School of Optometry and Vision Sciences
Cardiff University

Low-Level Night-Time Light Therapy for Age-Related Macular Degeneration

David Grant Robinson

2017

A thesis submitted to Cardiff University for the degree of Doctor of Philosophy

Supervisors:
AM Binns
TH Margrain

Advisor:
A Wood

For Catherine

Acknowledgements

Firstly, I would like to thank my two inspirational supervisors, Dr Ali Binns and Prof Tom Margrain for their guidance and encouragement throughout this PhD.

I would also like to thank Dr Ashley Wood and Dr Matt Dunn for their help and advice over the years. Many thanks also go to the office staff at the Optometry department, especially the wonderful Sue Hobbs who has provided fantastic support since day one.

A huge thank you to everyone in the Bristol Eye Hospital Clinical Research and Retinal Imaging Units for all of the hard work you have contributed to this PhD. In particular, I would like to thank Ms Clare Bailey and my fantastic trial manager Gemma Brimson. I would also like to extend my gratitude to all of the participants that agreed to take part in my studies.

A heartfelt thanks goes to my fellow post-graduate friends, especially those in office 2.10. Thank you all for putting up with my distracting antics and grumpiness over the last 3 years. A special thanks goes to Nikki Cassels, who has been a constant source of encouragement and friendship since we first sat next to each other in 2013.

Finally, I would like to express my love and gratitude to my family. Especially to my wife Catherine, my parents, my siblings and to David for their enduring support and encouragement. You have always believed in me, for which I will forever be grateful.

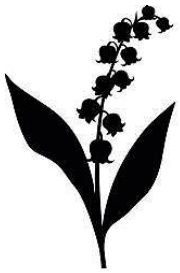

Table of contents

List of tables

List of figures

Acronyms

ABC	ABC-binding cassette
AE	Adverse events
AFC	Alternative forced choice
AMD	Age-related macular degeneration
ANCOVA	Analysis of covariance
ANOVA	Analysis of variance
AO	Adaptive optics
ApoE	Apolipoprotein
AR	Adverse reaction
AREDS	Age-Related Eye Disease Study
ATP	Adenosine triphosphate
AUC	Area under the curve
BCVA	Best-corrected visual acuity
BEH	Bristol Eye Hospital
bFGF	Basic fibroblast growth factor
CAD	Colour Assessment and Diagnosis test
CETP	Cholesterol ester transfer protein
CFH	Complement factor H
cGMP	Cyclic guanosine monophosphate
CI	Confidence interval
CIE	International Commission on Illumination
CNV	Choroidal neovascularisation
CNVM	Choroidal neovascular membrane
CONE τ	Time constant of cone photoreceptor recovery
CoR	Coefficient of repeatability
CRF	Case report form
CRU	Clinical research unit
CTGF	Connective tissue growth factor
DA	Dark adaptation
DHA	Docosahexaenoic acid
DNA	Deoxyribonucleic acid
ETDRS	Early Treatment Diabetic Retinopathy Study

EQ-5D	EuroQol-5D instrument
FIH	Factor-inhibiting hypoxia-inducible factor
FL	Fluid layer
GA	Geographic atrophy
GDF	Guanosine diphosphate
GTP	Guanosine triphosphate
HIF	Hypoxia inducible factor
HMCN	Hemicentin
HRE	Hypoxia response element
HSP	Heat shock protein
IPM	Inter-photoreceptor matrix
IQR	Inter-quartile range
IR	Inner retina
K^+	Potassium ion
LDF	Laser doppler flowmetry
LIPC	Hepatic lipase
LOCS	Lens Opacities Classification System
MHRA	Medicines and Healthcare products Regulatory Agency
MMSE	Mini mental state examination
Na^+	Sodium ion
nAMD	Neovascular age-related macular degeneration
ND	Neutral density
NHS	National Health Service
NICE	National Institute for Health and Clinical Excellence
NREM	Non-rapid eye movement
OCT	Optical coherence tomography
OLED	Organic light-emitting diode
ONH	Optic nerve head
OR	Outer retina
OST	Ocular surface temperature
PAI	Plasminogen activator inhibitor
PDE	Phosphodiesterase
PDF	Probability distribution function
PDT	Photodynamic therapy

PED	Pigment epithelial detachment
PEDF	Pigment epithelial derived factor
PHD	Prolyl hydroxylase domain protein
PIS	Patient information sheet
PO_2	Oxygen tension
PRISMA	Preferred Reporting of Items for Systematic Reviews
PSQI	Pittsburgh Sleep Quality Index
QUEST	Quick estimate by sequential testing
RAP	Retinal angiomatous proliferation
RCB	Rod-cone-break
RCT	Randomised controlled trial
REM	Rapid eye movement
RG	Red-green
RIU	Retinal imaging unit
ROC	Receiver operating characteristic
ROI	Reactive oxygen intermediate
RPD	Reticular pseudodrusen
RPE	Retinal pigment epithelium
SAE	Serious adverse events
SD-OCT	Spectral domain OCT
TIMP	Tissue inhibitor of matrix metalloproteinase
TSD	Theory of signal detection
VA	Visual acuity
VAS	Visual analogue scale
VEGF	Vascular endothelial growth factor
VFQ-48	Veterans Affairs Low Vision Visual Functioning Questionnaire
VHL	Von-Hippel-Lindau protein
WZ	Watershed zone
YB	Yellow-blue
ZEST	Zippy estimate of sequential testing

Summary

Age-related macular degeneration (AMD) is the leading cause of visual impairment in the developed world (Wong et al., 2014). The exact causes of AMD are unclear but hypoxia has been implicated (Stefánsson et al., 2011). If hypoxia has a role in the pathogenesis of AMD treatments that mitigate the effect of retinal hypoxia may slow disease progression.

This thesis aimed to establish the impact of light therapy, as delivered using a light emitting mask, on the progression of AMD. A phase I/IIa randomised controlled trial was implemented in which 60 participants with early and intermediate AMD were allocated to the intervention or the untreated control group in a 1:1 ratio and monitored over 12 months. The ability of secondary outcome measures (including: rate of cone dark adaptation, 14Hz flicker threshold and chromatic thresholds) to identify the likely risk of progression from early and intermediate AMD to advanced AMD was also assessed in a cross-sectional study evaluating the relationship between each baseline outcome measure and the severity of fundus changes.

Sixty participants were recruited of which 47 (20 intervention, 27 control) completed the 12 month follow-up period. No significant difference was found in the change of any parameter between groups apart from the time constant of cone-photoreceptor recovery (cone τ), which was increased to a greater extent in the treated group. An additional 40 participants were recruited to the cross-sectional study (n=100). Measurement of cone τ was identified as the best independent predictor of increased AMD severity based on the AREDS Simplified Severity Scale (Ferris et al., 2005).

Although a greater proportion of controls (48%) than mask wearers (38%) showed disease progression over the duration of the trial this difference did not reach statistical significance.

Chapter 1. Introduction

Age-related macular degeneration (AMD) is the leading cause of visual impairment in the UK and affects millions of people on a global scale. Currently there are no treatments for early AMD, intermediate AMD or geographic atrophy. The causes of AMD are not yet fully understood but hypoxia may play a role. Hypoxia has been found to be most acute at night when the retina is most metabolically active. By exposing the eye to very dim light at night the level of hypoxia is reduced. In practice, this can be achieved through low-level night-time light therapy provided by a light emitting mask. The overall objective of the work described in this PhD was to implement a clinical trial which aims to primarily assess the impact of low-level night-time light therapy on the progression of early and intermediate AMD, and retreatment rates for neovascular AMD (nAMD). The performance of a range of biomarkers for AMD and the safety and comfort of the light mask were also evaluated. This introductory chapter begins by providing an overview of the structure of a normal retina and retinal physiology in photopic and scotopic conditions. This is followed by a description of the risk factors, pathophysiology, classification, treatment and investigation of AMD. The latter part of the chapter provides an overview of visual psychophysics, focusing on the psychophysical investigative techniques of particular importance to the clinical trial. This chapter concludes with an outline of the specific aims of this PhD.

1.1. Normal retinal structure

In order to understand AMD pathogenesis and the value of potential therapeutics it is useful for the reader to have an understanding of the structure and function of a normal retina. With this in mind this section aims to provide an introduction to the retina and its component layers. Travelling from the outer to the inner retina, emphasis will be placed in this section on the layers that are of particular importance to AMD

pathogenesis. The retina is a light-sensitive layer of tissue that covers around 65% of the eye's interior surface (Oyster, 2006). It is situated between the choroid and the vitreous humour and extends from the optic nerve to the ora serrata (Figure 1.1) (Oyster, 2006). The retina acts as the primary stage of the visual processing pathway. Structurally it consists of nine individual layers including three layers of neuronal cell bodies interconnected by synapses (Figure 1.2) (Kolb, 2013).

When light focused by the cornea and lens strikes the photosensitive cells of the retina a cascade of chemical and electrical events is triggered. These events are collectively known as phototransduction and lead to the conversion of the incident light energy into an electrical signal. The signal is processed by the various neurons that reside within the retina and is transported via the optic nerve to the brain, where it is interpreted as an image (Forrester et al., 2016).

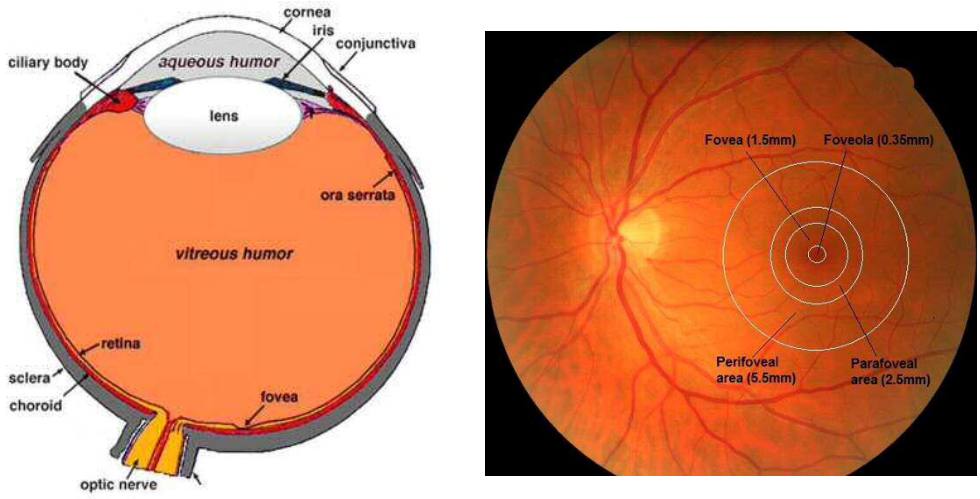

Figure 1.1. Diagram of a sagittal section of a human eye (left panel) and a healthy retinal appearance (right panel). The macular regions are circled and accompanied by typical measurements of diameter (Kolb, 2013; copyright permission from http://webvision.med.utah.edu/).

The direct appearance of the retina is displayed in Figure 1.1. When observed in this manner the optic nerve is referred to as the optic disc and can be seen as the pale circular area from which the major blood vessels of the retina radiate. The macula is an area of the retina located around 3.5mm temporally to the edge of the optic disc. It sits 1mm inferiorly to the centre of the optic disc and spans a diameter of 5-6mm

(Oyster, 2006). At the centre of the macula lies the fovea, an area specialised to provide high resolution visual acuity. The maximum resolving power of the eye is found at the centre of the fovea, known as the foveola, where the retinal thickness is at its minimum (Polyak, 1949). Surrounding the fovea is the parafoveal region which contains a large accumulation of retinal bipolar and ganglion cells. Outside of this lies the perifoveal region which ultimately merges with the peripheral retina.

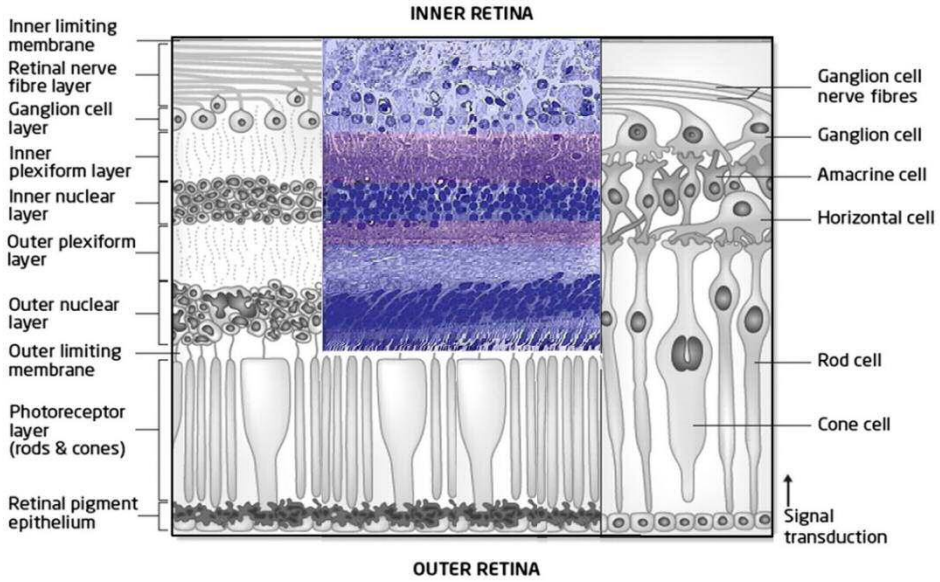

Figure 1.2. A diagrammatic representation of the retinal layers and neuronal cell bodies merged with a light micrograph (Wright et al., 2010; copyright permission from Elsevier [2018] licence 4274211239188*) of the central retina (Kolb, 2013; copyright permission from http://webvision.med.utah.edu/).*

1.1.1. Blood supply to the retina

The retina is extremely metabolically active and has one of the highest oxygen consumptions (per weight) of any tissue within the human body (Wong-Riley, 2010). It is served by a dual blood supply and maintains a blood-retinal barrier. The barrier is primarily upheld by the structural formation of the retina and is designed to promote the optimum environment for neural transmission.

The inner retinal layers are nourished via the central retinal artery which arises from the ophthalmic artery and enters the eye through the optic disc (Hayreh, 1962). Upon its emergence into the globe, the 100μm diameter central retinal artery divides into

superior and inferior branches which, in turn, separate into nasal and temporal arteries within the nerve fibre layer (Hayreh, 1962). Each subdivision of the artery is tasked with servicing a specific section of retinal tissue and is usually found in conjunction with similar subdivisions of the central retinal vein.

The temporal vessels make their way into the peripheral retina via an arching route around the macular region. This results in a 500μm diameter vessel-free area around the fovea (Oyster, 2006). In comparison, the nasal vessels run a more direct course to the ora serrata. Continued branching and bifurcation of the retinal vessels gives rise to the formation of a web-like capillary network within the nerve fibre or ganglion cell layer (known as the superficial network) and within the inner nuclear layer (known as the deep network) (Iwasaki and Inomata, 1986).

The retinal capillaries are characterised by their small luminal diameter (3.5 to 6μm), low flow rate and high oxygen exchange with surrounding tissue (Wang et al., 2011). Their structure is composed of a single layer of unfenestrated endothelium surrounded by a thick basal lamina (Ishikawa, 1963; Bernstein and Hollenberg, 1965). Pericytes overlie the basal lamina and are thought to facilitate the flow of blood due to their contractile nature (Chakravarthy and Gardiner, 1999). The vessels of this system do not anastomose with any other vascular structures and are therefore termed ‘end vessels’. This characteristic leaves the retina open to ischaemic assault in the event of an artery occlusion. The risk of complete inner retinal ischaemia in the case of central retinal artery occlusion is combated in 20-35% of the population by the cilioretinal artery which arises from the choroid (Justice and Lehmann, 1976).

Nutrition to the outer retinal layers is supplied by the choroidal circulation which, in turn, feeds off the short posterior ciliary arteries. In contrast to the retinal circulation, which is mainly influenced by local factors, the choroidal blood supply is controlled by sympathetic innervation and is not autoregulated (Delaey and Van De Voorde, 2000). The vascular structure of the choroid is generally divided into 3 layers. Moving from

the outermost to the innermost these are known as Haller's layer, Sattler's layer and the choriocapillaris. Vessel diameter is found to be largest within Haller's layer and gradually decreases towards the choriocapillaris (Hayreh, 1975). As the arteries decrease in size, the muscularis layer and internal elastic laminae are lost. The vessel walls become fenestrated, and therefore permeable, within the choriocapillaris layer. The choriocapillaris vessels are arranged into a network of individual lobules. Each lobule functions as an independent unit and, in a similar fashion to the retinal artery, derived vasculature does not anastomose (Hayreh, 1975). The greatest density of choriocapillary vasculature lies below the macula due to the high metabolic activity and avascular nature of this area.

All retinal layers that lie posteriorly to the outer plexiform layer are found to be avascular and rely heavily on the choroidal circulation for nourishment. The avascular macula region is also entirely dependent on the underlying choroidal blood supply (Nickla and Wallman, 2010). Before reaching their intended destination within the outer retina, metabolites are required to diffuse from the choriocapillary network and to pass through Bruch's membrane. This contributes to the choroidal circulation having a low rate of oxygen exchange in comparison to its high rate of flow (Nickla and Wallman, 2010).

1.1.2. The effect of luminance on retinal oxygen demand

In vivo oxygen (O_2) profiling of the macaque retina shows that, under light adapted conditions, retinal oxygen tension (PO_2) falls steeply between the choriocapillaris and photoreceptors (Wangsa-Wirawan and Linsenmeier, 2003). This is due to the high metabolic activity and oxygen demand of the photoreceptor inner segments. A more gradual reduction is then observed through the rest of the outer retina as shown in Figure 1.3 (Wangsa-Wirawan and Linsenmeier, 2003). The direction of this monotonic PO_2 gradient indicates that the choroid alone is responsible for photoreceptor oxygenation when light adapted (Ahmed et al., 1993).

When dark adapted, Figure 1.3 shows that the PO_2 level in the outer retina is considerably lower and approaches 0mmHg at the proximal side of the photoreceptor inner segments. Birol et al. (2007) found a decrease in PO_2 level from 48mmHg to 3.8mmHg when travelling from the choroid to the photoreceptor inner segment of the dark adapted macaque retina. Due to the O_2 gradient reversal seen at an inner segment level, retinal circulation has been found to be involved, alongside the choroid, with photoreceptor oxygenation when dark adapted (Ahmed et al., 1993).

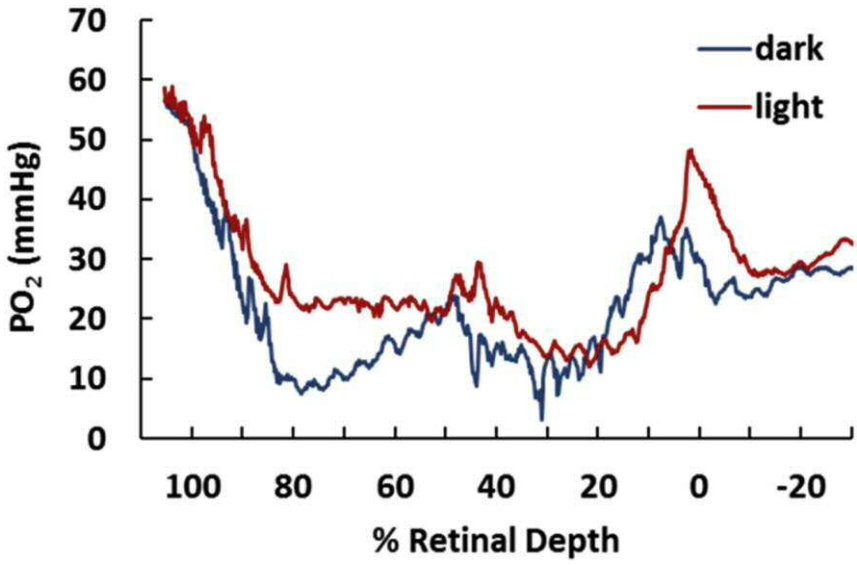

Figure 1.3. Intra retinal oxygen profile during light and dark adaptation. Note the near zero oxygen tension at 80% retinal depth observed in the dark (Linsenmeier and Zhang. 2017; copyright permission from Elsevier [2018] licence 4274230457173).

The increased oxygen demand displayed by the photoreceptors under scotopic conditions is attributable to the high metabolic demand of the 'dark current' in the approximately 92 million rods (Hagins et al., 1989; Sivaprasad and Arden, 2016). Oxygen profiles within this environment suggest that there is little O_2 reserve at the photoreceptor level. Increasing the volume of O_2 inhaled has been found to dramatically increase PO_2, in particular for the outer retina as the choroidal circulation does not autoregulate (Wangsa-Wirawan and Linsenmeier, 2003). The introduction of light under previously dark adapted conditions has also been found to reduce the O_2 consumption of the photoreceptors in the parafovea and fovea by 16-36% (Ahmed et al., 1993).

1.1.3. Bruch's membrane

Bruch's membrane is a thin modified connective tissue layer situated between the retinal pigment epithelium (RPE) and the choriocapillaris. The accepted model of Bruch's membrane structure involves 5 layers. This consists of the RPE basal lamina, an inner collagenous layer, a middle elastic layer, an outer collagenous layer and the basal lamina of the choriocapillary endothelium (Guymer et al., 1999). Histologically, Bruch's membrane appears as an acellular glassy layer of elastin and collagen rich tissue. Its structure aids to physically strengthen the RPE whilst also acting as a molecular sieve in order to regulate the exchange of biomolecules, nutrients, oxygen and metabolic waste between the retina and choroidal circulation (Booij et al., 2010). Bruch's membrane has been found to thicken with age. Ramrattan et al. (1994) documented a 2.7μm increase in thickness over ten decades. Other age-related changes include the accumulation of hydrophobic lipid-rich material within the inner collagenous zone and increased calcification of the elastic fibres (Huang et al., 2007; Booij et al., 2010). These changes have the potential to disturb normal function by acting as a diffusion barrier against metabolic exchange (Bird, 1992; Booij et al., 2010).

1.1.4. The retinal pigment epithelium

The RPE is the outermost retinal layer and is situated exteriorly to the neural layers of the retina. Located between the choroid and the photoreceptor outer segments, it exists as a monolayer of between 3 and 4 million regularly arranged hexagonal cells (Panda-Jonas et al., 1996). The cells are structured into a cuboidal formation which is densely packed and columnar in the central retina, but becomes shorter and flatter with increasing retinal eccentricity (Boulton and Dayhaw-Barker, 2001). Infoldings anchor the basal aspect of the RPE to Bruch's membrane whilst the apical surface extends microvilli towards the inter-photoreceptor matrix (IPM). The microvilli interact with the tips of the photoreceptor outer segments extending from the outer retinal

surface (Bonilha et al., 2006). The RPE cells are interconnected via gap junctions, which allow the controlled transfer of metabolites between neighbours, and tight junctions (zonulae occludens) which ensure a strong adhesion between cells (Hudspeth and Yee, 1973). Each cell contains melanin pigment which can vary in density between retinal areas, leading to a mottled fundus appearance. The melanin content of RPE cells also varies between individuals, leading to inter-individual variations in fundus appearance. The cell cytoplasm houses the smooth and rough endoplasmic reticulum, Golgi apparatus, mitochondria and lysosomes responsible for upholding the many functions of the RPE. Despite not being directly associated with the neural events of vision the RPE has been found to possess many physical, optical, metabolic and transport functions which play a critical role in the visual process (Bok, 1993; Strauss, 2005). These include:

1. Phagocytosis of shed photoreceptor outer segment discs.
2. Absorption of stray light and the prevention of light scatter within the eye.
3. Acting as a blood-retinal barrier between the choroid and neural retina.
4. Regeneration of visual pigment all-trans-retinal into its 11-cis configuration during the visual cycle.
5. Secretion of growth factors required for healthy choroidal maintenance.
6. Active exchange of nutrients with the choroid.
7. Facilitation of metabolite transport from the bloodstream to the photoreceptors.

The regular RPE array is often replaced by a more heterogeneous mixture of shapes and sizes through natural age-related changes. This is due to numerous changes including loss of melanin granules, thickening of Bruch's membrane, microvilli atrophy and basal infolding disorganisation (Bonilha, 2008). RPE function is also susceptible to disruption by the pigment granule lipofuscin which accumulates with age. Lipofuscin is composed of the lipid-containing residues of photoreceptor

phagocyctosis and has been found to correlate with RPE dysfunction, leading to apoptosis (Dorey et al., 1989; Holz et al., 1999; Suter et al., 2000).

1.1.5. The photoreceptor layer

There are two types of specialised neurons found within the retina, known as rod and cone photoreceptors. Both are capable of performing phototransduction by converting light energy into a neuronal impulse in order to generate information useful to the visual system (Hecht et al., 1942). Rods provide maximum sensitivity in scotopic conditions, although at the expense of temporal sensitivity and visual acuity. Cones operate under photopic conditions, and are responsible for high acuity vision and temporal resolution (Fu, 2010). Human colour vision is based on the three subtypes of cone photoreceptor, each of which is characterised by its response characteristics to different wavelengths of light (i.e. its spectral sensitivity curves). There are no subtypes of rods therefore the rod system is monochromatic (Lee, 2008).

There are approximately 92 million rods and 4.6 million cones found within the human retina, which vary in density with eccentricity (Curcio et al., 1990). The peripheral retina is dominated by rods which reach a density of 160,000 to 190,000 cells/mm^2 at 20-30° eccentricity (Ahnelt, 1998). The fovea exclusively houses cones, where they can be found at their greatest density of 200 000 cells/mm^2 (Curcio et al., 1990). Cone density decreases sharply with increasing retinal eccentricity as seen in Figure 1.4.

The major elements of a photoreceptor are shown in Figure 1.5. The photopigment, responsible for the capture and conversion of light energy, is located within the outer segment which is adjacent to the RPE. This is joined by a narrow connecting cilium to the inner segment which is filled with mitochondria in order to fuel metabolic activity (Hoang et al., 2002). An axon extends from the inner segment through the external limiting membrane and outer nuclear layer into the outer plexiform layer where it forms a synaptic terminal (Mustafi et al., 2009). Cones are associated with a complex network of postsynaptic cells, whereas the circuitry associated with rods is minimal.

Even though rods outnumber cones by approximately 20-fold, most mammalian retinas have 8-10 cone-driven neurons for every cell associated with the rod pathway (Masland, 2001).

A typical rod appears small in cell body but long and slender in inner and outer segment. Their shape is maximised for high density packing in order to enhance the capture of photons. Contained within their outer segments are the photopigment molecules embedded in a stack of around 600-1000 membranous discs (Sharma and Ehinger, 2003). Rod-based discs, unlike their cone counterparts, are free of attachment from the surrounding cell membrane and each is separated from the others. The discs of both rods and cones are produced at the base of the outer segment and are displaced to the tip by underlying newly formed discs (Young, 1971). Once at their final destination, the disc is encapsulated by the RPE microvilli, shed and phagocytosed (Young and Bok, 1969; Anderson et al., 1978). Cone outer segments are characteristically conical in shape measuring around 6μm at the base and 1.5μm at the tip. However, at the fovea their appearance is likened to rods due to the high density of the cones present (Borwein and Borwein, 1980). The discs contained within cones have a longer lifespan than their rod counterparts which take around 10 days to relocate from the base to the tip of the outer segment (Young, 1971).

The visual pigment found within the membranous discs consists of a variable protein component (opsin) and a bound chromophore which has been identified in humans as a vitamin A derivative (11-cis retinal). The photopigment found within rods has a peak spectral sensitivity of around 500nm and is known as rhodopsin (Wald and Brown, 1958). The visual pigment of cones is collectively termed iodopsin and exists in 3 forms (cyanolabe, chlorolabe and erythrolabe) corresponding to the peak wavelength absorption of each cone subtype (Lucas et al., 2013).

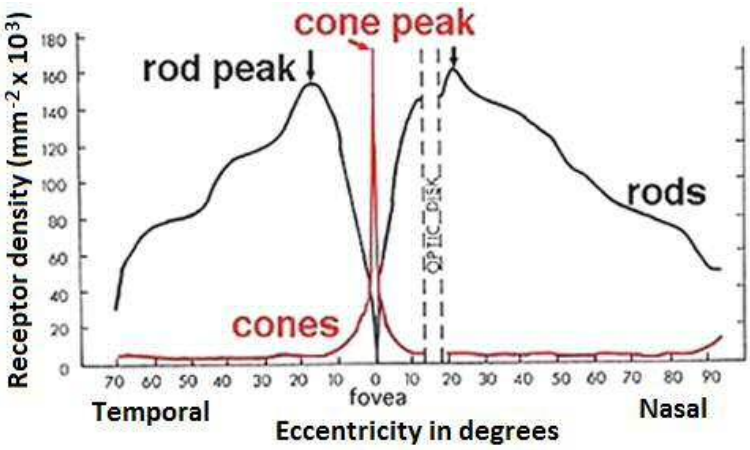

Figure 1.4. A graph displaying retinal rod and cone densities across the horizontal meridian (Kolb et al., 2013; copyright permission from http://webvision.med.utah.edu/).

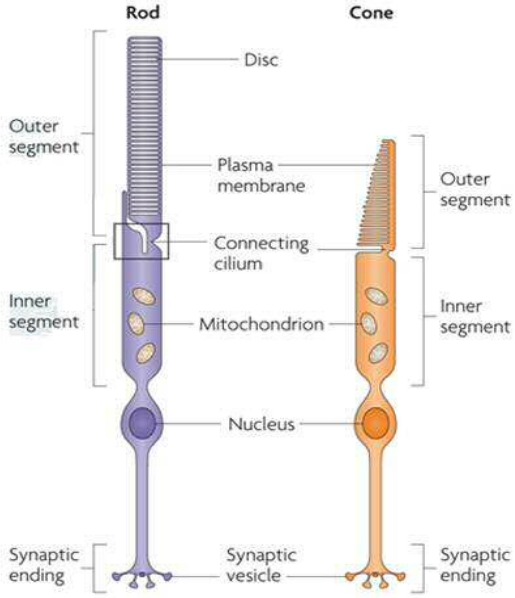

Figure 1.5. Schematic diagram of rod and cone photoreceptor structure (Wright et al., 2010; copyright permission from Elsevier [2018] licence 4274211239188*).*

1.2. Light and dark retinal physiology

Changes in light level elicit changes in visual function via the alteration of physiological processing at a retinal level. Therefore, retinal physiology can be found to differ under photopic and scotopic conditions. In the presence of light visual perception is initiated by activation of the visual pigment, this process is known as visual phototransduction. Adjustments to increases of light level are called light adaptation whereas adjustments to decreases are called dark adaptation. This section provides detail on

the photochemical changes that occur within the retina in both light and dark conditions.

1.2.1. Visual phototransduction cascade

Visual phototransduction is a process by which light is converted into electrical signals at a photoreceptor level. Once generated the electrical signals are transmitted through the visual pathway and ultimately processed into a visual interpretation of surroundings. The process of generating a visual signal in this manner is complex and consists of numerous stages. The following text provides a brief summary of the phototransduction pathway however for a more detailed description of the mechanism and its components the reader is directed to the excellent review articles by Lamb and Pugh (2004) and Yau and Hardie (2009).

- The visual phototranduction pathway is initiated when a photon is absorbed by visual pigment.
- The captured light energy causes the retinal found within the visual pigment to undergo a process known as photoisomerisation.
- Photoisomeration causes a structural change within the pigment as it alters from an 11-cis retinal to an all-trans retinal configuration.
- Opsin is unable to bind to all-trans retinal and is forced to undergo a conformational change into metarhodopsin II. At this stage the pigment is deemed to be ‘bleached’.
- Metarhodopsin II is unstable causing the pigment to split. This yields opsin and all-trans retinal.
- The free opsin activates a regulatory protein identified as transducin. This event causes transducin already bound to guanosine diphosphate (GDF) to dissociate and bind to guanosine triphosphate (GTP) instead.
- Once bound with GTP, the alpha subunit of transducin dissociates from its beta and gamma subunits.

- The alpha subunit-GTP complex activates phosphodiesterase (PDE).
- PDE breaks down cyclic guanosine monophosphate (cGMP).
- The decrease in cGMP causes photoreceptor Na^+ channels to close (Ebrey and Koutalos, 2001).
- The closure of photoreceptor cation channels results in a reduction in the current of ions between the photoreceptor and its surrounding extracellular matrix. The photoreceptor is deemed to be 'hyperpolarised' at this stage.
- Hyperpolarisation of the photoreceptor results in a reduction of neurotransmitter release which in turn leads to the generation of a physiological nerve signal.
- Once generated the electrical signal is propagated down the visual pathway.

This aforementioned process relies upon the presence of light. When the photon source is removed the events of phototransduction cease. The deactivation of the phototransduction cascade begins when transducin is driven to hydrolyse its bound GTP into guanosine diphosphate (GDP). This in turn halts the action of PDE. Following this, upregulation of guanylate cyclase obtained from calcium within the photoreceptor causes the transformation of GTP into cGMP. This leads to the replenishment of cGMP levels and the reopening of Na^+ channels.

1.2.2. Recycling of visual pigment

Visual pigment is recycled following phototransduction. In addition to the summary provided below, the mechanism via which bleached pigment is regenerated can be seen in Figure 1.6. For greater detail the reader is directed to the review articles by Lamb and Pugh (2004) and Yau and Hardie (2009).

- Phosphorylation of metarhodopsin II initiates visual pigment recycling.
- Once phosphorylated metarhodopsin II loses its affinity for transducin.

- Following this, the deactivation of metarhodopsin II is completed when it is bound by arrestin.
- Simultaneous phototransduction cessation at this point causes the release of the neurotransmitter glutamate to be resumed.
- All-trans retinal is then found to be reduced into all-trans retinol by an enzyme driven reaction (Wang and Kefalov, 2011).
- The all-trans retinol is transferred into the RPE where it is transformed into all-trans retinyl via the addition of an ester bond.
- RPE derived enzymes are then instrumental in the isomerisation of all-trans retinyl into 11-cis retinol.
- The 11-cis retinol is stored or converted into 11-cis retinal and diffused back into the photoreceptor.
- Once back in the outer segment the regeneration of visual pigment is completed via the recombination of 11-cis retinal and opsin.

Due to repeated recycling, retinol is susceptible to degradation over time and cannot be replaced by direct human synthesis. Levels required for phototransduction can be maintained via the sufficient intake of Vitamin A in the diet (Blomhoff and Blomhoff, 2006).

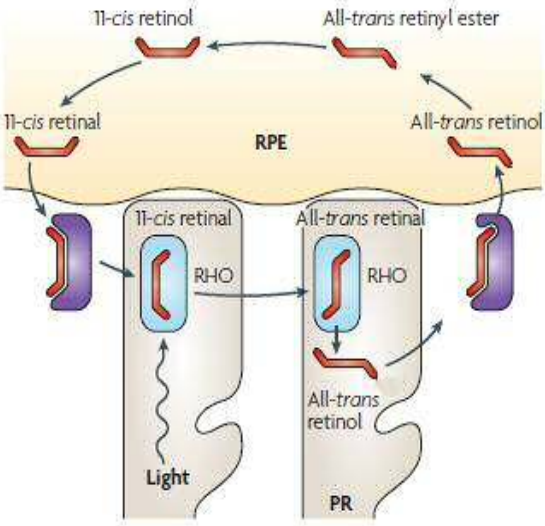

Figure 1.6. The process via which 11-cis retinal is recycled following usage within the phototransduction cascade. Rhodopsin is denoted as RHO (Wright et al., 2010; copyright permission from Elsevier [2018] licence 4274211239188*).*

1.2.3. Alternative method of visual pigment regeneration

Evidence based on a number of animal models has implicated Müller cell activity in the regeneration of cone photopigment (Das et al., 1992; Mata et al., 2002; Wang and Kefalov, 2011). The RPE derived protein RPE65 has been identified as an integral part of all-trans retinyl to 11-cis retinal conversion during the regeneration of rhodopsin (Redmond et al., 1998). However evidence suggests there is a secondary or substitute mechanism which results in retinoid production within a RPE65 deficient environment (Wang and Kefalov, 2011). Müller cells have been suggested as the alternative source due to their cellular content of 11-cis-retinyl-ester synthase and all-trans-retinol isomerase. It is proposed that these enzymes allow the conversion of all-trans retinol into 11-cis retinol which is later procured and utilised by cone photoreceptors (Mata et al., 2002). Rod photoreceptors are unable to facilitate photopigment regeneration via this method due to their lack of the enzyme 11-cis-retinol dehydrogenase. Therefore, this pathway is specific to the regeneration of cone visual pigment.

1.2.4. The dark current

Under scotopic conditions, cation channels located in the outer segment are kept open. The channels are controlled by cyclic guanosine monophosphate (cGMP) which is present at a high level under scotopic conditions (Miller, 1985). Sodium ions (Na^+), which passively enter the cell through these channels, travel into the inner segment via the connecting cilium and are actively pumped out of the photoreceptor via a sodium/potassium ion pump (Na^+/K^+) (Arshavsky et al., 2002). This process reduces the membrane potential of the photoreceptor and in combination with the steady inflow of Na^+ into the outer segment keeps the cell depolarised at around minus 40mV. The flow of Na^+ through the photoreceptor is known as the dark current. These conditions favour the release of the neurotransmitter glutamate which in turn transfers the neuronal signal onto synapsing bipolar cells. Off-centre bipolar cells are hyperpolarised by glutamate release at the synapse whilst on-centre bipolar cells are hyperpolarised in response to the downregulation of glutamate release. The photoreceptor Na^+/K^+ pump is driven by ATP, and generates a high metabolic demand in conditions of darkness.

Assessment of the effect of light intensity on the toad (Hamer et al., 2005) and salamander (Koutalos et al. 1995; Hamer et al., 2005) rod circulating current has suggested that progressively increasing the intensity of a background adapting light causes a progressive decrease in the rod circulating current. Complete cessation of the dark current occurs at a light intensity which varies between species (see Figure 1.7). An intensity of approximately 46 and 30 scotopic trolands (Td) is needed to reduce the rod circulating current by half in salamander (Nikonov et al., 2000) and mice (Lyubarsky et al., 1999), respectively. In comparison, a higher intensity is necessary to illicit the same reduction of rod circulating current in humans. Based on the assessment of one subject, Pepperberg et al. (1997) found that exposure to a luminance of 100 scotopic Td was required to reduce the rod current by 50%. Thomas

and Lamb (1999) used an electrophysiological technique to determine the attenuation of the maximal response of rod photoreceptors achieved at different background levels in 8 subjects. Their data suggested that a steady-state background intensity of 70 scotopic Td resulted in a 50% reduction in the human rod circulating current.

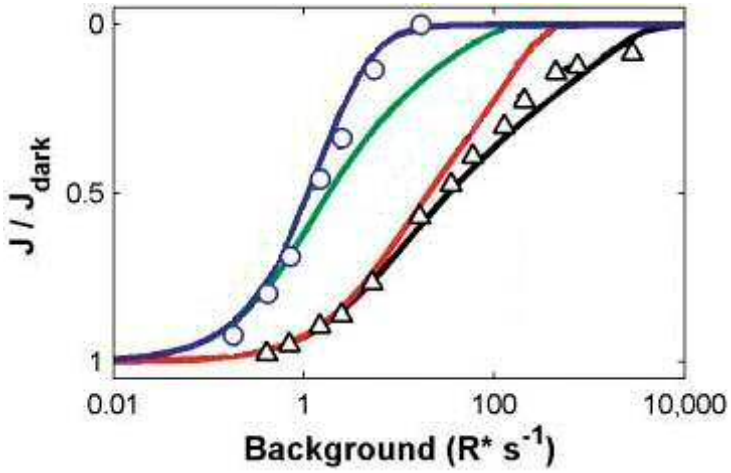

Figure 1.7. This unified model of light adaptation and its effects on circulating current in rods has been adapted from Hamer et al. (2005). It features data collected by both Hamer et al. (2005) and Koutalos et al. (1995). The figure plots steady-state circulating current as a function of background light adaptation. The data points show Koutalos et al.'s (1995) control (triangles) and suppressed dark adaption (circles) data. The solid curves form the basis of Hamer et al.'s (2005) predictions of suppression as based on their unified model. The data from Koutalos et al. (2005) has been shifted along the horizontal axis to compensate for differences in sensitivity between the salamander and the more sensitive toad model used by Hamer et al. (2005; copyright permission from Cambridge University Press [2018] licence 4274230980679).

1.3. Age-related macular degeneration

Age-related macular degeneration is a condition that typically manifests over the age of 55 (Klein et al., 2006) and affects the macular region of the retina. With progression over time it can lead to severe central vision loss in those affected. At present AMD is recognised as the principal cause of blindness in developed countries and is responsible for 8.7% of blindness worldwide (World Health Organisation, 2009). AMD can be classified into the following four subtypes (Ferris et al., 2013); early and intermediate AMD, which aren't associated with marked visual loss, and two forms of late AMD, geographic atrophy (GA) which causes a slow progressive visual loss, and nAMD which causes rapid loss of central vision if untreated.

Studies show that AMD has a high prevalence and correlation with visual impairment in North America (Chou et al., 2013), Asia (Kawasaki et al., 2010) and the United Kingdom (UK) where it is recognised as the primary source of sight impairment registration (Bunce et al., 2010; 2015). The AMD subtype that leads to slightly more than half of registrations of sight impairment in the UK is GA, this is due to the widespread adoption of intravitreal treatment for nAMD (Bunce et al., 2015). The actual prevalence however is thought to be even higher than registration figures suggest due to the exclusion of those who choose not to be registered with a visual impairment. Around 600,000 people in the UK are estimated to have advanced AMD, a figure that is expected to rise to around 750,000 by 2020 (Minassian et al., 2011). When combined with those who exhibit only early signs the total number of UK residents with AMD is estimated to be over 1.5 million (Owen et al., 2012).

Future projection suggests that due to population ageing, AMD cases within the UK are likely to increase by a third between 2012 and 2020 (Owen et al., 2012). This prevalence renders AMD a significant and growing socio-economic burden due to the cost of detection, treatment and provision of social care (Owen et al., 2012). With the potential to cause devastating effects on an individual's lifestyle AMD has also been linked to loss of independence and depression (Brody et al., 2001; Casten and Rovner, 2013; Jivraj et al., 2013; Zheng et al., 2017), loss of ability to carry out daily tasks (Scilley et al., 2002; Gopinath et al., 2017; Ugurlu et al., 2017), increased risk of falling (see reviews by Dhital et al., 2010 and Moenter et al., 2014), and reduced quality of life (Hassell et al., 2006; Coleman et al., 2010). On a global scale, based on the analysis of 39 population-based studies, it is expected that 196 million people will exhibit some form of AMD by 2020. This figure is predicted to rise to 288 million by 2040 (Wong et al., 2014).

1.3.1. Risk factors for AMD

There are many risk factors associated with the development and progression of AMD. Age is widely accepted as the greatest unpreventable risk factor for advanced AMD development (AREDS, 2000; Klein et al., 2006; Buch et al., 2005; Wang et al., 2007; Srinivasan et al., 2017) however other key risk factors have been identified and are documented in the following summary. In addition to those mentioned, refractive error (Wang et al., 1998; Wong et al., 2002; Tao and Jonas, 2010), cataract surgery (Wang et al., 2003a; Klein et al., 2002a), gender (AREDS, 2000; 2005; Owen et al., 2012; Grassmann et al., 2015), iris colour (Frank, 2000; Klein et al., 2014a; Schick et al., 2016), exposure to sunlight (Mitchell et al., 1998; Schick et al., 2016; AREDS, 2000; 2005; Fletcher et al., 2008), alcohol consumption (Adams et al., 2012) and diet/nutrition (Seddon et al., 2001; Smith et al., 2000; San Giovanni et al., 2009; AREDS, 2001a; AREDS2, 2013; see Section 1.3.2.1) have also been associated with AMD risk. For additional information the reader is directed to the excellent reviews by Chakravarthy et al. (2010) and Lambert et al., (2016).

1.3.1.1. Genetics

It has been estimated that between 46 and 71% of AMD risk is attributable to genetic variation and that first degree relatives of those with late AMD are at a substantially elevated risk of developing the condition themselves (Seddon et al., 2005; Klaver et al., 1998; Priya et al., 2012). Based on a study of 506 twin pairs, Hammond et al. (2002) found the phenotype of large soft drusen (>125μm) and the presence of ≥20 hard drusen were the most hereditable components of AMD. Genetic susceptibility was also confirmed via the finding of a higher concordance of AMD in monozygotic twins when compared to dizygotic twins. The risk of developing advanced AMD has been found to be increased nearly 4-fold for those with a family history of AMD, particularly in cases of nAMD (Smith and Mitchell, 1998). The presence of an immediate family member with AMD amplifies this risk, which has been estimated as

a 28 times and 12 times increase in risk for those with an affected parent or sibling, respectively (Shahid et al., 2012).

To date, approximately 40 genes have been identified that may be associated with the development of AMD (Lambert et al., 2016). It is likely that more genes will be identified in the future given the continued exploration of the seven previously unidentified loci associated with AMD highlighted by the AMD consortium in 2013 (AMD Gene Consortium, 2013).

The genes currently identified as being involved in AMD pathogenesis can be broadly classified into 5 groups depending on their biological pathway: the complement system, cholesterol metabolism, extracellular matrix remodeling, oxidative stress and retinal-specific function (Haddad et al., 2006). Genetic variants within each of these functional groups have been found to be particularly associated with the prevalence of AMD. It is estimated that nearly 50% of the risk of developing AMD can be attributed to gene mutations within the complement system (Klein et al., 2013; Shen et al., 2015). In particular, complement factor H (CFH), complement factor B, complement factor D, and complement components C2, C3, and C5 have been identified as relevant genes contributing to AMD risk (Maller et al., 2006; Gold et al., 2006; Yates et al., 2007; Jakobsdottir et al., 2008; Wu et al., 2013). From the remaining groups mutations in the hepatic lipase (LIPC), hemicentin-1 (HMCN1), apolipoprotein E (ApoE), ABC-binding cassette A1 (ABCA1), tissue inhibitor of matrix metalloproteinase-r (TIMP-3), cholesterol ester transfer protein (CETP) and the age-related maculopathy susceptibility 2 (ARMS2) gene have all been implicated with risk of AMD (Allikmets et al., 1997; Schultz et al., 2003; Yang et al., 2006; Yu et al., 2011; Baird et al., 2006; Chakravarthy et al., 2013a; Fritsche et al., 2015; Wang et al., 2015; Neale et al., 2010; Levy et al., 2015; Paun et al., 2015). For further information on each genetic variant the reader is referred to the review articles by Leveziel et al. (2011) and Lambert et al. (2016).

1.3.1.2. Race

Multiple studies have demonstrated that those of a white racial origin have a consistently higher incidence of AMD when compared to people of other ethnic backgrounds (Bressler et al., 2008; AREDS, 2005; Eye Disease Prevalence Research Group, 2004; Rein et al., 2009; Klein et al., 2011). In particular, a higher prevalence of both nAMD and GA has been found in white people when compared to black people (Klein et al., 2006; 2011; Bressler et al., 2008). It has also been identified that whilst black, Asian and Hispanic people manifest early AMD with almost the same prevalence as white people, they are subsequently less likely to progress to the end-stage of the disease (Friedman et al., 1999; Chang et al., 2008; Varma et al., 2010; Vanderbeek et al., 2011). The reason for the difference in AMD prevalence between these racial groups is not fully understood. It was originally speculated that, due to its ability to scavenge free radicals, melanin plays a protective role against disease progression in those where it is found in increased concentrations (Jampol and Tielsch, 1992). This is supported by the prevalence of AMD in different racial groups, which suggests that the degree of ocular pigmentation could be a significant protective factor, with white Caucasians showing the highest rates (5.4%), followed by Chinese (4.6%), Hispanics (4.2%) and those of black racial origin (2.4%) (Klein et al., 2006; Priya et al., 2012). Advances in genetic research have also identified various genotypes which increase an individual's vulnerability to AMD (see Section 1.3.1.1). Each genetic variant presents with varying frequency within different racial groups and therefore has the potential to influence AMD incidence and progression (Klein, 2011).

1.3.1.3. General Health

An association has been found between AMD and cardiovascular disease on numerous occasions (Tan et al., 2008a; Hogg et al., 2008, Wu et al., 2014). The strength of association has been found to be maximal when referring to advanced

AMD, where those with cardiovascular disease may be twice as likely to develop late stage manifestations of the disease (Chakravarthy et al., 2010). Conversely evidence has also been reported which shows that the presence of cardiovascular disease does not increase the risk of advanced AMD (DelCourt et al., 2001).

The presence of AMD has also been found to be positively associated with systemic hypertension (Hyman et al., 2000; AREDS, 2000; Churchill et al., 2006; Klein et al., 2003; Tan et al., 2008a; Duan et al., 2007). In comparison to normotensive individuals, a study by Klein et al. (2003) found that patients with both treated and uncontrolled blood pressure have a three-fold increase in the development of nAMD. The findings of the aforementioned studies included in this section indicate that AMD, atherosclerosis and cardiovascular disease may have similar pathogenic pathways. Other associations between general health and AMD have been identified, such as reduced blood triglyceride levels, increased body mass index and elevated fibrinogen levels. However, more investigation is required in order to solidify current, unsubstantial evidence regarding these factors (Seddon et al., 2003; AREDS, 2005; Hogg et al., 2008; Ngai et al., 2011).

1.3.1.4. Smoking

Cigarette smoking is the strongest environmental risk factor for nAMD (Pons and Marin-Castano, 2011). Cigarette smokers have consistently been identified as being 2-3 times more likely to develop AMD when compared to those who have never smoked (Thornton et al., 2005; Evans et al., 2005). They are also at risk of developing AMD on average 10 years earlier than non-smokers (Mitchell et al., 2002). Cigarette smoking has been found to increase the risk of both early AMD (Klein et al., 2002b) and end-stage AMD, with the strongest correlation to the development of nAMD (Vingerling et al., 1995; AREDS, 2005; Thornton et al., 2005; Woo et al., 2015). Furthermore, evidence suggests that smoking has a dose-dependent relationship with AMD risk, which increases with the number of pack years smoked (Seddon et al.,

1996; Chang et al., 2008). The cessation of smoking has also been found to lead to a subsequent reduction in AMD risk especially in those who have previously smoked fewer than 20 cigarettes per day (Christen et al., 1996; Khan et al., 2006). This finding is however not definitive as some studies have significant findings to suggest that former smokers are still at an increased risk (Smith et al., 2001; Thornton et al., 2005). The mechanism underlying the association between smoking and AMD remains unclear. Theories proposed include smoking induced vascular changes (Solberg et al., 1998), similar to those seen in atherosclerosis, complement pathway activation (Kew et al., 1985) and the reduction of antioxidants as induced by the multitude of chemicals found in tobacco smoke (Bernhard and Wang, 2007; Connell et al., 2009).

1.3.2. AMD pathogenesis

The precise mechanism behind AMD development and progression is unknown, Current evidence suggests that its pathogenesis is a multi-factorial process in which oxidative stress, age-related changes to Bruch's membrane, lipofuscin formation, chronic inflammation, hypoxia and choroidal vascular changes have all been implicated. Visual loss resulting from AMD pathogenesis ultimately arises via the dysfunction of photoreceptors secondary to an atrophic or neovascular event. This section gives a brief overview of the three most widely accepted mechanisms of AMD pathogenesis. For greater detail on the aforementioned factors and how they are implicated in AMD pathogenesis the reader is directed to the review papers by Ambati et al. (2003), Stefánsson et al. (2011) and Luthert (2011).

1.3.2.1. Oxidative stress

Oxidative stress is a mechanism of cellular damage resulting from the byproducts of oxygen metabolism during aerobic respiration. Energy required by the human body is primarily obtained through the oxidation of dietary carbohydrates, proteins and lipids. This is achieved through a series of reactions known as the tricarboxylic acid cycle. Products created via this method are transported to mitochondria where a process of

high oxygen consumption, known as oxidative phosphorylation, occurs (Beatty et al., 2000). This culminates in the creation of usable units of energy in the form of adenosine triphosphate (ATP). As well as generating intended ATP, this pathway has also been found to result in the formation of reactive oxygen intermediates (ROIs). ROIs are molecules found to be in an unstable or reactive state. They are formed as byproducts from active sites of enzymes, for example ATP synthase used in oxidative phosphorylation (Beatty et al., 2000). Stimuli including ageing, irradiation, inflammation and cigarette smoking have all been linked to the production of ROIs, such as free radicals, hydrogen peroxide and singlet oxygen (Beatty et al., 2000; Cui et al., 2012). Reactions between ROIs and other cellular molecules are often unfavourable as they can lead to direct apoptosis, inhibition of function or the formation of more harmful ROIs. It is for this reason that cumulative damage arising from reactions involving ROIs was originally proposed as a mechanism for ageing and age-related disorders (Harman, 1956).

The retina is particularly susceptible to the generation of ROIs. This is due to a number of factors including:

- Its high oxygen consumption.
- Its exposure to a high level of natural irradiation through visible light.
- The readily oxidised structure of its photoreceptor outer segments, due to high levels of polyunsaturated fatty acids.
- Excess ROI generation by neighbouring RPE phagocytosis.
- The presence of photosensitising agents such as lipofuscin, which promote further oxidation (see Beatty et al. 2000 for review).

In humans the activity of ROIs is suppressed by antioxidants, such as vitamin C, glutathione and carotenoids. The primary antioxidants found at the macula are the macular carotenoids, lutein and zeaxanthin. With increasing age, the changes that

manifest at the macula can be attributed to the ever growing imbalance between rising numbers of ROIs in comparison to antioxidants that naturally reside within the area. As a long-term result of unregulated ROI activity it is hypothesised that clinical features of AMD such as photoreceptor death and vascular endothelial growth factor (VEGF) upregulation are in some part resultant from the mechanism of oxidative stress (Beatty et al., 2000).

Numerous studies such have investigated the link between oxidative stress and AMD progression (Seddon et al., 2006; San Giovanni et al., 2007; Tan et al., 2008b; AREDS, 2001a; AREDS2, 2013; Weikel et al., 2012). Oxidative protein modifications have been identified as a component of drusen (Crabb et al., 2002; Hollyfield et al., 2003) and slower rates of disease progression have been found in those who take oral supplements high in antioxidant (AREDS, 2001a; AREDS2, 2013; Chew et al., 2014). The Age-Related Eye Disease Study (AREDS) demonstrated the efficacy of zinc-antioxidant supplements for preventing or delaying progression of early AMD to late AMD in those who are at high risk (AREDS, 2001a; AREDS2, 2013). The study showed that antioxidant supplementation reduced the 5-year risk of progression to advanced AMD by 25% for those with intermediate AMD or unilateral nAMD at baseline (AREDS, 2001a). This is supported by other studies that have reported a reduced risk of long-term incident AMD for those with a high dietary intake of lutein and zeaxanthin (Tan et al., 2008b) and naturally high levels of systemic carotenoids (Zhou et al., 2011). The reverse is also true, in that those who smoke or have a naturally high predisposition to ROI formation have been found to be at an increased risk of AMD development (Khandhadia and Lotery, 2010).

1.3.2.2. Chronic inflammation and immune response

Inflammatory involvement in AMD pathogenesis was hypothesised following evidence from numerous studies documenting the presence of immunological proteins within drusen (Hageman et al., 2001; Johnson et al., 2001; Anderson et al., 2002). It was

suggested by Roth et al. (2004) that drusen and other debris generated as a result of ageing and AMD release a pro-inflammatory signal which, in turn, initiates part of the innate immune system known as the complement cascade. This hypothesis has since been substantiated via the finding of other raised inflammatory markers involved with blood clotting and pathogenic defence in those with AMD (Shankar et al., 2007; Chakravarthy et al., 2010).

As introduced in Section 1.3.1.1, associations have also been found between genetic polymorphisms in genes which govern complement pathway activity, and increased risk of AMD. These polymorphisms have the potential to lead to altered cellular responses to assault or injury and unregulated complement activation (Donoso et al., 2005). Mutation of the CFH gene has been found to display an association with all stages of AMD (Despriet et al., 2006; Li et al., 2006; Sparrow et al., 2012). The Tyr402His polymorphism associated with CFH has been found to affect its binding properties and thus impair function (Donoso et al., 2010). Based on the results of three separate investigations assessing the relationship between CFH polymorphism and AMD development, Haddad et al. (2006) concluded that close to a half of all AMD cases in adults may be attributable to the CFH gene. In accordance with this, those who carry two copies of the polymorphism may have over a 10 fold increased risk of developing AMD compared to those who do not display the mutation (Despriet et al., 2006).

1.3.2.3. Outer retinal hypoxia

Changes have been found to occur to the choroidal vasculature and circulation in early AMD that may result in outer retinal hypoxia (Feigl, 2009). This has the potential to cause the formation of a choroidal neovascular membrane (CNVM) or direct cell apoptosis leading to GA, via the upregulation of hypoxia inducible factor (HIF) (Arjamaa et al., 2009). In addition to decreases in choroidal flow and volume, hypoxia in AMD may be exacerbated by such factors as increased scleral rigidity, Bruch's

membrane thickening and vitreoretinal adhesion, all of which reduce the diffusion of oxygen across the outer retina (Stefánsson et al., 2011). The reader is referred to Chapter 2 where the implication of hypoxia in the pathogenesis of AMD is discussed in detail.

1.3.3. Clinical features of AMD

Visual loss as a result of AMD is associated with the advanced forms of the disease as opposed to early manifestation. The clinical features that represent the 2 end-stage subtypes of AMD differ, however manifestations of early and intermediate AMD can appear in combination. This section provides an overview of clinical features encountered in AMD.

1.3.3.1. Drusen

Drusen represent an accumulation of extra-cellular material that is deposited between the RPE and the inner collagenous layer of Bruch's membrane, or between the RPE and its basement membrane. Identified morphologic phenotypes of drusen include hard, soft, calcified, reticular, large colloid, cuticular and basal laminar subgroups. The particular category that drusen are assigned to depends on their size, shape, colour, elevation, location within the retinal layers and definition. Drusen within each category also differ in component structure and may contain a combination of hydrophilic (e.g. CFH), hydrophobic (e.g. esterified cholesterol) and amphiphilic (e.g. Apolipoprotein B) factors (Anderson et al., 2002; Li et al., 2007; Curcio et al., 2010). Drusen < 63μm in diameter are referred to as small drusen or drupelets, drusen between 63μm and up to 125μm in diameter are classified as medium drusen, whilst those over 125μm in diameter are large drusen (Ferris et al., 2013).

Hard drusen consist of hyaline material and appear as small hemispherical yellow or white discrete deposits with well-defined borders (Figure 1.8). The formation of hard drusen is generally regarded as being part of the normal ageing process although the impact of their presence has been linked to mechanical disruption of the RPE and

photoreceptors (Al-Hussaini et al., 2009; Johnson et al., 2003). The presence of multiple hard drusen is a risk factor for AMD onset (Klein et al., 2002b; 2015). In contrast, the presence of soft drusen is diagnostic for early AMD. Soft drusen are larger than hard drusen (often exceeding 125μm in diameter), and their boundary may be distinct or indistinct. Appearing as yellow or grey in colour, they can arise independently or stem from pre-existing hard drusen (Sarks et al., 1994). The appearance of soft drusen is indicative of underlying diffuse changes to Bruch's membrane (basal laminar and linear deposits) (Sarks et al., 1994). Upon enlargement, several soft drusen may coalesce into a confluent form. The presence of soft drusen in large numbers has been associated with a significant risk of AMD progression (Wang et al., 2003b; Klein et al., 2008a). Once visible, drusen may persist as a clinical feature or regress over time via calcification and macrophage removal (Querques et al., 2014). Regression can be accompanied by the appearance of RPE pigmentary change and choriocapillary atrophy, or may precede the onset of choroidal neovascular growth (Yehoshua et al., 2011).

Reticular pseudodrusen (RPD), also known as subretinal drusenoid deposits, appear as yellowish interlacing networks of drusen which are deposited internal to the RPE (Mimoun et al., 1990; Hogg, 2014). RPD have similar constituents to soft drusen and are most commonly found in conjunction with other AMD features such as drusen, pigmentary changes, or late AMD (Zweifel et al., 2010; Sarks et al., 2011). Multiple longitudinal studies have revealed RPD as a strong predictor for progression to both nAMD (Ueda-Arakawa et al., 2013; Sarks et al., 2011; Cohen et al., 2007; Lee et al., 2012; Sawa et al., 2014; McBain et al., 2011; Klein et al., 2008b; Smith et al., 2006) and GA (Smith et al., 2006; Joachim et al., 2014; Finger et al., 2014; GAP Study Group, 2011). Despite this, the prevalence and specific role of RPD in AMD pathogenesis is unclear. Several of the studies reporting a relationship between RPD and nAMD also reported an association between RPD and retinal angiomatous

proliferation compared with other subtypes of nAMD (Ueda-Arakawa et al., 2013; Cohen et al., 2007; Sawa et al., 2014; McBain et al., 2011). As RPD are best visualised using infrared imaging or spectral domain optical coherence tomography, future analysis of epidemiological data using multimodal imaging will enable a more accurate determination of the population prevalence and risk factors associated with its development. Furthermore, the localisation of RPD internal to the RPE suggests that AMD may be a 2-component disease comprising of both subretinal and choroidal changes, however further research is needed to clarify whether choroidal changes associated with AMD pathogenesis are secondary to changes internal to the RPE (Sivaprasad et al., 2016).

1.3.3.2. Pigmentary abnormalities

The effect of AMD progression upon RPE melanin concentration results in clinically evident pigmentary changes as seen in Figure 1.8. Focal hyperpigmentation results from increased melanin, cell proliferation or migration of pigment epithelial cells within the RPE. The areas of pigment clumping appear darker than the surrounding healthy RPE tissue and can be found to overlie both soft and hard drusen (Bressler et al., 1994). The presence of focal hyperpigmentation has been reported as a risk factor for the development of neovascular AMD (Klein et al., 2002b). Focal hypopigmentary changes are also characteristic of AMD and manifest due to RPE degeneration (Klein et al., 2008a). The loss of melanin granules with age is a normal occurrence, however, the loss through AMD as a result of RPE atrophy or thinning leads to visible areas of mottled RPE appearance (Bonilha, 2008).

1.3.3.3. Geographic atrophy

Geographic atrophy is considered to be the end stage of dry AMD. It is defined by a well demarcated round or oval area of hypopigmentation in which choroidal vessels are more visible than in the surrounding retinal tissue (Figure 1.8). It is characterised by RPE and photoreceptor degeneration which results in a dense scotoma

corresponding to the area of atrophy. The development of GA is gradual. During progression initial paracentral loss is typically accompanied by foveal sparing until late in the disease process (Sunness et al., 2007; Holz et al., 2014). Over time GA has the potential to significantly impair visual function and can result in difficulty when performing tasks such as reading, watching television and recognising faces (Sunness et al., 1997). As a result, those with bilateral GA may require low vision aids and the provision of social services in order to maintain their independence (Klein et al., 1995).

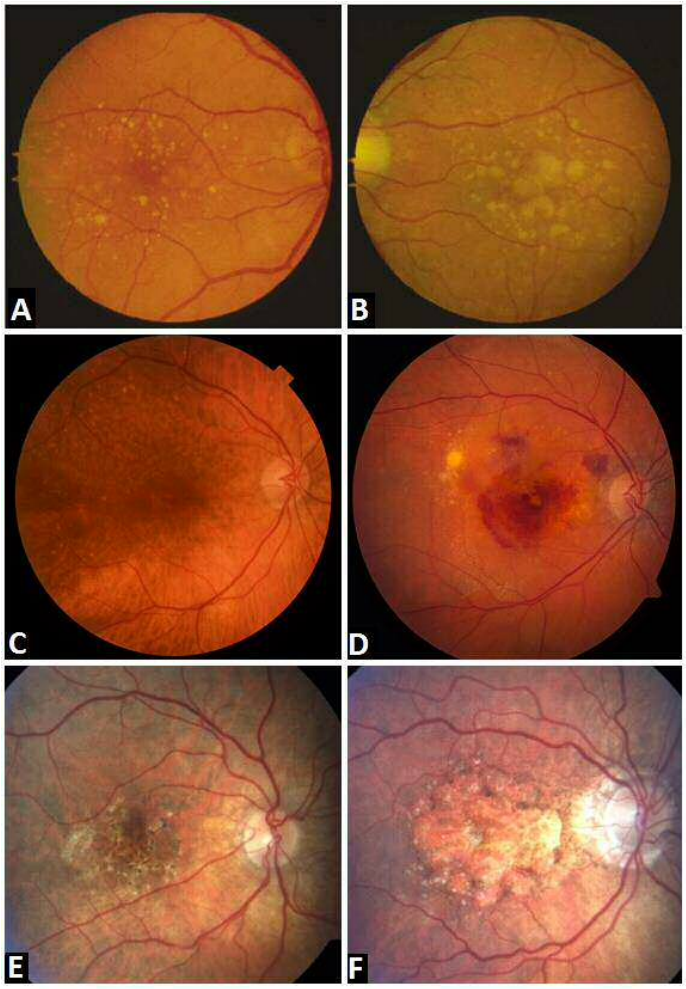

Figure 1.8. The fundus appearance of (A) hard drusen, (B) soft drusen, (C) reticular pseudodrusen, (D) neovascular AMD, (E) pigmentary changes at the macula and (F) geographic atrophy.

1.3.3.4. Choroidal neovascularisation

Choroidal neovascularisation is a feature of neovascular AMD, and occurs as a result of an imbalance between anti- and pro-angiogenic growth factors responsible for choroidal maintenance in healthy eyes. In advanced AMD the up-regulation of VEGF outweighs its anti-angiogenic counterpart, pigment epithelial derived factor (PEDF), resulting in the new vessel growth (Schlingemann, 2004). These new vessels grow from the choroid, through Bruch's membrane and into the subretinal space. Their arrival at the RPE results in either cessation of their growth, or barrier penetration to form a CNVM between the RPE and sensory retina (Grossniklaus and Gass, 1998). Due to their fragility, the new vessels are prone to leakage and rupturing. At a retinal level this process may be visible via the appearance of haemorrhaging (sub or intraretinal), intraretinal or subretinal fluid, hard exudates or a pigment epithelial detachment (Figure 1.8). At this stage blurred vision or metamorphopsia may be experienced (Fine et al., 1986). Classically the symptom of straight lines appearing bent or kinked is reported. Diagnosis and classification is generally based on optical coherence tomography and fluorescein angiography. Based on the location of the CNVM the two main designations of nAMD are classic (the CNVM penetrates the RPE) and occult (the CNVM is sub-RPE). In contrast, prior to CNVM formation angiomatous proliferation originating from the retina has also been reported in a second subtype of nAMD known as retinal angiomatous proliferation (RAP). The retinal vessels evident in RAP extend posteriorly into the subretinal space and may eventually communicate with choroidal neovascularisation (Yannuzzi et al., 2001; Freund et al., 2008).

Visual loss through a CNVM occurs at a rapid rate when compared to the timescale of GA development, therefore early detection and treatment is imperative. If left untreated the retinal haemorrhaging will eventually lead to the formation of a disciform scar which defines the end stage of neovascular AMD (Green and Enger, 1993;

Green, 1999). The resultant macular scarring is accompanied by a scotoma and a reduction in BCVA which in turn has been shown to have a major impact on quality-of-life (Brody et al., 2001; Brown et al., 2001). In a clinical trial of those with unilateral nAMD of varying impact on BCVA (n=136) Berdeaux et al. (2004) found that vision-related quality-of-life in those with nAMD was found to be the sum of two independent factors: worst eye BCVA and best eye BCVA. Suggesting that, the preservation of minimal VA in the worst eye of those with nAMD would help maintain vision-related quality-of-life. The most affected quality-of-life aspects reported by those with nAMD were driving, close vision activities (for example cooking, sewing, using hand tools), mental health and dependency (Berdeaux et al., 2004).

1.3.3.5. Pigment epithelial detachment (PED)

Pigment epithelial detachments occur when the basal lamina of the RPE is physically displaced from the inner collagenous layer of Bruch's membrane. Serous, fibrovascular and drusenoid PED subtypes are associated with AMD and can be identified via angiographic methods (Zayit-Soudry et al., 2007). Clinically, a serous PED is visible as a well demarcated, dome-like elevation of the retina. A serous PED manifests due to the accumulation of fluid between the RPE and Bruch's membrane which may be as a result of leakage from a CNVM (around 80% of cases), or may be due to impaired movement of fluid from the RPE to the choroid due to increased hydrophobicity of Bruch's membrane. PEDs are seen in up to 62% of eyes with advanced AMD (Coscas et al., 2007) and around half of those with newly diagnosed PEDs will experience significant visual loss (>3 ETDRS chart lines) one year from diagnosis (Pauleikhoff et al., 2002).

1.3.4. AMD grading scales

In order to enhance the comparability of results between research studies, the Wisconsin Age-Related Maculopathy Grading Scale was devised (Klein et al., 1991). Since its creation, the scale has been used as a basis for grading in a number of

longitudinal AMD studies, including the Beaver Dam, Rotterdam and Blue Mountains studies (Klein et al., 1992; Vingerling et al., 1995; Mitchell et al., 1995). Although the grading fundamentals were retained, each study tailored the scale slightly based on individual requirements. This process ultimately lead to further refinement of the scale and the collaborative creation of the International AMD Classification and Grading System (Bird et al., 1995).

More recently, widely used grading scales include the Age-Related Eye Disease Study System (AREDS, 2001b), the Three Continent AMD Consortium Age-Related Macular Degeneration Severity Scale (Klein et al., 2014b), and the Clinical Classification of AMD system (Ferris et al., 2013). Due to its large cohort size, longitudinal design and multi-centre approach the AREDS scale was designed to emphasise repeatability between graders (AREDS, 2001b). Following the completion of the study it was redesigned using the 5 year longitudinal data into a scale that reflected the risk of conversion to advanced AMD (Davis et al., 2005). This scale utilises the identification of key disease features, such as drusen characteristics and pigmentary abnormalities, from colour stereoscopic fundus photographs.

In order to aid ease of grading during clinical examination and reduce demanding photographic procedures, the original AREDS 9-step scoring structure has also been further simplified into a 5-step system called the AREDS Simplified Severity Scale (Ferris et al., 2005). This scale is based on a scoring system that grades each eye independently, then sums the score across both eyes to determine the final grade. The severity grade determined is based on the assignment of risk factors for approximate 5-year risk of developing advanced AMD in at least 1 eye (Table 1.1).

When summed across eyes the risk factors form a 5-step scale (steps 0-4) for which the 5-year risk of advanced AMD developing in at least 1 eye increases as follows: 0 factors, 0.4%; 1 factor, 3%; 2 factors, 12%; 3 factors, 26%; and 4 factors, 47% (Ferris et al., 2005). In accordance with the scale those with late AMD in one eye are graded

≥2 depending on the clinical signs within their fellow eye (Table 1.1). The AREDS Simplified Severity Scale has been used throughout this thesis to supplement analysis of the predictive capacity to AMD progression of the visual function tests used.

Table 1.1. The AREDS simplified grading scale documenting the pathological attributes for which risk factors are assigned to each eye. The risk factors are summed to give a grading of 0-4 which reflects the percentage risk of developing late AMD over 5 years (Ferris et al., 2005).

Disease stage	Risk category	Clinical signs	Late AMD conversion
Normal	0	Small drusen in one eye/both eyes or intermediate drusen in one eye AND no pigmentary abnormalities	0.4%
Normal	1	Intermediate drusen in one eye/both eyes or large drusen in one eye AND no pigmentary abnormalities OR small drusen in one eye/both eyes or intermediate drusen in one eye AND pigmentary abnormalities in one eye	3%
Early AMD	2	Large drusen in both eyes AND no pigmentary abnormalities OR intermediate drusen in one eye/both eyes or large drusen in one eye AND pigmentary abnormalities in one eye OR small drusen in one eye/both eyes or intermediate drusen in one eye AND pigmentary abnormalities in both eyes OR GA or nAMD in one eye and small drusen in the fellow eye AND no pigmentary abnormalities	12%
Early AMD	3	Large drusen in both eyes AND pigmentary abnormalities in one eye OR intermediate drusen in one eye/both eyes or large drusen in one eye AND pigmentary abnormalities in both eyes OR GA or nAMD in one eye and large drusen or pigmentary abnormalities in the fellow eye	26%
Late AMD	4	Large drusen AND pigmentary abnormalities in both eyes OR GA or nAMD in one eye and large drusen and pigmentary abnormalities in the fellow eye	47%

Since its introduction the performance of the AREDS Simplified Severity Scale has been validated by Liew et al. (2016). Briefly, this validation study involved re-grading baseline, 5- and 10-year fundus photographs of those enrolled into the Blue Mountains Eye Study (n=2134) with the AREDS Simplified Severity Scale. Following this the 5- and 10-year risk of advanced AMD progression rate for each severity grade was re-calculated and compared with that of the original AREDS cohort. The results showed a high-degree of concordance between predicted (using the AREDS Simplified Severity Scale) and expected (using Blue Mountains Eye Study data) 5- and 10-year incident late AMD rates. It was suggested that this supports the robustness of the AREDS Simplified Severity Scale, which has been applied widely across different study types (Liew et al., 2016).

1.3.5. Prevention and treatment

At present, most treatments target the neovascular form of AMD. The first medical treatment to show promising results against the continued progression of nAMD was a technique known as focal laser photocoagulation. When performing this procedure a laser is used to directly seal the site of leakage. This technique is no longer in frequent use, however, due to its negative impact on healthy retina and high rate of CNV recurrence (Virgili and Bini, 2007). Verteporfin photodynamic therapy (PDT) has also been widely used to treat nAMD and has been found to successfully stop or reverse vision loss over a short-term period of around 1 year. Its effectiveness is however variable and very dependent on the type and location of the presenting macular lesion (Bressler and Bressler, 2000). Currently, the use of focal laser photocoagulation and PDT has been superseded by that of Anti-VEGF drugs as discussed in this section. In contrast, there are no effective treatments available for early AMD, intermediate AMD or GA. With regards to these conditions early patient management involves lifestyle and nutritional advice. Such preventative measures are, however, only aimed at reducing the risk of disease progression as opposed to reversing its effects (AREDS, 2001a; AREDS2, 2013). Following the onset of GA, the provision of low vision aids is often necessary in order to utilise any remaining central vision. Depending on their need, patients with untreatable visual impairment attributable to AMD may also be referred to their GP, social services, or voluntary sector organisations for further practical or emotional help. In addition to the treatments documented in this chapter further investigation into AMD treatment is currently being directed towards, Angiopoietin antagonists (ClinicalTrials.gov identifier: NCT02713204), VEGF C/D inhibitors (ClinicalTrials.gov identifier: NCT02543229), designed Ankyrin repeat proteins (Souied et al., 2014), topical eye drop treatment (ClinicalTrials.gov identifier: NCT02727881) and stem-cell therapy (Fields et al., 2016).

1.3.5.1. Anti-VEGF drugs

At present, anti-VEGF drugs are widely used as the first choice of treatment against the effects of nAMD. When compared to other treatments such as Verteporfin PDT, anti-VEGF therapy has been found to be more effective at preventing vision loss, and is the first treatment which is actually able to restore vision (Brown et al., 2006; 2009). The treatment itself addresses the imbalance between anti-angiogenic and pro-angiogenic growth factors, which is seen during CNVM formation. A number of anti-VEGF drugs are in existence, including ranibizumab (Lucentis; Novartis), pegaptanib (Macugen; OSI Pharmaceuticals), bevacizumab (Avastin; Genentech/Roche) and, more recently, aflibercept (Eylea; Bayer). National Institute for Health and Clinical Excellence (NICE) guidelines currently only approve the use of ranibizumab (NICE TA 155, 2008), and alfibercept (NICE TA 294, 2013) for the treatment of nAMD.

Ranibizumab is a monoclonal antibody fragment which binds to and inhibits the action of VEGF-A. It has been deemed appropriate for the treatment of all major types of CNVM and is administered via direct intravitreal injection (Mitchell et al., 2010). When investigating the effectiveness of ranibizumab two pivotal phase II trials known as MARINA and ANCHOR (MARINA, 2006; Brown et al., 2009) demonstrated best-corrected visual acuity (BCVA) outcomes far superior to any previously published study in the treatment of nAMD. Bevacizumab is a humanised monoclonal antibody originally developed for use with metastatic colon cancer. It is molecularly larger than ranibizumab however is still able to penetrate ocular tissue in order to inhibit VEGF activity (CATT Research Group, 2011; Chakravarthy et al., 2013b). Although a review of clinical research studies since 2008 has identified ranibizumab as the most effective treatment for nAMD (Lanzetta et al., 2013), clinical outcomes such as logMAR visual acuity and foveal thickness have been found to show minimal variation between ranibizumab and bevacizumab over a 1, 2 and 5 year treatment period (Martin et al., 2011; 2012; CATT Research Group, 2016). Despite its financially lower unit cost when

compared to ranibizumab, bevacizumab has been associated with a slightly elevated rate of serious systemic adverse events and therefore is still not licensed for National Health Service (NHS) usage within the UK (Martin et al., 2012; Lanzetta et al., 2013). When considering the long-term outcomes for the treatment of nAMD the initial increase in BCVA often exhibited following the initiation of ranibizumab or bevacizumab anti-VEGF treatment has not been found to be sustained over a 5-year period (CATT Research Group, 2016). The Comparison of AMD Treatment Trials (CATT) (CATT Research Group, 2016) showed that after 5 years the mean BCVA of 647 participants was 3 letters worse than at baseline (when anti-VEGF therapy was initiated) and 10 letters worse than after 2 years of anti-VEGF therapy. Despite this the average visual acuity reported after 5 years of anti-VEGF treatment remained far superior to previous visual acuity outcomes using PDT (CATT Research Group, 2016).

Aflibercept differs to the other VEGF inhibitors in that it is not an antibody or antibody fragment. It is a recombinant fusion protein composed of human VEGF binding portions fused to a portion of human IgG1 immunoglobulin (Khan et al., 2014). Due to its ability to bind to all isoforms of VEGF-A and VEGF-B, aflibercept is able to penetrate further into the retina and bind with greater affinity than existing treatments (Khan et al., 2014). A number of clinical trials have demonstrated that aflibercept has the same efficacy as ranibizumab but requires fewer subsequent intravitreal injections (Dixon et al., 2009; CATT Research Group, 2011; Heier et al., 2012; Trichonas and Kaiser, 2013; Schmidt-Erfurth et al., 2014). Furthermore, retrospective analysis of 88 patients with previously untreated nAMD showed good long-term outcomes in a clinical setting can be achieved by using aflibercept (Eleftheriadou et al., 2017). Anatomical improvement (Hatz and Prünte, 2017; Lim et al., 2017) and improved visual-related quality of life (Zhu et al., 2017) has also been attributed to aflibercept use in those who have previously shown a limited response to ranibizumab. A recent

phase II study has also shown promising results regarding the efficacy of a VEGF inhibitor known as brolucizumab (Dugel et al., 2017). This single-chain antibody fragment of smaller molecular weight than both ranibizumab and bevacizumab has been shown to demonstrate non-inferiority to aflibercept when both were administered on an 8-weekly treatment regimen (Dugel et al., 2017). Two phase III studies are currently underway to further investigate the efficacy of brolucizumab when compared to aflibercept (HAWK, 2014; HARRIER, 2015).

Although the advent of VEGF inhibitors has revolutionised the management of nAMD, there is some debate regarding the most effective regimen to mitigate the treatment burden for those with nAMD without compromising BCVA outcomes (Park et al., 2012). Initially, in accordance with the MARINA and ANCHOR studies a fixed monthly treatment regimen was considered. These studies did however report a biphasic treatment effect after the initial 3-month loading phase which raised the possibility that, after the loading phase, maintenance of VA may be achieved with less frequent injections. This was investigated in the CATT research trials (CATT Research Group, 2011; Rosenfeld 2011) which included 4 treatment arms comparing ranibizumab or bevacizumab administered on variable (pro re nata [PRN]) or fixed monthly schedules over 12 months. The results showed no difference between the 12 month change in BCVA for those treated with ranibizumab as necessary following monthly evaluation (PRN) when compared to those on a monthly fixed regimen. Quarterly ranibizumab administration following an initial 3-month loading dose has also been investigated but was shown to be inferior to monthly treatment when using change in BCVA as a primary outcome measure (Schmidt-Erfurth et al., 2011; Regillo et al., 2008; Abraham et al., 2010).

Presently in clinical practice intravitreous VEGF inhibitors are commonly administered in accordance with one of two approaches, both of which implement a ‘loading’ phase followed by a maintenance phase. The maintenance phase is modelled on a

traditional PRN (Spaide 2007) or a treat and extend (Brown and Regillo, 2007; Chiang and Regillo, 2011) regimen. Traditional PRN involves regular (often monthly) follow-up and treatment as necessary (Lalwani et al., 2009; Boyer et al., 2009; Tano and Ohji, 2010; Dadgostar et al., 2009; Gupta et al., 2010). In contrast to this, the treat and extend approach involves regular and frequent treatment until the macular is dry, followed by a gradual extension of the treatment interval and corresponding follow-up visit. To date, a number of ranibizumab comparator studies of treat-and-extend versus PRN have shown an improvement in both visual and anatomical outcomes using a treat-and-extend approach over a period of 6 months to 36 months (Oubraham et al., 2011; Calvo et al., 2014; Hatz and Prünte, 2016; 2017; Giannakaki-Zimmermann et al., 2016; Kvannli and Krohn, 2017). Using data from 11 treat-and-extend studies a general algorithm has been devised to facilitate optimal application of treat-and-extend regimens in clinical practice (Freund et al., 2015). The algorithm suggests the extension of treatment intervals by up to 2 weeks at a time (reaching a maximum extension period of 12 weeks) for those with continued absence or stabilisation of intraretinal fluid following initial dosage.

1.3.5.2. Nutrition

Even though there is currently no effective treatment for early or intermediate AMD, lifestyle advice such as the cessation of smoking (Smith et al., 2001; AREDS, 2005) and the adoption of an active lifestyle (Knudtson et al., 2006; Williams, 2009) can be advised as preventative strategies against disease progression. In addition, current evidence also suggests that dietary advice and the recommendation of nutritional supplementation may also be effective.

The importance of dietary intake relates to the susceptibility of the retina to oxidative damage, which has been suggested as a contributing factor to AMD pathogenesis (Beatty et al., 2000). Therefore, in order to prevent AMD progression, the dietary intake of elements such as vitamins and carotenoids has been proposed as being

advantageous due to their antioxidant properties (Weikel et al., 2012). The AREDS research group undertook a randomised placebo controlled trial of 3640 participants with AMD severity ranging from early to unilateral advanced, to investigate the effect of high dose antioxidants on disease progression. They documented a 25% reduction in the risk of progression to advanced AMD in those who took an anti-oxidant vitamin, zinc and copper formulation (500mg vitamin C, 400IU vitamin E, 15mg beta-carotene, 80mg zinc and 2mg copper) over a 5 year period for those with extensive intermediate drusen, large drusen, or non-central GA in 1 or both eyes, or advanced AMD in 1 eye at baseline (AREDS, 2001a).

Other dietary supplements that have shown promise with regards to the inhibition of AMD progression include xanthophylls and omega-3 fatty acids, neither of which can be synthesised by humans. Lutein and zeaxanthin are obtained through the dietary intake of a variety of fruit and vegetables. They are found at their highest concentration at the macula and are thought to play a protective role via the inhibition of light induced damage (Snodderly, 1995; Landrum and Bone, 2001). Long chain omega-3 fatty polyunsaturated fatty acid Docosahexaenoic acid (DHA) is primarily found within photoreceptor outer segments. Mainly obtained through sources such as fish and plant oils, the regular intake of DHA has shown promising results in reducing the risk of AMD onset and progression (Seddon et al., 2006; San Giovanni et al., 2007; Tan et al., 2009). Despite this, a subsequent follow-up to the AREDS study (AREDS2, 2013) investigating the potential benefit of adding omega-3 fatty acids, lutein and zeaxanthin to combinations based on the original AREDS formula reported less encouraging findings. The results indicated that there was no benefit to adding omega-3 fatty acids to the supplement, whilst the xanthophyll additions were only beneficial in those who had very low dietary levels of lutein and zeaxanthin at baseline (AREDS2, 2013).

1.3.6. Clinical investigation of AMD

A range of tests is available for the evaluation of AMD, each of which can be utilised to focus on various traits and manifestations of disease progression. Traditionally, in order to diagnose the presence of AMD, measurement of visual acuity, central visual field assessment (for example, using the Amsler Chart), fundus photography and fluorescein angiography have been employed. Advancements in retinal imaging, for example, ultra-high resolution optical coherence tomography and fundus autofluorescence, have increased the sensitivity of detection of AMD (Holz et al., 2007; Padnick-Silver et al., 2012). In recent years, it has become apparent that various other tests of visual function, such dark adaptation (Dimitrov et al., 2008; 2011; Gaffney et al., 2011; Jackson et al., 2014a; 2014b; Owsley et al., 2001; 2007; 2016; 2017), microperimetry (Cassels et al., 2017; Acton et al., 2012) and photostress recovery time (Wu et al., 1990; Midena et al., 1997; Bartlett et al., 2004) are more sensitive than VA in detecting early functional loss in AMD. The investigative techniques of particular importance to this study are hereby documented. For additional information on other techniques available the reader is directed to the review papers by Neelam et al. (2009) and Nivison-Smith et al. (2014).

1.3.6.1. Optical coherence tomography (OCT)

Optical coherence tomography (OCT) is a non-invasive, cross-sectional imaging technique which utilises the principle of interferometry in order to generate 3-D representations of the retina (Drexler et al., 1999). OCT images consist of individual data points representing the superimposition of two light waves. These data points exist as a-scans and comprise a series of reflectivity measurements at varying depths within the retina. The combination of a number of a-scans produces a cross sectional image of the retina known as a b-scan, as seen in Figure 1.9 (Huang et al., 1991). The introduction of spectral domain OCT (SD-OCT), optical coherence tomography angiography (OCTA), swept-source OCT (SS-OCT) and adaptive optics OCT (AO-

OCT) has provided the opportunity to study outer retinal structures and clinical characteristics of interest in AMD in greater resolution. For example AO-OCT can be used to visualise photoreceptor wellbeing via the assessment of photopigment disc renewal in the outer segment (Zhang et al., 2005; Zawadzki et al., 2005; Jonnal et al., 2016). An application of SD-OCT is the visualisation of drusen in fine detail. In addition to this, when coupled with segmentation algorithms, the high definition b-scans provided by SD-OCT can be used to extract quantitative information describing the 3-dimensional geometry of the RPE. Quantification of the deformations of the RPE provides an indication of the volume of underlying drusen. Drusen volume evaluation using the OCT has been shown to be highly reproducible (Gregori et al., 2011).

The structural measurement of drusen volume has been identified as a potentially useful biomarker of AMD (Yehoshua et al., 2011; Abdelfattah et al., 2016; Schlanitz et al., 2017). In a study of 100 patients Yehoshua et al. (2011) assessed the potential utility of drusen volume evaluation as a clinical end point in trials designed to investigate AMD treatment. The drusen volume within areas of 3mm and 5mm circumference, centred on the fovea, were measured at 6, 12 and 24 monthly intervals. The results showed that drusen have an undulating pattern of growth over time. Quantitatively, the volume was found to increase in 48% of eyes and decrease in 40% of eyes assessed over 12 months. Eyes with markedly decreasing drusen volume were also found to be at an increased risk of subsequent exudative AMD or GA development (Figure 1.10). This finding correlates with other evidence which suggests drusen size as an important risk factor for the development of advanced AMD (Bressler et al., 1990; Pauleikhoff et al., 1990a; Klein et al., 2008a). It also supports the applicability of drusen volume analysis as a viable clinical tool when determining the likelihood of AMD progression.

Numerous studies comparing measurements of drusen area taken manually from colour fundus photographs and via an automated SD-OCT algorithm have been

undertaken (Jain et al., 2010; Iwama et al., 2012; Yehoshua et al., 2013; Mokwa et al., 2013; Diniz et al., 2014). Despite the tendency of OCT based analysis to slightly underestimate drusen volume it has been documented as a reproducible and reliable method for use in studies including people with AMD (Yehoshua et al., 2013; Diniz et al., 2014).

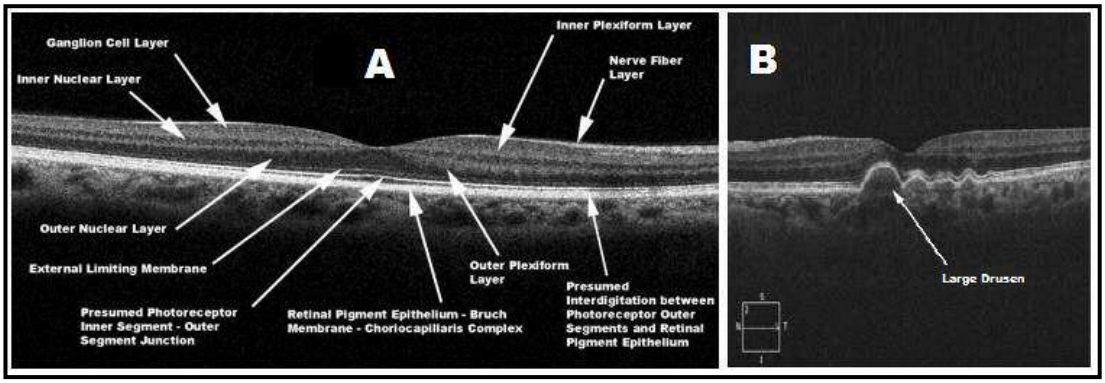

Figure 1.9. An SD-OCT horizontal b-scan displaying the outer retinal layers (A) and a large drusen underlying the macular region (B).

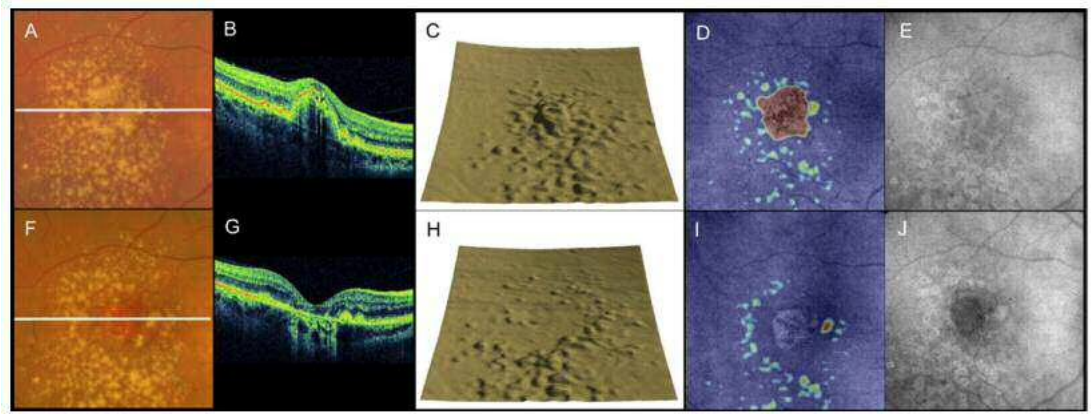

Figure 1.10. An example of the Zeiss Cirrus OCT drusen volume analysis software used by Yehoshua et al. (2011). Images displayed were taken from a 76 year old woman who displayed a reduction in drusen volume, prior to GA development. Images A-E show baseline measurements in comparison to F-J which document the changes seen 12 months later. The images represent a B-scan (A,F), horizontal B-scan (B,G), RPE segmentation map (C,H), hybrid OCT fundus image/drusen thickness map (D,I) and fundus autofluorescence (E,J).

1.3.6.2. Visual acuity

Within both optometric practice, hospital based optometry and in clinical trials, visual acuity (VA) is regularly used as a measure of visual function. Despite this, evidence suggests that measurements of VA do not correlate well with the visual performance

of everyday tasks in people with AMD (Hogg and Chakravarthy, 2005). Also, depending on the stage of progression and retinal pathology, VA amongst those with advanced AMD can be variable and changes are often masked by the 1-2 line test-retest variability of the Early Treatment Diabetic Retinopathy Study (ETDRS) chart (Arditi and Cagenello, 1993; Lovie-Kitchin and Brown, 2000). VA during earlier stages of disease progression is often found to exhibit minor or even no reduction, therefore the use of VA alone would not be sufficient to detect AMD until relatively late in disease progression (Klein et al., 1995).

1.3.6.3. Colour vision

Histopathological evidence suggests that cone photoreceptors are disrupted as a result of AMD at a functional and neuronal level (Curcio et al., 1996; Jackson et al., 2002; Shelley et al., 2009). Taking this into account, changes in visual performance relating to cone function, such as colour contrast sensitivity, can be measured in order to derive information on disease status and progression.

Using the Nagel Anomaloscope, Eisner et al. (1991) found that individuals with abnormal colour vision (denoted by a reduction in the effect of stimulus size on the red-green Rayleigh colour matching range, or rejection of all colour matches) had a high-risk fundus appearance for the development of nAMD. Further investigation by the same group resulted in the identification of red/green Rayleigh colour matching, when used alongside dark adaptation, as an effective predictive biomarker for nAMD development (Eisner et al., 1992). In a subsequent 2 year longitudinal study, Holz et al. (1995) measured tritan and protan colour contrast sensitivity using a bespoke computer graphics technique. The results indicated that measurement of blue colour contrast sensitivity at a foveal level may serve to monitor the progression of AMD prior to GA or exudative changes. These results were seconded by the finding that tritan thresholds are elevated in the presence of drusen (Frennesson et al., 1996; Arden

and Wolf, 2004) and continue to elevate in relation to the severity of AMD manifestation (Arden and Wolf, 2004).

The Colour Assessment and Diagnosis (CAD) test is currently used by the Civil Aviation Authority (CAA) as gold standard when testing colour contrast sensitivity. As seen in Figure 1.11, by employing dynamic luminance contrast noise to mask the detection of any residual luminance contrast cues, the test isolates red-green (RG) and yellow-blue (YB) thresholds along 16 directions of the International Commission on Illumination (CIE) chromaticity diagram (CAA, 2009). This allows the severity of colour vision loss to be quantified when compared to the pre-determined limits of 250 normal trichromats (Barbur et al., 2006). When implementing the CAD test on 18 participants with varying stages of AMD, O'Neill-Biba et al. (2010) found acquired loss of YB and, to a lesser degree, RG chromatic sensitivity. The exhibited threshold increase was found to be larger for YB chromatic sensitivity across all grades of AMD and exhibited a positive correlation to disease severity.

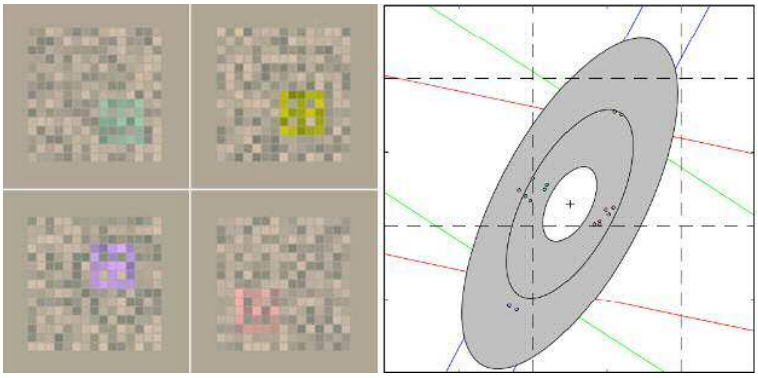

Figure 1.11. Coloured stimuli (overlying contrast luminance noise) as presented during the CAD test (left panel), and result plot generated following chromatic sensitivity measurement using the CAD test (right panel). A range of colours is shown in the left panel however during threshold testing a single colour is presented at any one time. During threshold testing the participant is asked to identify the direction of movement of the coloured square across the field of dynamic luminance contrast noise (Barbur et al., 2006). The range of chromatic threshold variation expected in normal colour vision falls within the grey shaded area of the CAD result plot shown in the right panel. Upon completion of the test measured thresholds are plotted as small red, green, yellow and blue circles upon the result plot. A subject's colour vision is considered normal if both RG and YB chromatic thresholds lie within the shaded area (CAA, 2009).

1.3.6.4. Temporal flicker sensitivity

Temporal sensitivity describes the ability of the eye to resolve and therefore respond to a flickering stimulus. The human eye is able to resolve flickering stimuli of up to 60-80Hz (Brown and Lovie-Kitchin, 1987). The ability of an individual to resolve a flickering stimulus can be clinically measured by increasing the temporal frequency whilst maintaining a constant background luminance until flickering can just be detected. Evidence suggests that in comparison to static stimuli, a flickering target increases the metabolic demand of the retina due to higher cortical processing rate via magno- and parvocellular neural pathways (Polak et al., 2002; Phipps et al., 2004). Haemodynamic studies have identified increases in retinal artery diameter and blood flow in response to flickering stimuli (Michelson et al., 2002; Polak et al., 2002) with peak vascular changes localised to the mid-perifoveal region. This, unsurprisingly, coincides with the location of the maximum ganglion cell and nerve fibre density (Kiryu et al., 1995). It is suspected that AMD-related pathological damage to both the outer retina and choriocapillaris results in compromised outer retinal metabolism and the inability to meet the increased flicker-induced metabolic demands (Neelam et al., 2009). Ultimately, this leads to a reduction in temporal sensitivity to a greater extent than expected through normal ageing (Kim and Mayer, 1994).

A series of studies conducted by Mayer et al. reviewed the effectiveness of foveal flicker sensitivity as a predictive measure for the development of nAMD in the fellow eye of those with a monocular manifestation (Mayer et al 1990; 1992a; 1992b; 1994). It was initially identified that a flickering stimulus of 10 or 14Hz was needed to correctly identify eyes at risk of nAMD development when compared to age-matched controls. This was with 78% accuracy on the basis of foveal flicker sensitivity alone (Mayer et al., 1992b). Subsequent investigations led to the conclusion that those at risk of nAMD development were found to have maximally reduced flicker sensitivity to mid-temporal frequencies (10-40Hz), leading to the designation of a 14Hz stimulus as optimal

(Mayer et al., 1992a). Participants who went on to develop nAMD were also found to have significantly lower sensitivities up to 9 months before the appearance of exudative retinal changes (Mayer et al., 1992b).

These findings are substantiated by Luu et al. (2012) who, following analysis of data from a 2-year longitudinal study also documented a reduced flicker sensitivity in eyes that went on to develop late AMD. In addition, based on severity grading, the reduction in foveal flicker sensitivity has been found to show significant concordance with related fundus changes typical of AMD progression (Mayer et al., 1994; Dimitrov et al., 2012; Luu et al., 2013). In a study of 293 participants with AMD Dimitrov et al. (2012) reported that 14Hz flicker threshold declined progressively along the continuum of AMD severity. Therefore, it was suggested that flicker threshold assessment had the potential to monitor disease progression and detect possible stabilisation or reversal of AMD pathogenesis with new treatments (Dimitrov et al., 2012).

The clinical value of temporal sensitivity testing was assessed in a study by Dimitrov et al. (2011) of 221 participants with varying AMD status. When evaluated against other steady state and dynamic tests, 14Hz foveal flicker sensitivity returned a modest diagnostic capacity of 34% of abnormal cases correctly identified. Despite this, when combined with scoring based on reproducibility and clinical applicability the test was ranked above dark adaptation and photostress recovery as a potential clinical tool for monitoring AMD progression within a research and clinical environment.

1.3.6.5. Dark adaptation

Due to its physiology, the visual system is generally able to adapt swiftly to changes in ambient illumination over a vast range of light intensity. This trait, however, is not upheld following extended retinal exposure to an intense adapting light source. The accumulation of a high concentration of ‘bleached’ or deactivated visual pigment leads to a slow, biphasic recovery of visual sensitivity which is known as dark adaptation

(DA) (Lamb and Pugh, 2004). Following exposure to the adapting light source, the threshold intensity needed to detect a visual stimulus over time can be plotted as a dark adaptation curve (Figure 1.12). When viewing the curve, the initial rapid reduction of visual threshold is mediated by the cone photoreceptors and is followed by the cone plateau. The subsequent slower threshold reduction is rod governed and is preceded by the rod-cone-break (RCB), which indicates a time-dependent shift in the dominant photoreceptor system. The appearance of the curve is dependent on multiple factors such as the percentage of photopigment bleached and stimulus specifics, such as size or retinal eccentricity (Hecht et al., 1935; 1937, Thomas and Lamb, 1999; Lamb and Pugh, 2004; Dimitrov et al., 2008, Gaffney et al., 2011; 2013).

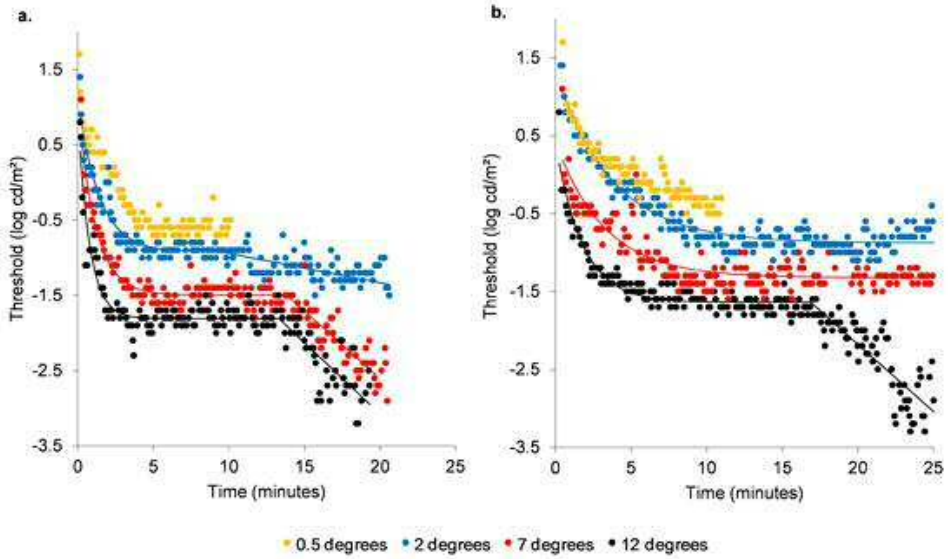

Figure 1.12. Dark adaptation functions in response to stimulus size for a typical healthy control (a) and in early AMD (b). For each stimulus size the raw data is shown with a best fitting model. To aid visualisation, the 12° data is correctly placed with regards to the y-axis however all other data have been displaced upwards. The 7 degree data has been displaced upwards by 0.3 log units from the 12 degree data, the 2 degree data has been displaced upwards by 0.3 log units from the 7 degree data and the 0.5 degree data has been displaced upwards by 0.3 log units from the 2 degree data (Gaffney et al., 2011; copyright permission from Wolters Kluwer Health [2018] licence 4274220230945).

The recovery of visual sensitivity in the dark is dependent on the regeneration of visual pigment via the retinoid cycle (Rushton and Campbell, 1954; Lamb and Pugh, 2004). This cycle is reliant on the integrity of the RPE and photoreceptors, and is supported by the choroidal circulation, via Bruch's membrane. Therefore pathology, such as AMD, that disrupts the outer retina and associated structures has been found to cause

prolonged dark adaptation in rods and cones (Eisner et al., 1991; Midena et al., 1997; Phipps et al., 2003; Dimitrov et al., 2008; 2011; Gaffney et al., 2011; Jackson et al., 2014a; Owsley et al., 2001; 2007; 2016; 2017). Rod-mediated parameters of dark adaptation, such as time to RCB and rod recovery rate, have been consistently found to be delayed in early AMD (Owsley et al., 2001; 2016; Dimitrov et al., 2008; Jackson and Edwards, 2008). Rod-mediated dark adaptation has also been found to be delayed over a 2 year period in those with intermediate AMD (Owsley et al., 2017).

Accurate measurement of the threshold changes that occur during the rapid initial stages of cone dark adaptation has been found to be a difficult process. Consequently initial evidence, recorded at 12° retinal eccentricity by Owsley et al. (2001), documented disturbances in rod mediated dark adaptation only in early AMD. Since this, studies by Dimitrov et al. (2008, 2011) and Gaffney et al. (2011, 2013), utilising larger visual stimuli and longer bleach durations, have provided compelling evidence that cone recovery dynamics in dark adaptation are also significantly impaired in AMD and can be used as a powerful diagnostic tool. This correlates with the histological findings of cone synapse irregularity, alongside loss of rods, in early AMD (Pow and Sullivan, 2007; Shelley et al., 2009). It may also reflect the underlying diffuse pathology of the RPE, Bruch's membrane and choroidal circulation in AMD, which will affect regeneration of both rod and cone photopigments.

When compared to a battery of other dynamic and steady state threshold tests by Dimitrov et al. (2011), the recovery parameters of dark adaptation were found to have excellent diagnostic capacity. Assessment using receiver operating characteristic (ROC) area under curve (AUC) analysis showed rod and cone recovery yielded 0.93 ± 0.016 and 0.86 ± 0.023 respectively using a 2° stimulus at 3.5° eccentricity in the inferior field. Quantitatively, the dark adaptation parameters of rod and cone rate of recovery were found to detect 86% and 62% of abnormal cases, respectively, when compared to 14Hz flicker threshold (34%), cone photostress recovery time (64%) and

blue colour contrast threshold (41%) (Dimitrov et al., 2011). Despite the potential displayed as an effective diagnostic tool for early AMD, dark adaptation has not generally been considered as a clinically viable technique. However, issues such as test duration and patient friendliness are currently being addressed. Promising results suggest accurate measurement of photoreceptor recovery parameters are possible within a 10 minute time frame (Gaffney et al., 2011; Jackson et al., 2014b) and that dark adaptation may be used as a suitable functional end point when evaluating treatments for early (Jackson et al., 2014b; Owsley et al., 2016) and intermediate AMD (Owsley et al., 2017). Recent longitudinal analysis of those graded 1 (normal) on the Age-Related Eye Disease Study System (AREDS, 2001b) showed that those with delayed rod-mediated DA at baseline were twice as likely to have AMD after 3 years when compared to those with normal DA (Owsley et al., 2016). This finding further supports the usefulness of this visual functional measure as a biomarker for early AMD.

1.3.6.6. Functional biomarkers for AMD

Biological markers (biomarkers) can serve many unique purposes, including confirmation of diagnosis, monitoring treatment effects or disease progression, and prediction of clinical outcomes (Biomarkers Definitions Working Group, 2001). The theoretical advantage of using validated biomarker outcomes in definitive trials includes smaller, faster and less expensive studies (Holloway and Dick, 2002). For this reason, structural and functional biomarkers are often adopted in research as primary endpoints for clinical trials (Law and Miles, 2013; Moyer and Barrett, 2009; Lesko and Atkinson, 2001). A high level of stringency is required when a biomarker response is substituted for a clinical outcome. The scientific program for evaluating biomarkers must be planned as early as possible with a blueprint to bring the biomarker into clinical trials and establish the link between the biomarker and clinical outcome (Fleming and DeMets, 1996). Evaluation of a biomarker can be based on an

exploratory process of determining how many of the characteristics of an ideal biomarker are met relative to the context of its use. Characteristics of biomarkers that underpin their utility include: clinical relevance, sensitivity, specificity, reliability and practicality (Lesko and Atkinson, 2001). There are multiple pathways to validate a biomarker for an intended use. Validation data itself often rises from the totality of evidence provided by preclinical animal studies and longitudinal analysis including clinical studies in healthy volunteers and late-phase efficacy/safety trials in patients with a targeted disease (Lesko and Atkinson, 2001; Fleming and DeMets, 1996).

Visual loss in AMD occurs due to the dysfunction and death of photoreceptors (rods and cones) secondary to the death or dysfunction of RPE cells, or a neovascular event (Ambati and Fowler, 2012). Therefore, psychophysical tests of vision, which depend on the functional status of the photoreceptors, RPE and associated structures, may detect subtle alterations in the macula before morphological fundus changes become visibly apparent. They also have the potential to not only identify those with early AMD but to also act as prognostic biomarkers for disease progression.

A number of visual function tests have been investigated in order to determine a potential biomarker for AMD. Three promising candidates (chromatic sensitivity, dark adaptation and flicker sensitivity) have been used throughout this thesis. As briefly mentioned in Sections 1.3.6.3 (colour vision), 1.3.6.4 (flicker sensitivity) and 1.3.6.5 (dark adaptation) each of these visual function tests has a body of evidence to support their relationship with disease severity and as such their usefulness as a biomarker for AMD progression. Whilst these visual function tests have been identified as functional biomarker candidates, further validation of their capability as surrogate biomarkers, as achieved through longitudinal evaluation, is still necessary.

Early AMD develops very slowly over time (Davis et al., 2005) and, therefore, it is not practicable to use end stage disease as an outcome measure in phase I/II trials of new interventions. Hence, the use of validated functional biomarkers is imperative for

the development of modern treatment strategies for early AMD. This necessitates the identification of biomarkers that may be used as surrogate outcome measures in clinical trials such as that presented in this thesis. For greater detail on AMD biomarkers and biomarker validation the reader is directed to the review articles by Lambert et al. (2016) and Lesko and Atkinson (2001).

1.4. Visual psychophysics

Psychophysics is the scientific study of the relation between stimulus and sensation (Gescheider, 1997). Its relevance to this study is paramount as many of the data collection techniques used are based on psychophysical methods. These methods rely upon the concept of threshold testing and are introduced in this section.

1.4.1. Classical psychophysical methods

Visual psychophysics commonly relies upon the presentation and detection of a stimulus. The stimulus can be manipulated in order to investigate various visual perception thresholds however in all cases it must exceed a critical strength, known as a sensory threshold, before a subject can be aware of its presence (Graham, 1965). There are two kinds of thresholds: absolute and difference. The lowest level of stimulus energy for which detection is achievable is known as the ‘absolute threshold’ (Gescheider, 1997). When discriminating between stimuli, the ‘difference threshold’ is the magnitude of the smallest detectable difference (also known as a ‘just noticeable difference’) between two stimuli (Gescheider, 1997).

There are three documented classical psychophysical methods of threshold testing:

1. The method of adjustment.
2. The method of limits.
3. The method of constant stimuli.

In order to determine a threshold using the method of adjustment or the method of limits an observer is asked to respond to a series of ascending (stimulus going from

non-seen to seen) and descending (stimulus going from seen to non-seen) steps. The threshold is ultimately obtained from the averaged value of responses (Kalloniatis and Luu, 2013). Even though threshold determination is similar the methods differ in that during the method of adjustment the observer is given the responsibility of controlling the stimulus level. The method of constant stimuli does not employ a sequential series of presentations. Instead, the stimulus is presented multiple times at each intensity, in a random order to the observer (Norton et al., 2002). The responses are then used to create a psychometric function which plots the probability of a correct response at a range of stimulus intensities in order to determine the threshold (Figure 1.13) (Kalloniatis and Luu, 2013).

During visual psychophysics, detection of a stimulus is often confirmed via a subjective response. However, the variability in response patterns found between participants can lead to the determination of inaccurate threshold levels (Gescheider, 1997). In order to counteract this effect stimuli are often presented repeatedly at each intensity and threshold levels are determined in probabilistic terms via a psychometric function.

The repetitive and time consuming nature of performing consecutive trials also leads to habituation and anticipation errors. Particularly when performing the method of limits habituation errors occur when a subject becomes accustomed to reporting that they perceive a stimulus. As a result they may continue reporting the same way even beyond threshold (Norton et al., 2002). Alternately when performing the method of adjustment a subject may anticipate that a stimulus is about to become detectable or undetectable and make a premature judgement. These errors can be minimised by preventing a sequential series or presentation as with the method of constant stimuli (Gescheider, 1997).

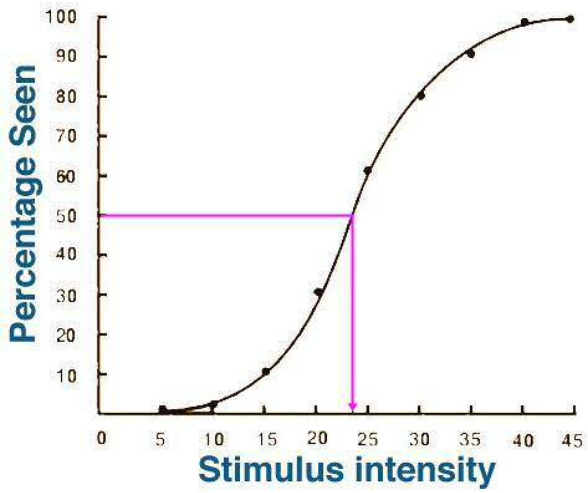

Figure 1.13. A psychometric function. Threshold is often taken as the stimulus intensity at which detection occurs for 50% of the presentations (Kalloniatis and Luu, 2013; copyright permission from http://webvision.med.utah.edu/).

1.4.2. Adaptive psychophysical methods

Adaptive psychophysical methods are widely regarded as more efficient than classical methods. This is because in adaptive methods stimuli presented are based on the observer's previous responses. This maximises the presentation of stimuli around the threshold value of the parameter of interest and minimises the time spent collecting data at points on the psychometric function that provide little information (Kalloniatis and Luu, 2013). Adaptive methods are classified into staircase and maximum-likelihood procedures, a summary of both has been provided here.

1.4.2.1. Staircase procedure

The staircase procedure can be considered as a modification of the method of limits (Cornsweet, 1962). A staircase procedure will usually begin with an easily detectable, high intensity stimulus. The stimulus intensity is then decreased in the initial series until the observer is no longer able to detect it, at which point, the presentations are reversed and the stimulus intensity is increased until the observer once again indicates their perception of the stimulus, which marks the completion of the second series. With each passing series the stimuli presented start progressively closer to the threshold value. To determine the final threshold an average of the reversal values

is taken. Before a staircase procedure can be implemented there must be clarity on such factors as the step-size of the stimulus testing level and the termination procedure.

It is common when performing a staircase procedure to use an ‘n up, 1 down’ paradigm. For example, if the observer makes a correct response ‘n’ times in a row then the testing level is reduced by 1 step-size. If the observer does not identify the stimulus correctly then the testing level is increased by ‘n’ step-sizes. A 1 up, 3 down paradigm was utilised to collect dark adaptation data throughout this trial.

1.4.2.2. Maximum likelihood procedures

During a maximum likelihood procedure the testing level presented is based on a statistical estimation of threshold derived from all of the observers’ previous responses. After each trial, a new threshold estimate is calculated in order to determine the new stimulus level to be presented. The number of trials is pre-determined and should be enough to allow a final threshold level to be reached. Statistically this technique relies upon the assumption that the underlying psychometric function of the parameter in question has a specific form, for example Gaussian (cumulative normal distribution), logistic or Weibull (Gescheider, 1997).

Before being able to perform a maximum-likelihood procedure prior knowledge of the distribution of threshold for a given stimulus must be known. This is often obtained through pilot studies or published data. From this data a probability distribution function (PDF) can be constructed which, in turn, allows the stimulus threshold that is most likely to correspond to the observer’s threshold to be determined. The PDF is modified according to the observer’s response to each stimulus presentation. This allows each subsequent presentation to be ever closer to the observer’s actual threshold until the stimulus intensity becomes stable. It is at this point that the final threshold is recorded. Procedures that utilise this method of threshold determination include ZEST (zippy estimate of sequential testing) and QUEST (quick estimate by

sequential testing). Although fundamentally similar these 2 methods differ in that the mean of the PDF is used to estimate stimulus intensity when performing ZEST (King-Smith et al., 1994), whereas the mode of the PDF is used when performing QUEST (Watson and Pelli 1983).

Throughout the course of this PhD temporal sensitivity data were measured using a QUEST Bayesian adaptive procedure. The QUEST psychometric method was developed by Watson and Pelli (1983) and relies upon the following assumptions:

- The psychometric function has the same shape under all conditions, when expressed as a function of log intensity.
- The subject's threshold does not vary from trial to trial.
- Individual trials are statistically independent.

QUEST relies upon Bayes' Theorum which can be used to combine the results of an experiment (in the form of the likelihood function) with pre-existing knowledge regarding the threshold parameter (in the form of a prior-probability distribution) to derive the probability distribution across possible values of the threshold parameter (Kingdom and Prins 2009). The use of prior knowledge regarding the threshold intensity when performing QUEST initially prevents excessive step-sizes into threshold intensities of little interest. As data collection proceeds however the prior knowledge plays a smaller and smaller role relative to the contribution of the data collected (Figure 1.14).

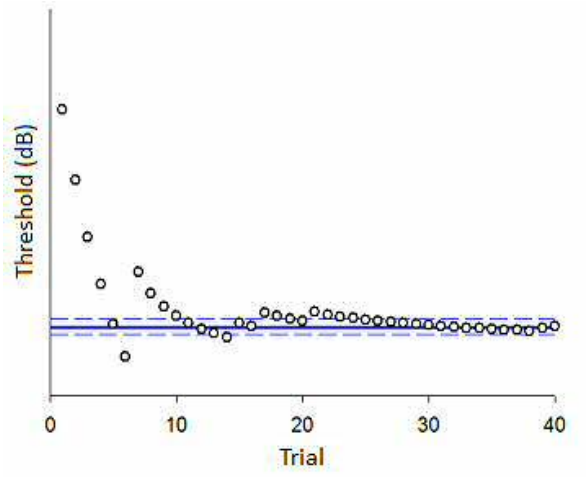

Figure 1.14. An example of data collected using the QUEST procedure. The circles represent successive stimuli (trials) presented to the observer. After each trial a new threshold estimate is calculated based upon previous responses. The final threshold level, after 40 trials, is represented by the solid blue line. The dashed lines display the standard deviation above and below the final threshold.

1.4.2.3. Forced-choice procedure

The forced-choice psychophysical method is based on the theory of signal detection (TSD). During this procedure the observer is forced to choose from alternative choices, one of which contains the stimulus. The exact procedure employed can be described by the number of alternative choices made available e.g. a procedure in which the observer chooses from 2 options is described as a 2-alternative forced choice procedure (2AFC). As the number of options available to the observer increases, the probability of a correct response due to chance alone declines (Gescheider, 1997). With every trial the stimulus alternatives are shown and the observer is required to select one stimuli as a response. The assumption can be made that in absence of response bias the observer chooses the option that contains the largest sensory stimulus (Gescheider, 1997). This results in the procedure being criterion-free. In order to determine the final threshold a psychometric function is often constructed. Figure 1.15 shows the psychometric function used for the colour assessment and diagnosis test used in this trial (4AFC procedure).

After any presentation the observer has at least a 25% chance of guessing correctly. This leads to a percentage of correct responses in which the observer did not in fact

detect the stimulus. The psychometric function allows the final threshold to be adjusted for chance in order to eliminate the effect of guessing. This is done by plotting the percentage of correct responses against the stimulus intensity and by selecting a value for percentage correctly identified to be designated as the threshold.

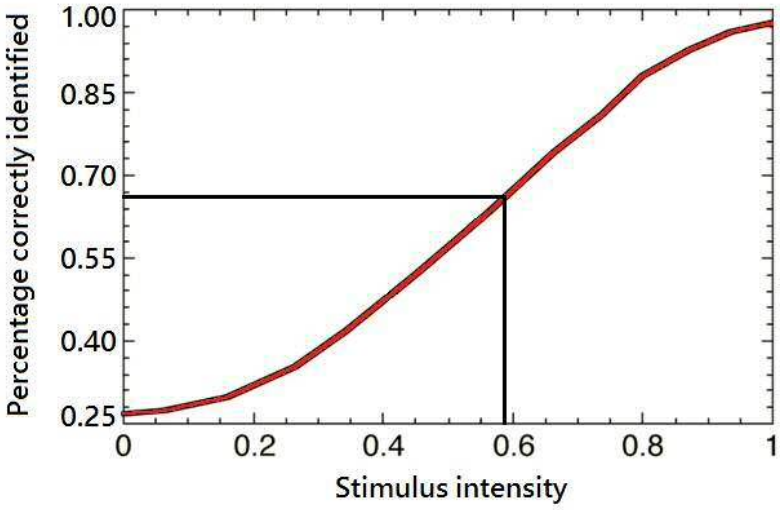

Figure 1.15. A psychometric function constructed from responses to a 4AFC procedure. In this example the final threshold value for this stimulus is recorded at the point where 66% of presentations were correctly identified.

1.5. PhD objectives

The overarching objectives of this PhD were:

1. To implement a longitudinal clinical trial (the ALight trial) in order to evaluate the impact of light therapy on the progression of early and intermediate AMD.
2. To carry out a simultaneous cross-sectional study alongside the longitudinal evaluation, in order to evaluate the trial outcome measures as biomarkers for AMD severity.

1.5.1. Pilot study aims

A further aim of this thesis was to perform 2 pilot studies to optimise and evaluate the psychophysical tests of visual function prior to recruitment for the ALight trial or cross sectional study. The specific aims of the pilot studies were:

1. To check the test sequence and time of the data collection techniques.

2. To verify that a new handheld photopigment bleach source could be used reliably in a dark adaptation experiment.
3. To optimise parameters of dark adaptation, flicker threshold and chromatic threshold measurement for use in the ALight clinical trial and cross-sectional study.

1.5.2. Cross-sectional study aims

A simultaneous cross-sectional study was conducted alongside the ALight clinical trial. The primary aim of this study was to evaluate the ability of dark adaptation, 14Hz flicker threshold, YB chromatic threshold and RG chromatic threshold tests to identify the likely risk of an increase in graded AMD severity (Chapter 4). The study also had two secondary aims:

1. To explore the relationship between the functional and structural outcome measures.
2. To determine the relationship between disease severity and the observed functional and structural deficits.

1.5.3. Longitudinal clinical trial (the ALight trial) aims

The primary aim of the ALight trial was to collect preliminary phase I/IIa proof of concept randomised controlled trial data from people with early or intermediate AMD in one eye and advanced nAMD in the fellow eye, in order to assess the effect of low-level night-time light therapy, compared with no intervention, on disease progression in the eye with early/intermediate AMD (Chapter 6).

An additional primary outcome measure was to assess the safety and tolerance of a CE marked device to deliver the light therapy (Noctura 500 light mask) within the cohort of participants with AMD (Chapter 5).

The secondary aims of the ALight trial (assessed in Chapters 5 and 6) were as follows:

1. To establish the effect of low-level night-time light therapy when compared to controls on:

i. The change in drusen volume over 12 months (measured using OCT software).
ii. The number of ranibizumab injections required on the fellow eye over 12 months.
iii. The change in visual function using the CAD test, BCVA and 14Hz flicker threshold.
iv. The change in self-reported quality of life (EuroQol-5D [EQ-5D]) (EuroQol Group, 1990) and visual function (VFQ-48 [Stelmack et al., 2004a; 2004b]).

2. To establish the acceptability of low-level night-time light therapy in those with AMD by monthly qualitative interviews.
3. To determine the effect of the light therapy on sleep patterns for those using the light mask intervention.
4. To evaluate the ability of all clinical tests to act as prognostic biomarkers for AMD progression.
5. To evaluate the ability of all clinical tests to act as predictive biomarkers for the effectiveness of low-level night-time light therapy in AMD.
6. To compare the sensitivity of all clinical tests to disease progression over 12 months.

1.6. Conclusion

Throughout the course of this chapter it has been stated that the causes of AMD are not yet fully understood but hypoxia may play a role. The ALight trial itself aims to reduce the level of hypoxia at night by exposing the eye to a dim light. In order to further evaluate the role of hypoxia in the pathogenesis of AMD a systematic review of literature is presented in the next chapter.

Chapter 2. Evaluating the role of hypoxia in the pathogenesis of AMD: a literature review

2.1. Introduction

The aetiology of AMD is multifactoral. There is evidence to suggest that hypoxia, oxidative stress, inflammation, mitochondrial disease and genetics are involved (Feigl, 2009; Stefansson et al., 2011; Ding et al., 2009; Coleman et al., 2008; 2013; Haines et al., 2005; Jarrett et al., 2008; Lin et al., 2011). The degree to which each factor contributes to AMD pathogenesis is unknown. Whilst all of these mechanisms may have a role in AMD this review examines the literature on hypoxia because any beneficial effects of low-level light therapy are likely to stem from increased tissue oxygenation.

Having one of the highest metabolic demands of any bodily tissue, the retina is particularly susceptible to the effect of hypoxia (Wangsa-Wirawan and Linsenmeier, 2003; Beatty et al., 2000). Hypoxia is defined as a decrease in available oxygen reaching the tissues of the body. The fact that humans thrive under varying environmental conditions, including at high altitude, dictates that it is possible for human beings to adapt to live under conditions of reduced oxygen tension (Moore et al., 1998; West, 2004). However, when human tissue oxygenation drops below 3-5% it is considered to be in a hypoxic state (Semenza, 2012) and as such may encourage damage at a cellular level.

As introduced in Section 1.1.2, using microelectrodes to measure the in vivo O_2 profile of the macaque retina shows that when the retina is dark adapted, the PO_2 level in the outer retina is low and approaches 0mmHg at the proximal side of the photoreceptor inner segments (Wangsa-Wirawan and Linsemeier, 2003). The increased oxygen demand displayed by the photoreceptors under scotopic conditions is attributable to the high metabolic demand of the ‘dark current’ in the approximately

92 million rods (Hagins et al., 1989; Arden et al., 2011). Oxygen profiles within this environment suggest that there is little O_2 reserve at the photoreceptor level. Therefore anatomical changes observed in AMD, such as increased thickening of Bruchs membrane (Chen et al., 1992; Schlingemann, 2004; Booij et al., 2010) and choroidal haemodynamic dysfunction (Pauleikhoff et al., 1999; Stefánsson et al., 2011), have the potential to impede the flow of oxygen to the outer retina and disrupt the fragile balance between metabolic demand and oxygenation still further, especially under dark adapted conditions. The physiological knife-edge of retinal oxygenation is exemplified, functionally, by the finding that dark adaptation in normals is incomplete at modestly reduced air pressures (McFarland and Evans, 1939), and by the adverse effects of hypoxia on colour vision (Karakucuk et al., 2004; Connolly et al., 2008; Vingrys and Garner, 1989), dark adaptation (Connolly and Hosking., 2006; Karakucuk et al., 2004; Vingrys and Garner, 1987; Brinchmann-Hansen and Myhre, 1989), mesopic sensitivity (Connolly and Hosking, 2009), and the electroretinogram (ERG) (Feigl et al., 2007; Tinjust et al., 2002; Feigl et al., 2008; Pavlidis et al., 2005; Schatz et al., 2014).

A number of hypotheses have been put forward regarding the relationship between hypoxia and the numerous metabolic and physical changes that manifest during AMD. These include that:

- Thickening of Bruch's membrane leads to hypoxia due to the increased distance over which oxygen must travel to diffuse from the choriocapillaris to the RPE complex (Chen et al., 1992; Schlingemann, 2004).
- Mechanical changes to the choroidal vasculature as a result of scleral rigidity and vitreoretinal adhesion lead to an increased vascular resistance within the short posterior ciliary arteries resulting in hypoxia (Friedman et al., 1995; Stefánsson et al., 2011).

- Reduced perfusion of the choroid leads to hypoxia, activation of molecular sensors and CNVM formation (Grundwald et al., 2005; Metelitsina et al., 2008; Mendrinos and Pournaras, 2009).
- Chronic inflammation leads to an increased retinal metabolic demand and exacerbates hypoxia (Arjamma et al., 2009).
- Interactions between hypoxia, oxidative stress and autophagy lead to impairment of RPE function (Blasiak et al., 2014).

However, it is still unclear if hypoxia is an initiating factor in AMD pathogenesis or a secondary product of the condition's development. To address this, the primary objective of this systematic review is to evaluate the literature regarding the role of hypoxia in the pathogenesis of AMD. A further aim is to identify any gaps in the current evidence base.

2.2. Literature review methods

The following eligibility criteria were used to determine which studies were included and which were excluded:

1. Studies had to specify AMD as a pathology considered and could investigate any form or stage of AMD.
2. Studies had to specify hypoxia or ischaemia in relation to the pathogenesis of AMD.
3. Studies could be of any design and could include human and/or animal models.
4. Studies had to be reported in the English language.
5. Studies had to be reported as full text articles. Conference abstracts were excluded.

2.2.1. Literature searching methods

In June 2017 a comprehensive literature search was undertaken of the following databases; Web of science (1900-June 2017), Embase (1947-June 2017), Ovid Medline (1946- June 2017).

The search terms were defined by AMD synonyms and the area of interest as displayed in Table 2.1. The use of an asterisk denotes that all variants of the word were searched for, i.e. hypoxia and hypoxic.

Table 2.1. Search terms used in order to find appropriate studies for inclusion within the review.

Age-related macular degeneration **OR** Age-related maculopathy **OR** Senile macular degeneration **OR** ARMD **OR** AMD	**AND**	Hypox* **OR** Ischaem* **OR** Ischem*

The reference lists of all included studies were hand searched along with selected relevant reviews (Feigl, 2009; Stefánsson et al., 2011; Arjamaa et al., 2009) to ensure that no applicable studies were overlooked. Once search results had been compiled, all titles and abstracts were read to evaluate the eligibility of each study for inclusion in the review. Relevant references identified from each of the databases were amalgamated and duplicate papers were removed. Full manuscripts were obtained and read for all studies that appeared to satisfy the inclusion criteria on first evaluation. Any studies which failed to meet the eligibility criteria on reading the full manuscript were excluded at this stage. The relevant data for each study were summarised in a data extraction table. This formed the basis of the table of included studies (see Appendix I).

Studies of any design were included in the review. No formal evaluation of the quality of included studies was carried out as the nature of the research question meant that a wide range of evidence was included, including basic science and animal studies, as well as studies including human participants. However, the text highlights the largest and/or most robust studies. Any particular issues with study design are also highlighted in the text. Furthermore, in the table of included studies, the study design is described and the identified limitations in each study are stated. No meta-analysis was carried out because of the diverse outcome measures incorporated by studies included in the review. Studies included in the review have been categorised into those that present 'direct evidence' and those that present 'indirect evidence' relating to the role of hypoxia in AMD pathogenesis.

2.3. Results

The results of the database search are summarised in Figure 2.1. After reading the titles and abstracts of 1527 articles identified by the literature searching strategy 53 appeared to meet the inclusion/exclusion criteria. All of these were confirmed as being relevant to the eligibility criteria after evaluating the full text, however only 52 were included as 2 studies reported the same data in 2 separate articles. Figure 2.2 shows the design of the 52 studies included within the review. The majority of studies were case-control to allow comparisons between those with AMD and healthy controls. All retrospective studies were based on haemodynamics as measured by fluorescein and indocyanine green angiography. All in vitro models used human or animal cells.

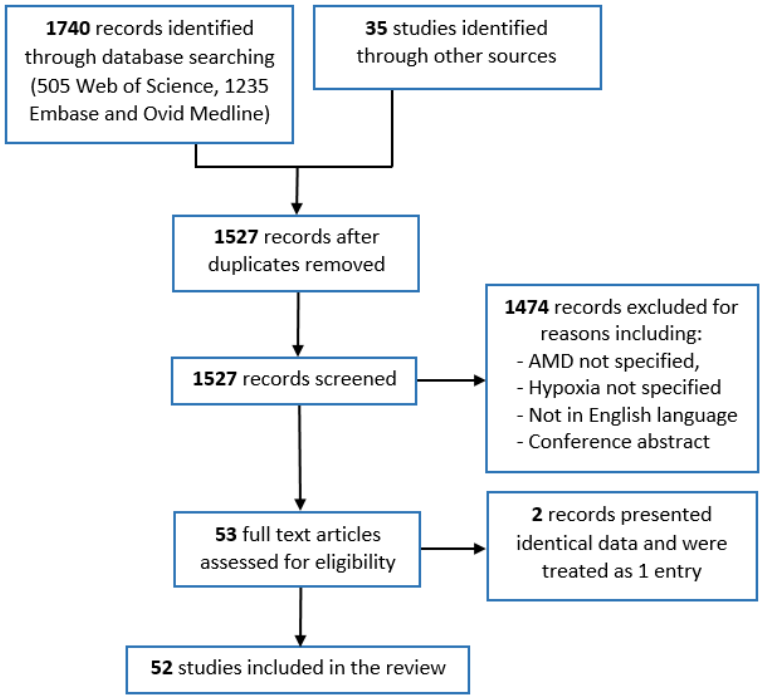

Figure 2.1. Preferred Reporting Items for Systematic Reviews and Meta-Analyses (PRISMA) flow diagram of the study identification pathway (Moher et al., 2009).

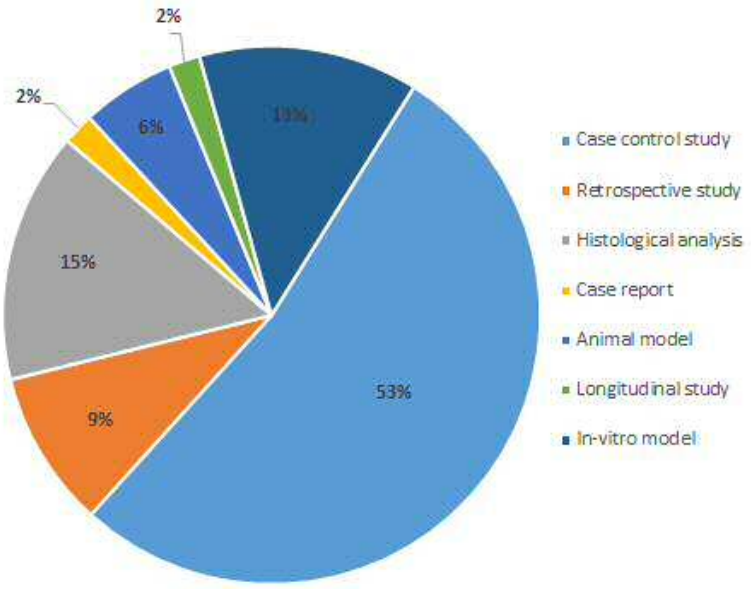

Figure 2.2. Breakdown of study design of studies included within the review.

2.3.1. Direct evidence of hypoxia in AMD

There is limited direct evidence of the role of hypoxia in the pathogenesis of AMD. The evidence which is available relates to the presence of HIF in the retina of individuals with AMD (Kvanta et al., 1996; Lopez et al., 1996; Sheridan et al., 2009;

Inoue et al., 2007). HIF is a transcription factor that responds to decreases in available oxygen in the cellular environment, or hypoxia. An additional 12 studies (6 animal models, 6 in vitro models) demonstrated evidence suggesting changes associated with AMD pathogenesis such as the upregulation of VEGF (Young et al., 2005; Lima Silva et al., 2007; Aiello et al., 1995; Iwase et al., 2013; Nishijima et al., 2007; Kurihara et al., 2016; Nakajima et al., 2013; Fuchshofer et al., 2009; Mousa et al., 1999; Coassin et al., 2010; Fooroghian et al., 2007; Liu et al., 2000). No studies found provided direct evidence against hypoxia as a factor in the pathogenesis of AMD. The following paragraphs describe the studies in more detail.

2.3.1.1. Relationship between hypoxia, HIF and VEGF in the retina

Hypoxia inducible factor has been identified as the master transcription factor responsible for mediating cellular activity in response to reduced oxygen. The dysregulation and overexpression of HIF-1 has been heavily implicated in the area of cancer biology, particularly in relation to angiogenesis (see review articles by Shi and Fang, 2004 and Wykoff et al., 2001). As HIF upregulation is a known indicator of hypoxia it is also of interest when discussing AMD pathophysiology. HIF isoforms (HIF-1α, HIF-2α and HIF-3α) are constantly produced under normoxic conditions but are short lived due to the natural process of hydroxylation via prolyl hydroxylase domain (PHD) proteins (Caprara and Grimm, 2012). When not under hypoxic strain, HIF-1α is tagged for degradation by the von Hippel-Lindau (VHL) protein and functionally obstructed by Factor-Inhibiting HIF (FIH) (Ohh et al., 2000; Mahon et al., 2001). When oxygen demand outweighs its availability the effectiveness of PHD, VHL and FIH are reduced, resulting in the accumulation of HIF-1α. The HIF-1α is translocated into the nucleus where it binds to HIF-1β and a co-activating protein (CBP/p300) at the hypoxia response element (HRE) (Caprara and Grimm, 2012). Following this, transcriptional activation of target genes can be initiated (Figure 2.3).

Within the retina the achievement of HIF stabilisation may also be dependent on the chaperone properties of heat shock protein 90 (HSP90) which, when blocked, results in reduced HIF-1α levels (Wu et al., 2007).

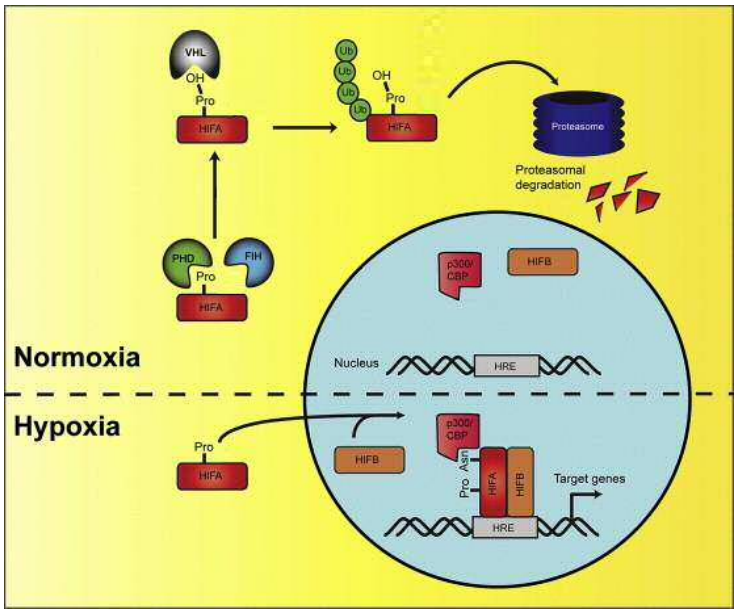

Figure 2.3. Schematic illustrating the activity of HIF-1α (HIFA) under normoxic and hypoxic conditions. Under normoxia after being functionally obstructed by Factor Inhibiting HIF (FIH) and tagged by Prolyl-4-hydroxylase (PHD) HIF-1α undergoes proteasomal degredation (Pro) and binds to the Von-Hippel Lindau (VHL). It then becomes polyubiquitylated (Ub) and targeted for proteosomal degradation. Under hypoxic conditions PHD activity is reduced, HIF-1α escapes hydroxylation and dimerises with HIF-1β (HIFB) and co-activating protein p300/CBP. Transcription of target genes then occurs at the hypoxia response element (HRE) (Caprara and Grimm, 2012; copyright permission from Elsevier [2018] licence 4274220739507).

At a retinal level HIF has been identified in both in vitro (Nakajima et al., 2013) and in vivo (Iwase et al., 2013) models of induced hypoxia. HIF-1 is known to induce transcription of more than 60 genes of varying function including angiogiogenesis and erythropoiesis, both of which assist the oxygenation of hypoxic areas. The HIF mediated signal protein responsible for new vessel growth is referred to as VEGF. Increased VEGF levels have been found in the presence of upregulated HIF-1α (Liu et al., 2000; Fooroghian et al., 2007) and HIF-2α (Sheridan et al., 2009). In addition to the stimulation of angiogenesis, VEGF has been found to play an active role in the maintenance of choroidal vasculature and neuroprotection of the retina (Nishijima et al., 2007). Therefore, it can be found at a background level within the retina even under normoxic conditions.

A strong relationship has been found between the induction of hypoxia and the resultant up-regulation of VEGF. Coassin et al. (2010) documented an 84% VEGF rise within cultured human RPE cells under a hypoxic (1% O_2) environment when compared to normoxia. This finding is consistent with that of Wu et al. (2007) who found a 3.4 fold rise in VEGF levels and Mousa et al. (1999) who documented a doubling of VEGF levels under similar hypoxic conditions. As VEGF increases in a time dependent manner the difference in levels of upregulation between each study is likely to be due to differences in time of RPE exposure to hypoxia (Mousa et al., 1999). In vitro animal studies also provide evidence of hypoxia induced VEGF up-regulation. Increased VEGF expression as a result of exposing cultured RPE cells to a hypoxic environment has been documented in rat (Young et al., 2005), mouse (Lima Silva et al., 2007; Kurihara et al., 2016) and bovine (Aiello et al., 1995) models. The relationship between HIF activity and VEGF production is further strengthened by the finding that the use of a HIF antagonist (doxorubicin) results in significantly reduced VEGF levels when compared to controls in mouse and rabbit models of stimulated choroidal neovascularisation (Iwase et al., 2013). Similarly, the use of a HIF antagonist results in longer VEGF restriction than the use of an anti-VEGF agent (Iwase et al., 2013).

2.3.1.2. Evidence of hypoxia mediated choroidal neovascularisation in AMD

Direct evidence of HIF-mediated, VEGF-induced angiogenesis can be found in-situ when analysing the components of CNVMs after surgical removal from nAMD patients (Kvanta et al., 1996; Lopez et al., 1996; Sheridan et al., 2009). Sheridan et al. (2009) analysed 9 CNVMs obtained from nAMD patients and found HIF-1α in 56% and HIF-2α in 89% of samples assessed. Both isoforms were most abundant in the outer retina which can be expected taking into account the location's dependence on oxygenation from the choroid. HIF-1α was localised within the RPE of 55% of samples analysed,

suggesting RPE hypoxia at some stage during nAMD pathogenesis. Inoue et al. (2007) also found evidence of HIF in 5 of 6 surgically removed CNVMs analysed. Although no HIF presence was found directly at the RPE level, both isoforms were detected in neighbouring macrophage and endothelial cells. In addition to VEGF, HIF has been linked to the transcription of other proteins found within the CNVM, such as connective tissue growth factor (CTGF) and plasminogen activator inhibitor-1 (PAI-1). As HIF-1 is known to induce the transcription of over 60 genes its capability to induce the transcription of targeted cells that not only lead to angiogenesis but also augment extra-cellular membrane deposit accumulation is currently under investigation (Fuchshofer et al., 2009).

2.4. Indirect evidence of hypoxia in AMD

Thirty-six studies provided indirect evidence of the role of hypoxia in the pathogenesis of AMD. The evidence which is available relates to changes to ocular structures affiliated with AMD pathogenesis, such as the choroid, Bruch's Membrane and RPE. The studies discussed in this section cover a wide range of study designs: 4 in vitro models, 1 longitudinal study, 1 case report, 1 histological analysis, 5 retrospective studies and 24 case control studies.

2.4.1. Choroidal blood flow volume and velocity

Given the evidence that the outer retina is principally oxygenated by the choroidal circulation (Wangsa-Wirawan and Linsenmeier, 1989; Ahmed et al., 1993), in addition to the evidence that the oxygen supply to the inner segments of the photoreceptors is barely sufficient to meet the demands of the dark adapted retina (Wangsa-Wirawan and Linsenmeier, 1989), it is logical to hypothesise that a deficiency in the haemodynamic profile of the choroidal circulation may result in outer retinal hypoxia.

Choroidal blood velocity in those with dry AMD was originally assessed using colour Doppler imaging by Ciulla et al. (1999). The peak systolic and end-diastolic blood velocity within the central retinal and posterior ciliary arteries of 25 patients with

drusen >63μm in diameter, RPE pigmentary changes or GA was compared to those without the disease. The flow velocity within the posterior ciliary arteries leading into the choroidal supply was found to be reduced in the presence of AMD. This finding was substantiated in another study via measurements of ocular surface temperature (OST) which is a method that provides an indirect assessment of blood perfusion below a structure (Sodi et al., 2014). When measured at three anterior ocular locations, the OST was lower in those with a range of AMD severities (n=142) than age-matched controls suggesting a potential underlying choroidal blood flow decrease beneath the sclera.

The reduction in choroidal blood volume and flow has been found to be proportional to disease severity in both advanced AMD subtypes (Grundwald et al., 2005; Metelitsina et al., 2008; Boltz et al., 2010; Berenberg et al., 2012; Chen et al., 2001) and has been associated with a risk of vision loss through disease progression (Piguet et al., 1992). One study that measured blood flow in the major retinal arteries as opposed to the choroid reported no significant difference between blood velocity or flow in healthy controls and those with AMD (Sato et al., 2006). In contrast, the opposite finding was reported by all other LDF studies, which reported choroidal (Grundwald et al., 2005; Metelitsina et al., 2008; Boltz et al., 2010, Berenberg et al., 2012) and ophthalmic artery (Üretmen et al., 2003) haemodynamic measurements.

Following the eventual emergence of a CNVM an increase in blood flow is measurable due to the filling of new vasculature (Pournaras et al., 2006). However, this is a temporary event. Due to fibrotic scarring as a result of new vessel leakage, the level of foveal blood velocity and flow eventually drops to a below-average level (Remsch et al., 2000; Chen et al,. 2001; Mori et al,. 2001).

Measurements of blood flow and volume indicate that hypoxia, if evident in AMD, may be a result of choroidal dysfunction (Grundwald et al., 2005). The finding of disturbed blood flow in both dry and nAMD subtypes further evidences this (Metelitsina et al.,

2008). Despite this, it is not possible to determine if the haemodynamic changes evidenced in AMD are unequivocally the only source of hypoxia. Other possible sources such as the structural changes that occur during AMD must also be considered.

2.4.2. Structural changes to the choroid

In addition to the evidence of changes in blood flow, the haemodynamic measurement of vascular resistance is also of interest when looking at the role of hypoxia in AMD pathogenesis. This measurement refers to the resistance that must be overcome to push blood through the circulatory system. Increased vascular resistance of the major temporal retinal arteries (as measured by resistivity index) has been documented in those with AMD (Sato et al., 2006). Similar results were found relating to the resistivity of the retrobulbar vessels as calculated from measurements of pulsatility and diastolic velocity (Friedman et al., 1995; Dimitrova et al., 2002). These results suggest that those with AMD have a more generalised circulatory abnormality proximal to the eye such as a stiffer, less compliant vasculature when compared to healthy age-matched normals. Such a haemodynamic change may be a result of sclerotic vessels trapped between an unyielding sclera one side and a stiff Bruch's membrane on the other. This in turn would cause a reduction of blood flow, the generation of a hypoxic environment and the presentation of drusen and other AMD clinical manifestations as demonstrated in Figure 2.4 (Friedman et al., 1989; Mullins et al., 2000; Pallikaris et al., 2006).

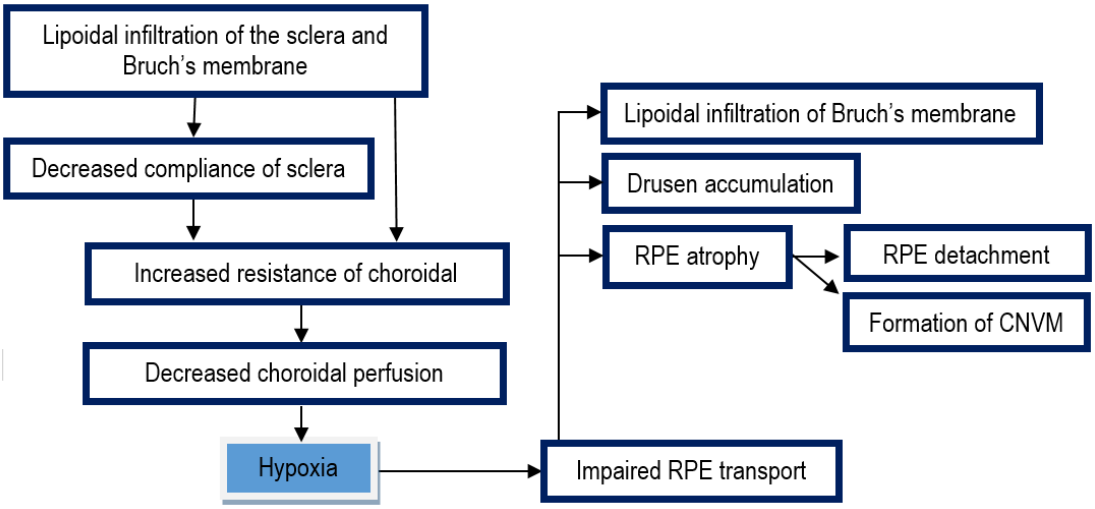

Figure 2.4. Proposed pathogenesis of AMD based on increased vessel rigidity. Retinal hypoxia caused by lipoidal infiltration with age or vascular disease disrupts RPE function leading to the propagation of Bruch's membrane thickening and RPE detachment or formation of a choroidal neovascular membrane (CNVM) (Friedman et al., 1989).

Histological analysis shows narrowed choriocapillary lumen found in those with early and established AMD when compared to controls (Kornzweig, 1977). Of the 31 AMD eyes reviewed by Kornzweig (1977), focal capillary atrophy was found in 59% and attributed to loss of cellular content and nuclei damage. Changes in choriocapillary density have also been found and are dependent on the stage of AMD, with early stages showing an increase (Spraul et al., 1996) and end-stages showing a reduction in density (Ramrattan et al., 1994; McLeod et al., 2009). This relationship is furthermore connected to RPE function. Regions of 100% RPE loss in people with geographic atrophy were found to be associated with a 51% mean decrease in vascular density, with the remaining 49% of functional vessels displaying lumen restriction (McLeod et al., 2002; 2009). Anatomically the use of high resolution ultrasound has identified Sattler's layer of the choroid as the site most susceptible to ischaemic damage in those with dry AMD. It has been postulated that damage to Sattler's layer at a cellular level is caused by vascular endothelial dysfunction or parasympathetic neuronal deterioration, however more research is required in order to substantiate this conclusion (Coleman et al., 2013).

2.4.3. Changes to choroidal blood flow perfusion

The use of videoangiograms has allowed proposed velocity and flow reduction of the choroidal vasculature to be visualised in relation to perfusion of blood throughout the macula. Anatomically, the choroidal blood supply originates from the posterior ciliary arteries and ultimately branches into segmented structures, each of which supplies one proportion of retinal tissue. Obstruction of a retrobulbar artery results in a periodic delay and incomplete filling of various areas of the choroid. Changes relating to AMD have shown preferential involvement of the perifoveal choroid (Ciulla et al., 2002). The locations most at risk of ischaemic insult are referred to as watershed zones, and represent the boundaries between regions supplied by different branches of the posterior ciliary arteries (Figure 2.5) (Hayreh and Baines, 1972).

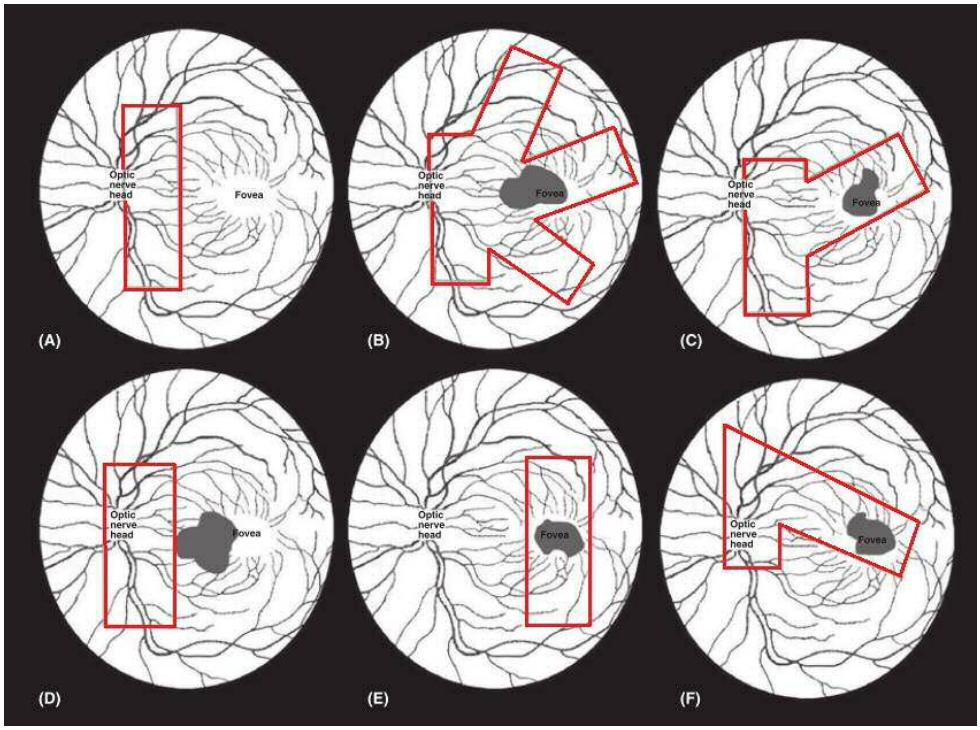

Figure 2.5. Schematic illustrations of different choroidal watershed zone (WZ) patterns and their relationships to neovascularisation in nAMD. Red lines denote the pattern of the WZ and dark grey areas represent neovascularisation. (A) Vertical pattern coursing through the optic nerve head (ONH) in a normal subject. (B) Stellate pattern WZ. (C) Vertical pattern coursing through the ONH and extending to the fovea. (D) Vertical pattern coursing through the ONH without foveal extension. (E) Vertical pattern coursing through the fovea. (F) Angled pattern of a WZ coursing through and adjacent to the ONH (Mendrinos and Pournaras. 2009; copyright permission from John Wiley and Sons [2018] licence 4274231455116).

Topographic analysis of the watershed zones shows that the boundaries between them often meet around the foveal region. As a result, the macula is deemed to be an area predisposed to chronic ischaemia (Mendrinos and Pournaras, 2009; Ross et al., 1998). The risk of ischaemia is compounded by the finding of delayed filling of the choroidal vessels in the presence of AMD (Melrose et al., 1987; Prünte and Niesel, 1988; Pauleikhoff et al., 1990b; Giovannini et al., 1994; Zhao et al., 1995). Such a delay results in poor perfusion of the macular tissue causing new vessel growth to be localised within the watershed zone boundaries in 70% of those with nAMD (Giovannini et al., 1994). Other pathological changes seen in AMD, such as the emergence of reticular pseudo-drusen and the formation of a CNVM, have also been associated with perfusion abnormality (Alten et al., 2013; 2016; Hartnett et al., 1996). In addition to neovascularisation, poor perfusion has been associated with localised areas of RPE atrophy and confluent drusen (Pauleikhoff et al., 1999). The degree of perfusion disruption is also proportional to the graded severity of drusen (Remulla et al., 1995; Staurenghi et al., 1992).

Figure 2.6 shows a potential mechanism of ischaemia-based AMD pathogenesis featuring impaired perfusion as a major contributing factor (Feigl, 2009). Reduced ocular blood flow is hypothesised to lead to impaired diffusion of factors necessary for the health of the choroidal circulation, which in turn exacerbates the existing choroidal perfusion abnormality. The resulting ischaemia is suggested to cause impaired RPE function leading to features such as increased deposition at the level of Bruch's membrane and the emergence of a CNVM (Feigl, 2009; Ciulla et al., 1999).

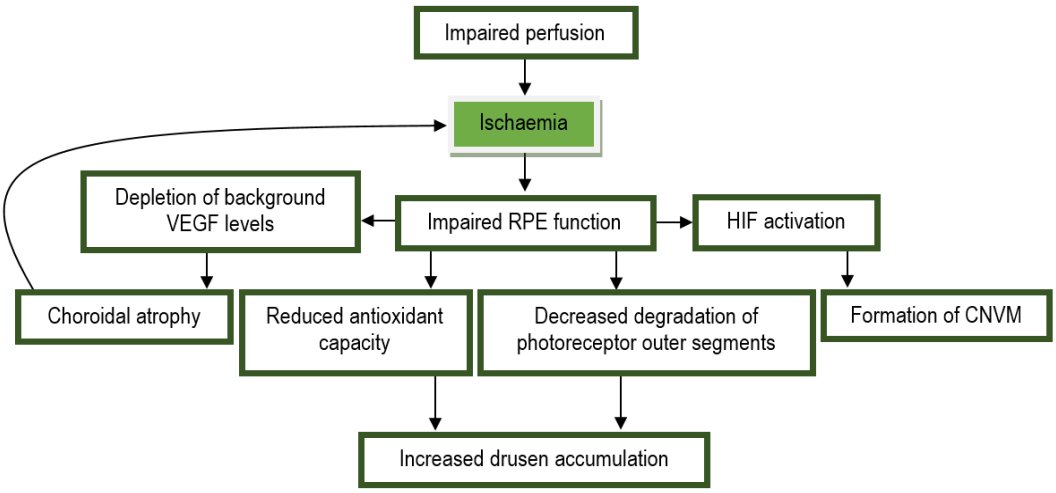

Figure 2.6. Proposed pathogenesis of AMD based on impaired perfusion leading to hypoxia. Adapted from the ischaemia hypothesis proposed by Feigl (2009). The initial cause of reduced ocular blood flow is not yet fully understood but has been proposed as increased resistance of choroidal vessels with age (Friedman et al., 1989).

2.4.4. Bruch's membrane and RPE dysfunction

Lipoid infiltration of Bruch's membrane is well documented in the process of normal ageing and is proposed to be exaggerated in the pathogenesis of AMD (Friedman, 1989). Such infiltration of Bruch's membrane is evidenced by thickening, degeneration of collagen, basal laminar deposition, drusen and calcification (Bird, 1992; Pauleikhoff et al., 1990a; Booij et al., 2010). The net result of such changes is an increase in distance between the retinal cells and choriocapillaris, via which aqueous based metabolites must diffuse (Schlingemann, 2004). This causes a lower oxygen tension at an outer retinal level in accordance with Fick's laws of diffusion, i.e. the rate of diffusion across a membrane is inversely proportional to the thickness of the membrane (Figure 2.7).

In addition, the transfer of metabolites across the RPE-Bruch's-membrane complex is further obstructed by a reduction in the hydraulic conductivity of Bruch's due to compositional change and the diffusion barrier caused by deposition of abnormal material (Chen et al., 1992; Booij et al., 2010). The spectrum of lipids infiltrating Bruch's membrane suggests that they originate, in part, from the phospholipids

derived from outer segment turnover. Their accumulation represents RPE inefficiency to remove retinal waste product (Booij et al., 2010).

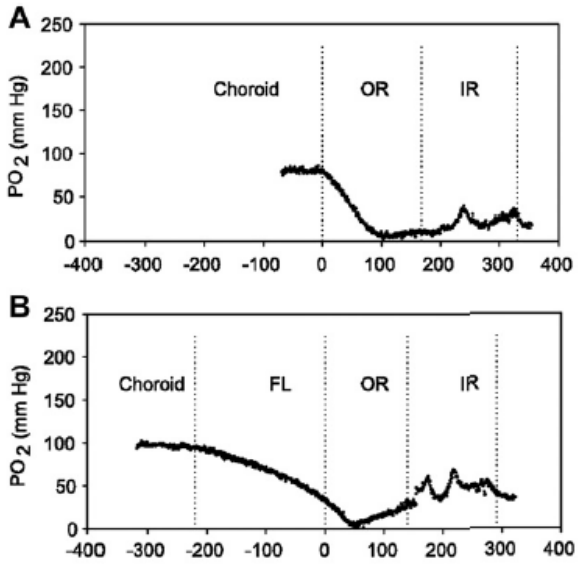

Figure 2.7. Examples of cat oxygen profiles collected at various retinal depths when breathing air. Increased distance between the choroid and retina can be seen to lower the oxygen tension at the outer retinal border as exhibited in the difference between (A) attached and (B) detached retina (IR: inner retina, OR: outer retina and FL: fluid layer under the retina) (Wang and Linsenmeier, 2007; copyright permission from ARVO).

Such RPE dysfunction and the resultant changes to the structure of Bruch's membrane are thought to contribute to choriocapillary degradation seen histologically in those with AMD. This degradation is attributed to a reduced level of RPE derived factors integral to vascular integrity reaching the choroid (McLeod et al., 2009; Spraul et al., 1996). The factors which have been shown to be affected include Basic fibroblast growth factor (bFGF), VEGF and endothelin-1 (McLeod et al., 2009). It is logical to suggest that a combination of increased RPE cell death and increased Bruch's membrane thickening as exhibited in AMD may both contribute to reduced RPE derived factors. This theory is supported by the finding of an increased venous oxygen saturation in end-stage AMD suggesting less oxygen extraction as a result of retinal cell death (Geirsdottir et al., 2014) and a reduction in large choroidal vein density in eyes with increased basil laminar deposit within the outer retina (Spraul et al., 1996; 1999). The resultant reduced level of blood flow within this region further

propagates the accumulation of cellular debris as a vicious circle develops between haemodynamic disruption, RPE dysfunction and the deposition of metabolic waste.

In addition to the impact on the choroid of RPE dysfunction, current evidence suggests that hypoxia-induced RPE metabolic stress results in a two-fold direct impact on RPE behaviour (Kurihara et al., 2016). Firstly, hypoxia alters RPE cellular activity resulting in changes in the rate of VEGF and metabolite secretion. Secondly, as opposed to oxidising glucose, the RPE cells commit to glycolysis upregulation in an attempt to gain energy at a faster rate. This allows the RPE cells to combat metabolic stress however doubles their glucose intake. As the RPE is the main supplier of glucose to the neurosensory retina this impacts photoreceptor function and survival (Kurihara et al., 2016).

2.4.5. Mitochondrial damage

The mitochondria are a vital intracellular organelle for retinal cell function and survival. Mitochondria are found at high densities within cells that are metabolically active, such as the RPE, where they perform roles including provision of chemical energy, regulation of programmed cell death and control of cellular metabolism. Mitochondrial dysfunction has been associated with theories of ageing (Druzhyna et al., 2008; Golden and Melov, 2001; Moosmann and Behl, 2008; Mandavilli et al., 2002; Weissman et al., 2007). Chronic dysfunction has also been associated with age-related macular degeneration (Blasiak and Szaflik, 2011; Jarrett et al., 2008; 2010; Lin et al., 2011; Karunadharma et al., 2010; Nordgaard et al., 2008). When studying the direct effect of hypoxia on mitochondrial structure, histological analysis shows that 90 minutes of acute ischaemia is enough to cause mitochondrial damage within both RPE and photopigment disc cells (Johnson and Foulds, 1978). Mitochondria exhibiting deoxyribonucleic acid (DNA) damage as a result of acute hypoxia also demonstrate reduced levels of ATP production which, in turn, is associated with RPE apoptosis (Bellot et al., 2001).

The precise mechanism by which hypoxia and mitochondrial dysfunction are associated is unclear. The oxidative stress hypothesis states that AMD pathogenesis occurs as a result of mitochondrial DNA damage incurred through the action of ROIs, the production of which has been shown to increase in acute ischaemia/reperfusion (Beatty et al., 2000). Although AMD is not an acute ischaemic condition, evidence suggests it involves a chronic vascular insufficiency such that similar mechanisms may apply (Feigl, 2009). A link between ROIs and HIF stabilisation has also been established during hypoxia and thus elevated ROI levels may act as a precursor to the activation of HIF transcription factors (Cash et al., 2007).

2.5. Discussion

The finding of HIF in the outer retina of those with AMD provides an indication that hypoxia is evident at some stage during pathogenesis (Kvanta et al., 1996; Lopez et al., 1996; Sheridan et al., 2009; Inoue et al., 2007). At present there is however a lack of further direct evidence to clarify whether hypoxia is a causative factor in the pathogenesis of AMD, or at what stage in the disease process it manifests. Measurements of perfusion pressure, oxygen tension and blood flow rate indicate that hypoxia, if evident, is likely a result of diminished choroidal blood circulation (Grundwald et al., 2005; Metelitsina et al., 2008). The consequence of such an impairment is poor perfusion, particularly throughout the macular region, which is a fragile area with a large oxygen demand.

The involvement of haemodynamic disruption as a source of hypoxia is further evidenced by:

- The fragile oxygen balance of the inner retina, in which even for a healthy retina the oxygen demand is only just met under dark adapted conditions (Wangsa-Wirawan and Linsenmeier, 2003).
- The positive correlation of reduced perfusion and AMD progression (Arjamaa et al., 2009).

- The finding of disturbed blood flow in both dry and nAMD subtypes (Metelitsina et al., 2008).

Although haemodynamic changes appear to contribute to the generation of a hypoxic environment it cannot be determined if these changes are unequivocally the only source of hypoxia. Increased thickening of Bruch's membrane, beyond that expected with normal ageing, causes a lower oxygen tension in the outer retina and may therefore provide another basis by which hypoxia could arise. In addition, lipid deposition and drusen formation cause further disruption to the transfer of metabolites between the choroid and the RPE which augments hypoxia long-term, for example by hindering the transport of RPE derived factors for maintaining the choroidal vasculature.

This review, through a systematic evaluation of the literature regarding hypoxia in the pathogenesis of AMD, has identified limited direct evidence through the emergence of HIF that hypoxia features within the pathogenesis of nAMD. Indirect evidence also supports hypoxic involvement in early AMD and GA. Due to the complexity of the pathogenesis it is not possible to determine whether hypoxia, if present, contributes as an initiating factor towards or emerges as a consequence of AMD pathogenesis. Furthermore, a number of the pathological traits evident in AMD have been associated with RPE dysfunction of which the relationship to hypoxia is still not clear. Such deficiencies in the literature have highlighted the need for more longitudinal human studies to characterise whether choroidal changes precede clinical signs of disease onset. In addition it would be useful to further investigate cellular indicators of hypoxia, particularly in relation to RPE dysfunction, in order to improve current understanding of the role of hypoxia in AMD pathogenesis.

It is also worth noting that all studies investigating HIF in relation to cultured human cells have focused on the RPE only. In accordance with the low oxygen tension when dark adapted (Wangsa-Wirawan and Linsenmeier, 2003) it is the inner retina as

opposed to the RPE that is of primary interest when investigating the effect of hypoxia on AMD pathogenesis. In order to further understand the role of hypoxia in AMD, deficiencies in the literature involving inner retinal HIF variation and level in response to light adaptation state need to be addressed. This would add to the rationale for studies which aim to manipulate the retinal oxygen level such as the ALight Clinical Trial for which the protocol is introduced in the next chapter.

Chapter 3. General methods and protocol development

Based on evidence to suggest that hypoxia plays a role in the pathogenesis of AMD the overarching objectives of this PhD were to evaluate the impact of light therapy on the progression of early and intermediate AMD, and to carry out a simultaneous cross-sectional study alongside the longitudinal evaluation, in order to evaluate the trial outcome measures as biomarkers for AMD severity.

This chapter begins with a section summarising the study design. The full trial protocol is not presented in this chapter, but is available in Appendix II, and has also been published (McKeague et al., 2014). The aims of the protocol development work described in the latter sections of this chapter were: (i) to optimise the original trial protocol in order to facilitate successful recruitment and data collection and (ii) to collect preliminary dark adaptation, flicker and chromatic threshold data from healthy control volunteers in order to assess the basic applicability of the techniques.

3.1. Overview of original protocol

The ALight trial was a Phase I/IIa proof-of-concept randomised controlled trial (RCT). To address the primary aim of the study (refer to Section 1.5 for a definitive list of trial objectives), 60 individuals with unilateral nAMD and early or intermediate AMD in the fellow eye were recruited from the Medical Retina unit of Bristol Eye Hospital (BEH). Participants were randomly allocated to receive either a light mask or no intervention (both groups continued to receive ranibizumab injections as required for the fellow eye). Safety was assessed through monitoring of progression rates to nAMD in the treated group, and through monitoring and reporting of adverse events (AE), serious adverse events (SAE) and adverse reactions (AR) relating to both eyes. This was done following a strictly defined protocol (McKeague et al., 2014). Figure 3.1 illustrates the patient pathway through the trial by means of a study flow diagram. The following sections will summarise the key features of the trial protocol.

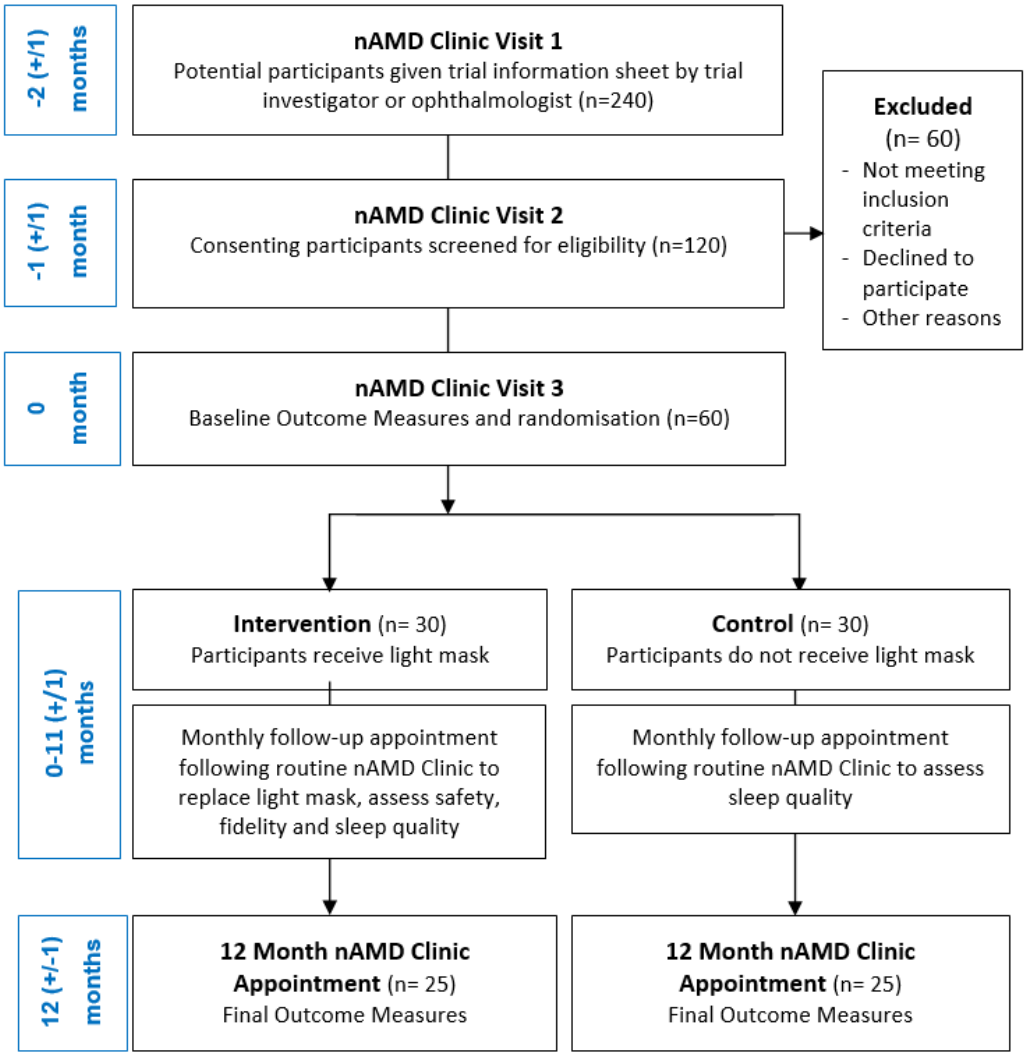

Figure 3.1. The participant pathway as displayed in flow diagram form (McKeague et al., 2014) The number of participants stated in each box represents the projected recruitment targets at the start of the trial.

3.1.1. Primary outcome measures

There were two co-primary outcome measures for the study - one a structural measure of disease progression based on retinal imaging, and one a measure of visual function:

i. The proportion of participants who showed disease progression in the eye with early/intermediate AMD. Disease progression was defined as the onset of advanced AMD or a 12 month increase in drusen volume beyond test-retest 95% confidence intervals.

ii. The change (baseline to 12 months) in the rate of cone dark adaptation (defined as the time constant of cone recovery [cone τ] after being exposed to a substantial photopigment bleach).

The introduction of SD-OCT has provided the opportunity to study drusen in greater detail (see Section 1.3.6.1). It was found by Yehoshua et al. (2011) that irrespective of initial drusen volume, approximately 50% of those with AMD show a significant increase in drusen volume over 12 months, i.e. beyond test-retest 95% confidence intervals. This finding makes disease progression based on an increase in drusen volume a useful outcome measure within a limited timeframe. Although the overall pattern is growth, some large drusen can shrink abruptly just before the onset of advanced disease. Therefore, we also considered conversion to nAMD as being an indicator of disease progression in the analysis. Data from a trial on a similar group indicated that about 10% of people meeting the inclusion criteria would develop advanced AMD within 12 months (Maguire et al., 2013). Hence, 60% of participants were expected to show progression based on increased drusen volume or progression to late AMD. It was felt that a clinically relevant reduction in this proportion would be 50% (i.e. from 60% to 30%). The development of advanced AMD was determined on the basis of ophthalmologist diagnosis at the monthly follow-up appointments within the nAMD clinic.

The rate of rod (Dimitrov et al., 2008; 2011; Owsley et al., 2001; 2007; 2016) and cone (Dimitrov et al., 2008; Gaffney et al., 2011; 2013; Jackson et al., 2014b) dark adaptation has been shown to be reduced in people with early AMD. Furthermore, longitudinal studies have shown that delayed cone adaptation is an indicator of increased risk of development of advanced AMD (Owsley et al., 2016; Sandberg et al., 1998). Therefore, the rate of retinal dark adaptation was chosen as a co-primary outcome measure as the functional measure which appears in the literature to be most sensitive to subtle changes in AMD status. The rate of cone, rather than rod, adaptation was chosen. This was done to allow a more rapid assessment of recovery

and based on evidence that cone adaptation is substantially delayed in people with AMD when a long duration bleach and large stimulus is used (Gaffney et al., 2011; 2013). Based on dark adaptation, the time constant of cone recovery (cone τ) was specified as the outcome measure assessed. Cone τ denotes the time to regenerate ~63% of cone photopigment, hence a larger cone τ denoted a slower recovery (i.e. greater impairment).

3.1.2. Secondary outcome measures

In addition to the primary outcome measures, a range of secondary outcome measures were also included to further evaluate the effectiveness of the intervention:

i. The change in drusen volume over the 12 months. The quantitative evaluation of drusen morphology by SD-OCT is highly reproducible (Gregori et al., 2011) and a study of the natural history of change in drusen volume has shown that, over 12 months, drusen exhibit an undulating pattern of growth whereby increase in overall volume is more likely than shrinkage. Mean cube root drusen volume increases significantly (P=0.006) by 0.016mm (SD 0.059) over 12 months (Yehoshua et al., 2011).

ii. The number of ranibizumab retreatments required on the fellow eye over 12 months. A review of medical records at the end of 12 months enabled us to quantify the impact of light therapy on the frequency of ranibizumab retreatment in eyes with active nAMD at baseline. Ranibizumab (as opposed to aflibercept) was chosen as a secondary outcome measure as at the time of study inception aflibercept was not widely used within Bristol Eye Hospital.

iii. The change in visual function using the CAD test, BCVA and 14Hz flicker threshold.

iv. The change in self-reported quality-of-life (EuroQol-5D [EQ-5D]) (EuroQol Group, 1990) and visual function (VFQ-48) (Stelmack et al., 2004a; 2004b).

To obtain detailed information about the time-course of any therapeutic action drusen volume was assessed at baseline and then at monthly intervals (using OCT images obtained at the regular nAMD clinic follow up appointments).

3.1.3. Participant eligibility criteria

All participants were aged between 55 and 88 years of age and had a BCVA in the test eye of logMAR score 0.3 (40 letters, Snellen 6/12) or better. A diagnosis of nAMD was made in one eye only. The fellow eye was classified as early or intermediate AMD, characterised by the presence of soft drusen and/or focal pigmentary changes, in the absence of signs of advanced AMD, e.g. retinal oedema, exudates, haemorrhage, GA (Ferris et al., 2013). In the original protocol those who had completed within the past month their initial 3 months of ranibizumab loading injections were deemed eligible. This was amended in January 2015 to also permit inclusion of those who were outside of their initial loading injections in the fellow eye – the rationale for this protocol amendment is discussed in Chapter 5. Participants also needed to be willing to adhere to the allocated treatment for the duration of the trial. Those recruited for the cross-sectional study were required to have grade 0 or 1 AMD (according to the AREDS Simplified Severity Scale) (Ferris et al., 2005). Any potential participant was excluded if they had:

- Ocular pathology other than macular disease, including: non-AMD related fundus changes, narrow anterior angles (≤grade 1 van Herrick), amblyopia, significant cataract (LOCS III graded, above grade 3 on any criterion), central corneal/media opacity, any posterior eye condition, glaucoma, history of prodromal symptoms of closed angle glaucoma.
- Significant systemic disease known to affect visual function (e.g. diabetes, Parkinson's disease, Alzheimer's disease).
- History of medication known to affect visual function (e.g. chloroquine, tamoxifen).
- An insufficient level of English language comprehension to be able to carry out the questionnaires and monthly interviews with study personnel.
- A history of falls, or a high risk of falling.

- A diagnosis of advanced AMD in both eyes.
- Significant systemic disease that would compromise participation in a 1 year study (e.g. motor neurone disease).
- Cognitive impairment as determined using an abridged Mini Mental State Examination (MMSE) (Schultz-Larsen et al., 2007).
- An illness requiring an oxygen mask to be worn at night.

3.1.4. Recruitment strategy

The basic recruitment strategy outlined in the original protocol was as follows. Potential participants were either directly identified by an ophthalmologist when attending their appointment at the eye hospital or by the trial investigator based on medical records. Once identified they were provided with an information sheet and asked for their permission to be contacted by the study investigator. Potential participants were contacted by telephone or letter (as preferred) at least two days after their receipt of the information sheet, and invited to meet the study investigator at their next visit to the nAMD clinic to discuss the trial, provide consent if they chose to participate, and carry out some basic screening tests. Participants were informed after this screening visit whether they were eligible to take part in the study. Approximately two months after receiving the participant information sheet (PIS) eligible participants were invited to attend for the baseline data collection (preferably coinciding with a regular visit to the clinic), and were randomised to the treatment or control group (see the flow diagram in Figure 3.1).

Participants with AMD severity grades of 0 and 1 according to the AREDS Simplified Severity Scale (Ferris et al., 2005) were recruited for the baseline cross-sectional analysis by local optometrists in Bristol and Cardiff, from Bristol Eye Hospital, from the list of research volunteers at the Cardiff University Eye Clinic and from staff and students of Cardiff University.

3.1.5. Withdrawal from trial: criteria and loss to follow-up

Any participant was withdrawn from the trial if they wished to discontinue the study or exhibited a serious adverse event/unexpected change deemed to be related to the intervention or to impact on their suitability to continue with the trial. Upon initial presentation any issue relating to the comfort of the intervention was attended to via adjustment of the mask. As necessary the tightness of the mask was altered and the patient reinstructed on adjustment so that they could manipulate this parameter at home. In order to improve comfort around the ears an alternative choice of mask strap was available if appropriate. In the event of continued discomfort the participant was given the option of withdrawing from the trial.

3.1.6. Registration

Details of eligible consenting participants were recorded on case report form 1 (CRF1) by the study investigator at the screening visit. Additional data arising from the baseline data collection visit were recorded on Case Report Form 2 (CRF2). All CRFs (see Appendix VIII) were stored in a secure locked room and the data were inputted into a password protected database designed by the study investigator. Details of those who decline to take part or those who did not meet eligibility criteria were also recorded on CRF1 providing they gave consent to have their anonymised data used.

3.2. Intervention

Participants were given a light mask (Noctura 500: Polyphotonix, UK) that presents illumination to both eyes, overnight. Illumination provided by the mask is based on organic light-emitting diode (OLED) technology. By positioning a series of organic (carbon based) thin films between two conductors and applying an electrical current the mask eyepieces emit a dim green light. The peak output of the light mask is 505nm which falls outside the range of short wavelength visible light that has been associated with RPE photochemical damage (Ham et al., 1976; Taylor et al., 1992; Arnault et al., 2013; Smick et al., 2013). Each OLED is powered by a 3V lithium cell battery. The

mask is depicted in Figure 3.2. It is activated when a touch sensor on the device is gently covered with a finger for 3 seconds. It deactivates if not worn continuously for the first 15 minutes, and after that, the light remains on for the remainder of the 8 hour treatment period. If the mask is removed or comes away from the face in this time data are still recorded to show that the mask is active but not being worn. In this trial, the masks were pre-programmed to function for a maximum of 8 hours within a time window, i.e. 8pm to 10am, to prevent misuse. Outside of these hours they did not illuminate if worn. Each mask was programmed using bespoke software (PPX Works) and hardware as developed by Polyphotonix, UK (Figure 3.3).

Figure 3.2. Principle components of the OLED sleep mask. The top panel shows the light-emitting 'pod' of peak output 502 nm. The bottom panel shows the cushioned fabric mask that houses the pod.

Treatment fidelity and acceptability were evaluated during a monthly interview with the study investigator, which coincided with the participant's routine nAMD clinic appointment. Both treatment arms attended this brief, monthly appointment to quantify sleep quality using the Pittsburgh Sleep Quality Index (PSQI) (Buysse et al., 1989). Compliance data were obtained at the monthly visit from the treatment group i) through evaluation of a diary of mask usage, ii) objectively through data collected on a chip in the mask itself (based on a capacitive sensor which logs when the mask is in contact with the face). This provided precise data on the hours the mask was worn each night. As each mask was programmed with the unique participant identification code, compliance data stored on-chip were non-identifiable except via the password protected electronic database.

Figure 3.3. A photograph of the hardware used to connect each mask to the PPX Works program. This system was used to program a mask before use, download compliance data at each monthly follow-up visit and record the return of a mask after 3 months wear.

For several reasons, it was not appropriate in this study to use a sham treatment. Firstly, if any light, even that of a different colour or intensity to the treatment, was presented to the control group overnight, there was the possibility that it could have had a physiological effect. Secondly, if a mask that didn't contain illuminated light-emitting diodes (LEDs) was to be used as a sham, the participants would be aware

that they didn't perceive light and so would be unmasked compared to the intervention group. Finally, a non-illuminated mask may have actually reduced the light levels entering the eye below the level that would normally be experienced in an urban environment, which may have impacted on the retinal physiology of the control group. The participants were not, therefore, masked as to whether they were in the intervention or control group.

The study investigator who collected the outcome data also provided the masks and instructions on usage, hence was also not masked to the intervention group. However, the primary outcome measure, disease progression, was an objective measure carried out by automated computer software. This minimised the potential for experimenter bias. The ophthalmologists at BEH who were seeing the participants for their regular anti-VEGF injections were masked as to whether individuals were in the intervention or control arm of the study. This was designed to prevent any bias in their retreatment decisions (which could impact on the secondary outcome measure of this trial which related to ranibizumab retreatment rates).

3.2.1. Determining the optimum light level for the intervention

The mask was set in this trial to provide a luminance of 75 photopic cd/m^2 (± 10%). When adjusted for the spectral sensitivity of rod photoreceptors, this equated to 186 scotopic cd/m^2. To convert this value into units of retinal illuminance (Td) in the closed eye, the luminance is multiplied by pupil area and adjusted for eyelid transmission. Studies investigating light attenuation by the human eyelid have found transmission to range between 0.3%-2% for light in the region of 500-505nm (Moseley et al., 1988; Robinson et al., 1991; Ando and Kripke, 1996). Therefore, we may assume an average lid transmission of 1%. Hence, a luminance of around 0.75 photopic cd/m^2 would be reaching the retina during periods of mask use. Under these conditions, pupil diameter in people in the age group 60-85 years is on average 5mm (Winn et al., 1994). This would result in a retinal illuminance in the order of 36 scotopic Td. In

humans, Thomas and Lamb (1999) used an electrophysiological technique to determine the attenuation of the maximal response of rod photoreceptors achieved with different background light levels. According to their data, the illumination of the dark adapted retina by 36 scotopic Td would cause an approximate 40% reduction in rod circulating current (Thomas and Lamb, 1999), which would impact substantially on the oxygen requirements of the dark adapted eye.

3.2.2. Maintenance of the light level

Each mask was replaced every 12 weeks at the participant's routine nAMD clinic appointment so that the total duration of mask usage was 12 months. Frequent replacement of the mask was designed to ensure that peak output was maintained throughout the duration of the trial. The measured output of one OLED of one mask assessed over 12 weeks is shown in Figure 3.4, in order to illustrate the typical change over time. Whilst there was some reduction in luminance over the 12 week period of usage, the mask output remained within 10% of the target 75cd/m^2. Mask condition was manually checked and function was verified on a monthly basis (via the collection of objective data documenting number of hours worn). As masks were programmed not to illuminate past 12 weeks of usage participants were given a new mask to use in advance of this date (up until when they were instructed to continue using their current mask).

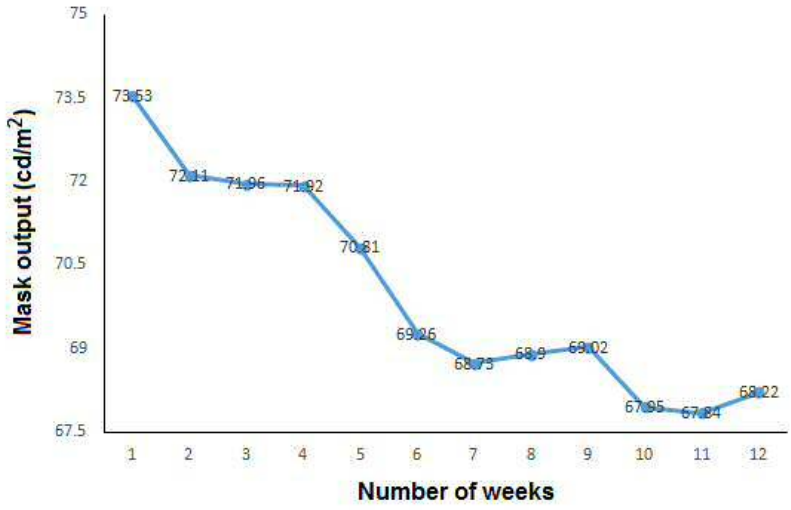

Figure 3.4. Luminance output of one eye of a Noctura 500 OLED mask over 12 weeks as measured weekly. The output of the mask was maintained to within (± 10%) of the desired output of 75 photopic cd/m2. The mask was illuminated for 8hrs nightly during collection of output data.

3.2.3. Circadian rhythm

A concern regarding the use of low-level night-time light therapy is the potential to cause a disturbance in sleep patterns via disruption of circadian rhythm. The term 'circadian rhythm' is used to describe a set of physical, mental and behavioural changes including sleep that follow a roughly 24 hour cycle. Current evidence suggests that a subgroup of photosensitive retinal ganglion cells containing the photopigment melanopsin are responsible for mediating light-dark cycles, thus regulating the secretion of the tiredness-inducing hormone melatonin (Lyubarsky et al., 1999; Berson et al., 2002; Hattar et al., 2002). Melatonin release has been found to be directly inhibited by light exposure (Lewy et al., 1980; Boyce and Kennaway, 1987) and a retinal luminance of 186 scotopic cd/m^2 has the potential to suppress secretion by 50-60% (Brainard et al., 2001). Despite this, to date the use of light therapy in this manner has been found to be well tolerated over a 12 month period (Arden et al., 2010; 2011). A secondary aim of this trial was to further investigate the potential disruption to circadian rhythm by monitoring self-reported sleep quality.

3.2.4. Ocular position during sleep

Our nightly sleep consists of several sleep cycles of non-rapid eye movement (NREM) and rapid-eye movement (REM) sleep. The first sleep cycle typically lasts around 90 minutes, with the succeeding cycles averaging around 100-120 minutes. Each cycle starts with NREM sleep which consists of 3 stages. An individual will typically proceed through stage 1, stage 2 and spend a period in stage 3 (Silber et al., 2007). The cycle is then reversed as the individual proceeds back down through stage 2. The return to stage 1 marks the end of NREM sleep. Following this REM sleep is entered. This is when most eye movement occurs during the sleep cycle. As the night progresses, the time spent in deep stage 3 sleep decreases and the time spent in REM sleep increases as seen in Figure 3.5.

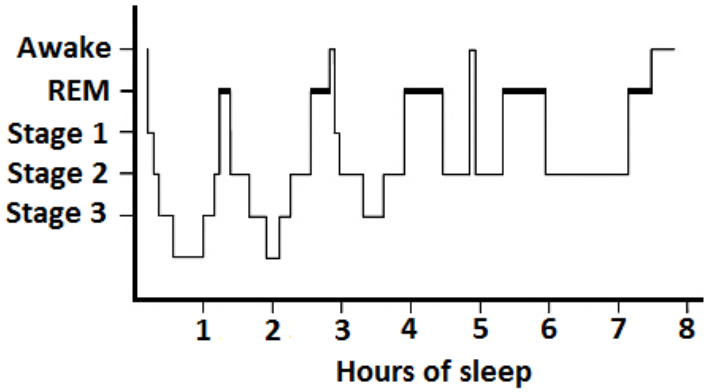

Figure 3.5. A hypnogram displaying a typical adult sleep pattern over 8hrs.

The eye movement which occurs during sleep was not anticipated to be an issue in this trial with respect to the provision of the correct retinal illuminance for two reasons. Firstly, it was not intended for the intervention in this study to provide a point focus of luminance on the macular, but rather, a ‘wall of light’ large enough to encapsulate the pupil in all positions of gaze. Secondly, older adults such as those enrolled in the trial, only spend around 10% of their total sleep time in REM sleep (Institute of Medicine, 2006). Therefore, trial participants are likely to only have spent around 30-60 minutes in REM sleep per night. Most of the time spent in this state will have dominated the latter half of the sleep period, especially the hours before waking.

3.3. Trial procedures

This section provides an overview of the procedures employed in the clinical trial and cross-sectional study.

3.3.1. Informed consent and screening

The study investigator was responsible for taking the informed consent of each participant at the beginning of the screening assessment. Following a full explanation of the study, they were invited to take part. Those who expressed interest in participating were then asked to sign the consent form. All investigators taking informed consent had received the appropriate training, i.e. “Good Clinical Practice” training provided by the National Institute for Social Care and Health Research.

3.3.2. Screening assessment

The screening assessment for potential participants in the clinical trial took approximately 30-60 minutes. Following a discussion of the study, and the obtaining of informed consent, the study investigator questioned the participant regarding their ocular and medical history in order to ensure the eligibility criteria had been met (documented in Section 3.1.3).

BCVA was measured for each eye with the participant’s habitual distance correction in place (following a brief refraction if necessary) using an ETDRS test chart (logMAR score and equivalent number of letters seen recorded). The letters displayed were altered for each eye to avoid repetition and memorisation. Prior to pupil dilation with 1% Tropicamide the drainage angle was measured using Van Herick’s method. Following this the media clarity was assessed for each eye and the lens was graded according to the LOCS III grading scale (Chylack et al., 1993). An abridged version of the MMSE test was used to assess for cognitive impairment (Schultz-Larsen et al., 2007). Those still deemed eligible for inclusion in the study also completed the following questionnaires through verbal interview with the investigator: visual function

(VFQ-48), health related quality-of-life (EQ-5D), Pittsburgh Sleep Quality Index (PSQI), smoking history (pack years), ocular vitamin supplementation and ethnic origin. Retinal photographs and OCT images were taken following pupil dilation and repeated if image quality was insufficient to allow evaluation. OCT and fundus photographs were assessed to check for eligibility.

3.3.3. Baseline assessment

The baseline assessment for those with AMD took approximately 75 minutes. OCT images (5 Zeiss Cirrus SD-OCT 4000, 6x6mm macular cube scans centred on the fovea) and fundus photographs (Topcon 3D-OCT 2000 45º photographs centred on the fovea) obtained during the participant's routine visit to the ranibizumab clinic were analysed to assess drusen volume and AMD grade, according to AREDS Simplified Severity Scale. If the images were of insufficient quality additional images were captured. Drusen volume analysis software was used to provide data regarding RPE elevation within $3mm^2$ and $5mm^2$ of the fovea (see Section 3.3.3.1 for further detail). Any changes in eligibility since screening were also addressed via ocular health examination. Repeated BCVA measurements (using a 4m ETDRS chart) were taken alongside auto-refraction (Topcon KR-7500) and data on current spectacle prescription. The following visual function tests were then completed:

- Colour vision testing. Chromatic thresholds were measured for the eye with early AMD using the CAD test (O'Neill-Biba et al., 2010) (City Occupational Ltd).
- Flicker thresholds. Contrast thresholds to a 14 Hz flickering stimulus were measured for the eye with early/intermediate AMD using the procedure outlined by Dimitrov et al. (2011).
- Dark adaptometry. Cone τ was determined using a psychophysical procedure described in publications by Gaffney et al. (2011). This involved an initial training phase, of around 5 minutes, then the adapting light was presented

(bleaching approximately 92% of macular cone photopigment), and finally recovery of visual thresholds was monitored for 25 minutes after exposure to the adapting light.

Details of the methods for collecting the visual function data are outlined in Section 3.6.3.1 (dark adaptation) and Section 3.7.1.2 (flicker threshold and chromatic thresholds).

3.3.3.1. OCT acquisition and drusen volume measurement

The Cirrus HD-OCT instrument was used to acquire 5 images for each participant from which the mean drusen volume measurement was recorded. All images were macular cube scans (200 x 200mm^3 A scans) covering a retinal area of 6 x 6mm^2 (20° x 20° visual angle). The scans were performed by experienced operators of the Bristol Eye Hospital Retinal Imaging Unit who assessed the quality of the scan during its acquisition. Scan quality assessment was based on signal strength, a parameter provided by the manufacturer of each OCT instrument. Signal strength ranges from 1 to 10, with lower scores indicating poorer quality. As with other studies that have used the same equipment to acquire drusen volume measurements in a cohort of those with AMD (Yehoshua et al., 2011; Abdelfattah et al., 2016), 5 scans were taken for the study eye and an image quality cut-off score of 7 or above was employed. Following image acquisition minor adjustments to head and participant positioning were made as necessary however there was no specific requirement to reset the instrument between scans. The Cirrus Advanced RPE Analysis Software (Version 7.0.1) was used to measure drusen volumes and areas within the 3- and 5mm circles (centred on the fovea) of the Cirrus grid. The algorithm compares a virtual RPE map free-from deposits (RPE floor) to the actual RPE geometry to derive a drusen profile (Figure 3.6).

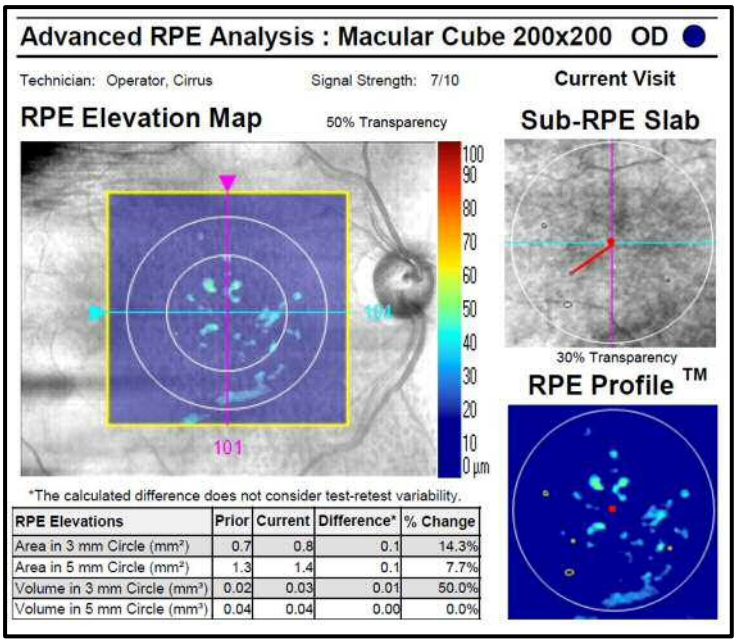

Figure 3.6. Example of quantitative measurements provided by the Cirrus automated algorithm. Drusen volume and area are measured within the 3- and 5mm concentric circles visible on the RPE elevation map. The sub-RPE slab denotes areas of atrophy and the RPE shows elevations in the RPE geometry when compared to a 'virtual' map.

3.3.3.2. Grading

The fundus images were graded according to the AREDS Simplified Severity Scale (Ferris et al., 2005) by two independent graders both of which were familiar with the clinical presentation of AMD. Where disagreement occurred between the two graders, the results were adjudicated independently by one of the PhD supervisors (AB). In accordance with the AREDS Simplified Severity Scale (Ferris et al., 2005), the severity of AMD was based on scoring each eye independently then summing the number of risk factors across both eyes to determine the final severity grading. Risk factors were assigned for each of the following retinal features:

- The presence of 1 of more large drusen (≥125µm; one risk point assigned per eye meeting this criterion).
- Any pigment abnormality (one risk point assigned per eye meeting this criterion).
- Bilateral intermediate drusen (≥63µm but <125µm) in the absence of large drusen (one risk point assigned if both eyes met this criterion).

Two risk factors were also assigned for any eye with advanced AMD. The summation of risk factors yielded a 5 step-scale (0-4). Hence, the 60 participants with unilateral nAMD had a severity grading of 2-4 and those included in the cross-sectional study without unilateral nAMD (n=40) had grades 0-1.

3.3.4. Enrolment

Following successful completion of the visual function tests the participant was randomised to the intervention or control arm of the study (see Section 3.5.1 for a detailed description of the randomisation process). Those individuals who were assigned to the treatment group were at this stage given a light mask, and provided with written and oral instructions on its use. Before leaving, all participants were reprised of the key information provided in the participant information letter about follow-up appointments. The participants were given written copies to take home of the PSQI questionnaire which they were asked to complete the night before their next monthly follow-up visit.

3.3.5. Monthly assessment of medical records

The investigator accessed the OCT images and medical records of all participants after they attended the nAMD clinic for each monthly follow up appointment. This was done in order to collect the measurement of drusen volume data on a monthly basis. The medical records also permitted monitoring of the conversion rate to advanced AMD in the control and intervention groups in the eye with early/intermediate AMD at baseline, and monitoring of ranibizumab retreatment rates in the eye with nAMD, for safety monitoring purposes.

3.3.6. Monthly follow-up appointment

Participants in both intervention groups attended a short, monthly follow-up appointment following their routine nAMD clinic appointment, during which both groups returned their completed PSQI sleep quality questionnaire. In addition, the

participants enrolled in the treatment group were asked to bring their mask along to each monthly visit to allow:

1. Objective compliance data (nightly hours of use) to be exported from the device onto a password protected computer.
2. Functionality of the mask to be checked.
3. Any broken or damaged masks to be replaced.
4. A new fabric strap to be provided and fitted.
5. A semi-structured interview to be carried out to determine the acceptability of the intervention.
6. Retraining in mask use if the participant had experienced any problems.

3.3.7. Final visit

This visit was the same as the baseline visit with the addition of a final semi-structured interview assessing compliance, an evaluation of the acceptability of the intervention and the oral completion of the self-report questionnaires (PSQI, VFQ-48, EQ-5D).

3.3.8. Data collection for the cross-sectional study

The collection of cross-sectional data from age-matched participants with grade 0 and 1 AMD severity in accordance with the AREDS Simplified Severity Scale (Ferris et al., 2005) consisted of the following:

- Informed consent was obtained following a discussion of the study.
- Ocular and medical history obtained verbally and recorded on structured proforma.
- BCVA was measured (logMAR score) for each eye at 4m. During measurement each eye was patched alternately and presented with a different EDTRS letter chart.
- Slit lamp examination of the anterior and posterior eye was performed. In order to minimise any risk of inducing closed-angle glaucoma during pupil dilation,

the Van Herick technique was used to assess the irido-corneal angle adjacent to the temporal limbus for each eye. A grading was made for each eye between 4 and 0, (the widest angle is denoted as a grade 4, whilst 0 indicates a closed angle). Those with a grade of 0-1 were excluded. Media clarity was assessed for each eye and the lens graded according to the LOCS III grading scale (Chylack et al., 1993). A volk lens was used to assess the retina.

- Tropicamide 1% was instilled into both eyes. The participant was only dilated if the Van Herick grading assessed in the slit lamp examination fell within the limits of the eligibility criteria.
- Auto refraction was carried out using the Topcon KR-7500. If a satisfactory auto-refraction result was unobtainable, the spectacle prescription from the participant's spectacles or last eye examination was recorded instead.
- Fundus photography and OCT were performed. Photographs of the retina (fundus) were obtained for each eye using the Topcon 3D-OCT 2000 (45° diameter photo centred on fovea) and digitally stored. The Topcon 3D-OCT 2000 was also used to capture 5 OCT images of the study eye (Macular cube scan 20°-20° centred on fovea).
- Visual function tests were performed: colour vision, flicker thresholds and dark adaptometry (as outlined in Sections 3.6.3.1 and 3.7.1.2).

3.3.9. Data collection environment and screen calibration

One room was used for all psychophysical data collection for the duration of the trial. The room, based within the clinical research unit (CRU) of Bristol Eye Hospital, was identified as an effective environment for dark adaptation due to its lack of windows. Light seepage under the door was rectified via the installation of a light excluder in order to further enhance the testing environment. OCT and fundus images were taken in a neighbouring room. The luminance output of the LCD monitor used to present psychophysical stimuli was γ corrected every 6-8 weeks using established techniques

as described by Metha et al. (1993). The monitor was activated 30 minutes before threshold testing was performed in order to account for variability in output due to warm-up characteristics. Output luminance of the monitor with and without γ correction and warm-up characteristics are shown in Appendix III.

3.3.10. Staff training

Each aspect of the data collection process was outlined to all affiliated CRU and retinal imaging unit (RIU) staff via a series of presentations delivered by the trial investigator from December 2014 until February 2015. Although the majority of baseline, monthly follow-up and final visits were carried out by the trial investigator, training was required for the BEH staff in case the trial investigator was absent for any reason. Although all staff members were introduced to the research study, one-to-one training was provided to the acting trial manager who was responsible for daily trial activity in the absence of the trial investigator. The trial manager was tutored on each data collection technique and shadowed the daily activity of the investigator on 5 separate occasions during which screening, baseline and monthly follow-up visits were witnessed. Familiarisation with the intervention including troubleshooting, collection of objective data and maintenance was also witnessed. The investigator assessed the trial manager for competency by observing the trial manager perform each type of study visit. The trial manager was permitted to perform unsupervised study visits only when deemed competent by the investigator.

3.4. Assessment of safety

For detailed information regarding the safety monitoring procedures and the classification of adverse events the reader is directed to the protocol in Appendix II.

3.4.1. Conversion to nAMD

One potential serious adverse event would be a conversion to nAMD in the study eye. An important aspect of the safety evaluation of the intervention was to ensure that it

did not increase the risk of progression to nAMD. Wong et al. (2008) carried out a meta-analysis of studies which looked at the progression to choroidal neovascularisation (CNV) in the fellow eye of people with unilateral nAMD at baseline. They reported that the cumulative 1 year incidence of CNV in the 426 patients enrolled in the 5 studies which evaluated this outcome was 12.2% (confidence intervals [CI], 1.7%–30.6%). Therefore, an upper limit on the number of people expected to convert to nAMD per month was devised:

Upper limit for conversion to nAMD from early/intermediate AMD:

n x (30.6% / 12 months)

Where n is the number of people in the trial who were using the light therapy light mask. It was deemed that should the percentage of participants using the light mask who develop nAMD exceed what might normally be expected (i.e. approximately 1% per month) we would notify the independent Trial Steering Committee, and the Device Manufacturer, who would notify the MHRA. Should the percentage exceed the upper confidence limit then the Trial Steering Committee would be contacted so that they could consider stopping the trial.

3.5. Statistical considerations

Given the potential benefit of participation, it was anticipated that the numbers of people withdrawing from the study from the intervention group would be low. By arranging follow-up appointments around scheduled visits to the nAMD clinic, we aimed to minimise drop-out within the control group. Data from a study involving diabetic patients and the same light mask intervention suggested that we would lose approximately 10% of people after 12 months due to lack of compliance or failure to attend follow-up appointments (Arden et al., 2011). It was also expected that further participants would withdraw for unrelated health reasons (Arden et al., 2011). Withdrawal from the study did not impact on patient care.

It should be noted that as a phase I/IIa proof-of-concept study this research was not powered to detect small effect sizes. In terms of the proportion of people showing disease progression, based on drusen volume and/or progression to advanced AMD, a sample size of 50 would allow for a 50% reduction in people showing progression to be detected at a probability level of 0.2, with a power of 80%. In terms of cone adaptation, based on parafoveal cone adaptation data from Gaffney et al., (2011), a sample size of 50 would allow a change in cone τ of 1 minute to be detected at a probability level of 0.05, with a power of 80%. This difference in cone τ is substantially smaller than the known effect of early AMD. Gaffney et al., (2011) reported a mean increase in cone τ of 2.85 mins compared to age-matched controls. In alignment with this we aimed to recruit 60 people which, allowing for 15% dropout through the year, would leave a final cohort of 51.

3.5.1. Randomisation

Participants were randomly allocated to either a control or a treatment group. Randomisation was generated by a random number generator. Computer generated random permuted blocks of size 2, 4 and 6 stratified for grade of AMD were used to allocate interventions to participants. In stratification, patients are formed into risk groups (strata) based on 1 or more prognostic factors, and a separate randomisation is conducted for each stratum. This helps to ensure balanced groups and is particularly important in a small study such as this. Randomisation was stratified into 3 layers (AMD grade 2, 3 or 4, according to the AREDS Simplified Severity Scale) (Ferris et al., 2005). The study investigator was provided with three piles of envelopes by the chief investigator in order to randomise the participant to either the intervention or control arm of the study. Each pile related to a different stratum of randomisation, i.e. grade 2, 3 or 4 of AMD, according to the AREDS Simplified Severity Scale. The envelopes in each pile were numbered, and contained the randomisation allocation for each participant.

3.6. Optimisation of outcome measures

On the basis of the current literature regarding the usefulness of visual function tests as potential AMD biomarkers (as introduced in Section 1.3.6.6), three functional tests were chosen for inclusion in the ALight protocol: cone dark adaptation, 14 Hz flicker thresholds and colour discrimination. Although numerous studies have investigated the effect of AMD on various aspects of visual function, there are few longitudinal data available to validate these outcome measures as potential trial endpoints. Therefore, this study not only used the psychophysical tests to evaluate the effectiveness of the trial intervention, but also used the 12 month follow up period of the trial as an opportunity to evaluate the prognostic and predictive capacity of the tests, and a baseline cross-sectional study to evaluate the relationship between the outcome measures and the severity of the fundus changes.

The following section outlines two pilot studies performed before recruitment for the ALight trial began to optimise and evaluate the psychophysical tests of visual function. The specific aims were:

1. To check the test sequence and time of the experiments.
2. To verify that a new handheld photopigment bleach source could be used reliably in a dark adaptation experiment.
3. To optimise parameters of dark adaptation, flicker threshold and chromatic threshold measurement for use in the ALight clinical trial and cross-sectional study.

3.6.1. Pilot Study to evaluate the effect of bleach intensity on characteristics of the dark adaptation function

As discussed in Section 1.3.6.5, dark adaptation parameters, including cone τ and time to RCB, have been identified as sensitive biomarkers for early AMD (Dimitrov et al., 2011; Gaffney et al., 2011). However, if assessment of dark adaptation is to be

employed as an outcome measure in a clinical trial, optimisation of the test parameters, such as bleach intensity, bleach duration and stimulus size, is essential, in order to maximise sensitivity to disease progression.

3.6.2. Selection of stimulus parameters

When assessing the diagnostic ability of three different sized annular stimuli, Gaffney et al. (2011) concluded that an annular stimulus of 12° radius was optimal for cone dark adaptation assessment in early AMD, displaying 90% sensitivity and specificity. However, a smaller annular stimulus of 2° radius was recorded as displaying a greater difference in means between those with AMD and controls. The diagnostic accuracy of the smaller stimulus was compromised by the greater between subject variability in results, which was attributed by the authors to a greater impact of focal retinal abnormalities on thresholds when sampling a limited retinal area. However, in a study of disease progression rather than diagnostic capacity, the between subject variability is of less interest than the between session variability. The inter-session repeatability of dark adaptation was addressed by McKeague et al. (2014) who found the use of a 2° spot stimulus to be more repeatable over two measurements than 7° and 12° annulus alternatives. When measuring cone τ it was determined that any change above the coefficient of repeatability (0.82) for this stimulus could be considered clinically significant. This number is considerably lower than the mean difference between healthy controls and those with AMD (McKeague et al., 2014).

In a study involving 221 participants with AMD and 109 healthy controls Dimitrov et al. (2011) measured the diagnostic potential of dark adaptation characteristics using a 4° foveal stimulus and a 2° stimulus at 3.5° and 10° eccentricity. All three locations tested showed deficits in AMD participants when compared to controls. Dimitrov et al. (2011) found the 2° stimulus at 3.5° eccentricity to be optimal as it provided a high diagnostic value (determined as the area under the ROC curve) for the parameters of cone τ (AUC 0.86 ± 0.023), rod recovery rate (AUC 0.93 ± 0.016) and time to RCB

(AUC 0.86 ± 0.027). As the 2° radius stimulus allows quantification of cone recovery rate within 10 minutes (Gaffney et al., 2011) and displays good diagnostic potential and repeatability when compared to other alternatives (Dimitrov et al., 2011; McKeague et al., 2014) it has been adopted for use within this experiment.

In addition to the stimulus area and size, the appearance of the dark adaptation function is also dependent on the intensity and duration of the pre-adapting bleaching light (Dimitrov et al., 2008; Gaffney et al., 2013). Gaffney et al. (2013) investigated the pre-adapting light intensity necessary to generate the maximal separation in the parameters of dark adaptation between those with early AMD and healthy controls. Participants were exposed to a 120s bleach of 3 adapting intensities termed low (71% and 51%), medium (84% and 74%) and high (91% and 90%) based on the percentage of photopigment (cone photopigment and rhodopsin, respectively) bleached. Their findings indicated that the medium and high intensities both provided equally good separation between groups, and sufficient data points to allow the time course of cone recovery to be monitored effectively. However, this study used a 12° radius annular stimulus. As a different retinal location will be targeted in the ALight trial (a circular region of 2° radius), the effect of bleach intensity needs further investigation before finalising the protocol.

Another difference between Gaffney et al. (2013) and the current study is the source of the bleaching light. The findings reported by Gaffney et al. (2013) were generated using a Maxwellian View optical system which requires precise head alignment in order to ensure the accuracy of the photopigment bleach delivered. In contrast, the bleaching source used in the trial was a hand-held alternative. In the absence of the Maxwellian View system alignment must be achieved via instructing the subject to look directly at the centre of the bleaching source.

This pilot experiment was designed in order to address the following aims:

1. To evaluate the effect of bleach intensity on dark adaptation parameters in healthy individuals using a 2° radius stimulus.
2. To compare results with those collected from healthy individuals by Gaffney et al. (2013) using a 12° radius stimulus.
3. To test the utility of a portable hand-held bleaching source.

3.6.3. Method and equipment

Healthy participants were recruited from among staff or students of the School of Optometry and Vision Sciences, Cardiff University. Any potential participant was excluded if they had:

- Ocular pathology: including narrow anterior chamber angles (≤grade 1 van Herrick), significant cataract (LOCS III graded, above grade 2 on any criterion), central corneal/media opacity, any posterior eye condition, glaucoma, history of prodromal symptoms of closed angle glaucoma.
- Significant systemic disease known to affect visual function.
- History of medication known to affect visual function.

To assess eligibility prior to retinal function testing anterior (slit lamp biomicroscopy) and posterior ocular health (indirect Volk Fundoscopy) were assessed for each potential participant. A full ocular and general health history was also recorded. Measurement of intraocular pressure was performed prior to and following dilation. The School's Research Ethics Committee approved the study, informed consent was obtained before data collection took place and all procedures were carried out in accordance with the tenets of the Declaration of Helsinki.

3.6.3.1. Experimental procedure

For participants assessed at all bleach intensities, measurements were taken over 2 separate days within a period of 2 weeks. All data could not be collected on a single visit due to the time required to perform repeated dark adaptation measurements.

Refractive correction for the test distance (140cm) was worn as required, and the non-study eye was occluded. Participants were dilated with one drop of 1% tropicamide prior to dark adaptation (mean pupil diameter after dilation = 6.8mm).

During the test procedure stimuli were presented on a calibrated, high-resolution monitor (NEC MultiSync PA241/W). The luminance of the monitor was γ-corrected in accordance with the method described by Metha et al. (1993). Cone dark adaptation thresholds were measured using a robust psychophysical method described in previous publications (Gaffney et al., 2011; 2012; 2013; 2014). The procedure is based on a '3 down, 1 up' paradigm with a 0.2 second stimulus presentation time and a 0.6 second response window denoted in the MATLAB code found in Appendix IV. Thresholds were recorded in response to a 2° radius solid yellow circular stimulus (chromaticity coordinates, 0.429, 0.413) under software control (MATLAB, R2009a, The MathWorks Inc). To aid fixation a white cross of variable intensity was generated under the stimulus. The fixation cross was always 3 fold brighter than the stimulus (Figure 3.7).

Participants were asked to wear goggles containing a 2.1 log unit neutral density filter, complete with side shields, throughout the duration of threshold measurement in order to minimise the distracting effect of light reflecting off the walls of the testing room. As the lower end of the linear luminance range approached, additional 2.1 ND and 1.8 ND filters were applied to the monitor to ensure that its output remained in the linear range.

Prior to commencement of threshold testing the subject was given verbal instructions and performed a training trial of 1 minute in order to familiarise themselves with the test. This training involved presentation of the test fixation target and suprathreshold stimuli without a photopigment bleach. The participant was deemed to have shown competency if they responded to all presentations (of varying brightness) without making any errors, i.e. missing a presentation or responding between presentations.

If the participant was unable to complete the training trial within three attempts they were deemed ineligible for the study. The tutorial session was repeated at the start of the second visit.

A hand-held bleaching source consisting of a 'white' LED overlaid with a diffusing (LEE Filters 216 'white diffusion') and amber filter (LEE Filters HT015 'deep straw') was used to deliver a 120s photopigment bleach. The amber filter provided protection from potentially harmful short-wavelength blue light (Figure 3.8) and also reduced the scotopic retinal luminance in order to attain an approximately equivalent cone photopigment and rhodopsin bleach. The unit was mounted onto a modified Royal Air Force (RAF) rule in order to ensure a precise viewing distance of 23.5cm, thus resulting in a 12° diameter bleach of the central retina (Figure 3.9; Figure 3.10). The bleach source was calibrated using a photometer (LS-110; Konica Minolta., Osaka, Japan). The luminance of the device was initially measured with no filters in place, then with 0.6 and 1.2 ND filters. The bleach intensities that ensued were documented as high, medium and low. Table 3.1 shows them alongside the expected cone photopigment and rhodopsin bleach.

To initiate threshold testing the desired bleach was applied for 2 minutes (Figure 3.10). The order of bleach intensities used was randomised. Upon termination of the bleach, spectacles were instantly replaced if necessary and the 2.1 log unit ND goggles were positioned over the eyes. Immediately following this, dark adaptation was monitored continuously for 25 minutes. The subject was reminded at the start of this process to maintain their fixation towards the centre of the cross target and indicate perception of the stimulus via the hand-held keypad. Although fixation was not monitored, the examiner gave verbal encouragement to the participant at regular intervals in order to ensure alertness and compliance. An experimental timeline of dark adaptation visits is shown in Figure 3.11.

Figure 3.7. A representation of the participant's view of the circular stimulus (left panel) and the fixation target alone (right panel) as seen on the NEC MultiSync PA24/W VDU monitor.

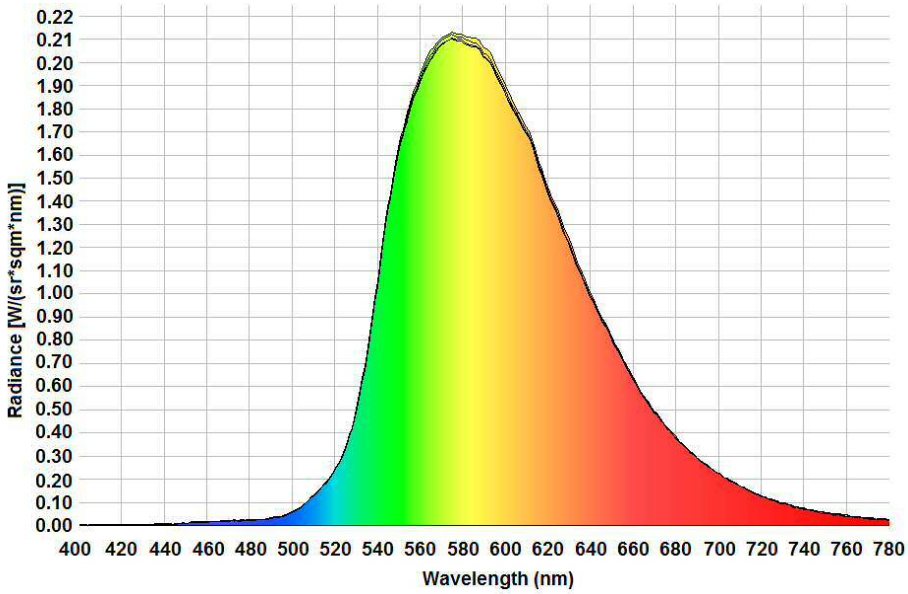

Figure 3.8. Transmission spectrum of the bleaching source overlaid with a white diffusion (LEE filter 216) and amber filter (LEE filter HT015). The spectrum was obtained using a Specboss 1201 Spectroradiometer (JETI Instruments, Germany). The multiple outlines of the spectrum represent repeated readings.

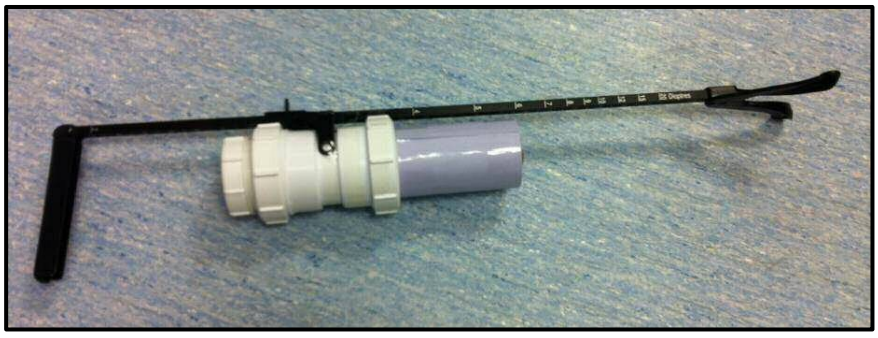

Figure 3.9. A photograph of the bleaching source setup. The portable device was mounted onto a modified RAF rule and connected to a mains voltage supply for use.

Table 3.1. Bleach characteristics of the 3 intensities used, calculated using equations by Thomas and Lamb (1999) and Paupoo et al. (2000). Measurements reported do not take into account the Stiles-Crawford effect.

Bleach intensity	Log photopic Trolands (duration: 120s, 7mm pupil)	Percentage cone photopigment bleach	Percentage rhodopsin bleach
HIGH	5.54	92.00	91.59
MEDIUM	4.92	72.32	53.10
LOW	4.37	37.91	19.81

Figure 3.10. The bleaching source was positioned in front of the study eye and held in place for 120s as seen in this photograph. Immediately after bleaching cessation the ND goggles were bought down over the participant's eyes and threshold testing began.

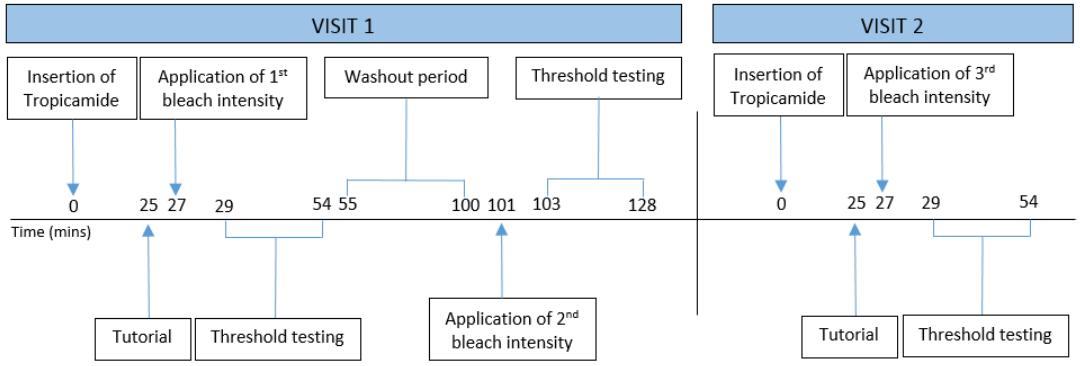

Figure 3.11. Experimental timeline for dark adaptation visits. Prior to dilation logMAR visual acuity was recorded at 4m and ocular health was verified. The timeline displays above shows activity related to the measurement of dark adaptation parameters across two visits (within two weeks apart).

3.6.4. Analysis

A single exponential, double-linear model (see Equation 3.1; McGwin et al. [1999]) was fitted to the data on a least squares fit basis using the Solver function of Microsoft

Excel. Statistical analysis of cone τ, time to RCB and final cone threshold was undertaken using statistical software (SPSS, Version 20) in order to determine whether parameters differed significantly between bleach intensities. A Shapiro-Wilk test indicated that the data were not normally distributed hence non-parametric analysis via the use of a Kruskal-Wallis test and pairwise post-hoc analysis was applied. Median and inter-quartile range (IQR) values were also calculated.

$$T(t) = (a + (b.exp^{(-t/\tau)})) + (c.(max[t - rcb,0])) + (d.(max[t - rrb,0]))$$

Equation 3.1. T represents the threshold (log cd/m2) at time t after cessation of the bleach, a is the final cone threshold, b is the change in cone threshold from t=0. τ is the time constant of cone recovery, c and d represent the second and final slopes of rod recovery, max is a logic statement, rcb denotes time to RCB from t=0 and rrb denotes the time from bleach offset to the transition between c and d.

3.6.5. Results

Thirteen healthy control participants took part in the study to evaluate the effect of bleach intensity on characteristics of the dark adaptation function. Mean age was 30.2 years (range = 23 to 49yrs). Eleven of the 13 participants were assessed at all bleach intensities. Of the remaining 2, due to time constraints and unavailability to re-attend for further testing 1 participant (GR) provided data for the high and low bleach intensities only whilst the other (TM) provided data for the medium bleaching intensity only. In accordance with this data from 12 participants was analysed for each bleach intensity.

The dark adaptation data for a typical participant are shown in Figure 3.12. Note that the rate of cone threshold recovery is slower and the time to RCB is later with increasing bleach intensity. When using the weaker bleach the rapid subsequent fall of threshold within the first half minute of measurement in all participants made data modelling difficult (Figure 3.13). Dark adaptation parameters for all participants are displayed in Table 3.2. Group median and IQR values for dark adaptation parameters are displayed in Table 3.3. Median values for each parameter at each bleaching

intensity are shown graphically in Figure 3.14. There was a significant difference in time to RCB between the highest bleach intensity and both the medium (P=<0.05) and low (P<0.05) intensities. There was no significant difference between bleach intensities for final threshold achieved (P>0.05). Cone τ was found to be significantly longer when using the highest bleach intensity level in comparison to the low (P<0.05) alternative.

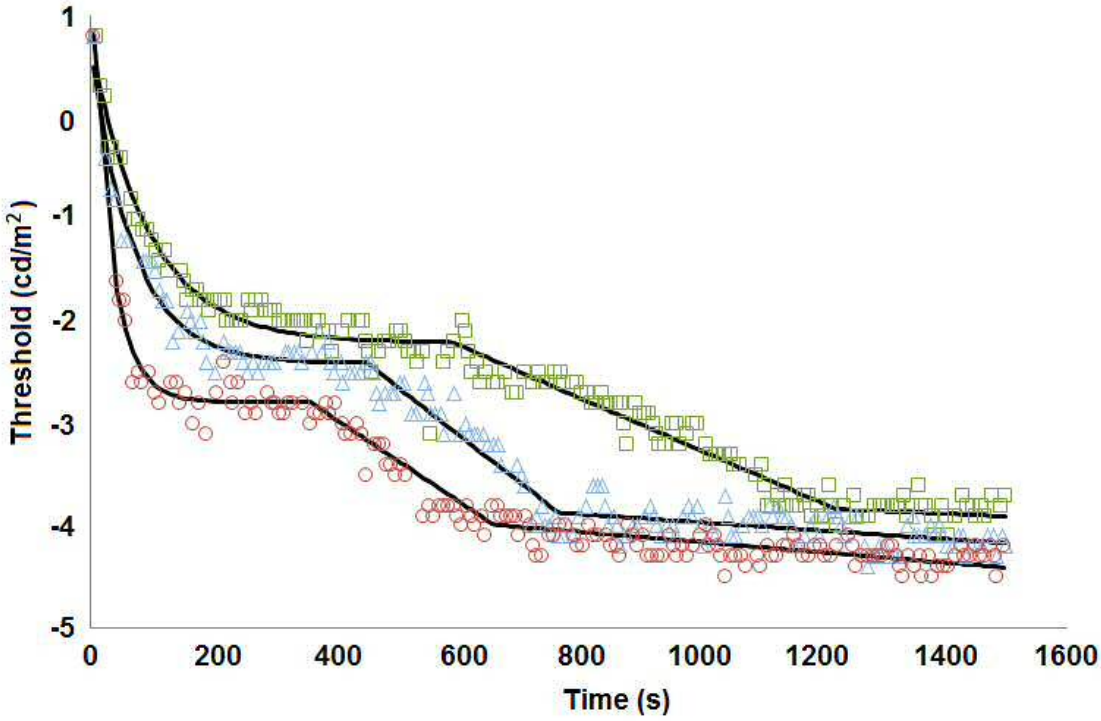

Figure 3.12. Typical dark adaptation curves recorded after exposure to three different photopigment bleach intensities. Each data set is represented by the raw data (squares high bleach, triangles medium bleach and circles low bleach) to which a best-fitting model has been applied (given by Equation 3.1).

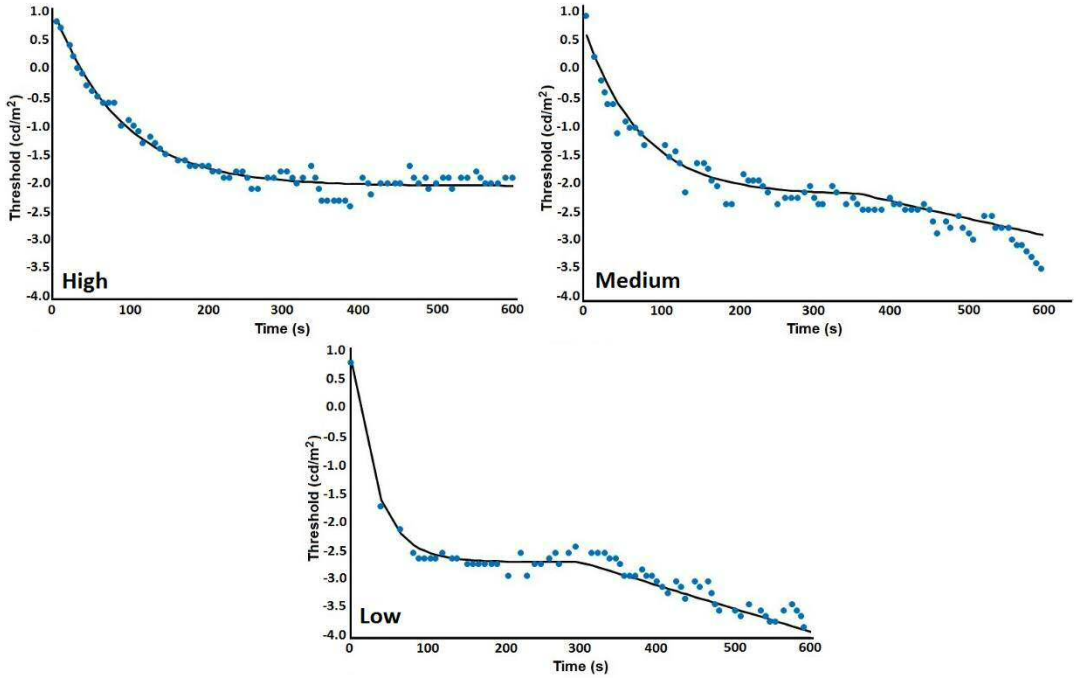

Figure 3.13. Sample curves of high, medium and low intensity bleach for one participant (TC) with the first 10 minutes of data plotted in order to magnify the cone proportion of the data. The blue circles represent the raw data values by which the best-fitting model (black line) has been applied (given by Equation 3.1). Take note of threshold measurement over the first 200 seconds, in which cone τ is recorded. The integrity of data modelling, on the basis of raw data values, can be seen to be more accurate for the high and medium bleach within this time frame. Due to the speed of recovery when using the low intensity bleach, few data points are available on which to fit the model.

Table 3.2. Individual participant data for cone τ and time to RCB dark adaptation parameters.

	Cone τ (mins)			Time to RCB (mins)		
Study ID	**High**	**Medium**	**Low**	**High**	**Medium**	**Low**
AB	2.09	1.67	1.51	11.27	4.05	3.91
AN	1.68	1.70	0.52	12.26	7.29	4.20
BF	1.60	1.17	0.55	9.87	7.56	6.00
CE	1.73	1.47	0.72	9.78	7.00	4.67
CJ	2.22	2.75	0.67	13.00	7.50	7.00
KB	1.77	1.26	0.62	11.01	7.00	5.50
LR	1.70	0.95	0.45	8.64	7.06	2.00
LT	1.68	1.49	0.55	13.25	9.65	4.62
NC	1.33	1.05	0.52	11.47	8.36	6.50
SJ	1.90	1.60	0.45	12.10	7.64	3.00
TC	1.45	1.24	0.55	10.92	6.00	5.00
GR	1.12	-	0.44	9.89	-	5.50
TM	-	1.05	-	-	5.74	-

Table 3.3. Comparison of median (inter-quartile range) of each bleach intensity used.

Bleach intensity	Cone τ (mins)	Final threshold (log cd/m^2)	Time to RCB (min)
High	1.69 (1.56, 1.80)	-2.23 (-2.34, -2.13)	11.14 (9.89, 12.14)
Medium	1.36 (1.14, 1.62)	-2.17 (-2.36, -2.02)	7.17 (6.75, 7.58)
Low	0.55 (0.50, 0.63)	-2.36 (-2.57, -2.24)	4.84 (4.13, 5.63)

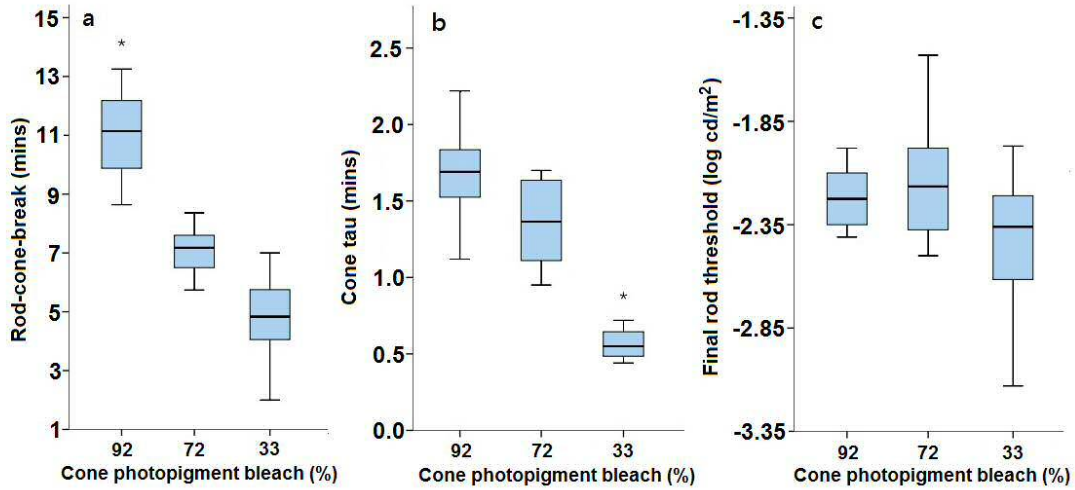

Figure 3.14. Summary of median time to RCB (a), cone τ (b) and final threshold level (c) at each bleach intensity level. Whiskers denote the highest and lowest data points collected within each intensity. For any given parameter a bleach intensity denoted by an asterisk (*) demonstrated a significant difference to all other bleach intensities investigated.

3.6.6. Discussion

The results suggested that bleaching levels of ≥70% cone photopigment and ≥51% rhodopsin (i.e. the medium and high bleach levels used in this study) were clinically viable for assessment of dark adaptation. Despite having the desirable characteristic of the shortest test duration to obtain parameters known to be affected in AMD, the weak bleach intensity was found most difficult to model as a result of the rapid recovery of threshold following cessation of the bleach. Such difficulty resulted in concerns about the integrity of the model outputs for the lowest bleach intensity, when compared to the high and medium intensity alternatives.

Cone τ did not differ significantly between the upper two bleach intensities. The high bleach τ of 1.69 mins (101.4 secs) and the med bleach τ of 1.36 mins (81.6 secs) fall broadly into agreement with data published by Hollins and Alpern (1973). They reported that when using a long duration equilibrium bleach cone τ was around 105

seconds, regardless of the percentage of photopigment bleached (from 30% to 100%). These published data, however, were obtained for one patient only.

Measurement of time to RCB was possible for each participant at each bleach intensity. However, this parameter has been shown to occur later in an older cohort than used in the present study and in those with AMD (Gaffney et al., 2013). Due to its diagnostic capacity, the measurement of this parameter has been shown to be of importance (Owsley et al., 2016). Using a stimulus with a diameter and bleach intensity comparable to that of the high bleach intensity used in the present study Gaffney et al. (2011) recorded average time to RCB as being over 5 minutes longer in a healthy control group than that reported here (n=10, mean age 70.5yrs), and over 9 minutes longer in those with early AMD (n=10, mean age 68.3yrs) than that found within this study (n=13, mean age 30.2yrs). This difference can be attributed to the age difference between the present cohort and that of Gaffney et al. (2011). The results suggest that dark adaptation to elicit rod parameters should be measured over a minimum period of 25 minutes in older adults and people with AMD, unless not permitted by participant fatigue.

Cone final threshold, as expected, did not differ significantly between bleach intensities. The diagnostic value of the cone final threshold has been reported to be relatively poor (Owsley et al., 2001). Gaffney et al. (2011) found no significant difference in final threshold between control and AMD groups. Comparatively, the threshold reported by Gaffney et al. (2011) was higher in both the control (-1.92 log cd/m^2) and AMD (-1.94 log cd/m^2) groups than reported in the present study (-2.23 log cd/m^2). This was expected and can be attributed, once again, to the on-average 40 year age difference between the study cohorts.

In conclusion, the results indicate that the dark adaptation parameters of cone τ, cone final threshold, and time to RCB are measurable following the use of a simple hand-held bleaching source. Based on current evidence regarding diagnostic capacity

(Dimitrov et al., 2011; Gaffney et al., 2011; 2013), cone τ and time to RCB were selected as outcome measures for the ALight trial. As the mean time to RCB for the early AMD cohort assessed by Gaffney et al. (2011) using a comparable stimulus was 20.39mins a recording period of 25mins was used for the ALight trial. It was expected that this timeframe would allow time to RCB data to be attained in the ALight cohort without excessive participant fatigue.

Results for the medium and high bleach intensities were consistent with other studies although direct comparison was not possible due to differences in cohort age (Gaffney et al., 2011) and stimulus size (Dimitrov et al., 2011). Overall the results suggested that either bleach intensity could be used for the ALight trial however, the high intensity was chosen to facilitate data modelling, particularly following bleach cessation when assessing cone τ.

Despite this, the pilot study indicated that dark adaptation data collection in this manner is time consuming and requires considerable concentration. Those recruited to the ALight trial would be required to perform this test alongside a number of other visually demanding tasks in a single visit. As a number of the participants in this pilot study commented on the effect of fatigue, it was decided to modify the ALight protocol to include an extra dark adaptation recording session to ensure that the integrity of data collected was not compromised. In alignment with this, dark adaptation was initially performed following the ALight trial screening visit. If necessary, due to poor quality data (as attributable to participant fatigue) dark adaptation was repeated at the baseline visit.

3.7. Pilot study to collect data for flicker threshold and colour vision tests

In addition to dark adaptation parameters, visual function measures of foveal flicker sensitivity and chromatic thresholds have also shown potential as biomarkers sensitive to the characteristics of early AMD (Neelam et al., 2009). The measurement of 14Hz flicker thresholds have been shown to distinguish healthy controls from those with early AMD (Mayer et al., 1991) because it targets the compromised retinal metabolism and blood flow in the presence of AMD (Mayer et al., 1991; Dimitrov et al., 2011). The Colour Assessment and Diagnosis (CAD) test has also been found to be a sensitive method of determining chromatic thresholds which may reflect photoreceptor disruption in AMD (Barbur et al., 2006; O'Neill-Biba et al., 2010). For further detail regarding these tests of visual function the reader is directed to Sections 1.3.6.4. (temporal sensitivity) and 1.3.6.3. (colour vision).

The aim of this experiment was to collect sufficient pilot data on normal subjects to ensure that the experimental methods, hardware and custom software scripts were sufficiently robust to include in the ALight trial.

3.7.1. Method and equipment

Healthy control participants were recruited from the staff and students of the School of Optometry and Vision Sciences, Cardiff University. All subjects had no history of ocular or systemic disease known to affect visual function (the inclusion/exclusion criteria and assessment methods for eligibility are given in Section 3.6.2). The cohort consisted of the same participants (except participant TM) that were included in the study to evaluate the effect of bleach intensity on characteristics of the dark adaptation function (Section 3.6.1). There were no previously reported colour vision defects within the cohort. The School's Research Ethics Committee approved the study, informed consent was obtained before data collection took place and all procedures were carried out in accordance with the tenets of the Declaration of Helsinki.

3.7.1.1. Generation of stimuli

Stimuli for both psychophysical tests were presented on a calibrated, high-resolution monitor (NEC MultiSync PA241/W). The monitor was calibrated with a 26cd/m^2 test background luminance for CAD testing via the bespoke LUMCAL program as supplied by City Occupational Ltd. For the measurement of 14Hz flicker thresholds the luminance of the monitor was also γ-corrected in accordance with the method described by Metha et al. (1993).

3.7.1.2. Experimental procedure

Both tests (CAD and flicker) were performed within a single session of testing following pupil dilation (1% Tropicamide). The eye with the best logMAR visual acuity at 4m was selected as the study eye, and the participant was seated 140cm directly in front of the monitor. Refractive correction was worn as necessary and the non-test eye was occluded. The CAD test was completed first, followed by a 15 minute recovery period before temporal flicker thresholds were assessed (Figure 3.15).

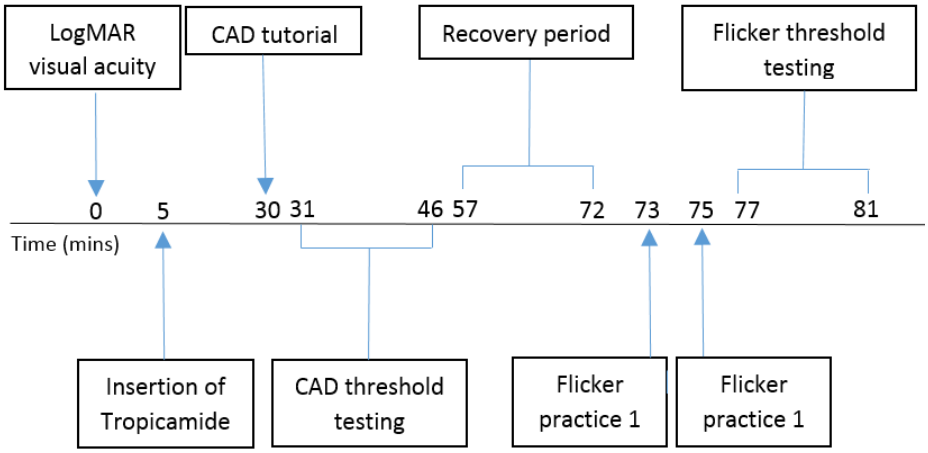

Figure 3.15. Experimental timeline for performance of the Colour Assessment and Diagnosis (CAD) and flicker threshold tests. Prior to visual acuity measurement ocular health was verified.

The Colour Assessment and Diagnosis Test (CAD) (Version 2.2.4. City Occupational Ltd., London, UK) was used to measure RG and YB chromatic sensitivity (Rodriguez-Carmona et al., 2012). RG and YB chromatic thresholds were measured by using

coloured stimuli moving against an achromatic background. By employing dynamic luminance noise to mask the detection of any residual contrast cues, the test isolates chromatic thresholds along 16 directions of the CIE (x,y) chromaticity diagram. The dynamic luminance noise background (chromaticity coordinates 0.305, 0.323; mean luminance 26 cd/m^2) comprised a checkerboard of 15 x 15 squares (total 3.3° diameter) which fluctuated randomly in luminance above and below the average background level. The luminance of each check was distributed with equal probability within ± 55% of the background luminance. The stimulus comprised of a colour-defined checkerboard of 5 x 5 squares (total 1.1° diameter) which over a 600ms duration moved diagonally across the luminance noise in 1 of 4 possible directions. The 16 directions of colour space (6 red, 6 green, 2 blue, 2 yellow) assessed were selected to correspond to the RG (140-175°) and S-cone isolating (58-68°) confusion lines of the CIE chromaticity diagram. Determination of the final RG and YB threshold was based on a 2-down, 1-up staircase in which colour intensity was reduced (by an initial step size of 0.006 CAD units) until the stimulus was not distinguishable against the background. This staircase procedure was repeated for nine reversals. For each reversal the step size was reduced by 0.001 CAD units until a final step size of 0.002 was reached. The chromatic distance in the CIE colour space for the last 4 staircase reversals was averaged in order to determine the final threshold.

The participant was given verbal instructions regarding the test procedure and the four-alternative forced choice nature of the test. The participant was instructed to press one of the four buttons on a hand-held keypad which corresponded with the perceived direction of movement of the stimulus on the screen (Figure 3.16). Each stimulus presentation was followed by an audible ‘beep’ as an indication of when a response was expected. The participant was prompted to respond even if the direction of stimulus movement was not detected. Initially a screening programme lasting 1 minute was run as a training and familiarisation exercise. Once a firm understanding

of test requirements had been demonstrated (deemed as a 100% correct response rate) the participant progressed onto the full threshold measurement program. Time to complete ranged from 12-20 minutes depending on response speed. Throughout the duration of the test the room was uniformly illuminated (69.2 cd/m^2) and the monitor was mounted with a peaked hood to provide optimum conditions for colour accurate viewing.

Figure 3.16. A representation of the participant's view when performing the CAD test (left). The direction of movement seen was responded to using the red keypad buttons shown on the USB remote (right).

Temporal sensitivity to flicker was measured using a well-established QUEST Bayesian adaptive procedure (Watson and Pelli, 1993; Brainard, 1997; Pelli, 1997). This method determines final threshold using the maximum likelihood estimate of threshold based upon the results of all previous trials (King-Smith et al., 1994). As per the code in Appendix V the QUEST procedure was implemented using routines available within MATLAB Psychophysics Toolbox (MATLAB, R2009a, The MathWorks Inc., Massachusetts, USA) to drive a go/no-go adaptive staircase (Brainard, 1997). The starting point for the final threshold estimate (40 trials) was determined from the results of the practice run (10 trials). Responses that occurred more than a second after stimulus offset were deemed as false-positives. The trial stimulus was situated in the centre of the screen and appeared as a 4° Gaussian blob (chromaticity coordinates, 0.305, 0.323; temporal frequency 14Hz) surrounded by a white circle to aid with fixation (Figure 3.17). The stimulus was presented to the fovea at random intervals for a duration of 2 seconds. The flickering stimulus was generated

by modulating a luminance increment according to a sinusoidal temporal profile. The mean luminance of the monitor was 48 cd/m^2. Following verbal instructions on the test procedure and fixation requirements, a familiarisation trial of 1 minute duration was performed before data collection. The subject pressed a button on a hand-held keypad as soon as they perceived the stimulus.

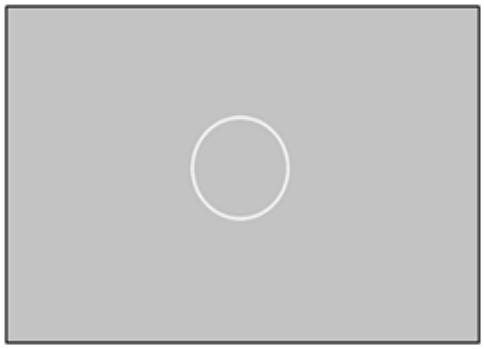

Figure 3.17. A representation of the participant's view when performing the 14Hz flicker threshold test. The white circle provides a fixation target within which each flicker perceived is responded to using the keypad shown in Figure 3.16.

The practice trial was repeated until the participant was able to demonstrate understanding of the test requirements, achieving two successive measurements within 1 standard deviation of each other with no more than 1 false positive over 10 presentations. This allowed progression to the full trial of 40 presentations, taking approximately 4 minutes to complete. The mean threshold value for each test, along with its standard deviation and range, was determined. In order to compare the tests according to the dispersion of values around their mean the coefficient of variation (the ratio of the standard deviation to the mean) was also calculated.

3.7.2. Results

Complete datasets were obtained and analysed from 12 participants. The age range of participants was from 23-48yrs (mean age = 28.7yrs). A sample flicker threshold dataset from one participant is shown in Figure 1.14. For the flicker assessment test, the solid blue line represents the final threshold achieved and the dashed lines either side denote the 95% confidence intervals. The 40 white circles represent the flickering

stimuli presented. Those in which the threshold is seen to elevate following presentation represent unseen stimuli. For the colour vision testing, threshold levels along 16 directions of colour space are represented by the coloured circles found within the larger grey ellipse of the CAD results diagram (Figure 1.11). As all circles fall within the boundary of the ellipse they are deemed to be within normal limits, hence the participant in question does not to have a colour deficiency. The flicker and colour contrast threshold data collected for each subject are presented in Table 3.4. Descriptive statistics relating to test thresholds are displayed in Table 3.5.

Table 3.4. 14Hz Flicker and CAD threshold data as collected from each individual participant.

Study ID	Flicker threshold	RG threshold (CAD units)	YB threshold (CAD units)
AB	-1.82	1.16	1.11
AN	-1.77	1.18	1.31
BF	-1.72	1.17	0.92
CE	-1.81	2.06	1.48
CJ	-1.89	0.96	1.10
GR	-2.00	1.30	1.35
KB	-1.81	1.85	1.89
LR	-1.74	1.32	1.41
LT	-1.70	2.22	1.85
NC	-1.83	1.35	1.28
SJ	-1.70	1.86	1.36
TC	-1.93	1.29	1.38

Table 3.5. Comparison of mean threshold, threshold range and coefficient of variation between each test performed.

Test (n=12)	Mean threshold (+/- SD)	Threshold range (max/min)	Coefficient of variation
14Hz Flicker	-1.81 (±0.09)	-0.30 (-1.70/-2.00)	4.97
CAD (RG)	1.48 (±0.41)	1.26 (2.22/0.96)	27.70
CAD (YB)	1.37 (±0.28)	0.97 (1.89/0.92)	20.53

3.7.3. Discussion

The chromatic sensitivity results obtained are in agreement with those of O'Neill Biba et al. (2010) who found the mean threshold value (± SD) within their control group (n=45, mean age = 56yrs) to be 1.47(± 0.17) for RG testing and 1.60 (± 0.15) for YB

testing. Both values fall within the statistically determined limits of the CAD test as based on analysis of 238 normal trichromats and 250 colour deficient observers by Barbur et al. (2006). In comparison, mean threshold values found for 18 participants at varying stages of AMD were documented outside the normal range as 5.58 and 7.03 (RG and YB respectively) by O'Neill Biba et al. (2010).

Even though flicker and colour vision parameters were not tested using the same units of measurement they may be compared with respect to their between-subject variability using the 'coefficient of variation' which expresses the standard deviation as a percentage of the mean. The least variable results were obtained when testing flicker sensitivity, followed by YB and finally RG colour contrast sensitivity. A higher level of between-subject variability can impact on the diagnostic capacity of a test. These results may help to explain the finding of Dimitrov et al. (2011) that 14Hz flicker threshold testing was better able to distinguish those with AMD from healthy controls (AUC ± SD, 0.84 ± 0.021), than colour threshold testing of both YB (AUC ± SD, 0.80 ± 0.020) and RG (AUC ± SD, 0.77 ± 0.026) parameters. Dimitrov et al. (2011) remarked that, within their cohort, between subject variation in chromatic thresholds may have been attributable to subtle lens opacities.

As the ALight trial measures within subject changes over time the between-subject variability is of less importance than the inter-session repeatability of these tests. In a population of healthy participants (n=30, mean age ± SD: 36.3 ± 14.1) McKeague et al. (2014) found from coefficient of repeatability analysis (CoR ± SD) that the RG CAD threshold test (0.390 ± 0.13) was significantly more repeatable than the 14Hz flicker test (0.015 ± 0.005) when recorded on 2 occasions over 2 days. There was no significant difference between the coefficient of repeatability of the RG (0.39 ± 0.13) and YB (0.43 ± 0.14) CAD thresholds. Threshold values reported by McKeague et al. (2014) were comparable with those presented here (Table 3.6). This was expected due to the similarity in cohorts.

Table 3.6. Comparison of threshold values obtained by McKeague et al. (2014) and those presented here. Bracketed numbers show the standard deviation.

	McKeague et al. (2014) Visit 1	McKeague et al. (2014) Visit 2	Pilot study cohort
RG Threshold (CAD units)	2.33 (±4.58)	2.22 (±4.58)	1.48 (±0.41)
YB Threshold (CAD units)	1.42 (±0.56)	1.33 (±0.56)	1.37 (±0.28)
14Hz Flicker (cd/m^2)	-1.85 (±0.012)	-1.93 (±0.17)	-1.81 (±0.09)

Pragmatically the CAD and flicker tests were performed without issue by all participants. The cohort for the ALight trial was however much older and it was expected that the fast responses and dexterity required for the CAD test might cause difficulty for some individuals. It was thought that this could potentially increase the test time to over 15 minutes. On this basis, the protocol was amended such that participants would be instructed to take regular breaks after 15 minutes had elapsed in order to minimise the effect of fatigue and boredom. It was noticeable that participants were intentionally not blinking regularly when performing the 14Hz flicker test. This, on occasion, caused the sensation that the fixation target had temporarily disappeared thus participants were encouraged to blink as normal during threshold testing. Despite these minor concerns the pilot data collected was found to be comparable with published data and no issue was uncovered relating to the experimental methods, hardware or custom software scripts used which were sufficiently robust to include in the ALight trial.

3.8. Conclusion

This chapter began by introducing the original trial protocol. Additional information was provided regarding the intervention and protocol modifications implemented prior to trial inception. Amendments were made to the protocol with the aim of improving logistical aspects such as the participant recruitment pathway, data collection environment and staff training.

Both of the preliminary experiments described in this chapter resulted in the successful collection of pilot data from normal subjects. Dark adaptation data collected allowed optimisation of the bleaching source and timeframe of threshold measurement. It was also determined that the hand held bleaching source could be used in dark adaptation measurement. The usefulness of each test to monitor disease progression in AMD could not be determined from this pilot experiment. In order to address this, secondary aims of this PhD were to determine the relationship between each functional outcome measure and AMD severity in a cross-sectional evaluation of those with and without AMD, and to use the longitudinal trial data to assess the ability of dark adaptation, colour vision, and flicker thresholds to act as prognostic biomarkers for AMD progression. The results of the cross-sectional analysis are presented in Chapter 4.

Chapter 4. The capacity of four visual function tests to predict an increase in age-related macular degeneration severity

Although hypoxia is implicated in AMD pathogenesis, the aetiology is multifactoral which increases the difficulty of developing targeted treatments. In accordance with this, current treatment is available only for those with nAMD. The early identification of individuals at the greatest risk of developing nAMD would enable targeted monitoring by clinicians. Furthermore, in planning clinical trials of interventions designed to prevent disease progression, identifying those individuals at greatest risk of progression enables an efficient study design to be implemented. This means that tests capable of predicting risk of disease progression are invaluable to both clinicians and researchers. This chapter details a cross-sectional study aiming to understand the prognostic capacity of a battery of psychophysical tests each of which has a body of evidence to support its relationship with AMD severity (Dimitrov et al., 2011; 2012).

4.1. Introduction

Currently, early and intermediate AMD are diagnosed by the presence of characteristic retinal features such as soft drusen and pigmentary abnormalities (Ferris et al., 2013). The standard approach used to determine AMD severity in both clinical and research settings is to grade the extent of these fundus changes using parameters such as size, number, appearance and location (Bird et al., 1995; Ferris et al., 2005; Davis et al., 2005; Ferris et al., 2013). However, the extensive longitudinal data provided by the AREDS trial led to the development of grading scales which not only allow the severity of AMD to be established, but also the 5-year risk of progression to advanced AMD to be determined (AREDS, 2005; Ferris et al., 2005). For example, the AREDS Simplified Severity Scale (Ferris et al., 2005) can be used to establish the risk of progression by summing risk factors (up to a maximum of 4) which include the presence of intermediate drusen in both eyes, the presence of large drusen or pigmentary abnormalities in either eye, and the presence of advanced AMD

in one eye (Ferris et al., 2005). The risk factors are summed across both eyes. The lowest and highest risk groups (0 risk factors and 4 risk factors) were estimated to exhibit a 0.5% and 50% chance, respectively, of progressing to advanced AMD over a 5 year period. However, the presence of drusen and pigmentary change alone is not sufficient to identify those likely to develop advanced disease (Dimitrov et al., 2011). This is exemplified by the low rate of advanced disease manifestation in those over 50 years of age displaying early clinical characteristics (Sunness et al., 1989; Van Newkirk et al., 2000; Smith et al., 2001) and reflected in the low specificity (around 55%) of fundus changes to predict disease progression (Sunness et al., 1989).

Another approach to predicting risk of disease progression may lie in the evaluation of retinal function or OCT-derived anatomical biomarkers. At present, When investigating changes relating to AMD, OCT-derived measurements of retinal thickness are commonplace within clinical and research settings. Retinal layer segmentation tools such as the Iowa Reference Algorithms also allow the assessment of individual retinal layers of specific interest in relation to AMD pathogenesis such as the RPE and photoreceptor layer (Garvin et al., 2009; Antony et al., 2011). Drusen volume analysis has also shown potential as a structural AMD biomarker (Yehoshua et al., 2011; Abdelfattah et al., 2016; Schlanitz et al., 2017). To date, a number of visual function tests have also been identified as potential biomarkers of AMD. These include dark adaptation (Owsley et al., 2007; 2016; Dimitrov et al., 2008; 2011; Gaffney et al., 2011), flicker threshold (Mayer et al., 1992a; 1994; Dimitrov et al., 2011) and chromatic sensitivity (Eisner et al., 1992; Arden and Wolf, 2004; O'Neill Biba et al., 2010). Longitudinal studies of colour-matching (Eisner et al., 1992), colour contrast sensitivity (Eisner et al., 1992; Holz et al., 1995), flicker threshold (Mayer et al., 1994; Luu et al., 2012) and dark adaptation (Owsley et al., 2016; Eisner et al., 1992) indicate that these functional measures also have a prognostic value. This

suggests that relatively simple visual functional tests may be used to identify those at greatest risk of disease progression. Despite this, no published evidence is available to establish the magnitude of the increased risk of progression associated with a worsening performance in each of these tests.

4.2. Aims

The primary aim of this study was to evaluate the ability of dark adaptation, 14Hz flicker threshold, YB chromatic threshold and RG chromatic threshold tests to identify the likely risk of an increase in graded AMD severity . Five-year progression to nAMD risk was determined using the AREDS Simplified Severity Scale (Ferris et al., 2005) as a surrogate. The measures were chosen as candidate functional biomarkers on the basis of strong evidence supporting a relationship with disease severity (Dimitrov et al., 2011; 2012) and preliminary evidence of predictive capacity (Eisner et al., 1992; Holz et al., 1995; Mayer et al., 1994; Luu et al., 2012; Owsley et al., 2016). The study also had two secondary aims:

3. To explore the relationship between the functional and structural outcome measures.
4. To determine the relationship between disease severity and the observed functional and structural deficits.

4.3. Methods

Recruitment for this study took place at the BEH Clinical Research Unit from July 2014 to August 2016. All participants were aged between 55 and 88 years of age and had a corrected ETDRS visual acuity in the test eye of 40 letters (logMAR 0.3, Snellen 6/12) or better. A detailed eligibility criteria list is provided in Section 3.1.3 however, in brief, participants with bilateral advanced AMD, including drusenoid pigment epithelial detachment (DPED) and non-central GA were not eligible to participate in the study. Exclusion criteria also included ocular pathology other than macular disease, significant systemic disease or history of medication known to affect visual

function and cognitive impairment as determined using an abridged MMSE (Schultz-Larsen et al., 2007).

In order to maximise recruitment posters were displayed within the waiting areas of all departments within the eye hospital. All participants were asked if they would pass on leaflets to friends that may participate. Avon Local Optometric Committee was contacted and asked to distribute information (via e-mail) regarding the study to all practices within the Avon area. The local Macular Society was also informed of the research study and provided with posters, leaflets and information at a talk designed to raise awareness regarding research at BEH.

4.3.1. Participants

One hundred participants were recruited to the study directly from BEH Medical Retinal Clinic. Sixty of those who took part were also participants in the ALight clinical trial addressed later in this thesis. All sixty within this cohort had early or intermediate AMD (as classified by the presence of soft drusen and/or focal pigmentary changes) in one eye and nAMD in their fellow eye (as confirmed by fluorescein angiography). The remaining 40 participants were normal or had early AMD in the study eye only, and were recruited from a list of research volunteers at Cardiff University Eye Clinic, clinic waiting rooms at BEH and from amongst the friends of those with nAMD enrolled onto the study. The AMD severity of all participants was graded (0-4 with increasing severity) in accordance with the AREDS Simplified Severity Scale (Ferris et al., 2005). The grading protocol is described in Section 3.3.3.2. In those with no or early AMD only, the eye with the best VA was designated as the test eye. In cases where VA and fundus status were the same, the right eye was assigned as the study eye. In the case of those with unilateral nAMD, the fellow eye (exhibiting signs of early AMD only) was selected for testing. All participants provided informed written consent prior to participation. The study was approved by the NHS Health Research Authority

National Research Ethics Service Committee North West – Greater Manchester South, and all procedures adhered to the tenets of the Declaration of Helsinki.

4.3.2. Experimental procedures

The data from the 60 participants enrolled in the ALight trial were collected at the baseline visit as described in Section 3.3.3. The experimental procedure for the 40 individuals who were not part of the larger trial is outlined here. The consent form and all templates used to record clinical data are shown in Appendix VI. Following a discussion of the participant information sheet, and provision of informed consent, all participants underwent a standardised examination procedure prior to undertaking the functional tests. These baseline tests included a clinical eye examination (slit lamp biomicroscopy of the anterior segment and indirect ophthalmoscopy), assessment of BCVA (4 metre logMAR), an assessment of cognitive function (MMSE; Schultz-Larsen et al., 2007) and an interview regarding ocular history, medical history and medication. Pupillary dilation was achieved using 1% tropicamide and confirmed through assessment of the photopic pupil reflex. The same room was used for all visual function tests for which only the study eye underwent the visual function testing regimen.

Each participant was seated 140cm directly in front of a calibrated high resolution LED monitor (NEC MultiSync PA24/W) when collecting dark adaptation, flicker and colour discrimination threshold data. Refractive correction was worn as required and the non-test eye was occluded. The order of tests used was randomised and all were performed on one visit. To prevent fatigue participants were given short breaks between tests and when necessary participants reattended to repeat a psychophysical test if completion was not possible at their initial visit. All repeat measurements were recorded within 4 weeks of initial assessment. Following visual function testing retinal images were obtained. The acquisition of SD-OCT images was performed using a Zeiss Cirrus SD-OCT 4000 (Carl Zeiss Meditec, Inc., California,

USA). Fundus photographs (30° diameter centred on the fovea) were taken using a Topcon 3D-OCT 2000 (Topcon Medical Systems Inc., New Jersey, USA) and digitally stored. All visual function tests were performed using the same methods and calibrated equipment as described in Chapter 3. For a detailed description of the dark adaptation (Section 3.6.3.1), chromatic threshold (Section 3.7.1.2) and flicker threshold (Section 3.7.1.2) testing regimen the reader is directed to the relevant bracketed section.

4.3.3. Examination of structural outcome measures

The Cirrus HD-OCT instrument was used to acquire 5 images for each participant from which the mean drusen volume measurement was recorded. All images were macular cube scans (200 x 200mm^3 A scans) covering a retinal area of 6 x 6mm^2 (20° x 20° visual angle). A detailed description of the OCT acquisition and drusen volume measurement regimen is described in Section 3.3.3.1. Retinal thickness analysis was performed using OCT Explorer 4.0. This program is part of the Iowa Reference Algorithms (Retinal Image Analysis Lab, Iowa Institute for Biomedical Imaging, Iowa, USA) and is a publicly available, device-independent, graph theory-based tool for segmentation of 10 retinal layers in volumetric OCT images (Garvin et al., 2009; Antony et al., 2011). Of the 5 images taken per participant, the scan with the highest signal strength was chosen for automated retinal layer segmentation. If there were several scans of a similar quality then one was chosen randomly. Retinal layer thickness values were obtained for the foveal subfield and the inner and outer rings of a standard ETDRS grid (Figure 4.1). The thickness of each retinal layer within each subfield was summed to derive a total retinal thickness (corresponding to the distance from the inner limiting membrane to the outer boundary of the RPE).

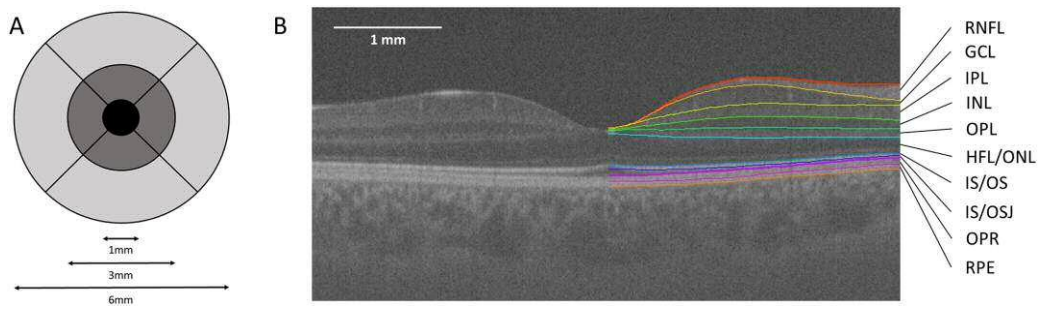

Figure 4.1. ETDRS grid and example 10 intraretinal layer segmentation. (A) Standard ETDRS grid showing three subfields: foveal (black), inner (dark grey) and outer (light grey). (B) Screenshot of 10 layer (11 boundary) segmentation of a long-wavelength OCT image, produced by the Iowa Reference Algorithms. The left half shows the image prior to segmentation. Layers 1-10 (top to bottom, as defined by the software): retinal nerve fibre layer (RNFL); ganglion cell layer (GCL); inner plexiform layer (IPL); inner nuclear layer (INL); outer plexiform layer (OPL); outer plexiform layer-Henle fibre layer to boundary of myoid and ellipsoid of inner segments (OPL-HFL ~ BMEIS); photoreceptor inner/outer segments (IS/OS); inner/outer segment junction to inner boundary of outer segment photoreceptor/retinal pigment epithelial complex (IS/OSJ ~ IB-RPE); outer segment photoreceptor/retinal pigment epithelial complex (OPR); retinal epithelium (RPE) (Terry et al., 2016; copyright permission from PLOS One).

4.3.4. Statistical analysis

All statistical analysis was performed in SPSS Statistics 20.0 (SPSS Statistics for Windows, R2011, IBM Corp., New York, USA). The functional measures used in this investigation may vary with age. Therefore, the first step was to analyse differences in age between graded severity groups using a one-way analysis of variance (ANOVA). The nominal level of statistical significance was set at α=0.05. Following this, to address significant differences between the groups, the second step was to make the data age independent. This was achieved using linear regression analysis to model the relationship between each functional outcome measure and age within the grade 0 AMD severity group (AREDS Simplified Severity Scale; Ferris et al., 2005). The functional outcome values of each participant were adjusted according to the linear regression equation, to that of the mean age of the entire cohort (75.37 ± 7.07 SD) (Figure 4.2). The drusen parameters were not age-adjusted as they are only associated with advancing disease.

The Shapiro-Wilk test was used to assess distributional assumptions. Group comparisons between outcome measures were conducted using the one-way

analysis of variance (ANOVA) test with post-hoc Bonferroni testing (for normally distributed data) or the Kruskal-Wallis with pairwise Mann-Whitney U-test post-hoc comparisons (for non-normally distributed data). In order to account for multiple comparisons P-values were adjusted in accordance with the Holm-Bonferroni adjustment procedure (Holm, 1979). Standard and multiple linear regression analyses were conducted to explore the relationship between the structural (predictor variable) and functional (outcome variable) outcomes. Regression assumptions were tested in accordance with methods described by Altman (1991). This involved testing the distribution of the residuals (calculated as the actual outcome variable value minus the value predicted by the regression model) for normality (Figure 4.3). P, R^2 and pseudo R^2 values were determined to describe the significance of the regression model alongside the percentage of variance explained.

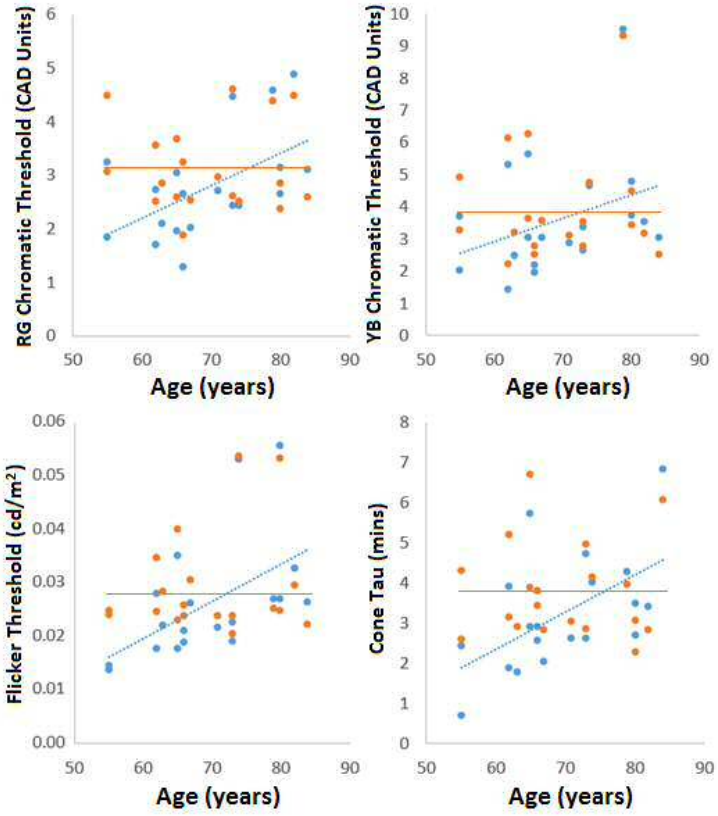

Figure 4.2. Scatter plots for the control group (AREDS Simplified Severity Grade 0; Ferris et al., 2005) showing raw data (blue circles) for each outcome measure and age-adjusted data (orange circles). Linear regression analysis was used to model the relationship between each functional outcome measure (blue regression line) and correct the data to the average age of the cohort (orange regression line).

The predictive value of the visual function tests was estimated using ordinal regression analysis. Ordinal regression models identified as statistically significant (P<0.05) were used to determine odds ratios (calculated as the exponential of each coefficient estimate) for individual and combinations of outcome measures. The assumption of multicollinearity was verified using the test of parallel lines and coefficient estimates were verified as significant (P<0.05, based on Wald test statistic) prior to odds ratio calculation. Odds ratios determined equated to the odds of moving up an AMD severity grade based on 1 unit increase of the outcome measure. The corresponding risk of 5-year progression to nAMD associated with each severity grade was designated as grade 0 (0.4%), grade 1 (3.1%), grade 2 (14.8%), grade 3 (35.4%), grade 4 (53.1%) in accordance with the AREDS Simplified Severity Scale (Ferris et al., 2005).

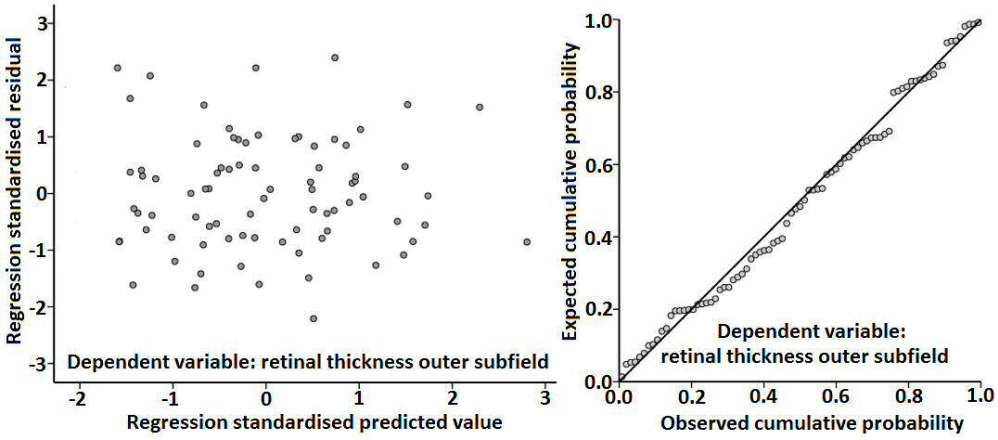

Figure 4.3. Normality testing of residuals in order to satisfy linear regression assumptions (Altman, 1990). Standardised residuals obtained from a retinal thickness regression model are shown in the left panel. The standardisation process involved rescaling each variable to have a mean of zero and a standard deviation of 1. For each case shown, the Y-axis value represents its difference from the mean of the original variable in number of standard deviations. For example, a value of 0.5 indicates that the value for that case is half a standard deviation above the mean. Variables have been standardised in this manner to allow direct comparison of cases and simplify interpretation of results. The X-axis shows the predicted value of retinal thickness for each case as based on the regression model, This value has also been standardised. The normal P-P plot of the standardised residuals shown in the right panel suggests normality indicating the variability of residuals shown in the scatter plot was not sufficient to cause assumption violation.

4.4. Results

The flow of participants through the study is shown in Figure 4.4. One hundred participants were recruited with AMD severity distributed from grade 0 to 4 (mean age 75.37 ± 7.07 SD; 55% female). Participants with an AMD severity of grade 0 (0 risk factors) in accordance with the AREDS Simplified Severity Scale (Ferris et al., 2005) were designated as control participants. The characteristics of each AMD severity group are shown in Table 4.1. All other participants had either early/intermediate AMD only (1-4 risk factors), or advanced AMD in one eye and early/intermediate AMD in the fellow eye (2-4 risk factors). In those with unilateral nAMD, the number of intravitreal injections received at the time of recruitment ranged from 3 to over 20. Mean BCVA in the fellow eye ranged from 0.08 to 0.45 logMAR across all AMD severity grades.

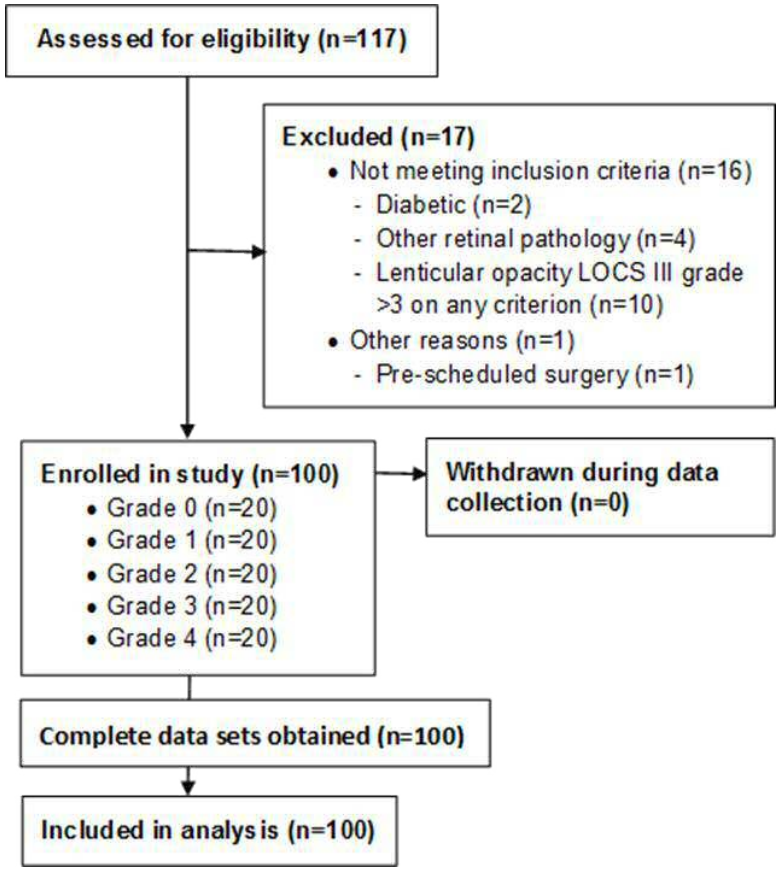

Figure 4.4. Flow diagram of cross sectional study participants. Specified 'Grade' relates to AMD severity as graded using the AREDS Simplified Severity Scale (Ferris et al., 2005). Those graded ≥2 also participated in the ALight clinical trial (results presented in Chapters 5 and 6).

Significant differences were found between the mean age of the grade 0 group (69.58 ± 8.73) and the grade 2 (76.56 ± 8.29; P=0.037), 3 (78.65 ± 6.52; P=0.001) and 4 (77.74 ± 5.37; P=0.006) groups. The relationship between age and each of the functional measures was verified as significant for each outcome measure within the control group (study-eye visual acuity, P=0.02; cone τ, P=0.01; 14Hz flicker threshold, P=0.05; red-green chromatic threshold, P=0.02; yellow-blue chromatic threshold, P=0.05). The functional data were therefore all corrected for the effect of age using the approach described earlier (Figure 4.2). The structural parameters were not age-adjusted as linear regression showed no significant relationship between age in the control group and the retinal thickness of the foveal (P=0.166), inner (P=0.436) and outer (P=0.571) subfields.

Table 4.1. Characteristics of each graded AMD severity group. Raw and age-adjusted means are provided for visual acuity measurements. "AREDS grade" refers to the number of risk factors assigned according to the AREDS Simplified Severity Scale (Ferris et al., 2005).

Participants		Age	Visual acuity (logMAR) Study Eye		Visual acuity (logMAR) Fellow Eye	
AREDS grade	*N (% female)*	Mean (±SD)	Mean (±SD)	Age-adjusted mean (±SD)	Mean (±SD)	Age-adjusted mean (±SD)
0	19 (52%)	69.58 (±8.73)	-0.01 (±0.07)	-0.02 (±0.07)	0.08 (±0.12)	0.05 (±0.15)
1	21 (66%)	74.33 (±6.44)	0.03 (±0.14)	0.03 (±0.14)	0.20 (±0.28)	0.19 (±0.28)
2	18 (44%)	76.56 (±8.29)	0.06 (0.15)	0.06 (±0.16)	0.30 (±0.31)	0.31 (±0.33)
3	23 (56%)	78.65 (±6.52)	0.08 (0.12)	0.08 (±0.12)	0.45 (±0.28)	0.46 (±0.28)
4	19 (58%)	77.74 (±5.37)	0.11 (0.11)	0.11 (±0.11)	0.45 (±0.35)	0.47 (±0.35)

4.4.1. Retinal function and disease severity

Cone τ, 14Hz flicker thresholds and chromatic thresholds were recorded for all participants. One participant was removed from red-green chromatic sensitivity analysis due to congenital protanopia as verified by the Ishihara test. In accordance with Shapiro-Wilk testing and as verified using normal Q-Q plots data were normally

distributed within each severity grade (Shapiro-Wilk, P>0.05) for the functional outcome measures (following log transformation).

Significant differences between groups for each normally distributed outcome measure is shown in Figure 4.5. The mean RG chromatic threshold was significantly lower in the grade 0 group than grades 2 (P<0.001), 3 (P=0.001) and 4 (P<0.001). No significant difference in RG chromatic sensitivity was found between grades 2, 3 and 4. However, the mean grade 1 threshold was significantly lower than grades 2 (P=0.006) and 4 (P<0.001). Fewer significant differences were found when assessing YB chromatic threshold. The grade 4 group was found to have significantly higher YB thresholds than all other groups (grade 0, P<0.001; grade 1, P<0.001; grade 3, P<0.021), except grade 2 (P=0.683). Unlike RG thresholds there were no significant differences found between those graded 1-3. Mean cone τ values were significantly lower in grade 0 than grades 3 (P=0.033) and 4 (P<0.001), and in grade 1 when compared to all subsequent grades (grade 2, P=0.032; grade 3, P=0.001; grade 4, P<0.001). Mean 14Hz flicker threshold values showed fewer significant mean differences across graded severities than any other functional outcome measure. The average flicker threshold value was significantly higher for those with the highest graded AMD severity when compared to all other grades (grade 0, P<0.001; grade 1, P<0.001; grade 2, P=0.015; grade, P<0.001). There was no difference found between controls and those graded ≤3.

Table 4.2. Differences in mean as derived from raw data and age-adjusted mean thresholds across all grades of AMD severity. The small difference between means and age-adjusted means indicates a limited effect of age of the effect of each outcome measure.

	Red-Green Threshold (Log CAD Units)		Yellow-Blue Threshold (Log CAD Units)		Flicker Threshold (Log cd/m²)		Cone τ (Log mins)	
AREDS Grade	Mean (±SD)	Adjusted Mean (±SD)	Mean (±SD)	Adjusted Mean (±SD)	Mean (±SD)	Adjusted Mean (±SD)	Mean (±SD)	Adjusted Mean (±SD)
0	0.97 (±0.35)	1.11 (±0.25)	1.19 (±0.44)	1.30 (±0.36)	-3.71 (±0.37)	-3.55 (±0.31)	1.07 (±0.50)	1.29 (±0.30)
1	1.39 (±0.67)	1.43 (±0.62)	1.43 (±0.51)	1.46 (±0.48)	-3.63 (±0.45)	-3.60 (±0.43)	1.14 (±0.51)	1.18 (±0.50)
2	2.06 (±0.69)	2.06 (±0.67)	1.86 (±0.57)	1.87 (±0.51)	-3.22 (±0.72)	-3.25 (±0.49)	1.55 (±0.36)	1.53 (±0.39)
3	1.84 (±0.47)	1.82 (±0.42)	1.73 (±0.55)	1.70 (±0.55)	-3.33 (±0.20)	-3.38 (±0.24)	1.67 (±0.15)	1.62 (±0.16)
4	2.33 (±0.70)	2.33 (±0.67)	2.17 (±0.39)	2.16 (±0.38)	-2.72 (±0.80)	-2.82 (±0.23)	1.89 (±0.34)	1.86 (±0.35)

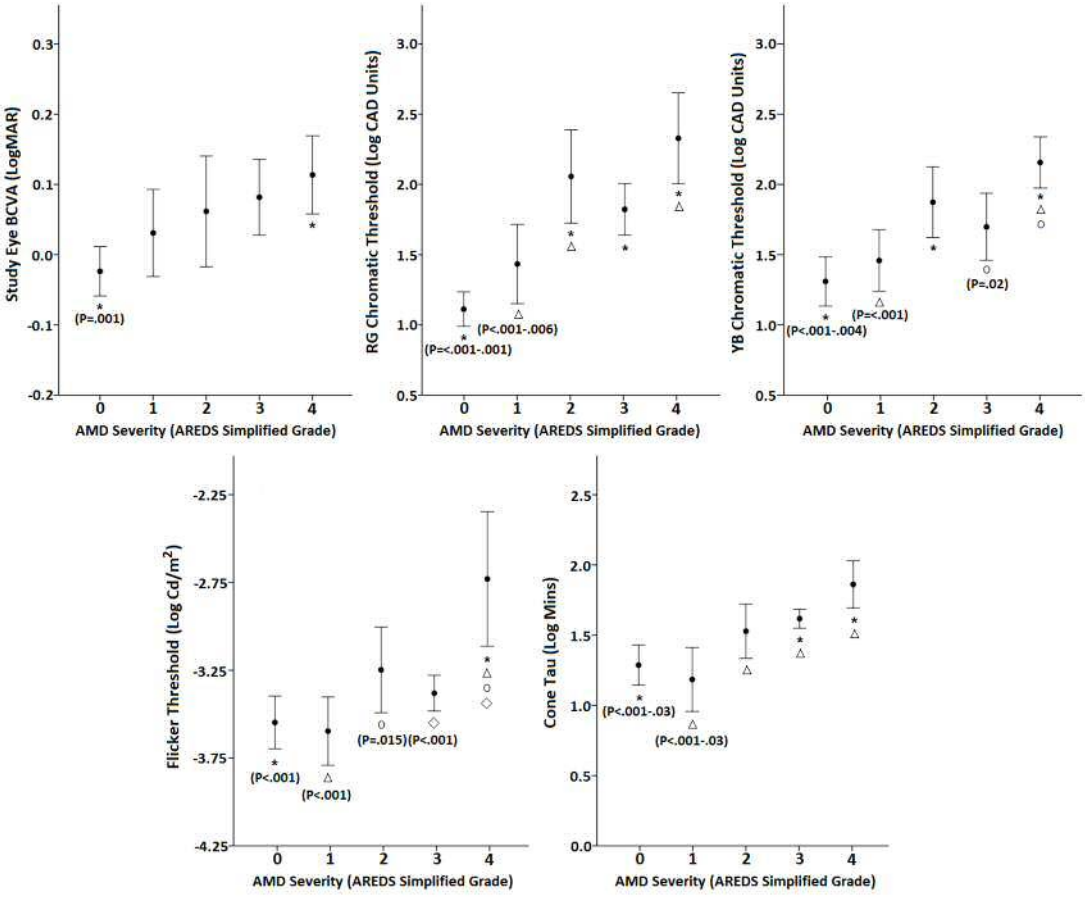

Figure 4.5. Graphs showing differences in age-adjusted means across AREDS grades for 5 functional measures: visual acuity, red-green chromatic sensitivity, YB chromatic sensitivity, 14Hz flicker threshold and cone τ. Significant differences between groups are denoted by the 4 symbols used (asterisk, triangle, circle and diamond). A symbol above a specified P-value denotes a significant difference between that severity grade and all others with the same symbol. When a significant difference exists between one grade and multiple others the range of P-values is displayed.

4.4.2. Retinal structure and disease severity

No data were omitted from the analysis of drusen area, volume and retinal thickness. Measurements of retinal thickness were normally distributed and as such were not log transformed. Drusen data were found not to be normally distributed even after log transformation, hence non-parametric statistics were used to analyse and describe these data. For those graded 0-2 median drusen volume and area measurements were found to be 0.00 (Table 4.3). As shown graphically in Figure 4.6 those graded ≥3 were found to have significantly larger drusen volume and area when compared to those graded ≤2. Retinal thickness data are provided in Table 4.4. Due to the imaging protocol chosen OCT image quality did not permit individual retinal layer segmentation. However, measurements of total retinal thickness were possible. When assessing retinal thickness, mean differences existed between severity groups at the foveal (P=0.040) and inner (P=0.001) subfield regions. The mean foveal subfield was found to be significantly thicker in those graded 0 when compared to those graded 4 (P=0.04). No significant differences in thickness were found between grades 0-3. Similarly, grade 4 subjects had a significantly thinner mean inner-subfield zone than those graded 0 (P=0.001), 1 (P=0.015) and 3 (P=0.018) (Figure 4.7).

Table 4.3. Median and inter-quartile-range (IQR) values for drusen characteristics.

	Drusen Volume (mm3)		Drusen Area (mm2)	
AREDS grade	3mm median (IQR)	5mm median (IQR)	3mm median (IQR)	5mm median (IQR)
0	0.00 (0.00, 0.00)	0.00 (0.00, 0.00)	0.00 (0.00, 0.00)	0.00 (0.00, 0.00)
1	0.00 (0.00, 0.00)	0.00 (0.00, 0.01)	0.00 (0.00, 0.02)	0.00 (0.00, 0.10)
2	0.00 (0.00, 0.00)	0.00 (0.00, 0.00)	0.00 (0.00, 0.05)	0.00 (0.00, 0.06)
3	0.01 (0.01, 0.03)	0.02 (0.01, 0.04)	0.38 (0.21, 0.69)	0.56 (0.32, 1.14)
4	0.01 (0.01, 0.02)	0.03 (0.01, 0.04)	0.40 (0.15, 0.55)	0.80 (0.41, 1.16)

Table 4.4. Mean and standard deviation values for 3 retinal thickness zones: foveal, inner and outer subfields.

	Retinal thickness foveal subfield (microns)	Retinal thickness inner subfield (microns)	Retinal thickness outer subfield (microns)
AREDS Grade	Mean (±SD)	Mean (±SD)	Mean (±SD)
0	288.26 (±24.28)	1331.13 (±56.65)	1147.95 (±54.71)
1	282.61 (±31.01)	1306.72 (±90.28)	1148.74 (±71.99)
2	272.15 (±21.47)	1264.59 (±91.40)	1093.87 (±67.16)
3	278.93 (±29.99)	1303.57 (±78.94)	1139.57 (±54.62)
4	261.75 (±29.22)	1219.33 (±99.74)	1112.75 (±73.44)

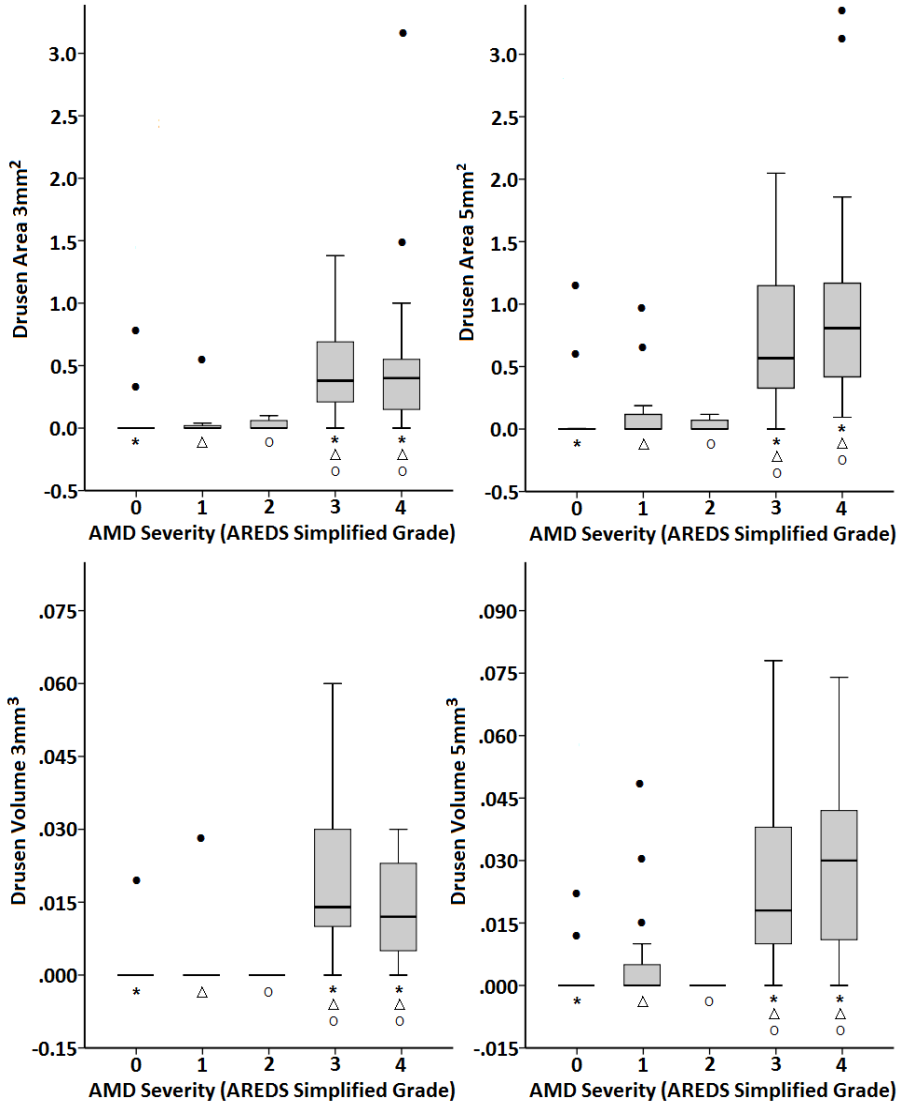

Figure 4.6. Boxplots for each structural outcome measure showing distribution of data across graded AMD severities. Black circles show outliers (calculated as 3 times above IQR). Significant differences between groups (P<0.01) are denoted by the symbols used (asterisk, triangle and white circle). When the same symbol is denoted by more than two groups each group has a significant difference with at least 1 other group denoted by the same symbol. One drusen volume outlier (GP15:1.66/1.74mm³ is not shown as their data extends beyond axis boundaries). A negative y-axis origin has been chosen in order to aid visualisation of the minimum value for all structural outcomes (0.00).

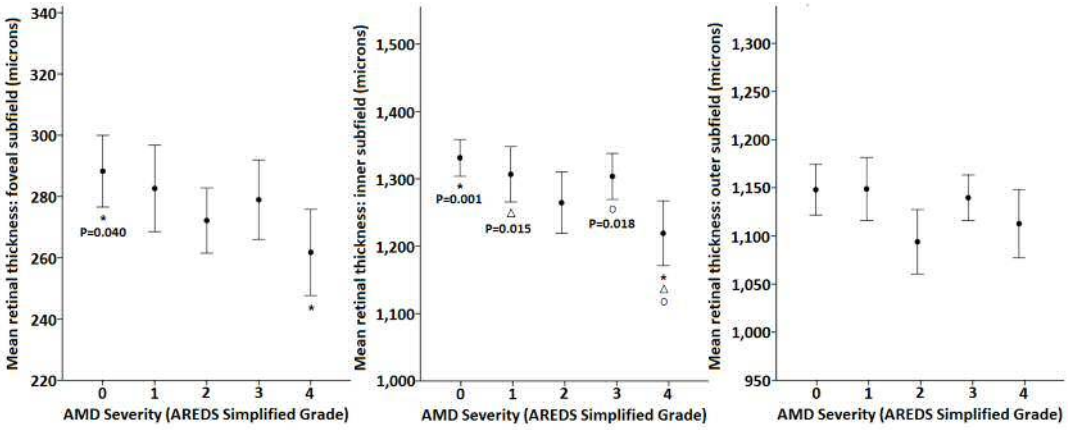

Figure 4.7. Graphs showing differences in means across AREDS grades for 3 subfields of retinal thickness: foveal, inner and outer. Significant differences between groups are denoted by the three symbols used (asterisk, triangle and circle).

4.4.3. Functional and structural outcome relationship

Standard linear and multiple regression were conducted (Table 4.5) to determine the relationship between functional and structural outcome measures. According to standard linear regression analysis the only variable which was a significant predictor ($P<0.05$) of drusen volume (3mm radius around fovea, R^2 0.06, P=0.035) and area (R^2 0.09, P=0.006) was cone τ (Figure 4.8). Despite this, according to the R^2 parameter of the model, cone τ was only able to predict <10% of the variation in drusen volume and area. When retinal thickness was assessed, independent predictors for mean foveal thickness (flicker threshold, R^2 0.06, P=0.035), mean outer retinal thickness (YB chromatic sensitivity, R^2 0.12, P=0.002) and mean inner retinal thickness (cone τ, R^2 0.13, P=0.001; YB chromatic sensitivity, R^2 0.22, $P<0.001$; flicker threshold, R^2 0.18, P=<0.01) were found. Models containing multiple parameters were also found to be significant predictors of mean inner retinal thickness. The most significant multivariate model to predict mean inner retinal thickness (adjusted R^2 0.30, $P<0.001$) included the parameters of YB chromatic sensitivity (P=0.018), cone τ (P=0.020) and flicker threshold (P=0.033). In comparison, a model containing just the parameters of YB chromatic sensitivity and cone τ was also found to be a

significant predictor of mean inner retinal thickness (adjusted R^2 0.28, P<0.001) however it explained slightly less variance.

Table 4.5. Linear and multiple linear regression results. Data are shown only for significant models (P<0.05 model fit). Where models contain more than one test of visual function a coefficient estimate and its corresponding 95% confidence intervals (CI) are shown for each test within the model.

	Variable predicted	β coefficient	95% CI bounds (lower, upper)	P	R^2
Cone τ	Drusen area ($3mm^2$)	0.329	0.095, 0.563	0.006	0.09
Cone τ	Drusen volume ($3mm^3$)	5.151	0.404, 9.898	0.035	0.06
Cone τ	Inner retinal thickness	-0.002	-0.003, -0.001	0.001	0.13
YB sensitivity	Outer retinal thickness	-0.003	-0.004, -0.001	0.002	0.12
YB sensitivity	Inner retinal thickness	-0.003	-0.004, -0.002	<0.001	0.22
Flicker threshold	Inner retinal thickness	-0.002	-0.004, -0.001	<0.01	0.18
Flicker threshold	Foveal thickness	-0.004	-0.009, 0.000	0.035	0.06
YB sensitivity and cone τ	Inner retinal thickness	-64.500 -54.815	-99.733, -29.267 -98.892, -10.742	<0.001	0.28
YB sensitivity and cone τ and flicker threshold	Inner retinal thickness	-46.340 -51.548 -39.870	-84.570, -8.117 -94.704, -8.399 -76.391, -3.350	<0.001	0.30

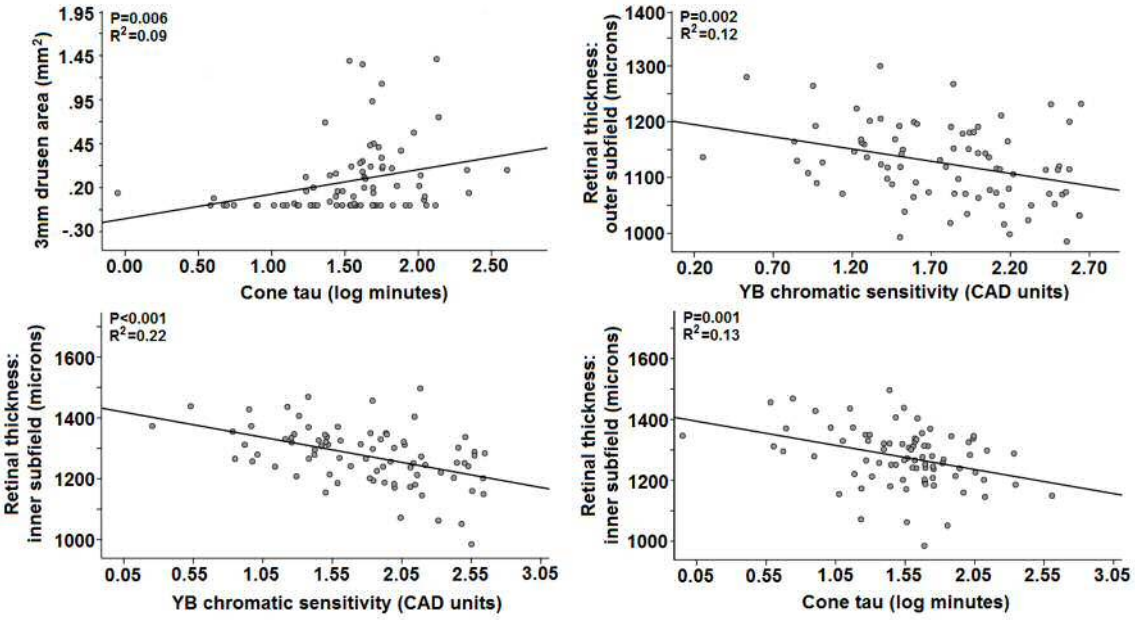

Figure 4.8. Scatter plots showing significant relationships between structural and age-adjusted functional tests.

4.4.4. Outcome measures as AMD predictors

According to the ordinal regression analysis, cone τ (pseudo R^2 0.35, P<0.001) and YB chromatic sensitivity (pseudo R^2 0.16, P<0.001) were found to be independent predictors of increased AMD severity (Table 4.6). The predictive capacity of cone τ and YB chromatic sensitivity together was higher still (pseudo R^2 0.39, P<0.01). When

both tests were used simultaneously odds ratios showed that with every log minute increase in cone τ and every CAD unit increase, the odds of moving up a severity grade are 2.5 and 20 times higher, respectively. For a participant progressing from severity grade 3 to 4 this equates to a 5-year progression risk increase from 35.4% to 53.1% in accordance with the AREDS Simplified Severity Scale (Ferris et al., 2005). Therefore, they are 2.5 times more likely to have a 17.7% increased risk of 5-year progression to nAMD based on 1 log minute increase in cone τ. Flicker threshold was only a significant predictor when used in combination with YB chromatic sensitivity (pseudo R^2 0.27, P<0.001). RG chromatic sensitivity was rejected as a significant predictor by all ordinal regression models. Foveal thickness was the only significant structural predictor (P=0.047) however it explained far less of the variance (pseudo R^2 0.05) than cone τ and was rejected by all multivariate models.

Table 4.6. Ordinal regression results. Data are only shown for significant models (P<0.05 model fit, P<0.05 coefficient estimate, P>0.05 test of parallel lines). P values <0.05 show that at least one coefficient in the model is a significant predictor of increasing disease severity based on the AREDS Simplified Severity Scale. A coefficient estimate is shown for each test incorporated within the regression model (as ordered in the first column). The P-value provided for each β coefficient shows the significance of that coefficient (as based on the Wald test statistic) in estimating an increase in AREDS Simplified Severity grade (Ferris et al., 2005).

			β coefficient 1			β coefficient 2		
	P	**Pseudo R^2**	**Estimate (P-value)**	**Odds ratio**	**95% Confidence interval**	**Estimate (P-value)**	**Odds ratio**	**95% Confidence interval**
Cone τ	<0.001	0.35	3.352 (<0.001)	28.56	2.022 – 4.681			
YB sensitivity	<0.001	0.16	1.408 (0.001)	4.09	0.607 – 2.209			
Retinal thickness: fovea	0.047	0.05	-0.014 (0.044)	1.00	-0.029 – 0.000			
YB sensitivity and cone τ	<0.001	0.40	0.916 (0.034)	2.50	0.069 – 1.763	3.018 (<0.001)	20.45	1.670 – 4.366
YB sensitivity and flicker threshold	<0.001	0.27	0.867 (0.054)	2.38	-0.140 – 1.748	1.587 (0.002)	4.89	0.568 – 2.607

4.5. Discussion

In order for clinicians and those undertaking clinical trials to identify high risk patients for closer monitoring the identification of visual function tests that may enhance the prediction of disease progression in those with early/intermediate AMD would be valuable. Although the hierarchy of early AMD changes based upon visual function tests has been established previously (Dimitrov et al., 2012) such functional outcomes have not previously been utilised to predict risk of progression. In the present study, using the AREDS Simplified Severity Scale as a surrogate, the best predictor of an increase in graded AMD severity was found to be cone τ. When compared to all other vision function tests, cone τ was better able to predict an increase in AMD severity. Out of the remaining 3 functional tests, YB chromatic sensitivity also showed some promise in predicting AMD progression based on severity grading, particularly when used in combination with other visual function tests. In comparison, flicker threshold and RG chromatic sensitivity showed only limited capacity and were least useful.

The present findings are in agreement with Dimitrov et al. (2012) who performed a cross-sectional study to assess the relationship between clinical macular changes and retinal function in 293 participants of varying AMD severity and 64 controls. The adaptational tests (cone and rod recovery) investigated by Dimitrov et al. (2012) were found to show a rapid decrease in functional outcomes at the earliest stage of AMD. The functional deficit exhibited continued to worsen with the manifestation of intermediate and soft drusen and remained stable thereafter, at a low-level of function following the onset of advanced disease. Therefore, it was suggested that adaptational tests would be valuable in identifying those with the earliest form of AMD. In comparison, steady-state measurements of visual function such as 14Hz flicker threshold and blue chromatic threshold have been shown to decrease consistently as clinical grading increases in severity (Dimitrov et al., 2012). Therefore, it was concluded that steady-state thresholds were particularly useful for monitoring AMD

progression over time. In light of the findings of the present study, it might be suggested that these outcomes are less effective as prognostic indicators.

When considering previous longitudinal studies that have examined endpoints predictive of progression to late AMD the present findings are consistent with that of Eisner et al. (1992). Eisner et al, (1992) used a battery of tests (including flicker threshold) and found that foveal dark adaptation rate and S-cone mediated colour-matching were the best predictors of nAMD development. Similarly, the strong performance of cone τ in the present study is also in agreement with a previous study by Owsley et al. (2016) who, by measuring rod dark adaptation, showed that those with delayed dark adaptation at baseline were twice as likely to have AMD in that eye when reassessed after 3 years. Owsley et al. (2017) also reported that rod-mediated dark adaptation may slow in intermediate AMD over 2 years and as such could be useful as a functional endpoint in proof-of-concept studies and clinical trials on intermediate AMD.

The overall delay in dark adaptation in AMD can be attributed to impaired outer retinal function. That is, the intimate relationship between photoreceptor outer segments and the RPE is fundamental to the regeneration of visual pigment molecules following photoisomerisation. Crucially, production of 11-cis retinal by the RPE is the rate limiting step in the regeneration of visual pigment molecules and hence dark adaption rate (Lamb and Pugh, 2004). AMD and the rate limiting set in the dark adaptation process share the same anatomical locus, the RPE cell, and it is for this reason that measures of dark adaptation are consistently associated with AMD, even at its earliest stages (Ambati et al., 2003).

The poor predictive capacity of red-green chromatic sensitivity in comparison to yellow-blue sensitivity is also consistent with current evidence as based on a longitudinal study of 47 subjects with macular drusen reported by Holz et al., (1995). The vulnerability of the blue cone pathway to retinal disease has been attributed to

the S-cone receptors and corresponding ganglion cells (Hood and Greenstein, 1988; Hood et al., 1984; Cho et al., 2000). The limited dynamic response range of the S-cone receptors compared to L and M counterparts has been postulated as a factor resulting in their increased susceptibility to pathological disturbance, such as the hypoxia and inflammation implicated in AMD pathogenesis (Hood et al., 1984). Conversely, the loss could also be due to structural changes that occur to the photoreceptors in early AMD (Curcio et al., 1996; Jackson et al., 2002) or alterations in the post-receptoral retinal mechanisms (Greenstein et al., 1992).

The current findings suggest that the usefulness of flicker sensitivity as a prognostic biomarker for AMD progression based on graded severity is limited. This conclusion appears to be at odds with a report that flicker threshold is decreased in eyes that eventually develop GA or choroidal neovascularisation (Mayer et al., 1994; Luu et al., 2012). However, the study undertaken by Mayer et al, (1994) included a relatively small cohort (n=16 subjects with AMD, n=20 controls). Secondly, comparison with the more robust longitudinal study conducted by Luu et al. (2012) is difficult as 'flicker perimetry' using a different frequency stimulus positioned at different retinal locations to those in the present study was implemented. Although the present findings suggest that flicker threshold is not likely to be a good predictor of the onset of advanced disease, based on other attributes the test has been identified a useful clinical biomarker (Dimitrov et al., 2011). Despite having a lower diagnostic capacity than cone recovery rate, flicker threshold testing was found to be a useful clinical biomarker when factors such as reproducibility, test difficulty and test-time were considered (Dimitrov et al., 2011). This conflicting evidence suggests that flicker threshold cannot be excluded as a potentially useful biomarker for AMD progression until further longitudinal investigation has been conducted.

A good functional biomarker would also be able to monitor disease progression with greater sensitivity than the widely used measure of visual acuity. Although visual

acuity displayed potential to differentiate between those with grade 0 AMD severity and those with the highest AMD severity grading, the tests that showed the largest difference between severity groups, and therefore may have the greatest potential to monitor disease progression were cone τ and chromatic sensitivity. These findings are consistent with a previous study by Dimitrov et al. (2011) who examined the diagnostic capacity, reproducibility and clinical applicability of a battery of visual function tests in 221 subjects with early AMD and 109 controls. Dimitrov et al. (2011) reported that the biomarker with the best diagnostic capacity to distinguish those with early AMD from controls was cone recovery rate. However, comparison of colour threshold with the present study is confounded given that Dimitrov et al. (2011) measured this using a staircase paradigm based on equiluminous foveal red and blue 2° diameter Gaussian blobs. Such a method is unable to mask the detection of any residual luminance contrast signals that may be present. In comparison, the CAD test uses dynamic luminance contrast noise to mask the detection of confounding signals allowing for greater precision when isolating colour thresholds (Birch et al., 1992; Barbur et al., 1994; 2004).

When considering retinal thickness, due to the imaging protocol chosen OCT image quality did not permit analysis of individual retinal layers. Although retinal morphology and macular OCT imaging have previously been shown to correlate well, the separation of adjacent tissues at a retinal level is restricted by the resolution of the OCT image, particularly when the neighbouring tissues have matching relative reflectivity such as the RPE and choroid, or the photoreceptor outer segments and photoreceptor nuclei (Toth et al., 1997). Other drawbacks of OCT imagining which may have impacted on image quality in the present study included: refractive index or media opacification effects, optical attenuation with increasing tissue depth and the misrepresentation of surface contours used to define total retinal thickness by the image processing algorithm (Toth et al., 1997).

Cone τ and YB chromatic sensitivity displayed the closest relationships with the structural measure of retinal thickness. Using OCT analysis a number of studies have evaluated retinal thickness in eyes with early/intermediate AMD (Camacho et al., 2017; Yang et al., 2016; Lee and Yu, 2015; Yenice et al., 2015; Rogala et al., 2015; Savastano et al., 2014; Wood et al., 2011; Schuman et al., 2009; Kaluzny et al., 2009; Malamos et al., 2009) and advanced AMD (Blair et al., 2010; Kashani et al., 2009; Yuda et al., 2010; Zhang et al., 2014). Wood et al. (2011) reported a reduction of mean retinal thickness at the fovea and at a number of extrafoveal points in those with early AMD (n=16) compared to age-matched controls (n=16). Other studies exploring retinal thickness in early AMD have documented focal thinning localised to drusen location but no evidence of a generalised reduction across the macular region (Rogala et al., 2015; Schuman et al., 2009; Kaluzny et al., 2009; Malamos et al., 2009). Localised thinning of the ganglion cell layer (Camacho et al., 2017; Lee and Yu, 2015; Yenice et al., 2015; Savastano et al., 2014) and photoreceptor layer (Schuman et al., 2009; Kaluzny et al., 2009) has also been found in early and intermediate AMD. The importance of Photoreceptor layer thickness measurement is further supported by the finding of an association between decreases in photoreceptor layer thickness in those with early AMD and a deterioration of retinal electrophysiological activity (Yang et al., 2016). In addition, the overall change in retinal thickness in those with GA has also been attributed to photoreceptor loss as assessed in human donor eyes (Curcio et al., 1996).

Due to the increased intraretinal fluid and pigment epithelial detachment, retinal thickness analysis as performed in the present study (using the standard IOWA reference algorithm approach) is prone to segmentation error in those with nAMD (Zhang et al., 2014). Alternatively an automated 3D method of retinal segmentation has been reported by Zhang et al. (2014) which can accurately quantify the outer retinal-subretinal layer thicknesses in the presence of fluid relating to nAMD. This

method, which is currently being assessed in a larger population, facilitates the investigation of thickness changes in the photoreceptor layer of those with nAMD whereas previous studies have targeted the retinal nerve fibre layer (Yuda et al., 2010) and outer-nuclear layer (Kashani et al., 2009).

Although further investigation of the individual intraretinal layer thicknesses and their relationship to functional outcomes in those with AMD is necessary, the findings of the present study in conjunction with current evidence suggest that any change of visual function associated with thinning of the macular region, especially in those with early AMD, may be a candidate biomarker to reflect an increase in graded disease severity.

Drusen volume and area measurement allowed clear differentiation between participants with early/intermediate and advanced disease grades. The lack of variation in drusen volume for those graded 0-2 was likely caused by the insensitivity of the Zeiss Cirrus Advanced RPE Analysis Software or the image protocol used. The elevation map generated by the software apparently permits measurement of drusen area and volume elevations >20μm (Gregori et al., 2011). It is suspected that the on-board Zeiss Cirrus drusen analysis software used in this study was not sensitive enough to identify small RPE deformations and therefore failed to detect drusen <20μm, as well as flat drusen or subretinal drusenoid deposits that are located above the RPE. Those with graded severity ≥3 tended to feature larger, easily measurable drusen, whilst those with lower grades tended to have drusen of a size which was not registered by the imaging software.

A limitation in this study was the reliance on the AREDS Simplified Severity Scale (Ferris et al., 2005) as a surrogate for risk progression to advanced AMD. Although the scale is based on large scale clinical trial data, the predicted progression risk is a marker for AMD progression and as such cannot be directly interpreted as being equal to the actual progression. In addition, multiple tests of significance were conducted to

discern relationships between outcome measures and an increase in AMD graded severity. Although steps were taken to reduce the likelihood of Type I error, repeated testing does increase the risk that significant results arose by chance alone. The study is strengthened by its large sample size, of which 60% of participants were recruited from a robust clinical trial cohort (McKeague et al., 2014). Also, the robust outcome measures tested each relate to a body of evidence supporting their use as effective AMD biomarkers.

4.6. Conclusion

In conclusion, alongside the aforementioned aims in Section 4.2 this chapter has addressed secondary aim 4 (Section 1.5) of this PhD which was to establish the relationship between baseline functional biomarker outcomes and severity of AMD. The identification of two different visual function testing modalities as independent predictors of increased AMD graded severity implies that cone τ and YB chromatic sensitivity may provide different information about the underlying pathological processes in AMD. This may be valuable when used alongside clinical estimation of severity as based on fundus changes and further advocates the use of visual function testing in AMD patients. However, this study evaluated cross-sectional data and evaluated the ability to predict risk of increased severity based on the fundus appearance graded using the AREDS Simplified Severity Scale (Ferris et al., 2005). Whilst this approach has identified promising candidate biomarkers, there is a need for a longitudinal evaluation of these functional measures over a period of years in order to definitively quantify the risk of progression associated with a change in these parameters. Similarly, whilst the significant difference in mean results between AMD grades might suggest that these tests are sensitive to disease progression, it is only through longitudinal evaluation that this hypothesis can be tested. Longitudinal testing as such would improve functional test selection for clinical trials investigating potential

new AMD treatments. An overview of one such clinical trial, as pertaining to this thesis, is provided in the next chapter.

Chapter 5. Overview of ALight trial implementation and intervention safety

To date, there have been three longitudinal studies which have reported on the safety and acceptability of night-time light therapy (Arden et al., 2010; 2011; Sahni et al., 2016). Over 6 and 12 month periods Arden et al. (2010; 2011) reported no difficulty in sleeping or mood alteration associated with the light therapy. Similarly, over a 3 month period Sahni et al. (2016) found no major safety concerns, although they did report a small impairment to daytime alertness and a moderate negative effect on wellbeing (Sahni et al., 2016). Although these studies have assessed the acceptability of sleep mask based night-time light therapy, they targeted the treatment of diabetic maculopathy (Arden et al., 2010; Arden et al., 2011; Sahni et al., 2016). As AMD is a condition that manifests over the age of 55 (Klein et al., 2004) the cohort investigated during the ALight trial allows the acceptability of light therapy to be assessed in an older population. Information regarding clinical trial implementation and intervention safety in a cohort with AMD will be useful not only in future longitudinal studies aiming to investigate the impact of light therapy on progression of this disease, but also for assessing light therapy as a potential long-term treatment for AMD and other pathologies in an ever ageing population.

This chapter begins by providing an overview of key aspects of the clinical trial, such as participant characteristics and recruitment. The chapter goes on to describe an evaluation of the safety and acceptability of the Noctura 500 light mask intervention during the ALight trial, including an analysis of compliance data, and concludes by describing withdrawals from the clinical trial.

5.1. Recruitment and participants

This section provides details regarding the recruitment of participants to the ALight trial which ran from July 2014 to November 2016. Specifically, there is an overview of patterns of recruitment and a description of a modification made to the protocol that

was designed to ensure that the recruitment target (n=60) was met. Participant characteristics are also described. For a detailed overview of the methods for the trial prior to its inception the reader is directed to Chapter 3 and to the published trial protocol (McKeague et al., 2014a) shown in Appendix II.

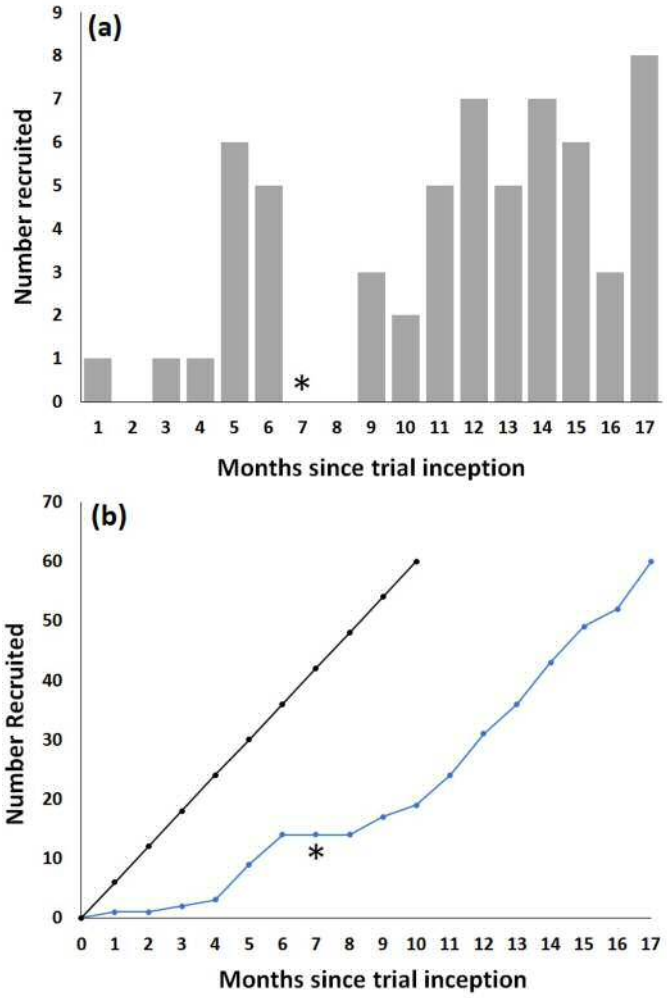

Figure 5.1. Timescale showing monthly (a) and cumulative (b) projected (black) and actual (blue) recruitment figures. The asterisk shows the point in time at which the protocol was amended to improve recruitment.

Figure 5.1 shows the predicted (n=6 per month over 10 months) and actual (n per month ± SD, 4 ±2.79 over 17 months) recruitment timescale. Over the course of the trial, 160 patient information sheets (PIS; Appendix VII) were distributed (n per month ± SD, 9 ± 5.6). The reasons given by those who declined to participate are documented in Figure 5.2. Over a third of those who declined to participate stated that

they did not want to wear a mask whilst sleeping (n=36). Nineteen were deterred by the duration of study appointments as they had others dependent on them or relied on others for transport to and from the hospital. Twelve were happy with the current standard level of care and eleven did not want the additional psychological strain of being involved in a clinical trial. The participants featured in the 'other' category did not wish to participate due to comorbidity issues or impending operations. Thirteen potential participants were identified as eligible using medical notes, and issued with a PIS, however further assessment revealed ineligibility.

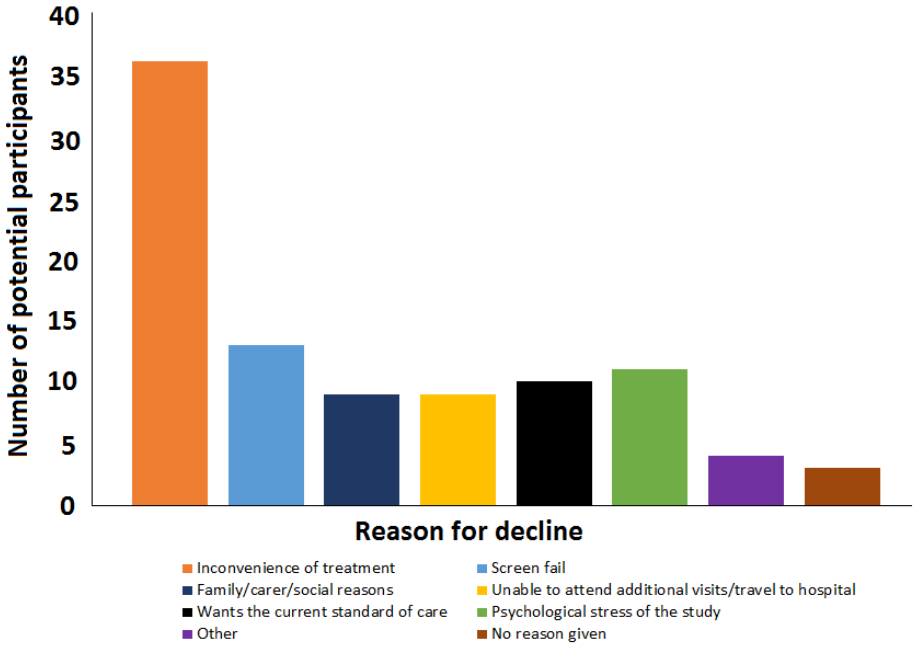

Figure 5.2. Bar chart displaying number of PIS distributed and reasons for decline in participants.

5.2. Recruitment enhancement for clinical trial

The lower than projected recruitment rate 4 months after trial inception not only resulted in a protocol amendment (to the eligibility criteria), but also prompted the original recruitment strategy (Section 3.1.4) to be further developed in order to maximise the number of participants receiving information about the trial. On a weekly basis the investigator was tasked with reviewing the eligibility of the entire list of patients attending the following week's nAMD clinic. Each day, the nAMD clinic patient list consisted of those attending the injection clinic and those booked into the Retinal

Imaging Unit. Potential eligibility, at this stage, was determined on the basis of NHS medical records. Lists of potentially eligible participants were distributed amongst the CRU, Retinal Imaging Unit and Medical Retina Unit staff. In addition, an email detailing the same information was sent to all staff within the CRU. This was done to ensure that eligible patients were not missed in the busy clinic. CRU staff were encouraged to actively search for the specified patient at the designated appointment time if for any reason they had not been contacted by the reception staff upon the patient's arrival. Using this approach, it was possible to ensure that longstanding hospital patients were being informed of the study as well as new referrals to the department.

The recruitment process is summarised in Figure 5.3. Upon arrival of the patient, staff based either at reception or within the Retinal Imaging Unit were advised to alert the study investigator or a member of the CRU immediately so that the potential participant could be provided with verbal and written information about the trial. At this stage, the potential participant was also allowed to examine the light-mask intervention.

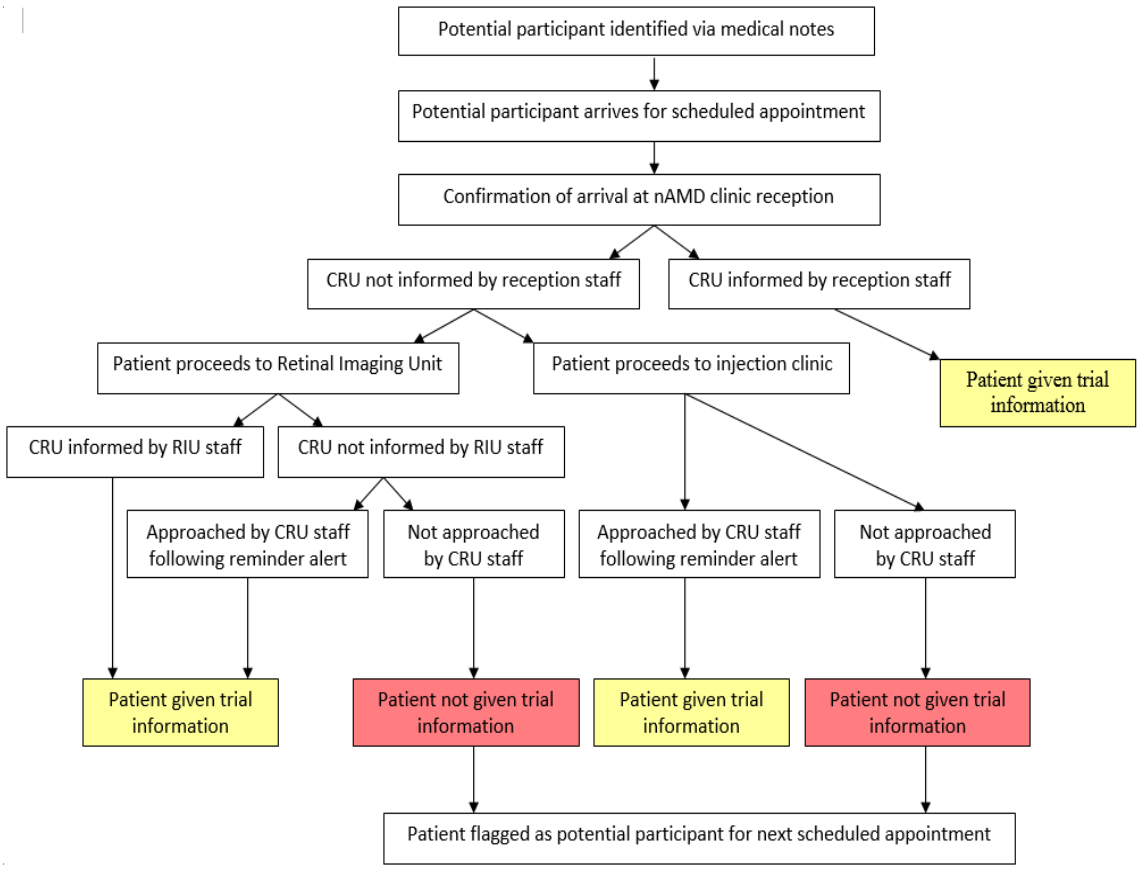

Figure 5.3. Flow diagram summarising distribution of patient information leaflets throughout the Bristol Eye Hospital AMD clinic.

5.3. Participant characteristics

Figure 5.4 shows the flow of participants through each stage of the ALight trial. The cohort in this study overlapped with that presented in Chapter 4, previously described characteristics are briefly mentioned however differences between the present cohort and that of the previous study are described in detail. The target of 60 participants were recruited from the BEH Medical Retina Clinic (average age ± SD, 77.65 ± 6.72; 53% female). Each participant was reviewed on a monthly basis over a 1 year period (+/- 1 month; average time on study ± SD, 372 ± 18.59 days). Case report forms (CRFs) for each study visit are shown in Appendix VIII. All those recruited had early or intermediate AMD (Ferris et al., 2013) defined by the presence of intermediate or large soft drusen and/or focal pigmentary changes in one eye and, nAMD in their fellow eye (as confirmed by fluorescein angiography). The number of unilateral

intravitreal injections received at the time of recruitment ranged from 3 to 36 (mean ± SD, 8.16 ± 8.00). All participants were aged between 55 and 88 years of age (mean age ± SD, 77.74 ± 6.76). BCVA ranged from 0.26 to -0.14 logMAR in the study eyes (mean BCVA ± SD, 0.09 ± 0.12) and 1.06 to -0.14 logMAR (mean BCVA ± SD, 0.39 ± 0.30) in the fellow eyes.

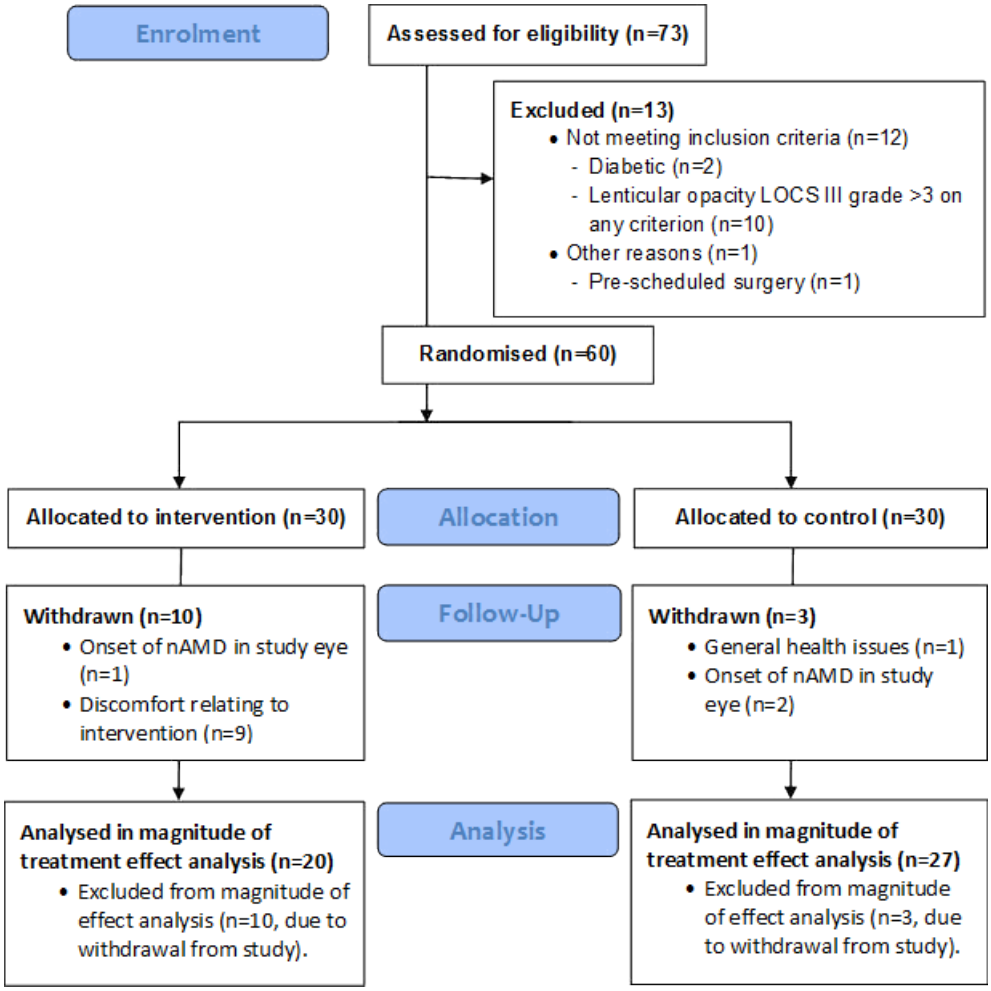

Figure 5.4. Consolidated standards of reporting trials (CONSORT) diagram showing the flow of participants through each stage of the ALight trial.

The grading of retinal images has been described in Section 3.3.3.2. Due to the presence of advanced AMD in one eye and early/intermediate AMD in the fellow eye, severity grades ranged from 2-4 (grade 2, n=18; grade 3, n=22; grade 4, n=20) of the AREDS Simplified Severity Scale (Ferris et al., 2005; Figure 5.5). During the course of the trial no participant displayed increased lenticular opacification beyond 1 LOCS

grade. Mean LOCS gradings (± SD) at baseline were: nuclear opalescence (1.5 ± 1.1), nuclear colour (1.68 ± 1.25), cortical cataract (1.0 ± 0.9) and posterior subcapsular cataract (0.5 ± 0.7). Eleven had an intraocular lens implant (8 bilateral, 3 monocular). No participant underwent cataract extraction within 6 months prior to study enrolment. Two were current smokers (mean pack years ± SD, 28.13 ± 29.17), 30 previously smoked (mean pack years ± SD, 24.43 ± 19.28) and 18 were regularly taking ocular supplements (mean years taken ± SD, 1.95 ± 0.96). A full breakdown of participant baseline characteristics is provided in Appendix IX. Table 5.1 provides descriptive characteristics of each randomisation group.

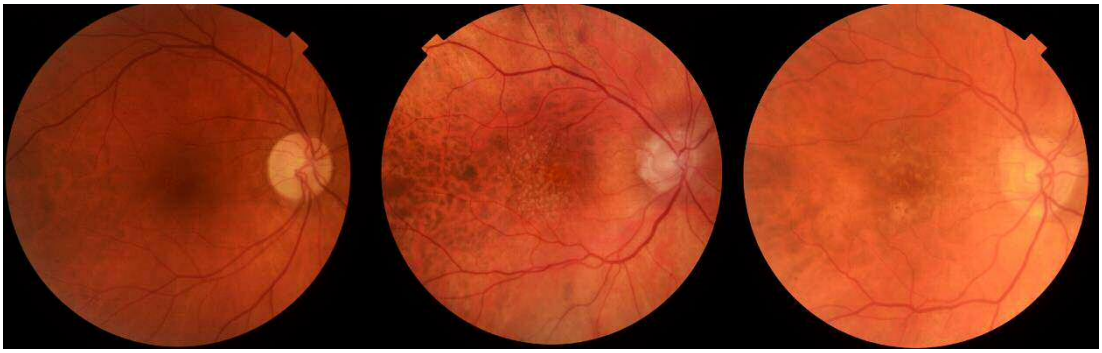

Figure 5.5. Study eye fundus photographs from participants with varying AMD severity grades. In all cases participants had nAMD in the fellow eye, which meant they were attributed 2 risk points from the non-study eye in addition to risk points attributable to large drusen and pigmentary change in the study eye. Severity grades 2 (KW010028), 3 (JC010004) and 4 (GP010015) are shown from left to right. Severity was graded in accordance with the clinical manifestation of drusen and pigmentary change: Grade 2, drusen <125µm only; grade 3, drusen/pigmentary changes ≥125µm only; grade 4, drusen and pigmentary changes ≥125µm (Ferris et al., 2005).

Table 5.1. Table of baseline descriptive statistics for ALight clinical trial participants.

	Intervention	**Control**
Number of participants	30 (60 % female)	30 (53% female)
Mean Age (±SD)	78.30 (± 6.56)	77.17 (± 6.95)
AREDS grade 2 (*N*)	9	9
AREDS grade 3 (*N*)	13	9
AREDS grade 4 (*N*)	8	12
Mean BCVA Study Eye (logMAR ± SD)	0.10 (± 0.12)	0.08 (± 0.12)
Mean BCVA Fellow Eye (logMAR ± SD)	0.38 (± 0.27)	0.39 (± 0.32)
Ocular supplement history (mean years taken ±SD)	0.93 (± 1.29)	0.32 ± 0.63
Smoking history (mean pack years ±SD)	13.89 (± 20.07)	12.42 (± 18.50)

5.4. Research appointment scheduling and protocol violation

During the course of the trial, a number of protocol violations arose relating to research appointment scheduling and the collection of drusen volume data. A total of 701 research appointments were scheduled over a 29 month period (73 screening, 60 baseline, 521 monthly and 47 final appointments) equating to approximately 700 hours. All appointments were carried out by trained study investigators, with over 95% of all appointments being undertaken by the primary investigator (DGR). The total number of study visits taking place in the trial per month ranged from 2 to 51 with no participant returning within 4 weeks of their last monthly follow-up visit. The number of monthly follow-up appointments performed peaked at a little over 40 between months 15 (September 2015) to 17 (November 2015). During this period a combination of baseline, monthly follow-up and final visits were being performed. Recruitment was completed by December 2015 resulting in a drop of study visits overall, however the monthly follow-up rate remained high. Final visits were initiated from June 2015 onwards, 12 months after the first participant was randomised. Half of all final visits were performed between June and October 2016 with the final participant completing their 12 month study cycle on 29th November 2016. For a visual representation of the study visit schedule throughout the trial the reader is directed to Figure 5.6.

The reliance on the BEH nAMD Clinic appointment schedule resulted in participants being seen every 4-6 weeks as opposed to monthly as originally planned. The mean frequency of follow-up visits (days ± SD) was 35 (± 2.06) days across the entire cohort with a range of 21 to 93 days. This resulted in the majority of participants (n=38) completing their 12 month study period with fewer than the expected 11 follow-up visits prior to their final visit. The mean number of follow-up visits per participant (n ± SD) was 9.50 (± 1.00). Forty-six percent of participants completed 10 of more follow-ups. The fewest monthly appointments performed for 1 participant was 7 owing to

their hospital appointment schedule and existing medical health conditions requiring intervention during the course of the study.

Final follow-up visits were carried out for all participants that did not withdraw from the trial. For 6 participants (4 control, 2 intervention) final appointments were conducted outside the proposed timescale of 12 months (± 4 weeks) due to scheduling issues arising from the hospital appointment structure. The intervention participants within this group were 6 and 7 days over the 12 months (± 4 week) schedule and continued to wear the mask through this additional time period. Despite these deviations from the planned structure it is worth noting that the mean number of active days (n ± SD) in the study for both the control (372 ± 18.59) and intervention (372 ± 14.94) participants showed only minimal deviation from the original target of 365 days.

The second cause of protocol violations resulted from a technical issue with the Zeiss Cirrus HD-OCT. Due to hardware malfunction the instrument was unusable for a 9 week period from May-July 2016. As a result, drusen volume data were not collected over 2 consecutive monthly follow-up visits for 24 participants. During this period, end-of-study appointments were still conducted in accordance with the participant timescale specified in the protocol. Following the end-of-study visit, mask wear ceased and missing data were collected as soon as possible following OCT repair. The mean delay in drusen volume measurement for the 5 participants (4 intervention, 1 control) affected by this issue was 7.20 (± 2.89) weeks post final study visit.

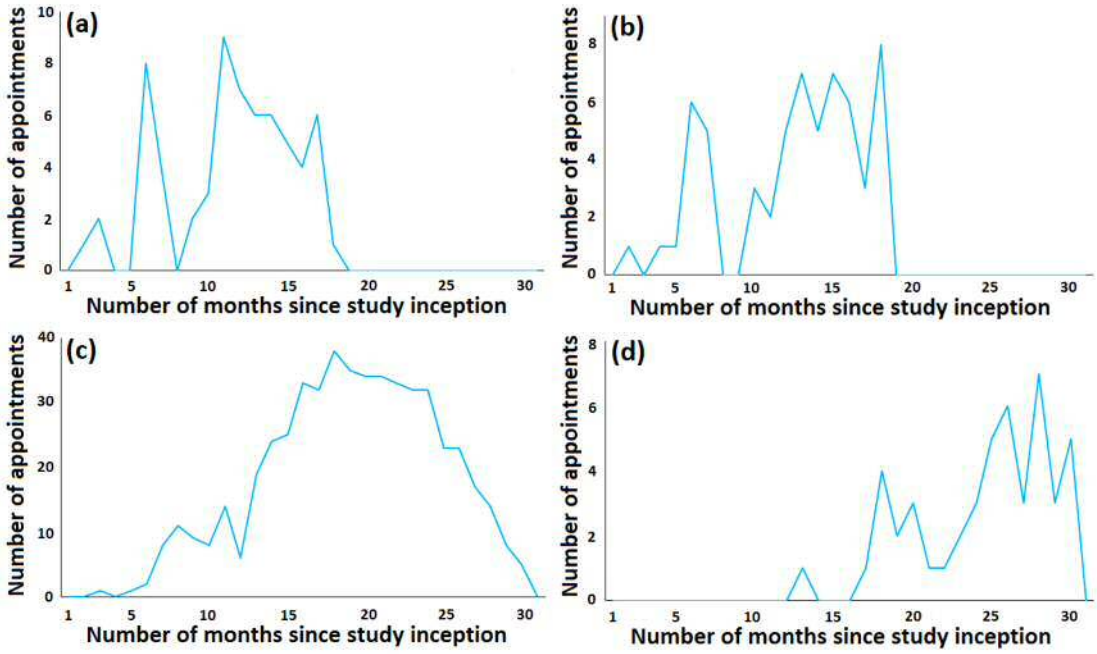

Figure 5.6. Plots depicting the number of screening (a), baseline (b), monthly follow-up (c) and final (d) assessments performed monthly throughout the duration of the trial.

5.5. Safety and acceptability of the intervention

A concern regarding the use of low-level night-time light therapy is potential sleep disturbance. This may occur because a subgroup of retinal ganglion cells containing the photopigment melanopsin has been found to be responsible for mediating light-dark cycles and melatonin secretion (Lyubarsky et al., 1999; Berson et al., 2002; Hattar et al., 2002). Studies that have investigated the nightly use of low-level light therapy (Arden et al., 2010; 2011; Sahni et al., 2016) aimed to investigate the effect in those with diabetic macular oedema, rather than AMD. In addition to this, the methods of suppressing the rod-circulating current and delivering light therapy are not all comparable with the present study (Figure 5.7). Therefore, it could not be assumed that the safety and tolerance to light therapy would be as well received by the participants in this study as it was by those in previous reports. As the illuminance used in the present study has the potential to suppress melatonin secretion by 50-60% (Brainard et al., 2001) the safety and acceptability of the intervention was

monitored throughout the duration of the trial via a number of mechanisms, each of which are introduced in this section.

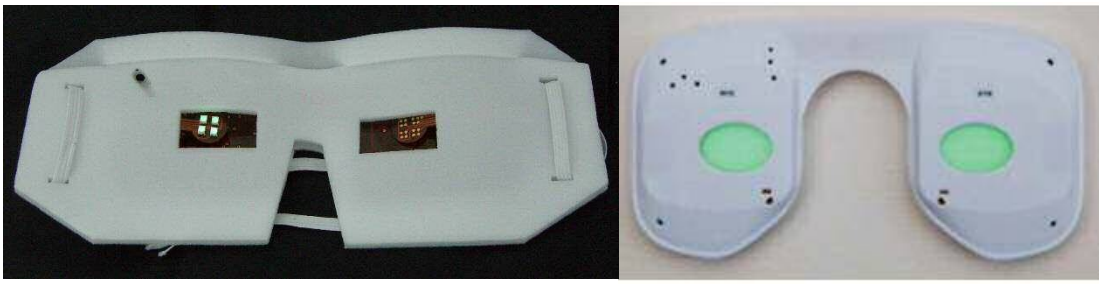

Figure 5.7. Photographs showing the difference in light therapy delivery as used by Arden et al. (2011) (left panel) and in the present study (right panel). The mask used by Arden et al. (2011) utilises four LEDs attached to plastic housing which was enclosed in a thick cotton cover and held in place by an elastic headband. In comparison, the sleep mask utilised in the present study uses OLEDs as an illumination source and is secured to the head via an adjustable velcro strap attached to a padded, synthetic housing.

5.5.1. Aims

This section presents results regarding the following specific aims of the trial: (i) to assess the safety of the intervention and (ii) to determine the acceptability of the sleep mask within a cohort of those with AMD. In order to address this overarching objective the following specific aims were established:

i. To report the number and cause of adverse events for each study group and identify any relationship with the intervention.
ii. To determine differences in sleep quality and total hours slept between the intervention and control groups.
iii. To report changes (and associated reasons) to nightly compliance data over the duration of the trial and seasonally for the intervention group.
iv. To report subjective feedback regarding the intervention from those within the intervention group.
v. To report the number and causes of withdrawals for each study group and identify any relation to the intervention.

5.5.2. Methods

Throughout the course of the clinical trial the safety of each participant was monitored by the recognition, documentation and appropriate management of any AEs or SAEs. For more information regarding the classification of AEs the reader is directed to the protocol in Appendix II. The relationship of any SAE to the intervention was determined by the chief investigator following accrual of any additional information needed to make an informed decision. Information relating to sleep disturbance, discomfort, changes to wakefulness during the day and number of hours slept per night were collected on a monthly basis using the PSQI. The PSQI was chosen due to its well-validated supporting internal consistency (Cronbach's alpha 0.80) (Buysse et al., 1989; Carpenter and Andrykowski, 1998) and discriminative validity (Carpenter and Andrykowski, 1998; Backhaus et al., 2002) across a variety of clinical and healthy populations.

Mask compliance data were collected as specified in Section 3.2. In brief, compliance data were collected at each monthly follow-up visit from a chip housed within the mask itself. The compliance data recorded within the chip were based on a capacitive sensor which logs when the mask is in contact with the face. The mask was connected to bespoke computer software (PPX Works, Polyphotonix Medical, UK) which extracted the data and displayed them graphically and in the form of daily, weekly and monthly tables of hours mask wear. Throughout the duration of the trial a monthly semi-structured interview for those within the intervention group allowed the collection of verbal feedback regarding their mask wear experience. Withdrawals were made as necessary in accordance with the onset of nAMD in the study eye or at participant request.

5.5.3. Analysis

Analysis was performed using IBM SPSS Statistics (SPSS Inc. SPSS for Windows, Version 20.0. Chicago, USA). The main analysis comprised descriptive statistics to

summarise safety concerns (adverse events and serious adverse events). The distribution of continuous data was assessed using the Shapiro-Wilk test. In accordance with the present consensus regarding Likert scale analysis (Sullivan and Artino, 2013; Norman, 2010; Carifio and Perla, 2008; De Winter and Dodou, 2010), questionnaire data were analysed with appropriate parametric and non-parametric tests based on data distribution. Sleep disturbance, as assessed using the PSQI, was scored using the methods described by Buysse et al. (1989). This scoring system uses the 19 individual PSQI items to generate 7 component scores, each reflecting a different component of sleep quality. Summation of the 7 component scores allowed the derivation of a global sleep score, with higher values reflecting greater sleep impairment.

Differences between groups for baseline, change in sleep quality (specified as change in global score from month 1 to month 12 of the study) and number of hours slept per night were compared using an independent samples t-test. Similarly, the independent samples t-test was also used to assess differences between the baseline global PSQI score of those who completed the full study duration and those who were withdrawn. Comparisons between number of hours slept before and during mask wear for the intervention group were made using the paired t-test. Seasonal variation in mask compliance was assessed using the 2016 northern hemisphere meteorological calendar in order to designate seasonal start and end dates (Met Office, 2017). Seasons were designated as: spring (1st March–31st May), summer (1st June–31st August), autumn (1st September–30th November) and winter (1st December–29th February).

For those within the intervention group, differences in monthly compliance over the duration of the trial and seasonal differences in compliance were investigated using a one-way ANOVA test. In accordance with the current consensus on randomised

controlled trials baseline characteristics between groups were not analysed (Roberts and Torgerson, 1999; Egbewale, 2015).

5.5.4. Results

5.5.4.1. Safety of the intervention

All 60 participants enrolled in the ALight trial were included in the analysis of intervention safety. During the course of the study, 33 mild/moderate AEs were recorded (Table 5.2). Most AEs occurred during winter (December-February) and fewest during spring (March-May). The reasons for each AE were assigned into three categories; ocular, general health and falls. All AEs were graded for severity and relatedness to the intervention, as described in the protocol.

Eight ocular AEs were recorded (4 control, 4 interventions; 24% of total AEs recorded) of which 2 occurred as a direct result of ranibizumab injection (MA010002 and PS010047). Ocular AEs recorded for intervention participants resulted in minor disruption to compliance in which mask wear was suspended for a maximum of 1-2 nights. Nineteen AEs (58% of total recorded AEs) were related to GP diagnosed general health issues; a third of which were attributed to cold/flu and sickness/diarrhoea symptoms. One participant (RG010035) reported a period of 4 night's non-compliance, citing nasal pressure caused by the mask leading to increased breathing difficulty during a period of cold/flu symptoms. Six participants (18% of total recorded AEs) suffered falls, all of which occurred during daylight hours. One mask wearer within this category required surgical intervention resulting in a period of sporadic compliance over a 2-week period.

The relationship of events to the study intervention was assessed by the chief investigator using the terms: associated or not associated (see the protocol in Appendix II for further details). Mask wear was deemed not to be associated with any reported adverse events. All ocular manifestations, although potentially aggravated

by mask wear, were a result of pre-existing ocular pathology within the eligibility criteria or occurred shortly after an intraocular injection. The proportion of participants in the intervention group who converted to nAMD was lower than the mean predicted conversion rate of 1% of per month (Section 3.4.1). Falls suffered by intervention participants occurred in daylight hours and all remaining adverse events recorded related to general health conditions commonly found within the age range of the cohort.

Table 5.2. Summary of AEs recorded throughout the data collection period.

Study ID	Date	Severity	Reason	Description	Study Arm
MA010002	Sep-14	Moderate	Ocular	conjunctival ulcer	Intervention
JN010005	Dec-14	Moderate	Muscular pain	Shoulder pain	Control
JN010005	Dec-14	Moderate	General health	Cystitis	Control
MA010002	Dec-14	Mild	Ocular	Dry eye	Intervention
JC010004	Jan-15	Mild	Ocular	Epiretinal membrane	Control
RG010035	Jul-15	Mild	General health	Cold/flu symptoms	Intervention
RH010024	Jul-15	Mild	Fall	Outdoors (daylight)	Control
RJ010021	Jul-15	Moderate	Fall	Outdoors (daylight)	Intervention
ML010036	Aug-15	Moderate	Fall	Outdoors (daylight)	Intervention
JC010011	Oct-15	Moderate	General health	Cold/flu symptoms	Control
CG010025	Nov-15	Moderate	General health	Shortness of breath	Control
PS010047	Nov-15	Moderate	Ocular	Stye	Intervention
JH010039	Dec-15	Moderate	General health	Gout	Control
ML010036	Dec-15	Mild	Fall	Outdoors (daylight)	Control
AW010051	Jan-16	Moderate	General health	Ankle swelling	Control
AW010060	Jan-16	Moderate	General health	Ankle swelling	Intervention
JW010017	Jan-16	Moderate	Muscular pain	Leg pain	Control
JW010043	Jan-16	Mild	Ocular	Epiretinal membrane	Control
AN010020	Feb-16	Moderate	Fall	Indoors (daylight)	Control
PS010047	Feb-16	Mild	General health	Cystitis	Intervention
PB010058	Mar-16	Moderate	General health	Cough	Control
AH010054	Jun-16	Moderate	General health	Sickness/diarrhoea	Control
JH010039	Jun-16	Mild	General health	Gout	Control
AW010048	Jul-16	Moderate	General health	Cold/flu symptoms	Control
AW010048	Jul-16	Mild	Ocular	Dry eye	Control
CE010059	Jul-16	Moderate	Fall	Indoors (daylight)	Control
DR010052	Jul-16	Moderate	Muscular pain	Neck pain	Control
HB010038	Jul-16	Moderate	Ocular	blunt trauma	Control
MM010045	Jul-16	Mild	Muscular pain	Foot pain	Control
RH010045	Jul-16	Moderate	General health	Sickness/diarrhoea	Intervention
PS010047	Aug-16	Mild	Ocular	Conjunctival haemorrhage	Intervention
AH010054	Sep-16	Moderate	General health	Sickness/diarrhoea	Control
AW010060	Sep-16	Moderate	General health	Hiatus hernia	Intervention

Nine serious adverse events took place during the course of the clinical trial (4 ocular and 5 general health related, see Table 5.3). Three participants (1 intervention, 2 controls) developed nAMD in their study eye and were withdrawn accordingly. For 1 participant (CA010016), mask wear was suspended for a month due to a retinal detachment following ranibizumab administration. General health issues that arose included undiagnosed heart disease and routine hip surgery. Two SAEs documented within a short time frame relate to a control participant (JW010023) who died shortly before completing their full study period.

Table 5.3. Summary of serious adverse events recorded throughout the data collection period.

Study ID	Date	Reason	Description	Study Arm
EA010007	Nov-14	Ocular	nAMD in study eye	Control
MA010002	Nov-14	General health	Heart disease	Intervention
CA010016	Aug-15	Ocular	Retinal detachment	Intervention
MH010029	Sep-15	Ocular	nAMD in study eye	Control
BP010040	Oct-15	Ocular	nAMD in study eye	Intervention
CA010016	Nov-15	General health	Hip surgery	Intervention
AH010054	Dec-15	General health	Heart disease	Control
JW010043	Aug-16	General health	Cancer	Control
JW010043	Aug-16	General health	Deceased	Control

5.5.4.2. Acceptability of the intervention: compliance data

Twenty intervention participants completed the study period (± 1 month). The masks' 12 week lifespan resulted in each participant receiving 5 masks in total over 1 year at various intervals. Due to reliance on the hospital AMD clinic timetable it was not possible to arrange a final study visit exactly 12 months after baseline therefore the number of days of mask wear over the study period differed for each participant. The mean number of night's worn (± SD), taking into account nights of complete non-compliance, was 372 (± 15). An example of monthly compliance data collection is shown in Figure 5.8 and final compliance data are shown in Table 5.4.

For those who completed the entire study duration, compliance data collected directly from the mask reported an average of 2067 (± 591) hours mask wear (± SD), taking into account nights of complete non-compliance, per participant over an average of 372 (± 15) days. This equated to 5.60 hours of mask wear per night or to 69% (± 19%) of the maximum achievable compliance (100% based on 8 hours of nightly mask wear). Monthly PSQI data specifying number of hours slept per night did, however, show that only a quarter of mask wearers reportedly slept 8 hours per night on average over the study duration. In order to derive a more realistic compliance rate, the compliance data were also assessed monthly by dividing each participant's average number of mask hours worn per night by their reported average number of hours slept per night (as specified by the PSQI response). The average compliance calculated for each participant across the 12 months was then averaged across participants to derive a final mean compliance rate of 78% (± 23%). The reported mean hours (± SD) slept per night as subjectively recorded from the PSQI was 7.19 (± 0.89) and the average nightly hours mask wear (± SD) as per objective mask data was 5.63 (± 1.54). No significant difference (one-way ANOVA with repeated measures, $P>0.05$) in mean hours of mask use per month was found over the study duration i.e. according to the number of months enrolled in the trial (Figure 5.9).

To explore seasonal variation, mean hours mask wear per participant were derived for each season in accordance with the 2016 northern hemisphere meteorological calendar (Met Office, 2017). The mean nightly hours worn (± SD) across all mask wearers (n=20) was highest during winter (5.73 ± 1.67), followed by summer (5.62 ± 1.77), spring (5.53 ± 1.98) and autumn (5.22 ± 1.67). No significant difference in mean hours of mask use per season was found over the study duration (one-way ANOVA with repeated measures, $P=0.33$).

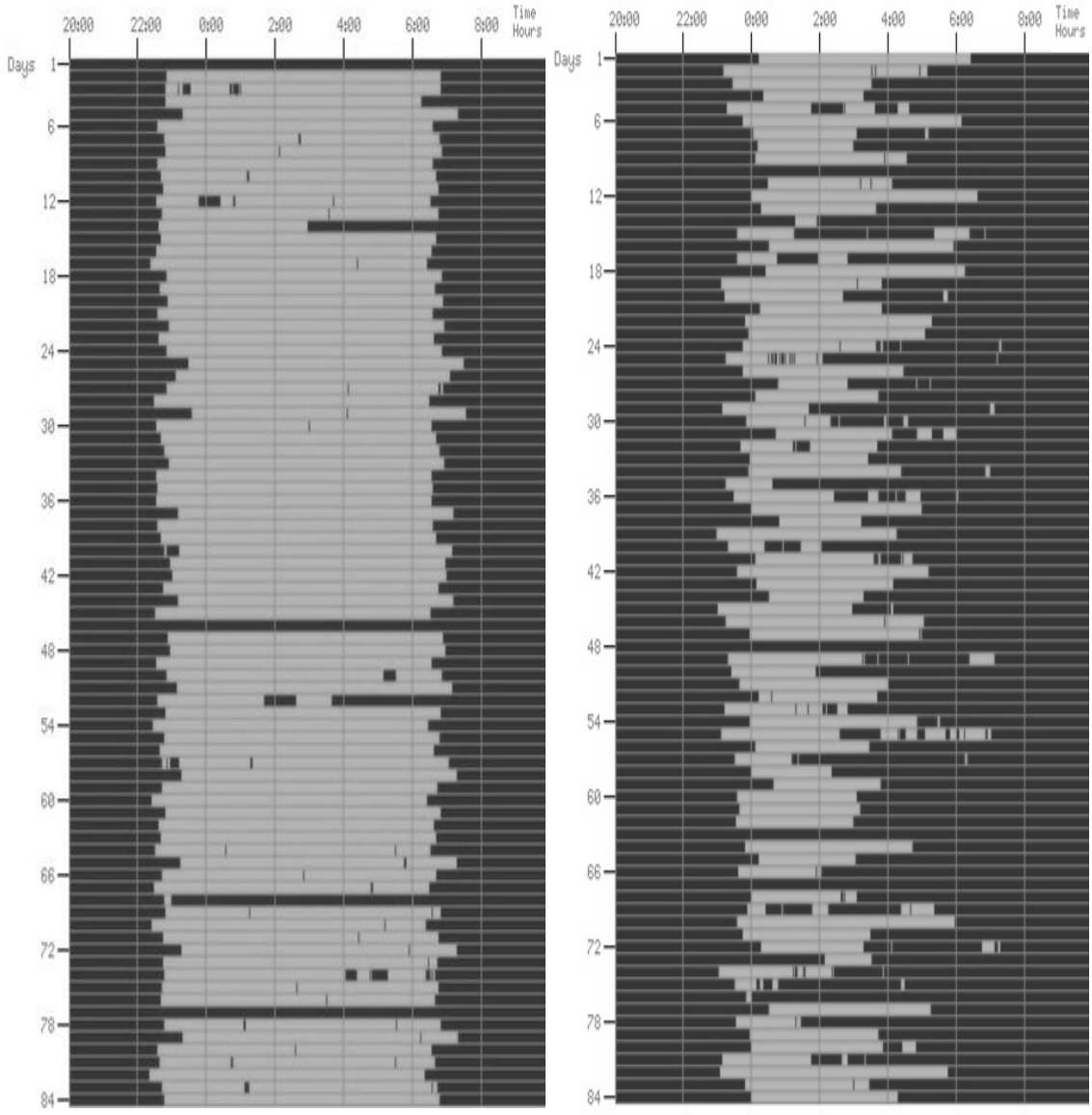

Figure 5.8. Twelve-week objective compliance data as collected directly from the masks of 2 participants. The left panel shows a compliant wearer (JG010014). The right panel shows a wearer reporting regular mask displacement throughout the night (MN010003).

Table 5.4. 12 month (±1 month) compliance data for the 20 intervention participants who completed the trial. All times are given in hours. Mean hours slept per night is derived from subjective feedback (PSQI questionnaire), total days worn and mean nightly hours mask wear are derived from objective mask compliance data.

Study ID	Total days worn	Total wearing time	Compliance rate (%)	Mean hours slept per night (±SD)	Mean nightly hours mask wear (±SD)
MN010003	383	1253.43	40.91	6.83 (± 0.42)	3.65 (± 2.10)
FC010009	370	2514.73	84.96	8.00 (± 1.33)	6.80 (± 1.91)
CS010012	364	2250.07	77.27	5.80 (± 1.30)	6.18 (± 1.65)
JG010014	400	2935.90	91.75	8.20 (± 0.25)	7.30 (± 1.69)
CA010016	393	2105.87	66.98	6.35 (± 0.40)	5.90 (± 3.21)
JB010019	364	2249.40	77.25	7.25 (± 1.27)	6.25 (± 2.41)
RJ010021	387	1925.47	62.19	7.58 (± 0.36)	4.93 (± 3.27)
RH010024	357	1720.87	60.25	8.55 (± 0.77)	4.95 (± 3.45)
KW010028	388	2716.30	87.51	7.90 (± 0.30)	7.15 (± 1.79)
DB010031	356	2203.20	77.36	6.40 (± 0.60)	6.22 (± 1.58)
AB010032	374	2250.13	75.20	6.98 (± 0.41)	6.03 (± 2.11)
SG010033	363	2191.77	75.47	7.55 (± 0.45)	5.97 (± 1.62)
RG010035	376	186.27	6.19	8.30 (± 0.32)	0.47 (± 0.76)
WB010037	353	1985.23	70.30	6.08 (± 0.30)	5.62 (± 2.00)
VB010042	399	2408.07	75.44	7.93 (± 0.16)	5.95 (± 1.63)
RH010045	364	1970.97	67.68	8.10 (± 0.42)	5.37 (± 2.19)
GL010046	356	2047.07	71.88	6.18 (± 0.40)	5.77 (± 2.39)
PS010047	357	2120.47	74.25	6.50 (± 0.47)	5.95 (± 2.14)
JL010056	364	1588.50	54.55	7.40 (± 0.64)	4.25 (± 2.76)
AW010060	373	2714.13	90.96	5.87 (± 0.56)	7.28 (± 0.89)

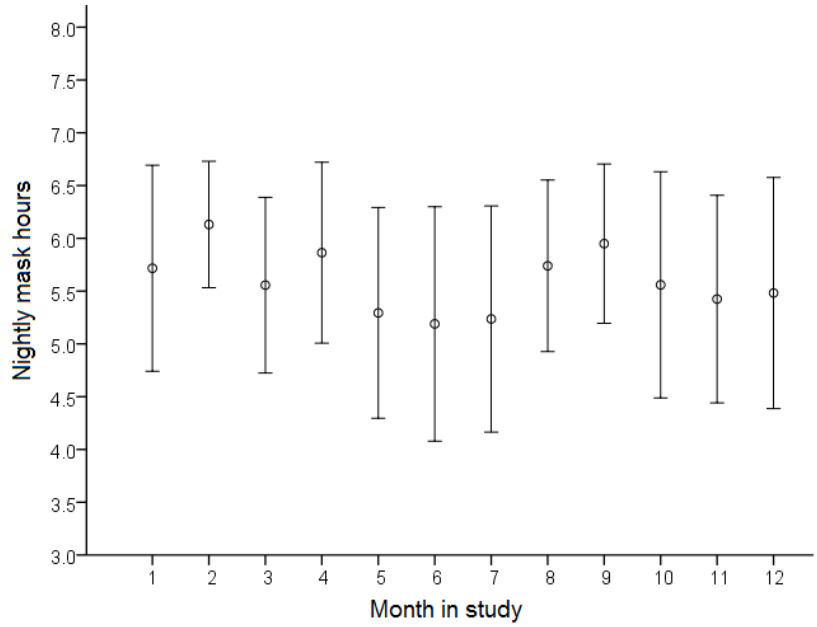

Figure 5.9. Means plots for average nightly hours mask wear each month over a 1 year period. Error bars represent 95% confidence limits.

5.5.4.3. Acceptability of the intervention

Subjective feedback regarding mask wear from those within the intervention group is introduced in detail in this section. Participants reported issues relating to mask comfort, design and disturbance to habitual routine throughout the trial in their monthly semi-structured interviews. Figure 5.10 provides an overview of negative participant feedback relating to the intervention.

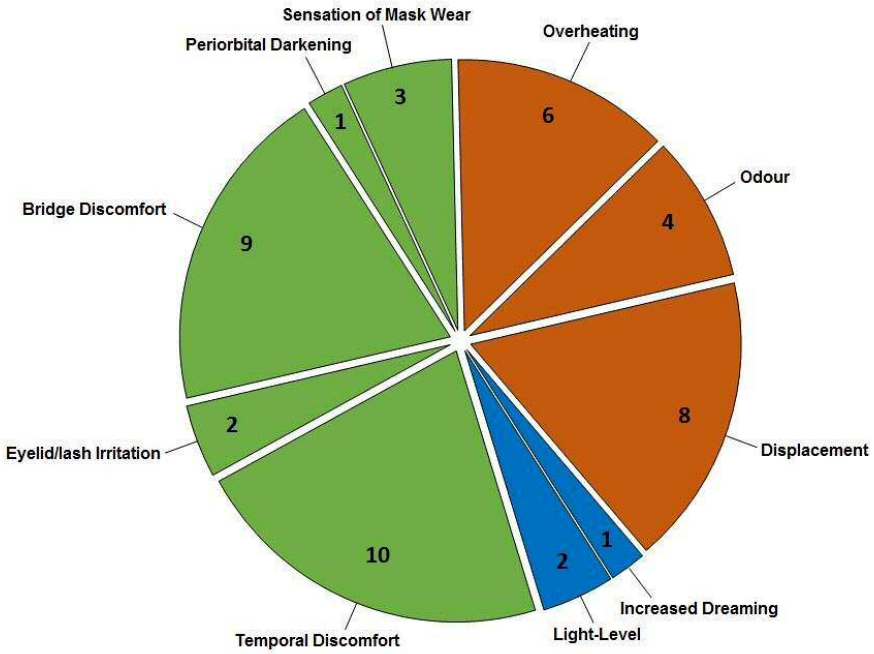

Figure 5.10. Negative mask wear feedback divided into three groups; comfort (green), design (orange) and sleep disruption (blue). Numbers denote the number of participants that reported each observation.

Of the original 30 mask wearers, 10 cited discomfort as a result of temporal pressure caused by mask wear when sleeping in a sideways posture. This issue contributed to the withdrawal of 3 participants and was reported most commonly by physically smaller participants who also cited issues with the mask size in general. One participant (GL010046) was able to successfully adopt a new sleeping posture to avoid this issue. Another source of discomfort arose as a result of contact between the mask housing and the eyelids/lashes (n=2). The irritation attributed to this sensation caused increased tearing in one participant resulting in damp mask fabric and skin friction. Pressure on the nasal bridge was experienced by 9 mask wearers,

3 of which were eventually withdrawn. The nasal pressure resultant from mask weight was reported to cause bridge indentation following overnight usage (n=2) and disrupted nasal breathing (n=2), particularly in the presence of cold/flu symptoms. All discomfort issues were reported on a constant basis for the duration of the trial. In order to alleviate nasal pressure a number of participants modified their masks (Figure 5.11)

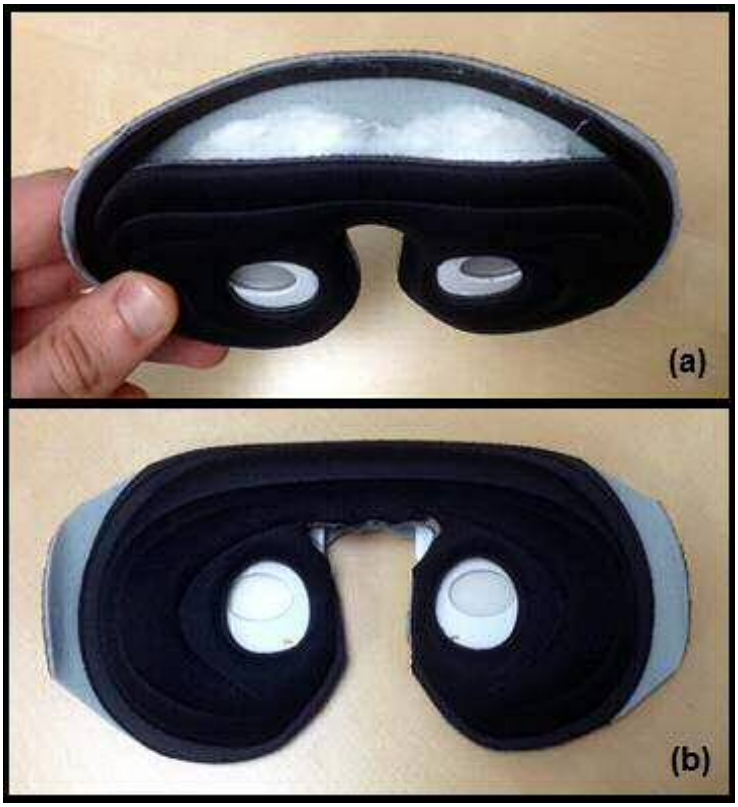

Figure 5.11. Photograph of mask modifications as performed by participants in an attempt to improve comfort. The padding applied in (a) was performed by a number of participants using cotton wool and folded fabric. As verified by the trial investigator this modification did not inhibit effective compliance data collection or light therapy administration. In contrast the modification displayed in (b) was potentially damaging the mask at a functional level. The mask wearer in (b) was eventually withdrawn due to persistent mask discomfort.

One participant (JG010014) encountered no discomfort, however subjectively reported increased periorbital darkening 2 months following initiation of mask wear. As this event was isolated, ophthalmic examination revealed no underlying pathological cause and the symptom did not worsen with continued wear. It was therefore not attributed to the intervention. Despite having no specific complaint of physical discomfort, 3 participants were unable to use the intervention on a nightly

basis as they became anxious with the concept of mask wear, preferring not to be visually enclosed upon awakening. This problem continued beyond 2 months for only 1 participant (RG010035) who described a ‘claustrophobic’ sensation encountered during mask usage.

The synthetic housing used for the mask was repeatedly reported to cause two issues relating to temperature and odour. Six participants cited the fabric as a cause of facial overheating. Although seasonal, this effect was a common complaint for all participants demonstrating a compliance <65% of the maximum achievable annually. New fabric housing was also described as emitting a ‘chemical’ smell for up to 1 week post initial usage. Despite causing some participants to wash the mask housing this reported issue was always temporary.

Loss of compliance as a result of mask displacement throughout the night was a common finding. Eight of the 30 original mask wearers reported waking up without the mask in position in at least 1 monthly follow-up appointment. 2 participants (MN010003 and JL010056) cited this as the primary reason for reduced compliance. Both participants also reported that tightening the mask fit until displacement ceased resulted in increased frontal/nasal pressure beyond tolerance. All participants who repeatedly reported displacement felt that once affixed the strap strength alone was adequate to prevent mask dislocation via general head movement during sleep. Displacement was instead speculated to be resultant of subconscious manual removal.

No mask malfunction was reported throughout the duration of the trial. Monthly inspection revealed damage to the fabric housing only as a result of usage (Figure 5.12). Participants were regularly given extra fabric sleeves to use if they felt wear and tear to the current mask housing was sufficient to warrant changing. No issues arose regarding activation of the mask. Two participants who reported nasal discomfort returned their pods with bridge damage (Figure 5.12). This issue did not

disrupt mask function despite the potential for connectivity damage between eyepieces.

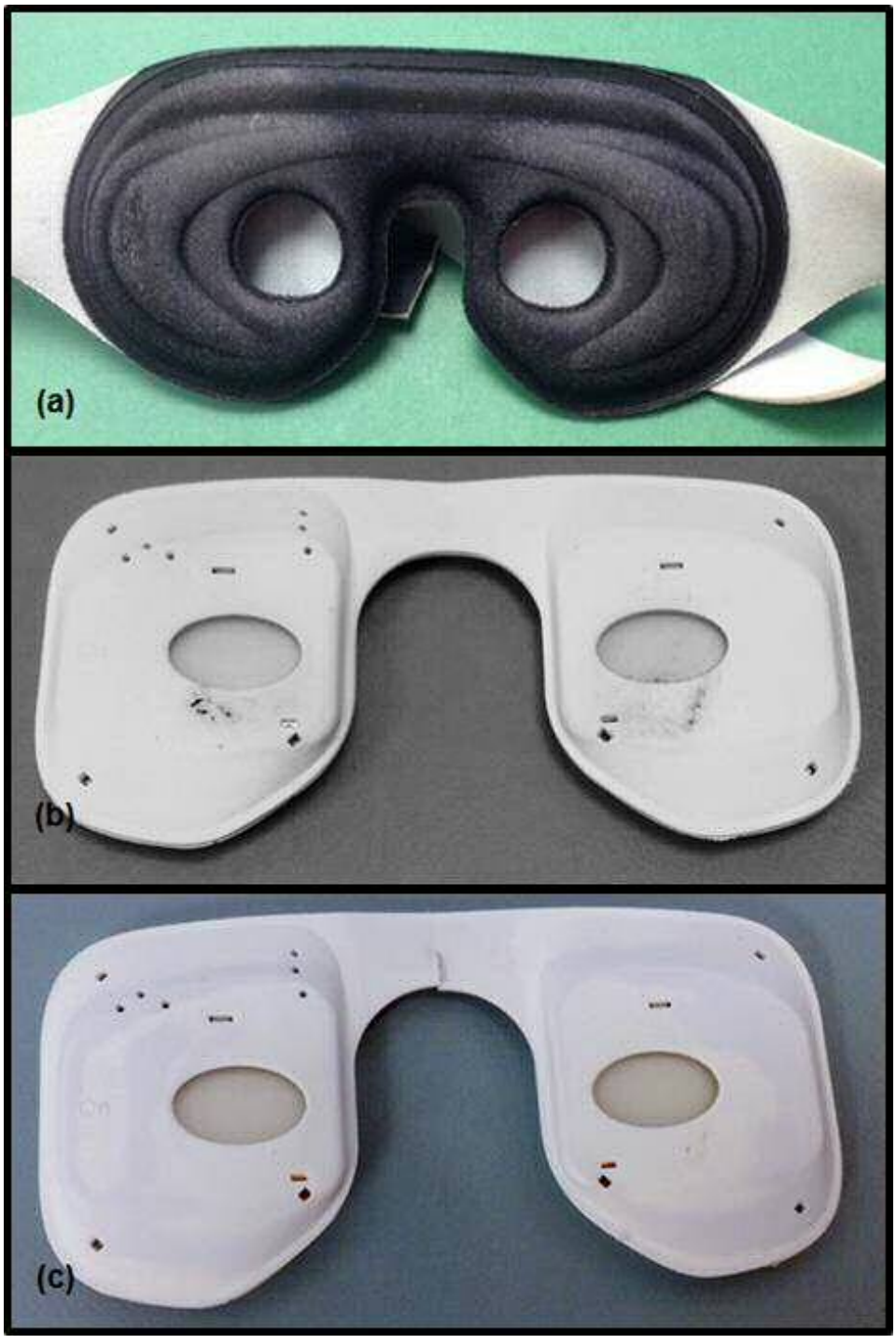

Figure 5.12. Photograph of (a) housing, (b) pod and (c) bridge damage as a result of usage.

5.5.4.4. Sleep disturbance questionnaire data

No major disruption to falling asleep or increased daytime lethargy was reported for any participant. One participant experienced a sustained increase in dream/nightmare regularity after initiating mask wear which subsided after a 2 month period. At first exposure, the light level was tolerated well by the majority of participants. Described sensations of glare (RH010045) and dazzle (RG010035) were found to subside within an 8-week period after which no further issues relating to luminance were reported. Continuing nightly exposure to low-level light therapy post 8 months resulted in the most compliant wearers (n=2) describing the illumination as 'comforting', aiding their ability to fall asleep. Three participants reported buying non-illuminating sleep masks for post-trial use attributing their improved sleep habits to the introduction of mask wear.

In addition to the subjective feedback, further analysis regarding sleep disturbance was conducted on the PSQI data of the 47 participants (27 controls, 20 intervention) who completed the full study cycle. No significant difference was found between the study groups for the mean baseline global score (independent samples t-test; P=0.16) suggesting that neither group contained more inherently poor sleepers. Mean baseline and 12 month global scores for each group are shown in Table 5.5. At the 12 month stage no significant difference was found in the proportion of each group designated as a 'poor' sleeper in accordance with the PSQI global score (control, 59%; intervention, 60%; Chi squared test, P=0.46). Similarly, over the study duration there was no significant difference in PSQI global score change between groups despite a higher proportion of mask wearers (65%) than controls (41%) reporting greater sleep disturbance after 12 months (independent samples t-test, P=0.19). Usable post-baseline PSQI data were only available for 8 of the 10 withdrawn mask wearers as 2 intervention participants did not surpass their 1 month follow-up. No significant difference was found between the baseline PSQI score of those who

remained within the study and those who were withdrawn (independent samples t-test, P=0.29).

There was no significant difference in the subjectively reported mean number of hours slept per night (± SD) for the mask wearers (7.19 ± 0.89) and the controls (6.78 ± 1.20) over the study duration (independent samples t-test, P=0.36). There was also no significant difference between mean hours slept before (7.23 ± 0.93) and after (7.17 ±1.07) mask wear (matched pairs t-test, P=0.49) or in mean hours slept at baseline (7.20 ± 1.12) and final (7.28 ± 1.22) study visits (matched pairs t-test, P=0.77) for the intervention group.

Table 5.5. Monthly mean global PSQI scores for participants who completed the full study period. Global scores shown represent the sum of mean monthly component scores relating to subjective sleep quality (component 1), sleep latency (component 2), sleep duration (component 3), habitual sleep efficiency (component 4), sleep disturbances (component 5), use of sleeping medication (component 6) and daytime dysfunction (component 7).

	Mean PSQI global score (±SD)	
Month	**Intervention**	**Control**
Baseline	3.97 (± 2.27)	5.40 (± 3.32)
1	5.38 (± 3.81)	5.56 (± 3.49)
2	4.79 (± 2.89)	5.64 (± 3.82)
3	5.30 (± 2.60)	6.04 (± 3.39)
4	5.11 (± 2.14)	5.29 (± 3.17)
5	5.57 (± 2.90)	5.80 (± 3.56)
6	5.33 (± 2.70)	6.25 (± 4.13)
7	5.93 (± 2.95)	5.45 (± 3.42)
8	6.06 (± 3.51)	5.63 (± 3.73)
9	6.11 (± 3.48)	6.38 (± 3.66)
10	5.82 (± 3.32)	6.04 (± 3.69)
11	5.05 (± 3.17)	6.20 (± 3.76)
12	5.10 (± 2.65)	5.59 (± 3.32)
1-12	5.35 (± 2.95)	5.79 (± 3.57)

5.5.5. Withdrawals from the study

Thirteen participants were withdrawn throughout the course of the trial (3 control, 10 intervention). As the trial follow-up visits were conducted in conjunction with scheduled hospital appointments, no participants were withdrawn due to repeated failure to attend. Of the control subjects 2 developed nAMD in their fellow eye and 1 died within 12 months of randomisation. The reasons for intervention withdrawals are detailed in Table 5.6. Thirty-three per cent of all intervention participants withdrew from the study. Seventy per cent of all intervention withdrawals occurred within 65 days of randomisation with only 2 intervention participants unable to complete less than 1 month of mask wear. Consistent with the semi-structured questionnaire feedback, the majority of withdrawals relating to mask wear were caused by temporal and bridge discomfort. The mean number of mask wear nights before withdrawal did not differ significantly between those who reported temporal (53 days) and bridge (47 days) discomfort.

Analysis of the characteristics between those withdrawn (n=13) and those who completed the entire study duration (n=47) was performed in order to investigate any potential bias in the study caused by the withdrawn cohort. This was done to establish whether the results had been skewed in a more favourable direction by the withdrawal of participants for whom the intervention was having either no effect, or an adverse effect. The baseline characteristics of the withdrawn and completed study groups are shown in Table 5.7. Independent samples t-test analysis showed no significant difference between the age (P=0.94), ocular supplement history (P=0.12), smoking history (P=0.52) or baseline VA (P=0.28) of those withdrawn and those who completed the entire study duration. Similarly, there was no difference in gender balance between the groups (chi-squared test, P=0.36).

Table 5.6. Mask wearer withdrawal timescale and primary reason for ceased participation.

Study ID	Date randomised	Date withdrawn	Days on study	Mask wear (hours)	Reason for withdrawal
MJ010001	11/07/2014	05/08/2014	25	85.80	Overheating
JE010010	03/12/2014	03/01/2015	31	142.00	Temporal discomfort
MA010002	06/10/2014	06/01/2015	92	137.50	Bridge discomfort
GW010018	22/04/2015	27/04/2015	5	21.33	Bridge discomfort
GF010034	20/07/2015	01/09/2015	43	20.30	Bridge discomfort
BP010040	13/07/2015	28/10/2015	107	591.50	Conversion to nAMD
GC010055	20/10/2015	22/12/2015	63	310.90	Temporal discomfort
MP010057	24/11/2015	22/12/2015	28	37.43	Psychological
PC010050	02/11/2015	05/01/2016	64	31.23	Temporal discomfort
BJ010041	25/08/2015	25/01/2016	153	582.73	Eyelid/lash irritation

Table 5.7. Baseline characteristics of participants who were withdrawn and those who completed the full study period of 12 months. Standard deviation values are shown in brackets.

	Withdrawn	Completed study
N	13	47
Grade 2 (n)	3	15
Grade 3 (n)	6	16
Grade 4 (n)	4	16
Age (± SD)	77.15 (± 8.25)	77.34 (± 7.06)
Ocular supplement history (years taken ± SD)	1.08 (± 1.30)	0.50 (± 1.12)
Smoking history (pack years ± SD)	19.66 (± 16.36)	11.35 (± 18.97)

5.6. Conclusion

This chapter has described the implementation of the ALight trial, provided information on trial logistics, participant characteristics and reports the results of a study designed to determine the safety and acceptability of nighttime light mask wear. Challenges relating to recruitment, appointment scheduling and the day-to-day operation of a longitudinal clinical trial investigating AMD have been described. Such information may be useful for future longitudinal studies aimed at assessing AMD.

In the present study, the mask was well tolerated by 90% of participants. Minor issues relating to brightness shortly after commencing mask wear were found to subside in concordance with the Troxler effect (Martinez-Conde et al., 2004). Reports of “glairiness” did not pose an issue beyond 2 months and no participant withdrew citing luminance level as a key contributing factor. The main reason for withdrawal was

mask discomfort of which 60% was attributed to issues with bridge or temporal discomfort. The overall withdrawal rate as a result of mask issues alone (26%) was in agreement to that reported for a similar age cohort (21%) in the one other study that has also used a sleep mask containing an OLED device as a potential therapy for retinal disease (Sahni et al., 2016). From month 1 to 3 the number of participants withdrawn per month due to mask-issues was equal (n=2) suggesting no 'critical-period' of habitualisation immediately after the initiation of mask wear. However, as the majority (75%) of withdrawals caused by mask-issues occurred within 64 days post randomisation, future studies may expect a low withdrawal rate beyond 3 months wear. The mask itself was found to be a robust method of delivering light therapy with no malfunction or operational issues reported throughout the duration of the trial.

The compliance rate of 70% was similar to that reported by Sahni et al. (2016) (76%) when a similar intervention was assessed in those with diabetic macular oedema (n=15) and healthy controls over 2 age groups (18-30 years, n=45 and 50-70 years, n=24). The mean age (± SD) of the older group was comparable with the present study (77.65 ± 6.72). Sahni et al. (2016) reported that the compliance within their older cohort was better and more consistent over time than their younger cohort. In the present study, disruption to compliance was minimal and primarily caused by ranibizumab administration. The complaints relating to mask comfort reported by those who completed the full 12 month study duration were not reflected in the self-reported PSQI analysis of sleep quality when baseline and final data was compared. For the majority of mask wearers, PSQI data suggested that any discomfort encountered relating to the mask was not sufficient to have a significant impact on sleep quality. This, in combination with a similar mean number of reported hours slept per night for both the intervention (7hrs 7mins) and control (6hrs 47mins) groups, suggests that sleep quality was not substantially affected by mask wear.

Although the level of retinal illuminance used had the potential to suppress the rod circulating current by 40% (Thomas and Lamb, 1999) whilst having a minimal effect on melatonin production as influenced by the photoreceptive melanopsin-containing ganglion cells (Brainard et al., 2001; Berson et al., 2002), there was a possibility that the nightly delivery of light therapy could disrupt circadian rhythm (see Section 3.2.3). In accordance with the PSQI, which was included as a means of evaluating self-reported sleep quality, the nightly delivery of low-level light therapy had no negative impact on any sleep component assessed including sleep quality, duration or latency. Although this is in agreement with other studies that reported no serious adverse events associated with mask wear (Arden et al., 2010; 2011; Sahni et al., 2016) it is not in agreement with the small impairment to daytime alertness reported by Sahni et al. (2016). Direct comparison is however confounded given several differences in the design of the current study. In the study by Sahni et al. (2016) the mean age of participants was substantially lower (45.18 years) than the present study (77.74 years), the masks were only worn for 3 months as opposed to the 12 month duration of the present study and daytime dysfunction was measured using response time as opposed to the PSQI. It can be suggested that the cohort assessed by Sahni et al. (2016) was more likely to be in full-time employment and, as a result, more likely to appreciate daytime dysfunction than the primarily retired cohort of the present study. Participants in the present study also wore the mask 4 times longer hence were given greater time to become accustomed to sleeping in the device.

The results described here provide evidence that the use of an OLED sleep mask is an acceptable and safe method of delivering nightly low-level light therapy. Although it must be noted that the number of withdrawals along with the high incidence of discomfort reported suggest that a proportion of individuals will find mask wear intolerable. The next chapter presents results of the analysis of the magnitude of the effect of light therapy on AMD progression.

Chapter 6. ALight trial magnitude of treatment effect

This chapter presents results relating to the magnitude of the effect of low-level night-time light therapy as delivered using a sleep mask on AMD progression in the ALight trial cohort. Functional (dark adaptation, chromatic sensitivity and flicker sensitivity), structural (drusen volume) and subjectively-reported (visual function and quality of life) changes are reported. Firstly, the results describe the impact of low-level night-time light therapy, compared to no intervention, on disease progression in early and intermediate AMD. Secondly, the effect of low-level night-time light therapy on retinal function, subjectively reported outcome measures and ranibizumab retreatment rate in the fellow eye is described.

6.1. Introduction

There is a critical need to evaluate potential therapeutic interventions aimed at treating AMD prior to the onset of the advanced stages of GA and nAMD. Presently, ageing retinal function has shown to be improved with near infrared light (Sivapathasuntharam et al., 2017) and an LED based multi-wavelength treatment (photobiomodulation therapy) has been shown to improve functional outcomes in those with early/intermediate AMD (Merry et al., 2016). In addition, two phase III clinical trials are also underway investigating a potential new GA treatment (CHROMA, 2014; SPECTRI, 2014) however, to date, the only treatment currently available is for those with the neovascular form of the disease. For the majority of individuals with intermediate AMD or GA no such treatment exists. The potential treatment introduced in this PhD was developed in response to evidence implicating hypoxia in AMD pathogenesis (see Chapter 2). The availability of oxygen at a retinal level can be increased by the inhalation of a greater volume of oxygen or manipulation of metabolic demand. As the retina is most metabolically active under scotopic conditions any approach aimed at preventing full dark adaptation at night could potentially reduce the need for oxygen, thereby delaying progression of conditions

with a hypoxic aetiology (Arden et al., 2011). In practice, this effect can be achieved on a nightly basis via the provision of low-level light therapy. To date, a number of studies have assessed the impact of low-level light therapy in those with diabetic macular oedema (Arden et al., 2010; 2011; Sahni et al., 2016). These studies have shown an improvement in chromatic sensitivity and a reduction in diabetic retinal oedema in those who underwent light therapy in comparison to controls. Both of which were attributed to the prevention of night-time hypoxia (Arden et al., 2011; Sahni et al., 2016). This PhD sought to establish if the same intervention would have a therapeutic effect on people with early and intermediate AMD.

6.2. Aims

The primary aim of the ALight trial was introduced in Section 1.5. Briefly the aim was to assess the impact of low-level night-time light therapy, compared to no intervention, on AMD progression. Disease progression was defined on the basis of two co-primary outcome measures:

i. The proportion of people showing disease progression in the eye with early or intermediate AMD. Disease progression was defined as the onset of advanced AMD or increase in drusen volume beyond test-retest 95% confidence intervals.

ii. The rate of retinal adaptation (time taken for photoreceptors to recover their sensitivity after being exposed to a bright adapting light).

Secondary aims addressed in this chapter were to establish the effect of low-level night-time light therapy on:

i. The change in drusen volume over 12 months.

ii. The number of ranibizumab injections required in the fellow eye over 12 months.

iii. The change in chromatic sensitivity and 14Hz flicker threshold over 12 months.

iv. The change in self-reported quality of life and visual function over 12 months.

v. The ability of all clinical tests to act as prognostic biomarkers for AMD progression.

vi. The ability of all clinical tests to act as predictive biomarkers for low-level night-time light therapy in AMD.

6.3. Methods

For a detailed description of the ALight trial methods the reader is directed to the published trial protocol (McKeague et al., 2014) or the relevant sections throughout this thesis: eligibility criteria (Section 3.1.3), withdrawal criteria (Section 3.1.5), assessment of safety (Section 3.4), randomisation (Section 3.5.1), fundus grading (Section 3.3.3.2), experimental procedure (Section 3.6.3 and 3.7.1) and examination of structural outcome measures (Section 3.3.3.1).

In brief, the data presented relate to the participants who completed the trial. The baseline assessment (Section 3.3.3) involved the collection of drusen volume data (via optical coherence tomography: 5 Zeiss Cirrus OCT 2000 images, 6x6mm macular cube scans centred on the fovea), fundus photographs (Topcon OCT 2000 45° photographs centred on the fovea), BCVA, computer-based tests of visual function (chromatic thresholds, 14Hz flicker threshold and dark adaptation), and self-reported quality of life (EQ-5D) and visual function (VFQ-48) data. Following successful completion of the visual function tests, the participant was randomised to the intervention or control arm of the study. On a monthly basis, participants within each study group attended a short, follow-up appointment during which OCT images and ranibizumab retreatment data were collected. The final visit was conducted 12 months post-randomisation. At the final visit, data relating to retinal function were collected in the same manner as per baseline visit. The reader is directed to the relevant appendices for an example of the PIS (Appendix VII) consent form and CRFs (Appendix VIII) relating to this study.

In order to expand on the magnitude of effect analysis post-hoc data relating to the AMD status of participants who showed no disease progression during the trial was reviewed 6 months following their end-of-study visit (Appendix X). In addition, post-hoc testing was performed on the baseline difference of visual function between those who remained and those who withdrew from the trial. This was done to establish any potential bias in the study caused by the withdrawn cohort and to address the possibility that results had been skewed in a more favourable direction by the withdrawal of participants for whom the intervention was having either no effect, or an adverse effect.

6.4. Statistical analysis

All analysis was performed using IBM SPSS Statistics (SPSS Inc. SPSS for Windows, Version 20.0. Chicago, USA). There was no interim analysis. However, conversions to nAMD in the treated eye were monitored for safety reasons. This study was designed as a phase I/IIa proof of concept study and so was designed to estimate the magnitude of any potential therapeutic effect, rather than to detect small effect sizes.

Given the phase I/II nature of the trial, the main analysis comprised descriptive statistics to summarise the demographic characteristics and outcome measures of the two study arms. The primary outcome measure, disease progression, was based on the rate of retinal adaptation and also on nAMD onset or an increase in drusen volume beyond test-retest 95% confidence intervals (Gregori et al., 2011). The highly reproducible algorithm for drusen volume change as developed by Gregori et al. (2011) states that the change in drusen volume within a 3mm radius circle centred on the fovea of a given eye would only be significant if the new measured drusen volume were smaller than: $[(\text{baseline volume})^{1/3} - 0.025]^3$ or larger than $[(\text{baseline volume})^{1/3} + 0.025]^3$. Substitution of 0.025 with 0.028 allows for the calculation of confidence intervals for drusen volume measured within a 5mm radius circle centred on the fovea. In accordance with the consensus relating to randomised controlled trials, differences

in baseline characteristics between groups were not assessed (Roberts and Torgerson, 1999; Egbewale, 2015).

Prior to analysis, guidance on appropriate analysis techniques was sought from an experienced statistician based in the South East Wales Trials Unit. To compare the proportion of people showing disease progression in each study arm, individual chi-squared tests relating to drusen volume change and onset of nAMD were performed initially. Following this, a stratified Mantel-Haenszel test was used. In order to address the assumption of odds ratio homogeneity prior to Mantel-Haenszel analysis, a Breslow-Day statistic was derived. The normality of the distribution of data was assessed using the Shapiro-Wilk test. For normally distributed data, the ANCOVA test was carried out to compare the change in cone τ, BCVA and the number of ranibizumab retreatments between the two arms across the duration of the trial, when controlling for covariates age, gender differences (binary controlled as 0 or 1 depending on sex per group), vitamin supplement intake (controlled by number of years taken per group), history of smoking (controlled by overall pack years until date of assessment per group), and baseline data relating to each outcome measure.

Data that remained non-parametric even after log transformation were the change in drusen volume, 14Hz flicker threshold and chromatic thresholds. For these outcomes the Kruskal-Wallis test was performed to analyse and compare the change in the outcome measures over 12 months between the two groups. Note that all analysis apart from the ranibizumab retreatment rate relates to the eye with early/intermediate AMD.

Questionnaire data were analysed with appropriate parametric (ANCOVA) or non-parametric (Kruskal-Wallis) tests (according to data distribution). Self-reported visual function was assessed using the VFQ-48 scoring system (Stelmack and Massof, 2007). The scoring system allowed the derivation of a ‘person measure’ for each subject, with smaller values corresponding to a greater deficit in self-reported visual

function. Self-reported health related quality of life data were assessed using the EQ-5D (3 level version; EuroQol Group, 1990). This consisted of two questions. The first question, known as the EQ-5D self-classifier, consisted of five items for which an index-based 'summary score' was calculated using an algorithm developed from a general UK population based validation study (Dolan, 1997; Rabin and De Charro, 2001). The summary score is typically interpreted along a continuum with a lower score reflecting poorer self-reported quality of life. For the second question, the subjects rated their health using a 20 centimetre visual analogue scale (VAS) that ranged from 0 (worst imaginable health state) to 100 (best imaginable health state). VFQ-48 and EQ-5D data remained non-parametric even after log transformation hence these were assessed using the Kruskal-Wallis test.

A post-hoc analysis (not specified in the published protocol) was carried out to investigate the change over 12 months in the total retinal thickness (Kruskal-Wallis), visual acuity (ANCOVA) and AMD status as based on clinical severity between groups. Retinal thickness values were derived from the on-board Zeiss Cirrus SD-OCT 4000 retinal thickness algorithm which specifies total thickness for three subfields of the ETDRS grid (Figure 3.6). In addition, a comparison of the baseline characteristics and the computer-based visual function tests of those who were withdrawn and those who remained for the entirety of the study duration was also conducted. In order to investigate the prognostic capacity for AMD progression of the visual function tests ROC curves were constructed for each test plotting the sensitivity for AMD progression against the false-positive rate (1-specificity). The AUC was used to express the diagnostic capacity of each test. A post-hoc assessment of AMD status was also conducted 6 months after trial closure via review of hospital medical records.

6.5. Results

6.5.1. Participant characteristics

Twenty-one intervention and 29 control participants either completed the trial or withdrew as a result of nAMD, and are included in the magnitude of effect analysis (Table 6.1). Those that completed the full study period (20 intervention, 27 control) are included in the secondary outcome analysis. Fifty percent of the intervention group and 41% of the control group who completed the entire study duration were recruited within their ranibizumab loading phase.

Table 6.1. Table of baseline descriptive statistics for participants who completed the 1 year study duration and are included in the magnitude of effect and secondary outcome analysis.

	Intervention	Control
Number of participants	21	29
Mean age (±SD)	78.43 (±7.03)	77.00 (±7.02)
Gender balance	43% female	48% female
Mean BCVA study eye (ETDRS letter score ±SD)	0.09 (±0.13)	0.07 (±0.12)
Mean BCVA fellow eye (ETDRS letter score ±SD)	0.40 (±0.28)	0.39 (±0.33)
Ocular supplement history (mean years taken ±SD)	0.76 (±1.38)	0.33 (±0.63)
Smoking history (mean pack years ±SD)	12.43 (±20.21)	12.68 (±18.77)
Ranibizumab injection history (mean number ±SD)	8.45 (±8.94)	8.07 (±7.45)

6.5.2. Disease progression on basis of change in drusen volume or onset of nAMD

Characteristics relating to the change in drusen volume of the 50 participants who are included in the magnitude of effect analysis are shown in Table 6.2. Thirty-three percent (n=7) of intervention and 41% (n=12) of control participants were found to exhibit an increase in drusen volume beyond the 95% test-retest confidence intervals within a circle of 5mm diameter centred on the fovea. Five percent (n=1) of intervention participants and 7% (n=2) of control participants progressed to nAMD during the course of the study and were withdrawn. When combined with those who showed significant drusen growth, 38% (n=8) of the intervention group and 48% (n=14) of the control group showed disease progression over the course of the trial.

Although the proportion of people showing disease progression was reduced in the intervention group this did not reach statistical significance when onset of advanced AMD and increased drusen volume were assessed individually using a chi-squared test (drusen volume, $\chi^2 = 0.34$, P=0.39 [Table 6.3]; onset of nAMD, $\chi^2 = 0.10$, P=0.62 [Table 6.4]) or combined and analysed using the Mantel-Haenszel test (common odds ratio = 0.76, P =0.50 [Table 6.5]).

Table 6.2. Drusen volume characteristics of each study group. Percentages given relate to total number in each cohort included in the magnitude of effect analysis (intervention, 21; control, 29). Measurements were classified as showing significant growth/shrinkage using test- retest confidence intervals (CI) as derived from Gregori et al. (2011).

	Intervention		Control	
Change in drusen	**N (%)**	**Mean (±SD)**	**N (%)**	**Mean (±SD)**
Growth	8 (38%)	0.012 (±0.006)	16 (55%)	0.018 (±0.030)
Growth beyond 95% CI	7 (33%)	0.013 (±0.005)	12 (41%)	0.027 (±0.035)
Shrinkage	5 (24%)	0.036 (±0.047)	5 (17%)	0.018 (±0.024)
Shrinkage beyond 95% CI	5 (24%)	0.036 (±0.047)	4 (14%)	0.022 (±0.025)
No change	7 (33%)	0.000 (±0.000)	6 (21%)	0.000 (±0.000)

Table 6.3. Tabulated variables for assessment of disease progression (as based on nAMD onset) using the chi-squared test of independence.

Study Arm	**Onset of nAMD**	**Frequency**
Intervention	Yes	1
	No	20
Control	Yes	2
	No	27
χ^2 statistic	0.10	
P	0.62	

Table 6.4. Tabulated variables for assessment of disease progression (as based on increase of drusen volume beyond 95% test-retest confidence intervals) using the chi-squared test of independence.

Study Arm	**Increase drusen volume**	**Frequency**
Intervention	Yes	7
	No	14
Control	Yes	12
	No	17
χ^2 statistic	0.34	
P	0.39	

Table 6.5. Tabulated variables for assessment of disease progression (as based on increase of drusen volume beyond 95% test-retest confidence intervals and onset of nAMD) using the Mantel-Haenszel Test.

Study Arm	Onset of nAMD (n)	Significant increase in drusen volume (n)	Frequency
Intervention	Yes (1)	No (14)	15
	Yes (1)	Yes (7)	8
	No (20)	No (14)	34
	No (20)	Yes (7)	27
Control	Yes (2)	No (17)	19
	Yes (2)	Yes (12)	14
	No (27)	No (17)	44
	No (27)	Yes (12)	39
Odds ratio	0.76		
P	0.50		

6.5.3. Disease progression on the basis of cone dark adaptation

Data relating to the assessment of disease progression on the basis of change in cone τ are displayed in Figure 6.1 and Table 6.6. At baseline, the mean cone τ was 0.61 minutes faster in the intervention cohort than the controls. When measured again after 12 months, the average cone τ of the mask wearers was 1.59 minutes slower than initially recorded. A similar change was exhibited by the control group albeit by a smaller increment of 0.70 minutes. No significant difference in cone τ was found between the study groups at either baseline or the final visit. Despite this, analysis showed that the mean overall change of cone τ (±SD) in the control group (0.66 ±0.49 mins) was significantly less (P=0.018) than the intervention group (1.66 ±0.61 mins) when adjusted for covariates as shown in Figure 6.1. Therefore, cone τ increased significantly more in the mask wearing group over 12 months than it did for the control group.

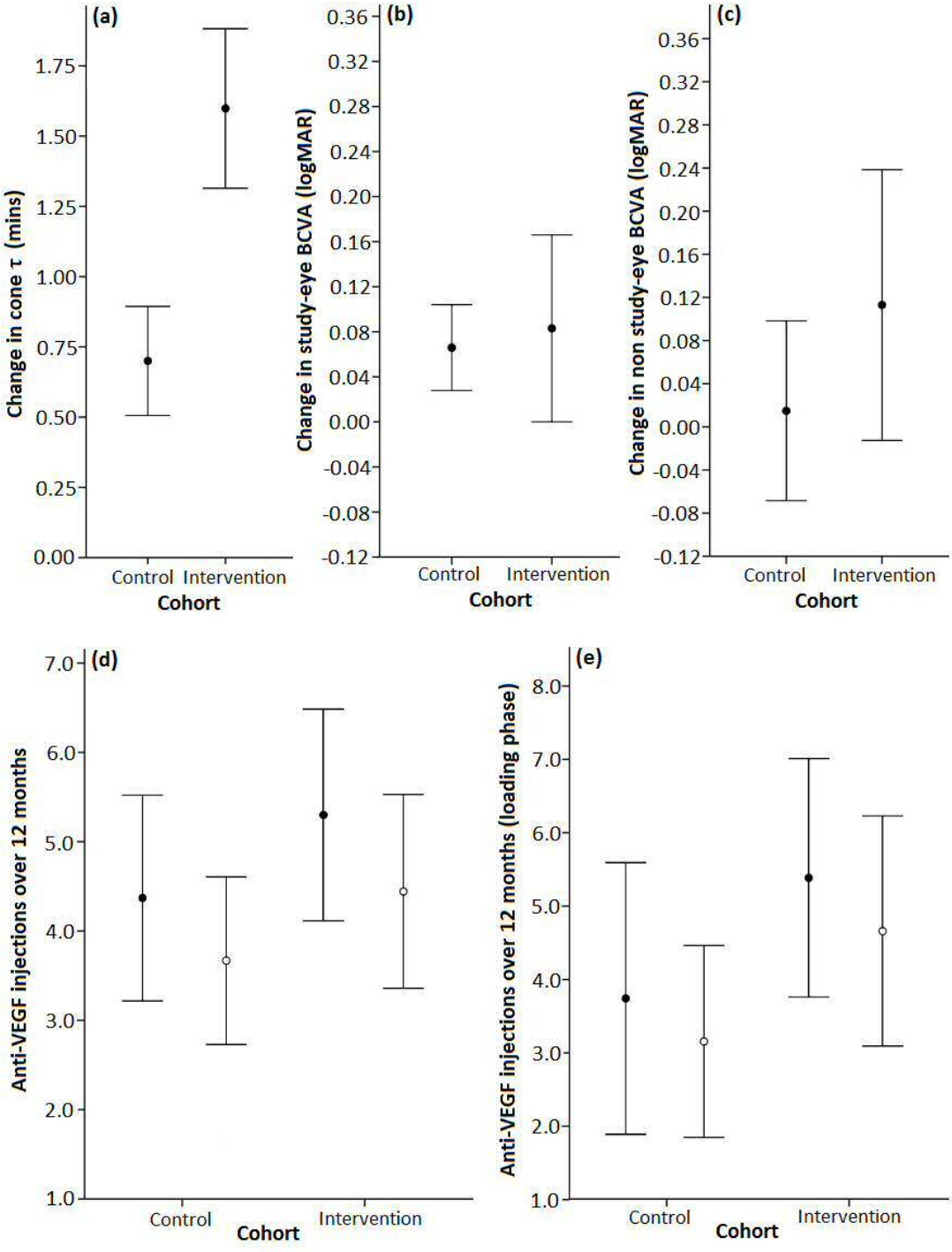

Figure 6.1. Means plots showing change in cone τ (a) and visual acuity (b-c) over 12 months. Plots (d) and (e) show the number of anti-VEGF injections administered over the study duration for the entire study cohort (d) and those recruited within their loading phase only (e). Black circles represent total injections (ranibizumab and aflibercept) and white circles represent those treated only with ranibizumab for the study duration. Whiskers denote 95% confidence intervals.

Table 6.6. Cone τ characteristics between study groups. Baseline and final mean cone τ are shown alongside the mean change prior to and after ANCOVA correction for differences in age, vitamin supplement intake, smoking history and baseline cone τ. The P-values specified relate to the significance of the difference in mean cone τ between study groups for each row. Cone τ measurements are given in minutes.

	Intervention (mean ±SD)	Control (mean ±SD)	P
Baseline	5.27 (± 1.81)	5.88 (± 1.58)	0.219
Final	6.86 (± 2.64)	6.58 (± 2.13)	0.689
Change over 1 year	1.60 (± 1.17)	0.70 (± 1.50)	0.031
ANCOVA corrected change	1.66 (± 0.61)	0.66 (± 0.49)	0.018

6.6. Secondary outcome measures

The secondary outcome measures (drusen volume, chromatic threshold and 14Hz flicker threshold data) were not normally distributed, even after log transformation. Hence, the Kruskal-Wallis test was used to evaluate change (baseline to 12 months) in each parameter. The results of this analysis are presented in Table 6.7. A number of outliers across all functional tests were identified, each of which has been specified in Figure 6.2. No evidence suggested that any of the outliers occurred as a direct result of any AE, mechanical fault or poor quality OCT scans. Information relating to the outliers was collected by the study investigator throughout the trial. Information of particular interest included:

- CA010016 encountered a number of health issues throughout the duration of the study resulting in general and ocular (non-study eye) surgery.
- CS010012 was increasingly anxious for a large proportion of the study (including the collection of final result data) due to the unexpected and sudden ill health of her partner.
- MB010023 OCT scans were reviewed by a hospital ophthalmologist at the time of nAMD diagnosis. In agreement with the study investigator hospital

records suggest that the study eye exhibited only dry AMD changes in the form of drusen and pigmentary abnormality.

As there was no evidence of a mistake and the outlier values were plausible analysis was performed on the entire dataset (Altman, 1991).

Spearman correlation analysis showed no significant correlation between baseline results and 12 month change for RG chromatic threshold (control correlation coefficient = 0.129, P=0.520; intervention correlation coefficient = -0.211, P=0.373), YB chromatic threshold (control correlation coefficient = -0.120, P=0.550; intervention correlation coefficient = 0.150, P=0.950), flicker threshold (control correlation coefficient = -0.170, P=0.933; intervention correlation coefficient = 0.251, P=0.286) or baseline drusen volume (control correlation coefficient = 0.348, P=0.076; intervention correlation coefficient = -0.139, P=0.559) (Figure 6.2). Therefore no correction for difference in baseline status between groups was required.

Table 6.7. Twelve month change in non-parametric outcome measures for each study group. Medians alongside inter-quartile range (bracketed) values are shown. For each functional outcome measure shown a larger threshold relates to poorer retinal function. The EQ-5D scores are based on the summary index score and the visual analogue scale score (0% relating to worst imaginable health state and 100% relating to best imaginable health state). For functional outcomes a larger value represents a decrease in retinal function. For the structural outcomes a negative value represents a reduction in drusen volume or retinal thickness over 12 months. A higher EQ-5D summary index score reflects an increased self-reported quality of life whereas a larger VFQ-48 person measure shows fewer self-reported visual function issues. Total retinal thickness values relate to the three subfield areas of the ETDRS grid.

Outcome measure	Intervention (IQR)	Control (IQR)
Drusen volume (mm^3)	0.00 (0.00, 0.01)	0.00 (0.00, 0.01)
14Hz flicker threshold (cd/m^2)	0.004 (0.001, 0.053)	0.001 (-0.006, 0.007)
RG chromatic threshold (CAD units)	-0.01 (-1.79, 2.84)	0.91 (-0.49, 2.17)
YB chromatic threshold (CAD Units)	0.245 (-0.23, 1.49)	0.170 (-0.31, 1.49)
EQ-5D summary index score	0.00 (-0.22, 0.00)	0.00 (-0.06, 0.00)
EQ-5D visual analogue scale %	1.25 (-5.00, 6.25)	1.00 (-4.00, 10.00)
VFQ-48 person measure score	3.42 (2.92, 3.65)	3.25 (2.65, 3.42)
Retinal thickness: central subfield (microns)	-7.50 (-11.25, -2.00)	-2.00 (-7.50, 2.00)
Retinal thickness: inner subfield (microns)	-4.63 (-7.50, -1.56)	-4.25 (-5.75, -2.13)
Retinal thickness: outer subfield (microns)	-2.38 (-3.88, -1.13)	-2.50 (-5.63, -0.25)

Over 12 months the median change in drusen volume (IQR) was the same for the intervention and control groups (0.000 [0.00, 0.01] mm^3). The largest increase reported within the control group was 0.12mm^3. This was 6 times larger than the peak increase reported by any intervention participant (0.02mm^3). In the intervention group, the median change in RG chromatic threshold over 12 months (IQR) showed an overall improvement by 0.01 (-1.79, 2.84) CAD units for mask wearers whereas the control group exhibited an overall decline of 0.91 (-0.49, 2.17) CAD units. The opposite was found when assessing YB chromatic thresholds where the median decline in function was 0.08 CAD units greater for mask wearers (YB chromatic threshold [IQR], 0.25 [-0.23, 1.49] CAD units) than controls (YB chromatic threshold [IQR], 0.17 [-0.31, 1.49] CAD units). The median change in 14Hz flicker threshold (IQR) over 12 months corresponded to a decline in function for both the intervention (0.004 [0.001, 0.053] cd/m^2) and control groups (0.001 [-0.006, 0.007] cd/m^2).

Analysis of median change in secondary outcome measures relating to visual function showed no significant difference between study groups (Kruskal-Wallis: drusen volume [P=0.66], RG chromatic threshold [P=0.46], YB chromatic threshold [P=0.79], 14Hz flicker threshold [P=0.10]) over the 12 month period (Figure 6.3).

At baseline, all participants were on a structured ranibizumab treatment regimen at BEH. This consisted of a loading phase (3 injections over 3 months) immediately after nAMD diagnosis followed by monthly assessment and subsequent injection as necessary. During the course of the study ranibizumab use was ceased in favour of aflibercept for 7 participants (4 intervention, 3 control). Twenty-one participants (10 intervention, 11 control) were recruited within their initial ranibizumab loading phase. Table 6.8 shows the injection characteristics of each study group. At baseline the average number of injections administered across the entire cohort was 8 (± 8.20). When all participants were included (from both ranibizumab and aflibercept regimens) the mean (± SD) number of injections administered over 12 months was slightly higher

in the intervention (5.30 ± 2.57) than the control (4.37 ± 2.91) group, although a higher number of intervention participants switched treatment regimen resulting in a 3-injection loading dose of aflibercept. No significant difference was found between the mean (± SD) total number of anti-VEGF injections received by the intervention (5.28 ± 2.54) and control (4.38 ± 2.91) groups despite non-mask wearers receiving on average 1 fewer anti-VEGF injection over a 12 month period (ANCOVA: P=0.30). As shown in Figure 6.1 this finding was also evident when considering those from each group who were retained on ranibizumab only (ANCOVA: P=0.57) and those who were recruited within their 3 month ranibizumab loading phase (ANCOVA: P=0.27) (Table 6.8). ANCOVA analysis relating to ranibizumab administration between the groups was performed specifying age, gender, vitamin supplement intake and history of smoking and baseline data relating to each visual function test as covariates.

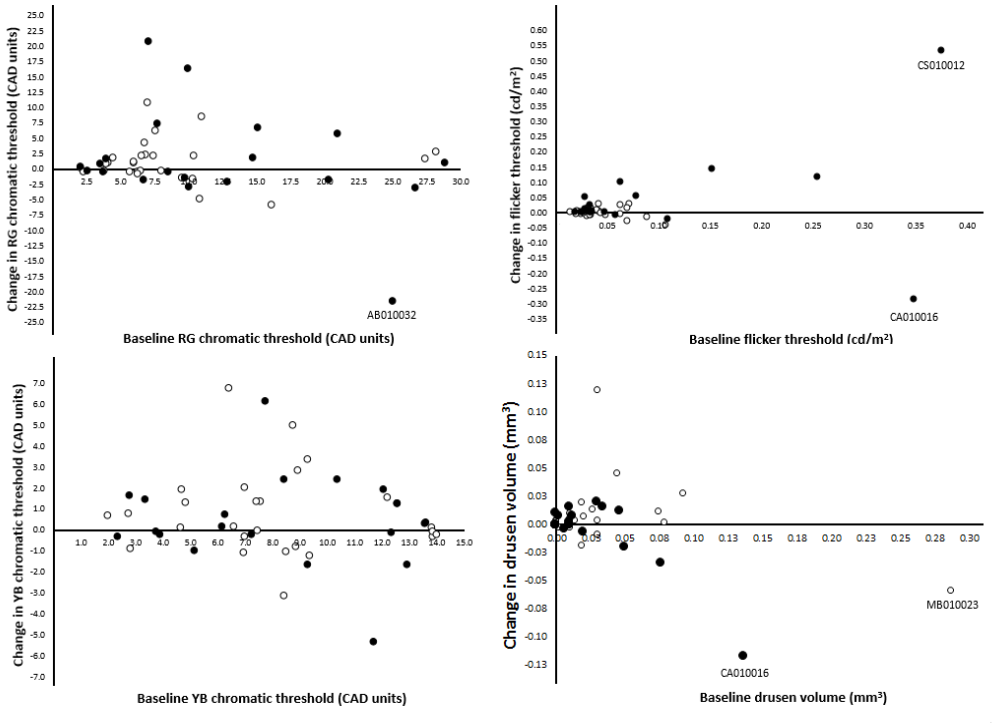

Figure 6.2. Scatter plots showing change of chromatic threshold, flicker threshold and drusen volume as a function of baseline data for all ALight clinical trial participants who completed the 12-month study period. Mask-wearers (intervention) are represented by black circles and non-mask wearers (controls) are represented by white circles. Outliers have been specified with the participant ID that they relate to.

Visual function (VFQ-48) and quality of life (EQ-5D) data are shown in Table 6.7. A large proportion (80%) of the entire cohort reported an overall improvement in self-reported visual function over the duration of the study in accordance with the VFQ-48 questionnaire. There was, however, no evidence of a significant difference between groups (Kruskal-Wallis: P=0.32) (Figure 6.3). The median change (IQR) in EQ-5D scores for the intervention and control groups was 0.00 (-0.22, 0.00) and 0.00 (-0.06, 0.00), respectively. This change was not significantly different between groups (Kruskal-Wallis: P>0.05). When using the EQ-5D visual analogue scale (0% relating to worst imaginable health state and 100% relating to best imaginable health state) the median change in health state was an increase from 85-88% in the control group and 80-83% in the intervention group over the study duration. There was no significant difference in the change of quality of life between study groups when analysing the visual analogue scale score (Kruskal-Wallis: P=0.85).

Table 6.8. Table showing mean number of anti-VEGF injections received by participants in each group over the duration of the ALight clinical trial. At the time of randomisation all participants enrolled into the clinical trial were on a ranibizumab treatment regimen. Data within the table relating to each study arm are divided into 'entire group' (the total number of intervention/control participants to complete the entire study duration) and 'loading phase' (data relating only to those who were recruited during their ranibizumab loading phase). 'Ranibizumab only' refers to those who were retained on a ranibizumab treatment regimen for the duration of their participation within the clinical trial. 'Treatment regimen changed'' refers to those for whom their treatment regimen was changed from ranibizumab to aflibercept during the course of their participation within the clinical trial. 'Ranibizumab pre-randomisation' refers to the mean number of ranibizumab injections received prior to randomisation. 'Mean total injections'' refers to the mean combined total of ranibizumab and aflibercept injections administered over the study duration for each study arm. 'Mean ranibizumab' refers only to those who were retained on a ranibizumab regimen for the duration of the clinical trial and denotes the mean number of ranibizumab injections administered for each study arm over the study duration. 'Mean total injections/ranibizumab (ANCOVA)' relates to corrected mean values obtained following ANCOVA analysis specifying age, smoking history, vitamin supplement intake and number of injections at baseline as covariates. Standard deviations are shown in brackets.

	Intervention (n±SD)		**Control (n±SD)**	
	Entire group	**Loading phase**	**Entire group**	**Loading phase**
Ranibizumab only	16	8	24	10
Treatment regimen changed	4	2	3	1
Ranibizumab pre-randomisation	8.45 (±8.94)	3.00 (±0.00)	8.07 (±7.45)	3.00 (±0.00)
Mean total injections	5.30 (±2.57)	5.40 (±2.27)	4.37 (±2.91)	3.73 (±2.76)
Mean total injections (ANCOVA)	5.28 (±0.77)	5.40 (±0.95)	4.38 (±0.67)	3.73 (±1.51)
Mean ranibizumab	4.44 (±2.03)	4.43 (±1.77)	3.67 (±2.22)	3.10 (±1.91)
Mean ranibizumab (ANCOVA)	4.23 (0.74)	4.86 (±0.86)	3.80 (±0.55)	3.10 (±0.93)

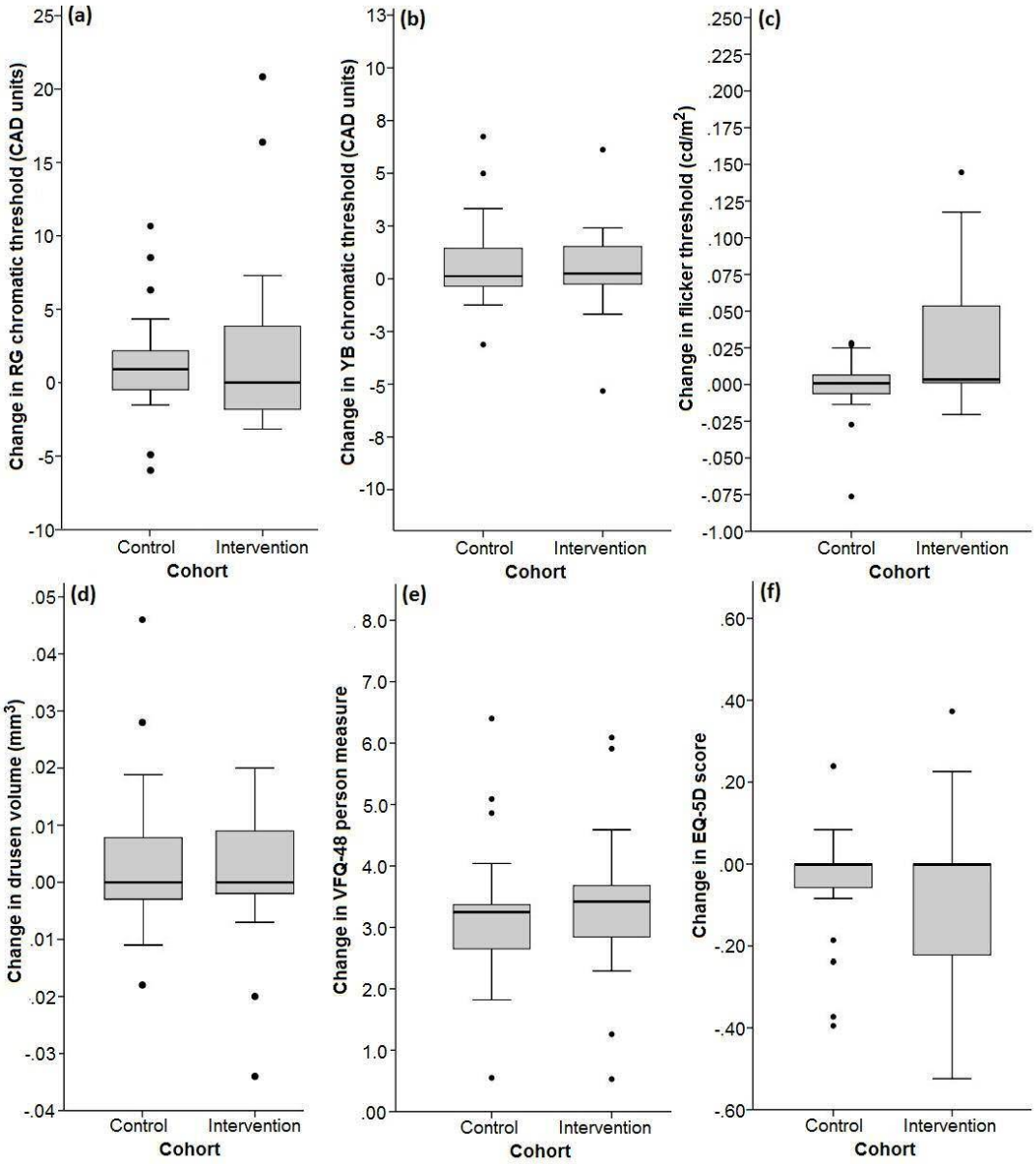

Figure 6.3. Boxplots showing 12 month change in RG chromatic threshold (a), YB chromatic threshold (b), 14Hz flicker threshold (c), drusen volume (d), VFQ-48 person measure (e) and EQ-5D instrument VAS validated score (f). Median is shown as the horizontal black line within the box. The box boundaries represent upper and lower quartiles with range minima and maxima at ends of vertical lines. Outliers (outside 2 inter-quartile ranges) of the median are shown as single points. For change in drusen volume 3 outliers (2 control: -0.058; 0.120 and 1 intervention: -0.120) have not been included in order to aid visualisation.

6.7. Post-hoc analyses

No significant difference (P>0.05) was found between the withdrawn and remain study groups for any visual function test. Data relating to retinal thickness measurements for the ETDRS subfields are displayed in Table 6.7. Assessment of thickness change over 12 months between study groups showed that the median reduction in thickness

was significantly greater in the central subfield of mask wearers when compared to controls (Kruskal-Wallis: P=0.044). No significant difference (P>0.05) was found when considering the median change of the other subfields.

As logMAR visual acuity is still used as a primary diagnostic tool within the hospital setting, this functional measure was also assessed for the study eye on a post-hoc basis. Over the course of the study a mean loss (± SD) of 4 (± 9) letters in the intervention and 3.5 (± 4.5) letters in the control group was found. This change was not significantly different between the two groups (ANCOVA: P=0.69) (see Figure 6.1). The change in AMD as based on clinical severity grading was also investigated. During the course of the trial the AMD severity of 2 intervention and 2 control participants increased by at least 1 AREDS Simplified Severity Scale grade. As the number of participants exhibiting a change in AMD severity as based on clinical grading was so few no statistical analysis was performed on this outcome measure.

6.8. Prognostic and predictive capability of visual function tests

Twenty-nine control participants were included in the ROC analysis of prognostic capability of the visual function tests. The control participant omitted was withdrawn during the study due to general health issues. The ROC curves for each test of retinal function assessed are shown in Figure 6.4. All parameters assessed at baseline showed limited capability to discriminate participants who went on to show progression from those who didn't. Cone τ yielded the highest area under the curve (AUC ± standard error) of 0.53 (± 0.11). This equated to an approximate 60% sensitivity and 40% specificity of the mean cone τ (5.88 mins). The other parameters did not exceed an area under the curve of 0.5, indicating that the prognostic capacity was no better than chance alone. The predictive capacity of the tests as biomarkers for low-level light therapy was not investigated as there was no statistically significant treatment effect.

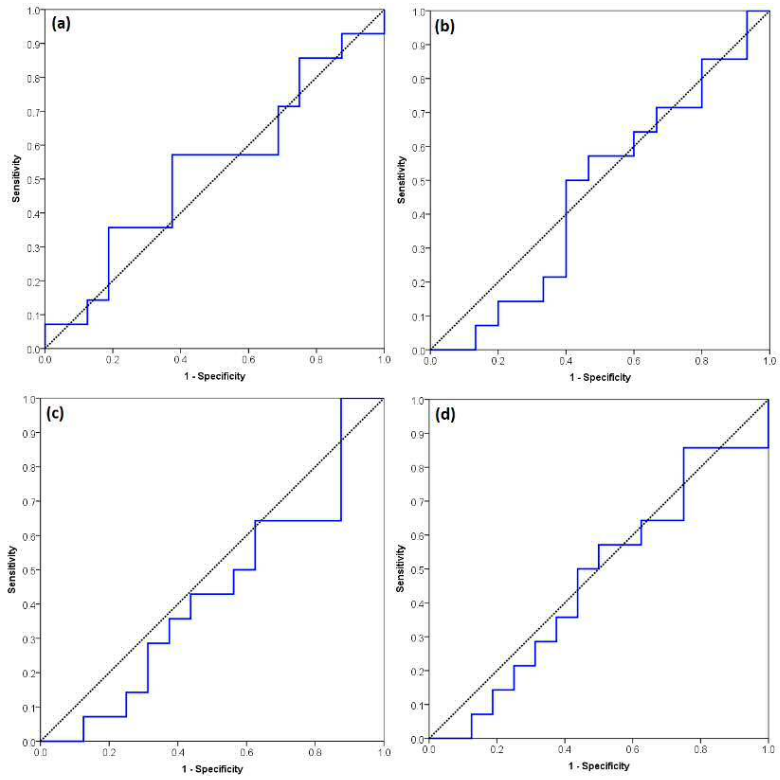

Figure 6.4. Receiver operating characteristic curves for cone τ (a), flicker threshold (b), yellow-blue chromatic threshold (c) and red-green chromatic threshold (d). Each plot shows the sensitivity of the parameter to disease progression in AMD against the false detection rate (1-specificity for all 29 participants).

6.9. Discussion

The findings of this exploratory study suggested that low-level night-time light therapy had no effect on disease progression in patients with early/intermediate AMD over 12 months. A greater proportion of controls (48%) than mask wearers (38%) showed disease progression over the duration of the trial, where progression was defined by either an increase in drusen volume (beyond 95% test-retest confidence intervals) or the onset of advanced AMD in the study eye. Whilst this difference failed to reach statistical significance, it must be noted that this was an exploratory study and as such was not powered to detect small differences between study groups.

The use of OCT-derived drusen volume measurement as a surrogate for disease progression was based on recent published evidence that drusen volume shows an overall pattern of growth for people with early/intermediate AMD over time

(Abdelfattah et al., 2016; Schlanitz et al., 2017; Yehoshua et al., 2011). The proportion of the intervention (35%) and control (44%) participants for which drusen volume increased significantly over the 12 month follow up period was roughly in agreement with that expected (48%) on the basis of published data (Yehoshua et al., 2011). The slightly higher than expected proportion of participants in the control group showing an increase in drusen volume could be attributable to the fact that all participants in this study had unilateral nAMD, and might therefore be considered to be at higher risk of progression than a randomly selected cohort with non-exudative AMD (Schlanitz et al., 2017; AREDS, 2005). This is reflected in the fact that none of Yehoshua's cohort of 143 people with drusen progressed to nAMD within the 12 month follow up, compared to 3 participants in the current cohort of 60.

In the present study a greater proportion of individuals in both groups showed drusen shrinkage (25% intervention, 15% controls) than had previously been reported (Yehoshua et al., 2011). This may, again, reflect a more advanced disease state in the 'early/intermediate AMD' eyes enrolled in the current study compared to Yehoshua et al. (2011), as a spontaneous regression of drusen appears to occur prior to the onset of advanced AMD (Schlanitz et al., 2017; Abdelfattah et al., 2016; Sallo et al., 2009). For the purposes of this trial, drusen shrinkage was not included as an outcome measure as it was not possible to distinguish between regression preceding late stage AMD and regression which may indicate a reduction in disease severity. However, there was no significant difference (chi-squared test, P=0.72) in the proportion of people (intervention, 25%; control, 19%) showing drusen shrinkage between groups. The post-hoc review of AMD status 6 months after the final visit also showed that none of the intervention participants who displayed significant drusen shrinkage throughout the trial progressed to nAMD up to 18-months post randomisation.

The findings of the present study show a 5% conversion rate to nAMD over a 12 month period for those with early/intermediate AMD at baseline. This is lower than the published rate of the same outcome (12.2%) as based on a meta-analysis of five studies of eyes free of advanced disease at study inception (Wong et al., 2008). Direct comparison with the published rate may be confounded as a number of participants included in the present study were taking an antioxidant supplement based on the AREDS formula (AREDS, 2001). Although, the exact impact of this possible confounding factor is unclear as the effect of the AREDS formula is based on one large trial of which the generalisability of the findings to other populations is unknown (Evans and Lawrenson, 2017).

In the present study, the only outcome measure to show a significantly different change over 12 months between the study groups was dark adaptation. There is an emerging body of evidence to suggest that dark adaptation is a sensitive biomarker of AMD (Eisner et al., 1987; 1991; Midena et al., 1997; Owsley et al., 2001; 2007; 2016; Binns and Margrain, 2007; Dimitrov et al., 2008; 2011; 2012; Gaffney et al., 2011; Jackson et al., 2014b), although there are limited longitudinal data to show the sensitivity of the test to disease progression (Eisner et al., 1992; Owsley et al., 2016; 2017) particularly when used over 1-year as opposed to a 2-year period (Owsley et al., 2017). The significant increase in cone τ seen in the intervention group when compared to the controls suggests that dark adaptation was selectively impaired in the treatment group. However, there is no published data regarding the long-term effect of reducing the rod-circulating current on the dynamics of cone adaptation. Hence, although the delayed dark adaptation metric may herald the progression of AMD, we cannot rule out the possibility that it is a consequence of disrupting retinal physiology. Although none of the changes in dark adaptation manifested in an increase in self-reported difficulty when moving from high to low illumination the VFQ-48 questionnaire is not sensitive to this aspect of visual function. A better alternative

to investigate this trait would be a questionnaire specific to low luminance such as the 32-item Low-Luminance Questionnaire (Owsley et al., 2006).

Despite the non-significant change in BCVA, a large proportion (80%) of the entire cohort reported an overall improvement in self-reported visual function over the duration of the study in accordance with the VFQ-48 questionnaire. This was not the case with self-reported quality of life as recorded using the EQ-5D instrument which showed no significant change. The primary reason for the improvement in self-reported visual function is likely to be continued anti-VEGF treatment as opposed to the intervention, as the effect was seen in both study groups. To date, a number of studies have reported an improvement in patients' vision-related quality of life after they started receiving anti-VEGF treatment for nAMD (Liew et al., 2015; Finger et al., 2013; 2014; Inoue et al., 2014). However, the positive impact of anti-VEGF treatment on a patient's vision-related quality of life was found to be dependent on improvement in visual acuity (Senra et al., 2016). In these studies, vision-related quality of life included not only aspects related to the use of vision in activities of everyday life but also mental health and social functioning. Therefore, a link has been suggested between VA and patients' perceptions of quality of life, functioning, and mental health (Senra et al., 2016). Such a link was not found in the present study however it is possible that comorbidities of the elderly ALight trial cohort, such as arthritis and osteoporosis, could have had a negative effect on quality of life (Mitchell and Bradley, 2006).

Although this trial found no significant effect of the therapy on progression of early/intermediate AMD, previous studies have suggested that the therapy is effective at improving retinal function (Arden et al., 2010; 2011) and reducing macular thickness (Arden et al., 2011) in those with diabetic macular oedema. Although both conditions are hypothesised to have a hypoxic aetiology this difference in effectiveness may be due to differing pathogenesis, as diabetic retinopathy primarily affects the inner rather

than the outer retinal circulation. In accordance with the current treatment regimen ranibizumab was issued on the basis of subretinal or intraretinal fluid without stable vision. In the present study, the potential influence of light therapy on the ranibizumab retreatment rate was found to be statistically not significant over a 12 month period. This analysis, however, was confounded by the implications of including those who switched to aflibercept and those who were not recruited within their loading phase.

Both study groups were found to show an overall decrease in retinal thickness (within a 6mm diameter circle centred on the fovea) over the course of the study. This is consistent with evidence suggesting that those with early/intermediate AMD have a generalised thinning of the macular region (Wood et al., 2011) compared to age-matched controls. The primary source of reduced retinal thickness in early/intermediate AMD has been attributed to thinning of the photoreceptor (Schuman et al., 2009; Kaluzny et al., 2009) and ganglion cell (Camacho et al., 2017; Lee and Yu, 2015; Yenice et al., 2015; Savastano et al., 2014) layers, particularly in regions overlying drusen (Rogala et al., 2015; Schuman et al., 2009; Kaluzny et al., 2009; Malamos et al., 2009).

Although retinal segmentation was not utilised in the present study to investigate intra-retinal changes, when considering total retinal thickness the retina thinned significantly more in mask wearers when compared to controls within the central subfield (1mm diameter circle centred on the fovea). Due to poor reproducibility of thickness measurements between OCT instruments of varying manufacturers, direct comparison of the change in retinal thickness found in the present study to that in the wider literature is not possible. This issue is primarily attributable to the different analysis algorithms used to set retinal boundaries within each OCT instrument (Giani et al., 2010; Kiernan et al., 2008). The finding of the present study could potentially be confounded by a number of causes. These include the effect of multiple comparisons increasing the risk of type I error, the effect of axial length which was not

accounted for (Song et al., 2010; Szigeti et al., 2015) and the possibility that some of the control group had retinal thickening attributable to incipient nAMD.

None of the visual function tests were able to predict AMD progression. This finding is not consistent with the potential biomarkers identified in Chapter 4, or with previous longitudinal reports assessing the usefulness of dark adaptation (Owsley et al., 2016) and flicker threshold (Mayer et al., 1994) as prognostic tools for AMD progression. Flicker threshold has been found to be reduced in eyes that eventually develop GA or nAMD (Mayer et al., 1994), however its efficacy as a marker for early disease onset or progression has not been established. It is hypothesised that the prognostic capability of flicker threshold measurement relies upon morphological changes to the L- and M- cone mechanisms as a result of AMD. These changes are postulated to cause the foveal cones to behave more like those within more peripheral retinal locations where they are less densely packed, have larger receptive fields and sensitivity loss at low temporal frequencies (Mayer et al., 1994). Alternatively, rod-mediated dark adaptation has been reported as a prognostic biomarker for early AMD (Owsley et al., 2016). The delay in dark adaptation has been attributed to impaired outer retinal function through changes that occur to structures underlying the retina, such as the photoreceptors, Bruch's membrane and the retinal pigment epithelium in AMD. For further detail on this process the reader is directed to Section 1.3.6.5. The poor prognostic performance of the visual function tests in the present study may be attributed to the relatively small cohort compared to the aforementioned longitudinal studies. In order to adequately establish the prognostic capacity of each test of visual function a much larger cohort would be required.

A weakness to the clinical trial was that an eligibility criteria change was required to improve the recruitment rate during the clinical trial (Section 5.1) thus reducing the power of the analysis with respect to number of injections in the eye with nAMD. It is also worth noting that throughout the study it was not possible to control variation in

pupil size between each intervention participant. Therefore the light therapy dosage each participant received may have varied slightly. For example, based on pupil measurements reported by Winn et al, (1994) the average pupil diameter for the youngest and oldest intervention participants during mask wear can be estimated as 5.5mm and 4.2mm, respectively. Assuming an average lid transmission of 1% this equates to a discrepancy in dosage of 20 scotopic Td per night between the 2 participants. Furthermore, when a possible difference in lid transmission between the participants is also considered the discrepancy in dosage may further increase. The effect of this discrepancy cannot be ruled out as a contributing factor to differences in the overall effect of light therapy between participants within the intervention cohort. The strengths of this study include the robust randomised controlled trial design, the successful masking of treating ophthalmologists, the high level of compliance, and the relatively low rate of withdrawal after the initial period of adaptation.

This study has collected important information about the safety and acceptability of the device in this patient cohort and the potential magnitude of the treatment effect for powering future trials. In conclusion, a larger cohort would be required to determine whether the lack of intervention effect on risk of AMD progression was a chance finding. Further work is also required to determine the potential effect of the treatment on subsequent progression to nAMD. Such future work, alongside a comprehensive discussion of this thesis, is presented in the following chapter.

Chapter 7. Discussion and future work

The overarching aim of the work presented in this thesis was to collect preliminary phase I/IIa proof of concept data about low-level night-time light therapy from people with early and intermediate AMD. The following chapter summarises the work in more detail.

7.1. Summary of thesis

Chapter 1 provided an overview of normal retinal structure and physiology in photopic and scotopic conditions. Current literature concerning the risk factors, pathophysiology, classification, treatment and clinical investigation of AMD was also reviewed. The concept of hypoxia in the AMD pathogenesis was introduced. Evidence regarding the fragile balance between metabolic demand and oxygenation of the retina, especially under dark-adapted conditions, was explored and attributed to the rod mediated dark current.

Chapter 2 reported a systematic literature review conducted to evaluate the role of hypoxia in the pathogenesis of AMD. The review identified direct evidence through the emergence of hypoxia-inducible factor (HIF) that hypoxia is evident at some stage during the pathogenesis of AMD (Kvanta et al., 1996; Lopez et al., 1996; Sheridan et al., 2009; Inoue et al., 2007). Indirect evidence was suggestive that the source of hypoxia resides in diminished choroidal circulation (Grunwald et al., 2005; Metelitsina et al., 2008). Considering that the macula is an area with a high oxygen demand and a fragile oxygen balance it seems reasonable to conclude that a consequence of irregularity in choroidal haemodynamic disruption would be hypoxia. However, there was no direct evidence from the review implicating hypoxia as a causative factor in the pathogenesis of AMD, or at what stage during the disease process it manifests. In addition, it could not be concluded whether the disturbance of choroidal circulation evidenced in AMD is unequivocally the source of hypoxia.

Chapter 3 detailed the study design for the ALight clinical trial, a prospective, longitudinal, randomised controlled trial to assess the impact of low-level night-time light therapy on the progression of early/intermediate AMD. In addition to elaborating and presenting amendments to the published protocol (McKeague et al., 2015), two pilot studies that aimed to optimise the parameters used within the main study were also reported. The results of the chapter indicated that the technique, parameters and equipment used to assess dark adaptation, chromatic sensitivity and flicker threshold prior to trial inception were clinically viable.

In chapter 4, the predictive capacity of the outcome measures used in the ALight trial was explored in the form of a cross-sectional study. Two different visual function tests (cone τ [pseudo R^2 0.35, $P<0.001$] and YB chromatic sensitivity [pseudo R^2 0.16, $P<0.001$]) were identified as independent predictors of increased AMD graded severity. When both tests are used simultaneously to predict an increase in AMD severity, odds ratios calculated show that with every log minute increase in cone τ and every CAD unit increase, the odds of moving up a AREDS Simplified Severity Scale grade (Ferris et al., 2005) are 2.5 and 20 times higher, respectively.

The finding supports the theory that a different underlying pathological process during AMD progression is responsible for dark adaptation and chromatic sensitivity deficits. These tests have been revealed as possible predictive biomarkers (Owsley et al., 2016; 2017; Eisner et al., 1992), however, as introduced in Section 6.8 following longitudinal evaluation dark adaptation, chromatic sensitivity and flicker threshold showed poor prognostic capacity for AMD progression during the ALight trial. Despite this, the poor performance of these visual function tests during the ALight trial may be attributed to the relatively small cohort compared to the aforementioned longitudinal studies. Therefore, the usefulness of these tests as AMD biomarkers is still unclear. Future clinical trials investigating potential new AMD treatments would benefit from further longitudinal evaluation of these potential biomarkers.

Chapter 5 provided an overview of the implementation of the ALight Clinical Trial. The safety and acceptability of the intervention was of particular focus. By examining the number of adverse events, subjective feedback and compliance data of the trial participants it was concluded that the use of an OLED sleep mask is an acceptable and safe method of delivering low-level night-time light therapy.

Chapter 6 presented the results relating to the magnitude of the effect of low-level night-time light therapy as delivered using an OLED sleep mask. These results formed the major findings of this thesis and as such are discussed in more detail below.

7.2. Key findings

The key findings of this thesis are presented with a view to addressing the original aims as specified in Section 1.5.

7.2.1. Effect of low-level night-time light therapy on AMD progression

The findings in relation to the primary objective suggested that low-level night-time light therapy, although well tolerated, had no effect on AMD progression. Although a greater proportion of controls (48%) than mask wearers (38%) showed disease progression over the duration of the trial, the study was exploratory and not powered to detect small differences between study groups. In addition to disease progression during the trial, a greater proportion of the control group (10%) than mask wearers (0%) also progressed to nAMD within 6 months after their end-of-study visit (Appendix X). Post-hoc analysis of baseline data showed that only RG chromatic threshold was a significant individual predictor of nAMD development over 18 months (binary logistic regression, $R^2 = 0.25$, $P=0.05$). Presently, no longitudinal study has investigated the usefulness of CAD-measured chromatic sensitivity as an AMD biomarker. These findings suggest that conversion to nAMD rates and effectiveness of the intervention ≥12 months may be worth exploring further in future studies.

Progression as based on the rate of retinal adaptation (time taken for the photoreceptors to recover their sensitivity after being exposed to a bright adapting light) showed a significant increase in cone τ in the intervention group when compared to the controls. The interpretation of this finding is not clear. It may represent a risk of increased rate of progression in the treatment arm (Eisner et al., 1992; Owsley et al., 2016). However, the finding that more participants from the control than the treatment arm showed increase in drusen volume or conversion to nAMD during the trial, and that more control participants converted to nAMD in the 6 months following the trial suggests that the intervention did not cause an increased risk of disease progression. It is possible that the delay in cone adaptation reported is a consequence of the long-term prevention of dark adaptation as opposed to AMD progression. At present, there is a deficit in the literature surrounding this as the two other longitudinal studies that have implemented similar methods of dark current suppression in a cohort of those with diabetic macular oedema did not measure dark adaptation parameters. Similarly, there is no evidence to clarify the effect of long-term light adaptation status on dark adaptation.

7.2.2. Acceptability of the intervention

Despite the limited impact on AMD progression the results of this thesis provide evidence that the use of an OLED sleep mask is an acceptable and safe method of delivering low-level night-time light therapy. The compliance rate (70%) was comparable with another study that utilised a similar intervention in a cohort of those with diabetic macular oedema (Sahni et al., 2016) and there were no serious adverse events or negative impact on sleep patterns to suggest safety concerns for future trials.

Although the use of an OLED sleep mask has been designated as an acceptable method of low-level night-time light therapy delivery there were a number of

withdrawals, and a high incidence of discomfort reported. During the course of the trial a number of design modifications were suggested to the mask which included:

i. Replacement of the synthetic material with a softer, lighter, natural fibre alternative to reduce overall mask weight.

ii. Perforation of mask housing or replacement with breathable material to prevent overheating.

iii. Tailoring fit by manufacturing the mask housing in a number of sizes.

iv. Incorporating memory foam into the housing to improve comfort through enhanced personalisation.

v. Modifying the strap fastener to prevent adhesion with bedding and hair.

vi. Applying a forehead buffer to alleviate pressure on bridge of nose by extending mask further outwards from the face.

vii. Redesigning access to the light sensor so the mask can be activated without removal from fabric sleeve.

viii. Enhancing the activation sensor location or colour to improve visibility.

These design modifications have since been relayed to the manufacturer and incorporated into the next generation OLED mask (Figure 7.1) prior to prospective implementation in future studies.

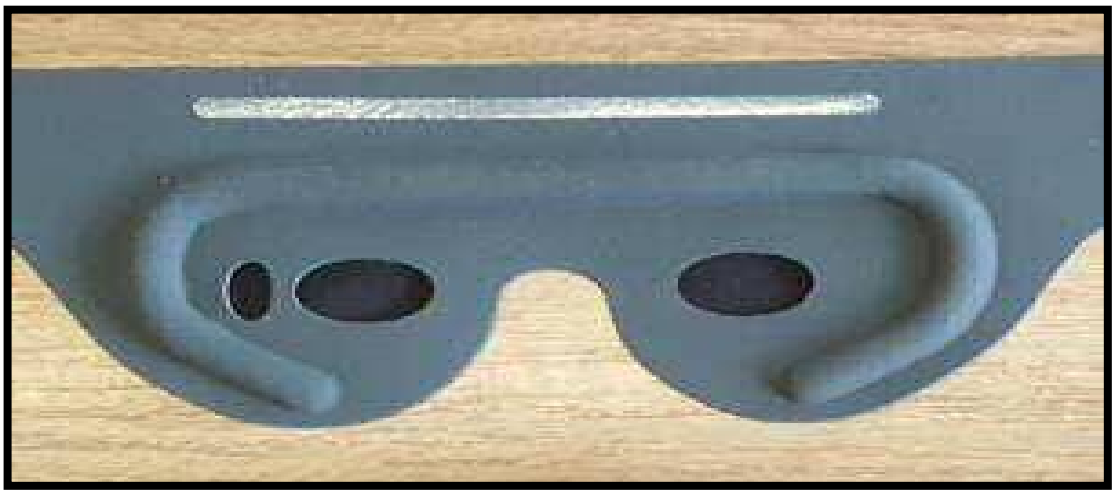

Figure 7.1. Photograph of the next generation OLED sleep mask housing as modified using feedback from the ALight study.

7.2.3. Effect of low-level night-time light therapy on secondary outcome measures

The findings relating to the secondary aims of this thesis were discussed in detail in section 6.6. Briefly, there was no evidence that low-level night-time light therapy had a positive effect on: the ranibizumab retreatment rate, change in drusen volume, change in health related quality of life (EQ-5D instrument) or change in visual function (as based on chromatic thresholds, 14Hz flicker threshold and ETDRS visual acuity). Although, 80% of the entire cohort reported an overall improvement in self-reported visual function over the duration of the study (in accordance with the VFQ-48 questionnaire) no significant difference between groups was found for this outcome measure.

7.2.4. Prognostic capacity of visual function tests for AMD progression

The evidence in this report suggests that none of the functional tests assessed at baseline were able to accurately predict disease progression during the 12 month follow up. Cone τ was the only measure to show an AUC exceeding 0.5, i.e. superior to chance alone at distinguishing between those who went on to progress in disease status, and those who did not. This finding is not consistent with previous longitudinal reports assessing the usefulness of dark adaptation (Owsley et al., 2016; 2017) and flicker threshold (Mayer et al., 1994) as prognostic tools for AMD progression. The predictive capability of dark adaptation parameters was recently evidenced in a longitudinal study by Owsley et al. (2016) who, by measuring rod dark adaptation, showed that those with delayed function at baseline and an otherwise normal retinal appearance were twice as likely to have AMD in that eye when reassessed after 3 years. In addition, both cone and rod dark adaptation parameters have also been found to show concordance with clinical macular changes in early/intermediate AMD (Dimitrov et al., 2012) further underlining the usefulness of this test. In comparison to

the results of the aforementioned studies, the poor performance of the visual function tests in the present longitudinal study may be attributed to the relatively small cohort (n=29). In order to adequately establish the prognostic capacity for nAMD onset of each test of visual function it would have been useful to have studied a larger cohort and to have followed them up for longer.

The cross-sectional analysis introduced in Chapter 4 showed that when using the AREDS Simplified Severity Scale as a surrogate for disease progression (Ferris et al., 2005) dark adaptation was the best predictive biomarker for increased AMD graded severity. Yellow-blue chromatic sensitivity also showed promise and as such is a useful test to supplement cone τ measurement. However, unlike dark adaptation, the predictive capacity of this measurement is not strengthened by a robust longitudinal study (Owsley et al., 2016; 2017). RG chromatic threshold and 14Hz flicker threshold were least useful as predictive biomarkers. This finding is contrary to current evidence suggesting that flicker threshold is found to be decreased in eyes that eventually develop GA and choroidal neovascularisation (Mayer et al., 1994; Luu et al., 2012). These differences can be attributed to the small cohort (n=36) of Mayer et al. (1994) and the different stimulus used by Luu et al. (2012) when compared to the present study. The finding that none of the visual function tests were accurately able to predict disease progression in the longitudinal component of this thesis is contrary to the identification of cone τ and YB chromatic sensitivity as independent predictors of increased AMD graded severity, as based on the cross sectional analysis conducted in Chapter 4. However, when considering the longitudinal analysis the sample size analysed (n=29) was far smaller than that of the cross-sectional study (n=100). In accordance with the lack of effect on AMD progression, the predictive capacity of the visual function tests as biomarkers for low-level night-time light therapy was not investigated.

7.3. Future work

7.3.1. Investigation of delayed dark adaptation cause

The precise cause of the delay in dark adaptation exhibited by the mask wearers of the present study is unclear. Longitudinal evaluation of a cohort of healthy participants could aid in further interpreting the present results. Such a study would involve a cohort of normals age-matched to the ALight trial cohort. Participants would be supplied with OLED light-emitting masks to wear nightly during sleep. Dark adaptation would be measured prior to mask wear and on a monthly basis until the end of the study period. This would determine any overall and progressive effect of dark current suppression on the rate of cone τ in those without AMD. Also, comparison of the change in cone τ (from baseline to final measurement) with the ALight cohort would suggest whether a delay in dark adaptation was related to suppression of the dark current or to the progression of AMD. In addition to this, a review of dark adaptation for the ALight trial intervention group would determine the permanency of the deficit found in the present study.

7.3.2. Anti-VEGF retreatment rate

The analysis of the ranibizumab retreatment rate in the present study was confounded by the implications of including those who had competed their initial loading phase and for those whom the treatment regimen was altered mid-trial. There is a strong rationale to support the presence of hypoxia in nAMD (see Chapter 2) and the present study has demonstrated acceptability and safety of the intervention. Therefore a future study specifically designed to investigate anti-VEGF retreatment rates in those with nAMD may still be valuable. It is, however, worth noting that in designing such a study the ‘treat and extend’ anti-VEGF administration programme will likely need to be considered as opposed to the standard monthly dosing regimen.

7.3.3. ALight follow-up study

The Alight trial was designed as an exploratory, proof of concept study. Although there was no evidence of an effect on disease progression the intervention was found to be safe and tolerable and, importantly, the absence of evidence is not evidence of no effect. In order to further investigate the effect of low-level night-time light therapy on AMD and build on the results of the ALight trial it is sensible to suggest a larger study, with a longer follow-up period utilising the same intervention. Post-hoc sample size calculations suggest that an approximate sample size of 381 per group would be required to power a future study to detect an effect of the magnitude seen in this exploratory trial (with 80% power, P=0.05) at 12 months. It is also worth noting that if nAMD conversions at 18-months are considered 59% of controls and 38% of the intervention group showed AMD progression (Appendix X). Powering a study to detect this magnitude of difference (80% power, P=0.05) would require an approximate sample size of 85 per group. When considering AMD progression over time using 18-month post-hoc data, the rate of progression (based on a significant increase in drusen volume or onset of nAMD) for participants within the intervention and control groups was 0.50 and 0.94 per month. Projected figures based on these progression rates show 57% (n=12) of the intervention group and 79% (n=23) of the control group displaying progression over 24 months. Powering a study to detect this magnitude of difference (80% power, P=0.05) would require an approximate sample size of 67 per group.

7.4. Final remarks

In conclusion, this exploratory study provides evidence that the use of an OLED sleep mask is an acceptable and safe method of delivering nightly low-level light therapy. A larger cohort would be required to determine whether the intervention has any effect on the progression of AMD. As AMD is a complex condition with a multi-factorial aetiology the development of a treatment is extremely difficult. Taking into account

the current global prevalence of AMD and the number of those who are presently registered as sight impaired or severely sight impaired as a result of AMD the need for a treatment aimed at preventing onset or progression is paramount. To that effect, it is hoped that the information here will not only inspire new thoughts regarding pathogenesis, but also aid in the design of future clinical trials aiming to drive us ever closer to a world where sight loss as a result of AMD no longer exists.

References

Abdelfattah NS, Zhang H, Boyer DS, Rosenfeld PJ, Feuer WJ et al (2016) Drusen Volume as a Predictor of Disease Progression in Patients With Late Age-Related Macular Degeneration in the Fellow Eye. *Investigative Opthalmology and Visual Science* **57**: 1839–1846.

Abdelfattah NS, Al-Sheikh M, Pitetta S, Mousa A, Sadda SR et al (2017) Macular Atrophy in Neovascular Age-Related Macular Degeneration with Monthly versus Treat-and-Extend Ranibizumab: Findings from the TREX-AMD Trial. *Ophthalmology* **124**: 215–223.

Abraham P, Yue H and Wilson L (2010) Randomized, Double-Masked, Sham-Controlled Trial of Ranibizumab for Neovascular Age-Related Macular Degeneration: PIER Study Year 2. American Journal of Ophthalmology 150: 315–324.

Acton J, Smith R, Hood D and Greenstein V (2012) Relationship between retinal layer thickness and the visual field in early age-related macular degeneration. *Investigative Ophthalmology and Visual Science* **53**: 7618-7624.

Adams M, Chong E, Williamson E, Aung K, Makeyeva G et al (2012) 20/20-Alcohol and age-related macular degeneration: the Melbourne collaborative cohort study: *American Journal of Epidemiology* **176**: 289-298.

Age-Related Eye Disease Study Group (AREDS) (2000) Risk factors associated with age-related macular degeneration: AREDS study report number 3. *Ophthalmology* **107**: 2224–2232.

Age-Related Eye Disease Study Group (AREDS) (2001a) A randomized, placebo-controlled, clinical trial of high-dose supplementation with vitamins C and E, beta carotene, and zinc for age-related macular degeneration and vision loss - AREDS report Number 8. *Archives of Ophthalmology* **119**: 1417–1436.

Age-Related Eye Disease Study Group (AREDS) (2001b) The Age-Related Eye Disease Study System for classifying age-related macular degeneration from stereoscopic color fundus photographs: the Age-Related Eye Disease Study report number 6. American Journal of Ophthalmology **132**: 668-681.

Age-Related Eye Disease Study Group (AREDS) (2005) Risk factors for the incidence of Advanced Age-Related Macular Degeneration in the Age-Related Eye Disease Study (AREDS) report number 19. *Ophthalmology* **112**: 533–539.

Age-Related Eye Disease Study Group 2 (AREDS2) (2013) Lutein, zeaxanthin and omega-3 fatty acids for age-related macular degeneration: the Age-Related Eye Disease Study 2 (AREDS2) randomized clinical trial. *Journal of the American Medical Association* **309**: 2005–2015.

Ahmed J, Braun R, Dunn R and Linsenmeier R (1993) Oxygen distribution in the macaque retina. *Investigative Ophthalmology and Visual Science* **34**: 516–21.

Ahnelt P (1998) The photoreceptor mosaic. *Eye* **12**: 531-540.

Aiello LP, Northrup JM, Keyt BA, Takagi H and Iwamoto MA (1995) Hypoxic regulation of vascular endothelial growth factor in retinal cells. *Archives of Ophthalmology* **113**: 1538-1544.

Al-Hussaini H, Schneiders M, Lundh P and Jeffery G (2009) Drusen are associated with local and distant disruptions to human retinal pigment epithelium cells. *Experimental Eye Research* **88**: 610–612.

Allikmets R, Shroyer N, Singh N, Seddon J, Lewis R et al (1997) Mutation of the Stargardt Disease Gene (ABCR) in Age-Related Macular Degeneration. *Science* **277**: 1805–1807.

Alten F, Clemens CR, Heiduschka P and Eter N (2013) Localized reticular pseudodrusen and their topographic relation to choroidal watershed zones and changes in choroidal volumes. *Investigative Ophthalmology and Visual Science* **54**: 3250–3257.

Alten F, Heiduschka P, Clemens CR and Eter N (2016) Exploring choriocapillaris under reticular pseudodrusen using OCT-Angiography. *Graefe's Archive for Clinical and Experimental Ophthalmology* **254**: 2165–2173.

Altman DG (1991) *Practical statistics for medical research*. 1st edition. London, Chapman and Hall.

Ambati J and Fowler B (2012) Mechanisms of age-related macular degeneration. *Neuron* **75**: 26-39.

Ambati J, Ambati BK, Yoo SH, Ianchulev S and Adamis AP (2003) Age-Related Macular Degeneration: Etiology, Pathogenesis, and Therapeutic Strategies. *Survey of Ophthalmology* **48**: 257–293.

AMD Gene Consortium (2013) Seven new loci associated with age-related macular degeneration. *Nature Genetics* **45**: 433–439.

Anderson D, Fisher S and Steinberg R (1978) Mammalian cones: disc shedding, phagocytosis, and renewal. *Investigative Opthalmology and Visual Science* **17**: 117–133.

Anderson D, Mullins R, Hageman G and Johnson L (2002) A role for local inflammation in the formation of drusen in the ageing eye. *American Journal of Ophthalmology* **134**: 411–431.

Ando K and Kripke D (1996) Light attenuation by the human eyelid. *Biological Psychiatry* **39**: 22–25.

Antony B, Abràmoff MD, Tang L, Ramdas WD, Vingerling JR et al (2011) Automated 3-D method for the correction of axial artifacts in spectral-domain optical coherence tomography images. *Biomedical optics express* **2**: 2403–2416.

Arden G and Wolf J (2004) Colour vision testing as an aid to diagnosis and management of age-related maculopathy. *British Journal of Ophthalmology* **88**: 1180–1185.

Arden G, Gündüz M, Kurtenbach A, Völker M, Zrenner E et al (2010) A preliminary trial to determine whether prevention of dark adaptation affects the course of early diabetic retinopathy. *Eye* **24**: 1149–1155.

Arden G, Jyothi S, Hogg C, Lee Y and Sivaprasad S (2011) Regression of early diabetic macular oedema is associated with prevention of dark adaptation. *Eye* **25**: 1546–1554.

Arditi A and Cagenello R (1993) On the statistical reliability of letter-chart visual acuity measurements. *Investigative Ophthalmology and Visual Science* **34**: 120–129.

Arjamaa O, Nikinmaa M, Salminen A and Kaarniranta K (2009) Regulatory role of HIF-1alpha in the pathogenesis of age-related macular degeneration (AMD). *Ageing Research Reviews* **8**: 349–358.

Arnault E, Barrau C, Nanteau C, Gondouin P, Bigot K et al (2013) Phototoxic action spectrum on a retinal pigment epithelium model of age-related macular degeneration exposed to sunlight normalized conditions. *PLOS One* **8**: e71398.

Arshavsky VY, Lamb TD and Pugh EN (2002) G proteins and phototransduction. *Annual Review of Physiology* **64**: 153–187.

Backhaus J, Junghanns K, Broocks A, Riemann D and Hohagen F (2002) Test–retest reliability and validity of the Pittsburgh Sleep Quality Index in primary insomnia. *Journal of Psychosomatic Research* **53**: 737-740.

Baird PN, Richardson ÃJ, Robman LD, Dimitrov PN, Tikellis G et al (2006) Apolipoprotein (APOE) gene is associated with progression of age-related macular degeneration (AMD). *Human Mutation* **27**: 337–342.

Barbur JL, Harlow AJ and Plant GT (1994) Insights into the Different Exploits of Colour in the Visual Cortex. *Biological Sciences* **258**: 327-334.

Barbur JL (2004) 'Double-blindsight' revealed through the processing of color and luminance contrast defined motion signals. *Progress in Brain Research* **144**: 243–259.

Barbur JL, Rodriguez-Carmona M and Harlow A (2006) Establishing the statistical limits of 'normal' chromatic sensitivity. *CIE Expert Symposium, CIE Proceedings*. Ottawa, Ontario.

Barthelmes D, Nguyen V, Arnold J, McAllister I, Guymer R et al (2016) Twelve-month outcomes of 'treat and extend' aflibercept therapy for neovascular age-related macular degeneration. *Investigative Ophthalmology and Visual Science* **57**: 521.

Bartlett H, Davies L and Eperjesi F (2004) Reliability, normative data, and the effect of age-related macular disease on the Eger Macular Stressometer photostress recovery time. *Ophthalmological and Physiological Optics* **24**: 594-599.

Beatty S, Koh H, Phil M, Henson D and Boulton M (2000) The role of oxidative stress in the pathogenesis of age-related macular degeneration. *Survey of Ophthalmology* **45**: 115–134.

Bellot JL, Palmero M, Garcia-Cabanes C, Sanz M and Orts A (2001) Effect of hypoxic stress in RPE cells: influence of antioxidant treatments. *Cutaneous and Ocular Toxicology* **20**: 29–38.

Berdeaux GH, Nordmann JP, Colin E and Arnould B (2005) Vision-related quality of life in patients suffering for age-related macular degeneration. *American Journal of Ophthalmology* **139**: 271-279.

Berenberg TL, Metelitsina TI, Madow B, Dai Y, Ying GS et al (2012) The association between drusen extent and foveolar choroidal blood flow in age-related macular degeneration. *Retina* **32**: 25–31.

Bernhard D and Wang X (2007) Smoking, oxidative stress and cardiovascular diseases: do anti-oxidative therapies fail? *Current Medicinal Chemistry* **14**: 1703–1712.

Bernstein MH and Hollenberg M (1965) Fine structure of the choriocapillaris and retinal capillaries. *Investigative Ophthalmology and Visual Science* **4**: 1016–1025.

Berson DM, Dunn FA and Takao M (2002) Phototransduction by retinal ganglion cells that set the circadian clock. *Science* **295**: 1070–1073.Bhatt A (2012) Protocol deviation and violation. *Perspectives in Clinical Research* **3**: 117.

Binns AM and Margrain TH (2007) Evaluating Retinal Function in Age-Related Maculopathy with the ERG Photostress Test. *Investigative Opthalmology and Visual Science* **48**: 2806–2813.

Biomarkers Definitions Working Group (2001) Biomarkers and surrogate endpoints: preferred definitions and conceptual framework. *Clinical Pharmacology and Therapeutics* **69**: 89-95.

Birch J, Barbur JL and Harlow AJ (1992) New method based on random luminance masking for measuring isochromatic zones using high resolution colour displays. *Ophthalmic and Physiological Optics* **12**: 133–136.

Bird A (1992) Bruch's membrane change with age. *British Journal of Ophthalmology* **76**: 166–168.

Bird A, Bressler N, Bressler S, Chisholm I, Coscas G et al (1995) An international classification and grading system for age-related maculopathy and age-related macular degeneration. *Survey of Ophthalmology* **39**: 367–374.

Birol G, Wang S, Budzynski E, Wangsa-wirawan ND and Linsenmeier RA (2007) Oxygen distribution and consumption in the macaque retina. *American Journal of Physiology* **293**: 1696–1704.

Blair MP, Gupta M, Blair NP and Shahidi M (2010) Association Between Retinal Thickness and Retinal Pigment Epithelium Elevation in Age-Related Macular Degeneration. *Ophthalmic Surgery, Lasers and Imaging* **41**: 175–181.

Bland JM and Altman DG (1986) Statistical methods for assessing agreement between two methods of clinical measurement. *Lancet* **8**: 307-310.

Blasiak J and Szaflik J (2011) DNA damage and repair in age-related macular degeneration. *Frontiers in Bioscience* **16**: 1291–1301.

Blasiak J, Petrovski G, Vereb Z, Facsko A and Kaarniranta K (2014) Oxidative stress, hypoxia, and autophagy in the neovascular processes of age-related macular degeneration. *BioMed Research International* **2014**: e768026

Blomhoff R and Blomhoff HK (2006) Overview of retinoid metabolism and function. *Journal of Neurobiology* **66**: 606–630.

Bok D (1993) The retinal pigment epithelium: a versatile partner in vision. *Journal of Cell Science* **17**: 189–195.

Boltz A, Luksch A, Wimpissinger B, Maar N, Weigert G et al (2010) Choroidal blood flow and progression of age-related macular degeneration in the fellow eye in patients with unilateral choroidal neovascularization. *Investigative Ophthalmology and Visual Science* **51**: 4220–4225.

Bonilha VL, Rayborn ME, Bhattacharya SK, Gu X, Crabb JS et al (2006) The retinal pigment epithelium apical microvilli and retinal function. *Advances in Experimental Medicine and Biology* **572**: 519–524.

Bonilha VL (2008) Age and disease-related structural changes in the retinal pigment epithelium. *Clinical Ophthalmology* **2**: 413–242.Booij JC, Baas DC, Beisekeeva J, Gorgels TF and Bergen AB (2010) The dynamic nature of Bruch's membrane. *Progress in Retinal and Eye Research* **29**: 1–18.

Borwein B and Borwein D (1980) The ultrastructure of monkey foveal photoreceptors with special reference to the structure, shape, size, and spacing of the foveal cones. *American Journal of Anatomy* **159**: 125–146.

Boulton M and Dayhaw-Barker P (2001) The role of the retinal pigment epithelium: topographical variation and ageing changes. *Eye* **15**: 384–389.

Boyce P and Kennaway DJ (1987) Effects of light on melatonin production. *Biological Psychiatry* **22:** 473-478.

Boyer DS, Heier JS, Brown DM, Francom SF, Ianchulev T et al (2009) A phase IIIb Study to Evaluate the Safety of Ranibizumab in Subjects with Neovascular Age-related Macular Degeneration. *Ophthalmology* **116**: 1731–1739.

Brainard DH (1997) The psychophysics toolbox. *Spatial Vision* **10**: 433–436.

Brainard GC, Hanifin JP, Greeson JM, Byrne B, Glickman G (2001) Action spectrum for melatonin regulation in humans: evidence for a novel circadian photoreceptor. *Journal of Neuroscience* **21**: 6405-6412.

Bressler SB, Maguire M, Bressler N and Fine S (1990) Relationship of drusen and abnormalities of the retinal pigment epithelium to the prognosis of neovascular macular degeneration. *Archives of Ophthalmology* **108**: 1442–1447.

Bressler NM, Silva JC, Bressler SB, Fine SL and Green WR (1994) Clinicopathologic correlation of drusen and retinal pigment epithelial abnormalities in age-related macular degeneration. *Retina* **14**: 130–142.

Bressler NM and Bressler SB (2000) Photodynamic therapy with Verteporfin (Visudyne): impact on ophthalmology and visual sciences. *Investigative Ophthalmology and Visual Science* **41**: 624–628.

Bressler SB, Munoz B, Solomon S and West S (2008) Racial differences in the prevalence of age-related macular degeneration. *Archives of Ophthalmology* **126**: 241–245.

Brinchmann-Hansen O and Myhre K (1989) The effect of hypoxia upon macular recovery time in normal humans. *Aviation, Space and Environmental Medicine* **60:** 1183–1186.

Brody B, Gamst A, Williams R, Smith A, Lau P et al (2001) Depression, visual acuity, comorbidity, and disability associated with age-related macular degeneration. *Ophthalmology* **108**: 1893–1901.

Brown B and Lovie-kitchin J (1987) Temporal function in age-related maculopathy. *Clinical and Experimental Optometry* **70**: 112–116.

Brown DM and Regillo CD (2007) Anti-VEGF Agents in the Treatment of Neovascular Age-related Macular Degeneration: Applying Clinical Trial Results to the Treatment of Everyday Patients. *American Journal of Ophthalmology* **144**: 627–637.

Brown MM, Brown GC, Sharma S, Bushee B and Brown H (2001) Quality of life associated with unilateral and bilateral good vision. *Ophthalmology* **108**: 643-648.

Brown DM, Kaiser PK, Michels M, Soubrane G, Heier JS et al (2006) Ranibizumab versus verteporfin for neovascular age-related macular degeneration. *New England Journal of Medicine* **355**: 1432–1444.

Brown DM, Michels M, Kaiser PK, Heier JS, Sy JP et al (2009) Ranibizumab versus verteporfin photodynamic therapy for neovascular age-related macular degeneration: Two-year results of the ANCHOR study. *Ophthalmology* **116**: 57–65.

Buch H, Nielsen NV, Vinding T, Jensen GB, Prause JU et al (2005) 14-year incidence, progression, and visual morbidity of age-related maculopathy: the Copenhagen City Eye Study. *Ophthalmology* **112**: 787–798.

Bunce C, Xing W and Wormald R (2010) Causes of blind and partial sight certifications in England and Wales: April 2007-March 2008. *Eye* **24**: 1692–1699.

Bunce C, Zekite A, Walton S, Rees A and Patel P (2015) Certifications for sight impairment due to age-related macular degeneration in England. *Public Health* **129**: 138–142.

Buysse, DJ, Reynolds CF, Monk TH, Berman SR and Kupfer DJ (1989) The Pittsburgh Sleep Quality Index: a new instrument for psychiatric practice and research. *Psychiatry Research* **28**: 193–213.

Calvo P, Ferreras A, Wang Y, Wai-Ching L, Devenyi R et al (2014) Treat and Extend Versus Treat and Observe Regimens in Wet Age-related Macular Degeneration Patients Treated with Ranibizumab: 3-year Surveillance Period. *Journal of Clinical and Experimental Ophthalmology* **5**: 1000324.

Camacho P, Dutra-Medeiros M and Paris L (2017) Ganglion Cell Complex in Early and Intermediate Age-Related Macular Degeneration: Evidence by SD-OCT Manual Segmentation. *Ophthalmologica **238**: 31-43.*

Caprara C and Grimm C (2012) From oxygen to erythropoietin: Relevance of hypoxia for retinal development, health and disease. *Progress in Retinal and Eye Research* **31**: 89–119.

Carifio J and Perla R (2008) Resolving the 50-year debate around using and misusing Likert scales. *Medical Education* **42**: 1150–1152.

Carpenter JS and Andrykowski MA (1998) Psychometric evaluation of the pittsburgh sleep quality index. *Journal of Psychosomatic Research* **45**: 5–13.

Cassels N, Wild J, Margrain T, Chong V and Acton J (2017) The use of microperimetry in assessing visual function in age-related macular degeneration. *Survery of Ophthalmology*. In press.

Cash TP, Pan Y and Simon MC (2007) Reactive oxygen species and cellular oxygen sensing. *Free Radical Biology and Medicine* **43**: 1219–1225.

Casten R and Rovner B (2013) Update on depression and age-related macular degeneration. *Current Opinion in Ophthalmology* **24**: 239–243.

CATT Research Group (2011) Ranibizumab and Bevacizumab for Neovascular Age-Related Macular Degeneration. *New England Journal of Medicine* **364**: 1897–1908.

CATT Research Group (2016) Five-year outcomes with anti-vascular endothelial growth factor treatment of neovascular age-related macular degeneration: the comparison of age-related macular degeneration treatment trials. *Ophthalmology* **123**: 1751-1761.

Chakravarthy U and Gardiner T (1999) Endothelium-derived agents in pericyte function/dysfunction. *Progress in Retinal and Eye Research* **18**: 511–527.

Chakravarthy U, Wong TY, Fletcher A, Piault E, Evans C et al (2010) Clinical risk factors for age-related macular degeneration: a systematic review and meta-analysis. *Biomedical Central Ophthalmology* **10**: 10–31.

Chakravarthy U, McKay GJ, De Jong PT, Rahu M, Seland J et al (2013a) ARMS2 increases the risk of early and late age-related macular degeneration in the European Eye Study. *Ophthalmology* **120**: 342–348.

Chakravarthy U, Harding SP, Rogers CA, Downes SM, Lotery AJ et al (2013b) Alternative treatments to inhibit VEGF in age-related choroidal neovascularisation: 2-year findings of the IVAN randomised controlled trial. *Lancet* **12**: 1258-1267.

Chang MA, Bressler SB, Munoz B and West SK (2008) Racial differences and other risk factors for incidence and progression of age-related macular degeneration: Salisbury Eye Evaluation (SEE) Project. *Investigative Ophthalmology and Visual Science* **49**: 2395–2402.

Chen JC, Firzke FW, Pauleikhoff D and Bird AC (1992) Functional loss in age-related Bruch's membrane change with choroidal perfusion defect. *Investigative Ophthalmology and Visual Science* **2**: 334–340.

Chen SJ, Cheng CY, Lee AF, Lee FL, Chou JC et al (2001) Pulsatile ocular blood flow in asymmetric exudative age-related macular degeneration. *British Journal of Ophthalmology* **85**: 1411–1415.

Chew EY, Clemons TE, Agrón E, Sperduto RD, Sangiovanni JP et al (2014) Ten-year follow-up of age-related macular degeneration in the age-related eye disease study: AREDS report number 36. *Journal of the American Medical Association* **132**: 272–277.

Chiang A and Regillo CD (2011) Preferred therapies for neovascular age-related macular degeneration. *Current Opinion in Ophthalmology* **22**: 199–204.

Cho NC, Poulsen G, Ver Hoeve J and Nork M (2000) Selective Loss of S-Cones in Diabetic Retinopathy. *Archives of Ophthalmology* **118**: 1393-1400.

Chou CF, Cotch MF, Vitale S, Zhang X, Klein R et al (2013) Age-related eye diseases and visual impairment among U.S. adults. *American Journal of Preventive Medicine* **45**: 29–35.

Christen W, Glynn R, Manson J, Ajani U and Buring J (1996) A prospective study of cigarette smoking and risk of age-related macular degeneration in men. *Journal of the American Medical Association* **276**: 1147–1151.

CHROMA (2014) A study investigating the efficacy and safety of lampalizumab intravitreal injections in participants with geographic atrophy secondary to age-related macular degeneration (CHROMA). *https://clinicaltrials.gov/ct2/show/NCT02247479*. [Accessed 15th May 2017].

Churchill A, Carter J, Lovell H, Ramsden C, Turner S et al (2006) VEGF polymorphisms are associated with neovascular age-related macular degeneration. *Human Molecular Genetics* **15**: 2955–2961.

Chylack LJ, Wolfe J, Friend J, Khu P, Singer D et al (1993) Quantitating cataract and nuclear brunescence, the Harvard and LOCS systems. *Optometry and Vision* **70**: 886–895.

Ciulla T, Harris A, Chung HS, Danis RP, Kagemann L et al (1999) Color Doppler imaging discloses reduced ocular blood flow velocities in non-exudative age-related macular degeneration. *American Journal of Ophthalmology* **128**: 75–80.

Ciulla T, Harris A, Kagemann L, Danis RP, Pratt L et al (2002) Choroidal perfusion perturbations in non-neovascular age-related macular degeneration. *British Journal of Ophthalmology* **86**: 209-213.

Civil Aviation Authority (CAA) (2009) Minimum colour vision requirements for professional flight crew, recommendations for new colour vision standards. *CAA Paper 2009/04* **1**: 1–57.

Coassin M, Duncan KG, Bailey KR, Singh A and Schwartz DM (2010) Hypothermia reduces secretion of vascular endothelial growth factor by cultured retinal pigment epithelial cells. *British Journal of Ophthalmology* **94**: 1678–1683.

Cohen S, Dubois L, Tadayoni R, Delahaye-Mazza C, Debibie C et al (2007) Prevalence of reticular pseudodrusen in age-related macular degeneration with newly diagnosed choroidal neovascularisation. *British Journal of Ophthalmology* **91**: 354–359.

Coleman AL, Yu F, Ensrud KE, Stone KL, Cauley JA et al (2010) Impact of Age-Related Macular Degeneration on Vision-Specific Quality of Life: Follow-up from the 10-Year and 15-Year Visits of The Study of Osteoporotic Fractures. *American Journal of Ophthalmology* **150**: 683–691.

Coleman DJ, Silverman RH, Rondeau MJ, Lloyd HO, Khanifar A et al (2013) Age-related macular degeneration: choroidal ischaemia? *British Journal of Ophthalmology* **97**: 1020–1023.

Coleman HR, Chan CC, Ferris FL and Chew EY (2008) Age-related macular degeneration. *Lancet* **372**: 1835–1845.

Connell PP, Keane PA, O'Neill EC, Altaie RW, Loane E et al (2009) Risk factors for age-related maculopathy. *Journal of Ophthalmology* **2009**: 1–39.

Connolly DM and Hosking SL (2006) Aviation-related respiratory gas disturbances affect dark adaptation: a reappraisal. *Vision Research* **46**: 1784–1793.

Connolly DM, Barbur JL, Hosking SL and Moorhead IR (2008) Mild hypoxia impairs chromatic sensitivity in the mesopic range. *Investigative Ophthalmology and Visual Science* **49**: 820–827.

Connolly DM. and Hosking SL (2009) Oxygenation state and mesopic sensitivity to dynamic contrast stimuli. *Optometry and Vision Science* **86**: 1368–1375.

Cornsweet T (1962) The staircrase-method in psychophysics. *American Journal of Psychology* **75**: 485–491.

Coscas F, Coscas G, Souied E, Tick S and Soubrane G (2007) Optical Coherence Tomography Identification of Occult Choroidal Neovascularization in Age-related Macular Degeneration. *American Journal of Ophthalmology* **144**: 592–599.

Crabb JW, Miyagi M, Gu X, Shadrach K, West KA et al (2002) Drusen proteome analysis: an approach to the etiology of age-related macular degeneration. *Proceedings of the National Academy of Sciences of the United States of America* **12**: 14682-14687.

Cui H, Kong Y and Zhang H (2012) Oxidative stress, mitochondrial dysfunction, and aging. *Journal of Signal Transduction* **2012**: 1–13.

Curcio CA, Sloan KR, Kalina RE and Hendrickson AE (1990) Human photoreceptor topography. *Journal of Comparative Neurology* **292**: 497–523.

Curcio CA, Medeiros N and Millican C (1996) Photoreceptor loss in age-related macular degeneration. *Investigative Ophthalmology and Visual Science* **37**: 1236–1249.

Curcio CA, Johnson M, Huang JD and Rudolf M (2010) Apolipoprotein B-containing lipoproteins in retinal aging and age-related macular degeneration. *Journal of Lipid Research* **51**: 451–467.

Dadgostar H, Ventura AA, Chung JY, Sharma S and Kaiser PK (2009) Evaluation of Injection Frequency and Visual Acuity Outcomes for Ranibizumab Monotherapy in Exudative Age-related Macular Degeneration. *Ophthalmology* **116**: 1740–1747.

Das S, Bhardwaj N, Kjeldbye H and Gouras P (1992) Muller cells of chicken retina synthesize 11-cis-retinol. *Biochemical Journal* **285**: 907–913.

Davis MD, Gangnon RE, Lee LY, Hubbard LD, Klein BE et al (2005) The Age-Related Eye Disease Study severity scale for age-related macular degeneration: AREDS report number 17. *Archives of Ophthalmology* **123**: 1484–1498.

De Winter J and Dodou D (2010) Five-point Likert items: t test versus Mann-Whitney-Wilcoxon. *Practical Assessment, Research & Evaluation* **15**: 10781922.

Delaey C and Van De Voorde J (2000) Regulatory mechanisms in the retinal and choroidal circulation. *Ophthalmic Research* **32**: 249–256.

DelCourt C, Michel F, Colvez A, Lacroux A, Delage M et al (2001) Associations of cardiovascular disease and its risk factors with age-related macular degeneration: the POLA study. *Ophthalmic Epidemiology* **8**: 237–249.

Despriet D, Klaver C, Witteman JC, Bergen AA, Kardys I et al (2006) Complement Factor H polymorphism, complement activators, and risk of age-related macular degeneration. *Journal of the American Medical Association* **296**: 301–309.

Dhital A, Pey T and Stanford M (2010) Visual loss and falls: a review. *Eye* **24**: 1437–1446.

Dimitrov PN, Guymer RH, Zele AJ, Anderson AJ and Vingrys AJ (2008) Measuring rod and cone dynamics in age-related maculopathy. *Investigative Ophthalmology and Visual Science* **49**: 55–65.

Dimitrov PN, Robman LD, Varsamidis M, Aung KZ, Makeyeva GA et al (2011) Visual function tests as potential biomarkers in age-related macular degeneration. *Investigative Ophthalmology and Visual Science* **52**: 9457–9469.

Dimitrov PN, Robman LD, Varsamidis M, Aung KZ, Makeyeva G et al (2012) Relationship between clinical macular changes and retinal function in age-related macular degeneration. *Investigative Ophthalmology and Visual Science* **53**: 5213–5220.

Dimitrova G, Tamaki Y and Kato S (2002) Retrobulbar circulation in patients with age-related maculopathy. *Eye* **16**: 580–586.

Ding X, Patel M and Chan CC (2009) Molecular pathology of age-related macular degeneration. *Progress in Retinal and Eye Research* **28**: 1–18.

Diniz B, Ribeiro R, Heussen FM, Maia M and Sadda S (2014) Drusen measurements comparison by fundus photograph manual delineation versus optical coherence tomography retinal pigment epithelial segmentation automated analysis. *Retina* **34**: 55–62.

Dixon JA, Oliver SC, Olson JL and Mandava N (2009) VEGF Trap-Eye for the treatment of neovascular age-related macular degeneration. *Expert Opinion on Investigational Drugs* **18**: 1573–1580.

Dolan P (1997) Modeling valuations for EuroQol health states. *Medical Care* **35**: 1095–1108.

Donoso LA, Kim D, Frost A, Callahan A and Hageman G (2005) The role of inflammation in the pathogenesis of age-related macular degeneration. *Survey of Ophthalmology* **51**: 137–152.

Donoso LA, Vrabec T and Kuivaniemi H (2010) The role of complement Factor H in age-related macular degeneration: a review. *Survey of Ophthalmology* **55**: 227–246.

Dorey CK, Wu G, Ebenstein D, Garsd A and Weiter JJ (1989) Cell loss in the aging retina. Relationship to lipofuscin accumulation and macular degeneration. *Investigative Ophthalmology and Visual Science* **30**: 1691–1699.

Drexler W, Morgner U, Kärtner F, Pitris C, Boppart S et al (1999) In vivo ultrahigh-resolution optical coherence tomography. *Optics Letters* **24**: 1221–1223.

Druzhyna NM, Wilson GL and LeDoux SP (2008) Mitochondrial DNA repair in aging and disease. *Mechanisms of Ageing and Development* **129**: 383–390.

Duan Y, Mo J, Klein R, Scott IU, Lin HM et al (2007) Age-related macular degeneration is associated with incident myocardial infarction among elderly Americans. *Ophthalmology* **114**: 732–737.

Dugel P, Jaffe G, Sallstig P, Warburton J, Weichselberger A et al (2017) Brolucizumab versus aflibercept in participants with neovascular age-related macular degeneration: a randomised trial. *Ophthalmology* **124**: 1296-1304.

Ebrey T and Koutalos Y (2001) Vertebrate photoreceptors. *Progress in Retinal and Eye Research* **20**: 49–94.

Egbewale B (2015) Statistical issues in randomised controlled trials: a narrative synthesis. *Asian Pacific Journal of Tropical Biomedicine* **5**: 354-359.

Eisner A, Fleming SA, Klein ML and Mauldin WM (1987) Sensitivities in older eyes with good acuity: eyes whose fellow eye has exudative AMD. *Investigative Ophthalmology and Visual Science* **28**: 1832–1837.

Eisner A, Stoumbos V, Klein M and Fleming S (1991) Relations between fundus appearance and function: eyes whose fellow eye has exudative age-related macular degeneration. *Investigative Ophthalmology and Visual Science* **32**: 8–20.

Eisner A, Klein ML, Zils JD and Watkins M (1992) Visual function and subsequent development of exudative age-related macular degeneration. *Investigative Ophthalmology and Visual Science*. **33**: 3091-3102.

Eleftheriadou M, Vasquez-Alfageme C, Citu C, Crosby-Nwaobi R, Sivaprasad S et al (2017) Long-term outcomes of aflibercept treatment for neovascular age-related macular degeneration in a clinical setting. *American Journal of Ophthalmology* **174**: 160-168.

EuroQol Group (1990) A new facility for the measurement of health-related quality of life. *Health Policy* **16**: 199-208.

Evans J, Fletcher A and Wormald R (2005) 28 000 Cases of age related macular degeneration causing visual loss in people aged 75 years and above in the United Kingdom may be attributable to smoking. *British Journal of Ophthalmology* **89**: 550–553.

Evans JR and Lawrenson JG (2017) Antioxidant vitamin and mineral suppliments for slowing the progression of age-related macular degeneration. *Cochrane Database of Systematic Reviews*. **31**: CD000254.

Eye Disease Prevalence Research Group (2004) Causes and prevalence of visual impairment among adults in the United States. *Archives of Ophthalmology* **122**: 477–485.

Feigl B, Stewart I and Brown B (2007) Experimental hypoxia in human eyes: implications for ischaemic disease. *Clinical Neurophysiology* **118:** 887–895.

Feigl B, Stewart I, Brown B and Zele AJ (2008) Local neuroretinal function during acute hypoxia in healthy older people. *Investigative Ophthalmology and Visual Science* **49**: 807–813.

Feigl B (2009) Age-related maculopathy - linking aetiology and pathophysiological changes to the ischaemia hypothesis. *Progress in Retinal and Eye Research* **28**: 63–86.

Ferris F, Davis M, Clemons T, Lee L, Chew E et al (2005) A simplified severity scale for age-related macular degeneration. *Archives of Ophthalmology* **123**: 1570–1574.

Ferris FL, Wilkinson C, Bird A, Chakravarthy U, Chew E et al (2013) Clinical Classification of Age-related Macular Degeneration. *Ophthalmology* **120**: 844–851.

Fields M, Cai H, Gong J and Del Priore L (2016) Potential of induced pluripotent stem cells (iPSCs) for treating age-related macular degeneration (AMD). *Cells* **8**: E44.

Fine AM, Elman MJ, Ebert JE, Prestia PA, Starr JS et al (1986) Earliest symptoms caused by neovascular membranes in the macula. *Archives of Ophthalmology* **104**: 513-514.

Finger RP, Wiedemann P, Blumhagen F, Pohl K and Holz FG (2013) Treatment patterns, visual acuity and quality-of-life outcomes of the WAVE study - A noninterventional study of ranibizumab treatment for neovascular age-related macular degeneration in Germany. *Acta Ophthalmologica* **91**: 540–546.

Finger RP, Wu Z, Luu CD, Kearney F, Ayton LN et al (2014) Reticular pseudodrusen: a risk factor for geographic atrophy in fellow eyes of individuals with unilateral choroidal neovascularization. *Ophthalmology* **121**: 1252–1256.

Fleming TR and DeMets DL (1996) Surrogate end points in clinical trials: Are we being misled? *Annals of Internal Medicine* **125**: 605-613.

Fletcher AE, Bentham G, Agnew M, Young I, Augood C et al (2008) Sunlight Exposure, Antioxidants, and Age-Related Macular Degeneration. *Archives of Ophthalmology* **126**: 1396–1403.

Fooroghian F, Razavi R and Timms L (2007) Hypoxia-inducible factor expression in human RPE cells. *British Journal of Ophthalmolology* **91**: 1406–1410.

Forrester J, Dick A, McMenamin P, Roberts F and Pearlman E (2016) *The Eye: Basic Sciences in Practice*. 4th edition. St Louis, Elsevier.

Frank R, Puklin J, Stock C and Canter L (2000) Race, iris color, and age-related macular degeneration. *Transactions of the American Ophthalmological Society* **98**: 109–115.

Frennesson C, Nilsson U and Nilsson S (1996) Colour contrast sensitivity in patients with soft drusen, and early stage of ARM. *Documenta Ophthalmogica* **90**: 377-386.

Freund K, Ho I, Barbazetto I, Koizumi H, Laud K et al (2008) Type 3 neovascularization - The expanded spectrum of retinal angiomatous proliferation. *Retina* **28**: 201–211.

Freund BK, Korobelnik JF, Devenyi R, Framme C, Galic J et al (2015) Treat-and-extend regimens with anti-VEGF agents in retinal diseases: a literature review and consensus recommendations. *Retina* **35**: 1489-1506.

Friedman E, Ivry M, Ebert E, Glynn R, Gragoudas E et al (1989) Increased scleral rigidity and age-related macular degeneration. *Ophthalmology* **96**: 104–108.

Friedman E, Krupsky S, Lane AM, Oak SS, Friedman ES et al (1995) Ocular Blood Flow Velocity in Age-related Macular Degeneration. *Ophthalmology* **102**: 640–646.

Friedman DS, Katz J, Bressler NM, Rahmani B and Tielsch JM (1999) Racial differences in the prevalence of age-related macular degeneration. *Ophthalmology* **106**: 1049–1055.

Fritsche LG, Igl W, Bailey JC, Grassmann F and Heid IM (2015) A large genome-wide association study of age-related macular degeneration highlights contributions of rare and common variants. *Nature Genetics* **48**: 134–143.

Fu Y (2010) Phototransduction in rods and cones. Webvision, *http://webvision.med.utah.edu/*. [Accessed 19th August 2017].

Fuchshofer R, Yu AL, Teng HH, Strauss R, Kampik A et al (2009) Hypoxia/reoxygenation induces CTGF and PAI-1 in cultured human retinal pigment epithelium cells. *Experimental Eye Research* **88**: 889–899.

Gaffney AJ, Binns AM and Margrain TH (2011) Topography of cone dark adaptation deficits in age-related maculopathy. *Optometry and Vision Science* **88**: 1080–1087.

Gaffney AJ, Binns AM and Margrain TH (2012) Aging and Cone Dark Adaptation. *Optometry and Vision Science* **89**: 1219–1224.

Gaffney AJ, Binns AM and Margrain TH (2013) The effect of pre-adapting light intensity on dark adaptation in early age-related macular degeneration. *Documenta Ophthalmologica.* **127**: 191–199.

Gaffney AJ, Binns AM and Margrain TH (2014) Measurement of cone dark adaptation: a comparison of four psychophysical methods. *Documenta Ophthalmologica* **128**: 33–41.

Garvin MK, Abràmoff MD, Wu X, Russell SR, Burns TL et al (2009) Automated 3-D intraretinal layer segmentation of macular spectral-domain optical coherence tomography images. *IEEE Transactions on Medical Imaging* **28**: 1436–1447.

Geirsdottir A, Hardarson SH, Olafsdottir OB and Stefánsson E (2014) Retinal oxygen metabolism in exudative age-related macular degeneration. *Acta Ophthalmologica* **92**: 27–33.

Geographic Atrophy Progression (GAP) Study Group (2011) Reticular Drusen Associated with Geographic Atrophy in Age-Related Macular Degeneration. *Investigative Opthalmology and Visual Science* **52**: 5009–5015.

Gescheider G (1997) *Psychophysics: the fundamentals*. 3rd edition. New Jersey, Lawrence Erlbaum Associates Inc.

Giani A, Cigada M, Choudhry N, Deiro AP, Oldani M, Pellegrini M et al (2010) Reproducibility of retinal thickness measurements on normal and pathologic eyes by different optical coherence tomography instruments. *American Journal of Ophthalmology* **150**: 815-824.

Giannakaki-Zimmermann H, Ebneter A, Munk MR, Wolf S and Zinkernagel MS (2016) Outcomes when Switching from a pro re nata Regimen to a Treat and Extend Regimen Using Aflibercept in Neovascular Age-Related Macular Degeneration. *Ophthalmologica* **236**: 201–206.

Giovannini A, Mariotti C, Ripa E, Sforzolini B and Tittarelli R (1994) Choroidal filling in age-related macular degeneration: indocyanine green angiographic findings. *Ophthalmologica* **208**: 185–191.

Gold B, Merriam JE, Zernant J, Hancox LS, Taiber AJ et al (2006) Variation in factor B (BF) and complement component 2 (C2) genes is associated with age-related macular degeneration. *Nature Genetics* **38**: 458–462.

Golden T and Melov S (2001) Mitochondrial DNA mutations, oxidative stress, and aging. *Mechanisms of Ageing and Development* **122**: 1577–1589.

Gopinath B, Liew G, Flood VM, Joachim N, Burlutsky G et al (2017) Combined influence of poor health behaviours on the prevalence and 15-year incidence of age-related macular degeneration. *Scientific Reports* **7**: 4359.

Graham CH (1965) *Vision and visual perception*. 1st edition. Oxford, Wiley.

Grassmann F, Friedrich U, Fauser S, Schick T, Milenkovic A et al (2015) A Candidate Gene Association Study Identifies DAPL1 as a Female-Specific Susceptibility Locus for Age-Related Macular Degeneration (AMD). *Neuromolecular Medicine* **17**: 111–120.

Green WR (1999) Histopathology of age-related macular degeneration. *Molecular Vision* **5**: 27.

Green WR and Enger C (1993) Age-related macular degeneration histopathologic studies. *Ophthalmology* **100**: 1519-1535.

Greenstein VC, Shapiro A, Zaidi Q and Hood DC (1992) Psychophysical evidence for post-receptoral sensitivity loss in diabetics. *Investigative Ophthalmology and Visual Science* **33**: 2781–2790.

Gregori G, Wang F, Rosenfeld PJ, Yehoshua Z, Gregori NZ et al (2011) Spectral domain optical coherence tomography imaging of drusen in nonexudative age-related macular degeneration. *Ophthalmology* **118**: 1373–1379.

Grossniklaus H and Gass J (1998) Clinicopathologic correlations of surgically excised type 1 and type 2 submacular choroidal neovascular membranes. *American Journal of Ophthalmology* **126**: 59–69.

Grunwald JE, Metelitsina TI, Dupont JC, Ying GS and Maguire MG (2005) Reduced foveolar choroidal blood flow in eyes with increasing AMD severity. *Investigative Ophthalmology and Visual Science* **46**: 1033–1038.

Gupta OP, Shienbaum G, Patel AH, Fecarotta C, Kaiser RS et al (2010) A Treat and Extend Regimen Using Ranibizumab for Neovascular Age-Related Macular DegenerationClinical and Economic Impact. *Ophthalmology* **117**: 2134–2140.

Guymer R Luthert P and Bird A (1999) Changes in Bruch's membrane and related structures with age. *Retinal and Eye Research* **18**: 59–90.

Haddad S, Chen C, Santangelo SL and Seddon J (2006) The genetics of age-related macular degeneration: a review of progress to date. *Survey of Ophthalmology* **51**: 316-363.

Hageman GS, Luthert PJ, Chong NV, Johnson L V, Anderson DH et al (2001) An integrated hypothesis that considers drusen as biomarkers of immune-mediated processes at the RPE-Bruch's membrane interface in aging and age-related macular degeneration. *Progress in Retinal and Eye Research* **20**: 705–732.

Hagins W, Ross P, Tate R and Yoshikami S (1989) Transduction heats in retinal rods: tests of the role of cGMP by pyroelectric calorimetry. *Proceedings of the National Academy of Sciences of the United States of America* **86**: 1224–1228.

Haines J, Hauser MA, Schmidt S, Scott WK, Olson LM (2005) Complement Factor H Variant Increases the Risk of Age-Related Macular Degeneration. *Science* **308**: 419–421.

Ham WT, Mueller HA and Sliney DH (1976) Retinal sensitivity to damage from short wavelength light. Nature **11**: 153-155.

Hamer R, Nicholas S, Tranchina D, Lamb T and Jarvinen J (2005) Toward a unified model of vertebrate rod phototransduction. *Visual Neuroscience* **22**: 417–436.

Hammond BR and Wooten BR (2002) Genetic influence on early age-related macular degeneration: a twin study. *Ophthalmology* **109**: 730-736.

HARRIER (2015) A Two-Year, Randomised, Double-Masked, Multicenter, Two-Arm Study Comparing the Efficacy and Safety of RTH258 6mg Versus Aflibercept in Subjects With Neovascular Age-Related Macular Degeneration. *https://clinicaltrials.gov/ct2/show/NCT02434328*. [Accessed 5th September 2017].

Harman D (1956) Aging: a theory based on free radical and radiation chemistry. *Journal of Gerontology* **11**: 298–300.

Hartnett ME, Weiter JJ, Staurenghi G and Elsner AE (1996) Deep retinal vascular anomalous complexes in advanced age-related macular degeneration. *Ophthalmology* **103**: 2042–2053.

Hassell J, Lamoureux E and Keeffe J (2006) Impact of age related macular degeneration on quality of life. *British Journal of Ophthalmology* **90**: 593–596.

Hattar S, Liao HW, Takao M, Berson DM and Yau KW (2002) Melanopsin-containing retinal ganglion cells : architecture, projections and intrinsic photosensitivity. *Science* **295** : 1065-1070.

Hatz K and Prünte C (2017) Intravitreal aflibercept in neovascular age-related macular degeneration with limited response to ranibizumab: a treat-and-extend trial. *Retina* **37**: 1185–1192.

Hatz K and Prünte C (2017) Treat and Extend versus Pro Re Nata regimens of ranibizumab in neovascular age-related macular degeneration: a comparative 12 Month study. *Acta Ophthalmologica* **95**: 67–72.

HAWK (2014) Efficacy and safety of RTH258 versus aflibercept. A Two-Year, Randomised, Double-Masked, Multicenter, Three-Arm Study Comparing the Efficacy and Safety of RTH258 Versus Aflibercept in Subjects With Neovascular Age-Related Macular Degeneration. *https://clinicaltrials.gov/ct2/show/NCT02307682*. [Accessed 5th September 2017].

Hayreh SS (1962) The ophthalmic artery III: branches. *British Journal of Ophthalmology* **46**: 212–247.

Hayreh SS and Baines J (1972) Occlusion of the posterior ciliary artery. I. effects on choroidal circulation. *British Journal of Ophthalmology* **56**: 719–735.

Hayreh SS (1975) Segmental nature of the choroidal vasculature. *British Journal of Ophthalmology* **59**: 631–648.

Hecht S, Haig C and Wald G (1935) The dark adaptation of retinal fields of different size and location. *Journal of General Physiology* **19**: 321–337.

Hecht S, Haig C and Chase A (1937) The influence of light adaptation on subsequent dark adaptation of the eye. *Journal of General Physiology* **20**: 831–850.

Hecht S, Shlar S and Pirenne M (1942) Energy, Quanta and Vision. *Journal of General Physiology* **25**: 819-840.

Heier JS, Brown DM, Chong V, Korobelnik JF, Kaiser PK et al (2012) Intravitreal Aflibercept (VEGF Trap-Eye) in Wet Age-related Macular Degeneration. *Ophthalmology* **119**: 2537–2548.

Hoang QV, Linsenmeier RA, Chung CK and Curcio CA (2002) Photoreceptor inner segments in monkey and human retina: mitochondrial density, optics, and regional variation. *Visual Neuroscience* **19**: 395–407.

Hogg RE and Chakravarthy U (2005) Visual function and dysfunction in early and late age-related maculopathy. *Progress in Retinal and Eye Research* **25**: 249–276.

Hogg RE, Woodside JV, Gilchrist SE, Graydon R, Fletcher AE et al (2008) Cardiovascular disease and hypertension are strong risk factors for choroidal neovascularization. *Ophthalmology* **115**: 1046–1052.

Hogg RE (2014) Reticular Pseudodrusen in Age-Related Macular Degeneration. *Optometry and Vision Science* **91**: 854–859.

Hollins M and Alpern M (1973) Dark adaptation and visual pigment regeneration in human cones. *Journal of General Physiology* **62**: 430–447.

Holloway RG and Dick AW (2002) Clinical trial end points – on the road to nowhere? *Neurology* **58**: 679-686.

Hollyfield JG, Salomon RG and Crabb (2003) Proteomic approaches to understanding age-related macular degeneration. *Advances in Experimental Medicine and Biology* **533**: 83-89.

Holm S (1979) A simple sequentially rejective multiple test procedure. *Scandinavian Journal of Statistics* **6**: 65-70.

Holz FG, Gross-Jendroska ME, Hogg C, Arden G and Bird A (1995) Colour contrast sensitivity in patients with age-related Bruch's membrane changes. *German Journal of Ophthalmology* **4**: 336–341.

Holz FG, Schutt F, Kopitz J, Eldred GE, Kruse FE et al (1999) Inhibition of lysosomal degradative functions in RPE cells by a retinoid component of lipofuscin. *Investigative Ophthalmology and Visual Science* **40**: 737–743.

Holz FG, Bindewald-Wittich A, Fleckenstein M, Dreyhaupt J, Scholl HP et al (2007) Progression of Geographic Atrophy and Impact of Fundus Autofluorescence Patterns

in Age-related Macular Degeneration. *American Journal of Ophthalmology* **143**: 463–472.

Holz FG, Strauss EC, Schmitz-Valckenberg S and Van Lookeren Campagne M (2014) Geographic atrophy: clinical features and potential therapeutic approaches. *Ophthalmology* **121**: 1079–1091.

Hood DC, Benimoff NI and Greenstein VC (1984) The response range of the blue-cone pathways: a source of vulnerability to disease. *Investigative Ophthalmology and Visual Science* **25**: 864–867.

Hood DC and Greenstein VC (1988) Blue (S) cone pathway vulnerability: a test of a fragile receptor hypothesis. *Applied Optics* **27**: 1025–1029.

Huang D, Swanson EA, Lin CP, Schuman JS, Stinson WG et al (1991) Optical Coherence Tomography. *Science* **254**: 1178–1181.

Huang JD, Presley JB, Chimento MF, Curcio C and Johnson M (2007) Age-related changes in human macular Bruch's membrane as seen by quick-freeze/deep-etch. *Experimental Eye Research* **85**: 202–218.

Hudspeth AJ and Yee AG (1973) The intercellular junctional complexes of retinal pigment epithelia. *Investigative Ophthalmology* **12**: 354–365.

Hyman L, Schachat A, He Q and Leske C (2000) Hypertension, cardiovascular disease, and age-related macular degeneration. *Archives of Ophthalmology* **118**: 351–358.

Inoue Y, Yanagi Y, Matsuura K, Takahashi H, Tamaki Y et al (2007) Expression of hypoxia-inducible factor 1alpha and 2alpha in choroidal neovascular membranes associated with age-related macular degeneration. *British Journal of Ophthalmology* **91**: 1720–1721.

Inoue M, Arakawa A, Yamane S and Kadonosono K (2014) Intravitreal injection of ranibizumab using a pro re nata regimen for age-related macular degeneration and vision-related quality of life. *Clinical Ophthalmology* **8**: 1711–1716.

Institute of Medicine (2006) *Sleep disorders and sleep deprivation: an unmet public health problem*. 1st edition. Washington DC, The National Academies Press.

Isikawa T (1963) Fine structure of retinal vessels in man and the macaque monkey. *Investigative Ophthalmology* **2**: 1–15.

Iwama D, Hangai M, Ooto S, Sakamoto A, Nakanishi H et al (2012) Automated Assessment of Drusen Using Three-Dimensional Spectral-Domain Optical Coherence Tomography. *Investigative Opthalmology and Visual Science* **53**: 1576–1583.

Iwasaki M and Inomata H (1986) Relation between superficial capillaries and foveal structures in the human retina. *Investigative Ophthalmology and Visual Science* **27**: 1698–1705.

Iwase T, Fu J, Yoshida T, Muramatsu D, Miki A et al (2013) Sustained delivery of a HIF-1 antagonist for ocular neovascularization. *Journal of Controlled Release* **172**: 625–633.

Jackson GR, Owsley C and McGwin G (1999) Aging and dark adaptation. *Vision Research* **39**: 3975–3982.

Jackson GR, Owsley C and Curcio CA (2002) Photoreceptor degeneration and dysfunction in aging and age-related maculopathy. *Ageing Research Reviews* **1**: 381–396.

Jackson GR and Edwards JG (2008) A short-duration dark adaptation protocol for assessment of age-related maculopathy. *Journal of Ocular Biology, Diseases, and Informatics* **1**: 7–11.

Jackson GR, Clark M, Scott I, Walter L, Quillen D et al (2014a) Twelve-month natural history of dark adaptation in patients with AMD. *Optometry and Vision Science* **91**: 925–931.

Jackson GR, Scott IU, Kim IK, Quillen DA, Iannaccone A et al (2014b) Diagnostic sensitivity and specificity of dark adaptometry for detection of age-related macular degeneration. *Investigative Ophthalmology and Visual Science* **55**: 1427–1431.

Jain N, Farsiu S, Khanifar AA, Bearelly S, Smith RT et al (2010) Quantitative comparison of drusen segmented on SD-OCT versus drusen delineated on color fundus photographs. *Investigative Ophthalmology and Visual Science* **51**: 4875–4883.

Jakobsdottir J, Conley YP, Weeks DE, Ferrell RE and Gorin MB (2008) C2 and CFB Genes in Age-Related Maculopathy and Joint Action with CFH and LOC387715 Genes. *PLOS One* **3**: e2199.

Jampol L and Tielsch J (1992) Race, macular degeneration, and the macular photocoagulation study. *Archives of Ophthalmology* **110**: 1699–1700.

Jarrett S, Lin H, Godley B and Boulton M (2008) Mitochondrial DNA damage and its potential role in retinal degeneration. *Progress in Retinal and Eye Research* **27**: 596–607.

Jarrett S, Lewin AS and Boulton M (2010) The Importance of Mitochondria in Age-Related and Inherited Eye Disorders. *Ophthalmic Research* **44**: 179–190.

Jivraj J, Jivraj I, Tennant M and Rudnisky C (2013) Prevalence and impact of depressive symptoms in patients with age-related macular degeneration. *Canadian Journal of Ophthalmology* **48**: 269–273.

Joachim N, Mitchell P, Rochtchina E, Tan AG and Wang JJ (2014) Incidence and Progression of Reticular Drusen in Age-related Macular Degeneration. *Ophthalmology* **121**: 917–925.

Johnson L, Leitner W, Staples M and Anderson D (2001) Complement activation and inflammatory processes in Drusen formation and age related macular degeneration. *Experimental Eye Research* **73**: 887–896.

Johnson NF and Foulds WS (1978) The effects of total acute ischaemia on the structure of the rabbit retina. *Experimental Eye Research* **27**: 45–59.

Johnson P, Lewis G, Talaga K, Brown M, Kappel P et al (2003) Drusen-Associated Degeneration in the Retina. *Investigative Ophthalmology and Visual Science* **44**: 4481–4488.

Jonnal RS, Kocaoglu OP, Zawadzki RJ, Liu Z, Miller DT et al (2016) A Review of Adaptive Optics Optical Coherence Tomography: Technical Advances, Scientific Applications, and the Future. *Investigative Opthalmology and Visual Science* **57**: 51–68.

Justice J and Lehmann RP (1976) Cilioretinal arteries. A study based on review of stereo fundus photographs and fluorescein angiographic findings. *Archives of Ophthalmology* **94:** 1355-1358.

Kalloniatis M and Luu C (2013) *Psychophysics of vision*. http://webvision.med.utah.edu/book/part-viii-gabac-receptors/psychophysics-of-vision/ [Accessed: 17th July 2017].

Kaluzny JJ, Wojtkowski M, Sikorski BL, Szkulmowski M, Szkulmowska A et al (2009) Analysis of the outer retina reconstructed by high-resolution, three-dimensional spectral domain optical coherence tomography. *Ophthalmic surgery, Lasers and Imaging* **40**: 102–108.

Karakucuk S, Oner AO, Goktas S, Siki E and Kose O (2004) Color vision changes in young subjects acutely exposed to 3,000 m altitude. *Aviation, Space and Environmental Medicine* **75:** 364–366.

Karunadharma PP, Nordgaard CL, Olsen TW and Ferrington DA (2010) Mitochondrial DNA Damage as a Potential Mechanism for Age-Related Macular Degeneration. *Investigative Opthalmology and Visual Science* **51**: 5470–5479.

Kashani AH, Keane PA, Dustin L, Walsh AC and Sadda SR (2009) Quantitative Subanalysis of Cystoid Spaces and Outer Nuclear Layer Using Optical Coherence Tomography in Age-Related Macular Degeneration. *Investigative Opthalmology and Visual Science* **50**: 3366-3373.

Kawasaki R, Yasuda M, Song SJ, Chen SJ, Jonas JB et al (2010) The prevalence of age-related macular degeneration in Asians: a systematic review and meta-analysis. *Ophthalmology* **117**: 921–927.

Kertes P, Sheidow TG, Williams G, Greve M, Galic I et al (2017) Canadian Treat and Extend Analysis Trial with Ranibizumab in Patients with Neovascular AMD: Interim Analysis of the CANTREAT Study. *Investigative Ophthalmology and Visual Science* **58**: 1200.

Kew R, Ghebrehiwet B and Janoff A (1985) Cigarette smoke can activate the alternative pathway of complement in vitro by modifying the third component of complement. *Journal of Clinical Investigation* **75**: 1000–1007.

Khan J, Thurlby D, Shahid H, Clayton D, Yates J et al (2006) Smoking and age related macular degeneration: the number of pack years of cigarette smoking is a major

determinant of risk for both geographic atrophy and choroidal neovascularisation. *British Journal of Ophthalmology* **90**: 75–80.

Khan M, Agarwal K, Loutfi M and Kamal A (2014) Present and possible therapies for age-related macular degeneration. *International Scholarly Research Notices Ophthalmology* **2014**: 608390.

Khandhadia S and Lotery A (2010) Oxidation and age-related macular degeneration: insights from molecular biology. *Expert Reviews in Molecular Medicine* **12**: 1–28.

Kiernan DF, Hariprasad S, Chin E, Kiernan C, Rago J et al (2008) Prospective comparison of Cirrus and Stratus optical coherence tomography for quantifying retinal thickness. *American Journal of Ophthalmology* **147**: 267-275.

Kim C and Mayer M (1994) Foveal flicker sensitivity in healthy ageing eyes II. Cross sectional aging trends from 18 through 77 years of age. *Journal of the Optical Society of America* **11**: 1958–1969.

Kingdom FA and Prins N (2009) Physcophysics: a practical introduction. 1st edition. London, Elsevier.

King-Smith P, Grigsby S, Vingrys A, Benes S and Supowit A (1994) Efficient and unbiased modifications of the QUEST threshold method: theory, simulations, experimental evaluation and practical implementation. *Vision Research* **34**: 885–912.

Kiryu J, Asrani S, Shahidi M, Mori M and Zeimer R (1995) Local response of the primate retinal microcirculation to increased metabolic demand induced by flicker. *Investigative Ophthalmology and Visual Science* **36**: 1240–1246.

Klaver C, Wolfs R, Assink J, Van Duijn C, Hofman A et al (1998) Genetic risk of age-related maculopathy: population-based familial aggregation study. *Archives of Ophthalmology* **116**: 1646–1651.

Klein R, Davis M, Magli Y, Segal P, Klein BE et al (1991) The Wisconsin age-related maculopathy grading system. *Ophthalmology* **98**: 1128–1134.

Klein R, Klein BE and Linton K (1992) Prevalence of age-related maculopathy: the Beaver Dam Eye Study. *Ophthalmology* **99**: 933–943.

Klein R, Wang Q, Klein BE, Moss S and Meuer S (1995) The relationship of age-related maculopathy, cataract, and glaucoma to visual acuity. *Investigative Ophthalmology and Visual Science* **36**: 182–191.

Klein R, Klein BE, Wong T, Tomany S and Cruickshanks K (2002a) The Association of Cataract and Cataract Surgery With the Long-term Incidence of Age-Related Maculopathy. *Archives of Ophthalmology* **120**: 1551–1558.

Klein R, Klein BE, Tomany SC, Meuer SM and Huang GH (2002b) Ten-year incidence and progression of age-related maculopathy: The Beaver Dam eye study. *Ophthalmology* **109**: 1767–1779.

Klein R, Klein BE, Tomany SC and Cruickshanks KJ (2003) The association of cardiovascular disease with the long-term incidence of age-related maculopathy. *Ophthalmology* **110**: 1273–1280.

Klein R, Klein BE, Knudtson MD, Meuer SM, Swift M et al (2006) Fifteen-year cumulative incidence of age-related macular degeneration: the Beaver Dam Eye Study. *Ophthalmology* **114**: 253–262.

Klein ML, Ferris FL, Armstrong J, Hwang TS, Chew EY et al (2008a) Retinal precursors and the development of geographic atrophy in age-related macular degeneration. *Ophthalmology* **115**: 1026–1031.

Klein R, Meuer SM, Knudtson MD, Iyengar SK and Klein BE (2008b) The Epidemiology of Retinal Reticular Drusen. *American Journal of Ophthalmology* **145**: 317–326.

Klein R (2011) Race/ethnicity and age-related macular degeneration. *American Journal of Ophthalmology* **152**: 153–154.

Klein R, Myers CE, Meuer SM, Gangnon RE, Sivakumaran TA et al (2013) Risk Alleles in CFH and ARMS2 and the Long-term Natural History of Age-Related Macular Degeneration. *Journal of the American Medical Association* **131**: 383–392.

Klein BE, Howard KP, Iyengar SK, Sivakumaran TA, Meyers KJ et al (2014a) Sunlight Exposure, Pigmentation, and Incident Age-Related Macular Degeneration. *Investigative Opthalmology and Visual Science* **55**: 5855–5861.

Klein R, Meuer SM, Myers CE, Buitendijk GH, Rochtchina E et al (2014b) Harmonizing the classification of age-related macular degeneration in the three-continent AMD consortium. *Ophthalmic Epidemiology* **21**: 14–23.

Klein R, Myers CE, Lee KE, Gangnon RE, Sivakumaran TA et al (2015) Small Drusen and Age-Related Macular Degeneration: The Beaver Dam Eye Study. *Journal of Clinical Medicine* **4**: 424–440.

Knudtson M, Klein R and Klein BE (2006) Physical activity and the 15-year cumulative incidence of age-related macular degeneration: the Beaver Dam Eye Study. *British Journal of Ophthalmology* **90**: 1461–1463.

Kolb H (2013) The organisation of the retina and visual system. In: Kolb, H, Fernandez, E, and Nelson, R [eds.] Webvision, *http://webvision.med.utah.edu/*. [Accessed 4th August 2017].

Kornzweig A (1977) Changes in the choriocapillaris associated with senile macular degeneration. *Annals of Ophthalmology* **9**: 753–756.

Koutalos Y, Nakatani K and Yau K (1995) The cGMP-phosphodiesterase and its contribution to sensitivity regulation in retinal rods. *Journal of General Physiology* **106**: 891–921.

Kurihara T, Westenskow PD, Gantner ML, Usui Y, Schultz A et al (2016) Hypoxia-induced metabolic stress in retinal pigment epithelial cells is sufficient to induce photoreceptor degeneration. *eLife* **5**: e14319.

Kvannli L and Krohn J (2017) Switching from pro re nata to treat-and-extend regimen improves visual acuity in patients with neovascular age-related macular degeneration. *Acta Ophthalmologica* **31**: 13356.

Kvanta A, Algvere PV, Berglin L and Seregard S (1996) Subfoveal fibrovascular membranes in age-related macular degeneration express vascular endothelial growth factor. *Investigative Ophthalmology and Visual Science* **37**: 1929–1934.

Lalwani GA, Rosenfeld PJ, Fung AE, Dubovy SR, Michels S et al (2009) A Variable-dosing Regimen with Intravitreal Ranibizumab for Neovascular Age-related Macular Degeneration: Year 2 of the PrONTO Study. *American Journal of Ophthalmology* **148**: 43–58.

Lamb TD and Pugh EN (2004) Dark adaptation and the retinoid cycle of vision. *Progress in Retinal and Eye Research* **23**: 307–380.

Lambert NG, El Shelmani H, Singh MK, Mansergh FC, Wride MA et al (2016) Risk factors and biomarkers of age-related macular degeneration. *Progress in Retinal and Eye Research* **54**: 64–102.

Landrum JT and Bone RA (2001) Lutein, zeaxanthin, and the macular pigment. *Archives of Biochemistry and Biophysics* **385**: 28–40.

Lanzetta P, Mitchell P, Wolf S and Veritti D (2013) Different antivascular endothelial growth factor treatments and regimens and their outcomes in neovascular age-related macular degeneration: a literature review. *British Journal of Ophthalmology* **97**: 1497–1507.

Law WP and Miles KA (2013) Incorporating prognostic imaging biomarkers into clinical practice. *Cancer Imaging* **13**: 332-341.

Lee B (2008) The evolution of concepts of color vision. *Neurociencias* **4**: 209-224.

Lee EK and Yu HG (2015) Ganglion cell-inner plexiform layer and peripapillary retinal nerve fibre layer thicknesses in age-related macular degeneration. *Investigative Ophthalmology and Visual Science* **56**: 3976-3983.

Lee MY, Yoon J and Ham DI (2012) Clinical Characteristics of Reticular Pseudodrusen in Korean Patients. *American Journal of Ophthalmology* **153**: 530–535.

Lesko LJ and Atkinson AJ (2001) Use of biomarkers and surrogate endpoints in drug development and regulatory decision making: criteria, validation, strategies. *Annual Review of Pharmacology and Toxicology* **41**: 347-366.

Leveziel N, Tilleul J, Puche N, Zerbib J, Laloum F et al (2011) Genetic factors associated with age-related macular degeneration. *Ophthalmologica* **226**: 87–102.

Levy O, Lavalette S, Hu SJ, Housset M, Raoul W et al (2015) APOE Isoforms Control Pathogenic Subretinal Inflammation in Age-Related Macular Degeneration. *Journal of Neuroscience* **35**: 13568–13576.

Lewy AJ, Wehr TA, Goodwin FK, Newsome DA and Markey SP (1980) Light suppresses melatonin secretion in humans. *Science* **210**: 1267–1269.

Li M, Atmaca Sonmez P, Othman M, Branham KE, Wade MS et al (2006) CFH haplotypes without the Y402H coding variant show strong association with susceptibility to age-related macular degeneration. *Nature Genetics* **38**: 1049–1054.

Li CM, Clark ME, Rudolf M and Curcio CA (2007) Distribution and composition of esterified and unesterified cholesterol in extra-macular drusen. *Experimental Eye Research* **85**: 192–201.

Liew G, Joachim N, Burlutsky G, Mitchell P and Wang JJ (2015) Validating Two Age-Related Macular Degeneration Classification Scales in A Population-based Cohort. *Investigative Ophthalmology and Visual Science* **56**: 3795–3795.

Lim RF, Gupta B and Simcock P (2017) Intravitreal aflibercept in neovascular age-related macular degeneration previously treated with ranibizumab. *International Journal of Ophthalmology* **10**: 423–426.

Lima Silva R, Shen J, Hackett SF, Kachi S, Akiyama H et al (2007) The SDF-1/CXCR4 ligand/receptor pair is an important contributor to several types of ocular neovascularization. *Federation of American Societies for Experimental Biology Journal* **21**: 3219–3230.

Lin H, Xu H, Liang F, Liang H, Gupta P et al (2011) Mitochondrial DNA Damage and Repair in RPE Associated with Aging and Age-Related Macular Degeneration. *Investigative Opthalmology and Visual Science* **52**: 3521–3529.

Liu LX, Lu H, Luo Y, Date T, Belanger AJ et al (2000) Stabilization of vascular endothelial growth factor mRNA by hypoxia-inducible factor 1. *Biochemical Biophysical Research Communications* **291**: 908–914.

Linsenmeier RA and Zhang HF (2017) Retinal oxygen: from animals to humans. *Progress in Retinal and Eye Research* **58**: 115-151.

Lopez PF, Sippy BD, Lambert HM, Thach AB and Hinton DR (1996) Transdifferentiated retinal pigment epithelial cells are immunoreactive for vascular endothelial growth factor in surgically excised age-related macular degeneration-related choroidal neovascular membranes. *Investigative Ophthalmology and Visual Science* **37**: 855–868.

Lovie-kitchin J and Brown B (2000) Repeatability and intercorrelations of standard vision tests as a function of age. *Optometry and Vision Science* **77**: 412–420.

Lucas RJ, Peirson SN, Berson DM, Brown TM, Cooper HM et al (2013) Measuring and using light in the melanopsin age. *Trends in Neurosciences* **37**: 1–9.

Luthert PJ (2011) Pathogenesis of age-related macular degeneration. *Diagnostic Histopathology* **17**: 10–16.

Luu CD, Dimitrov PN, Robman L, Varsamidis M, Makeyeva G et al (2012) Role of Flicker Perimetry in Predicting Onset of Late-Stage Age-Related Macular Degeneration. *Archives of Ophthalmology* **130**: 1450–1460.

Luu CD, Dimitrov PN, Wu Z, Ayton LN, Makeyeva G et al (2013) Static and flicker perimetry in age-related macular degeneration. *Investigative Ophthalmology and Visual Science* **54**: 3560–3568.

Lyubarsky A, Falsini B, Pennesi M, Valentini P and Pugh E (1999) UV- and Midwave-Sensitive Cone-Driven Retinal Responses of the Mouse: A Possible Phenotype for Coexpression of Cone Photopigments. *Journal of Neuroscience* **19**: 442–455.

Mahon PC, Hirota K and Semenza G (2001) FIH-1, a novel protein that interacts with HIF-1alpha and VHL to mediate repression of HIF-1 transcriptional activity. *Genes and Development* **15**: 2675–2686.

Maguire MG, Daniel E, Shah AR, Grunwald J, Hagstrom S et al (2013) Incidence of choroidal neovascularization in the fellow eye in the comparison of age-related macular degeneration treatment trials. *Ophthalmology* **120**: 2035-2041.

Malamos P, Sacu S, Georgopoulos M, Kiss C, Pruente C et al (2009) Correlation of High-Definition Optical Coherence Tomography and Fluorescein Angiography Imaging in Neovascular Macular Degeneration. *Investigative Opthalmology and Visual Science* **50**: 4926-4933.

Maller J, George S, Purcell S, Fagerness J, Altshuler D et al (2006) Common variation in three genes, including a noncoding variant in CFH, strongly influences risk of age-related macular degeneration. *Nature Genetics* **38**: 1055–1059.

Mandavilli BS, Santos JH and Van Houten B (2002) Mitochondrial DNA repair and aging. *Mutation Research* **509**: 127–151.

Margrain TH, Nollett C, Shearn J, Stanford M, Edwards RT et al (2012) The Depression in Visual Impairment Trial (DEPVIT): trial design and protocol. *Biomedical Central Psychiatry* **12**: 57.

MARINA Study Group (2006) Ranibizumab for Neovascular Age-Related Macular Degeneration. *New England Journal of Medicine* **355**: 1419–1431.

Martin DF, Maguire MG, Fine SL, Ying G, Jaffe GJ et al (2012) Ranibizumab and Bevacizumab for Treatment of Neovascular Age-related Macular Degeneration: Two-Year Results. *Ophthalmology* **119**: 1388–1398.

Martin DF, Maguire MG, Ying G, Grunwald JE, Fine SL et al (2011) Ranibizumab and Bevacizumab for Neovascular Age-Related Macular Degeneration. *New England Journal of Medicine* **364**: 1897–1908.

Martinez-Conde S, Macknik SL and Hubel DH (2004) The role of fixational eye movements in visual perception. *Nature Reviews Neuroscience* **5**: 229–240.

Masland RH (2001) The fundamental plan of the retina. *Nature Neuroscience* **4**: 877–886.

Mastin L (2013) Types and stages of sleep. *http://www.howsleepworks.com/types_cycles*. [Accessed 11th February 2016].

Mata NL, Radu R, Clemmons RC and Travis GH (2002) Isomerization and oxidation of vitamin a in cone-dominant retinas: a novel pathway for visual-pigment regeneration in daylight. *Neuron* **36**: 69–80.

Mayer M, Spiegler S, Kim C, Ward B and Glucs A (1990) Loss of foveal flicker sensitivity in eyes at risk for age-related maculopathy. *Investigative Opthalmology and Visual Science* **31**: 188.

Mayer M, Spiegler S, Ward B, Glucs A and Kim C (1992a) Foveal flicker sensitivity discriminates ARM-risk from healthy eyes. *Investigative Ophthalmology and Visual Science* **33**: 3143–3149.

Mayer MJ, Spiegler SJ, Ward B, Glucs A and Kim CB (1992b) Mid-frequency loss of foveal flicker sensitivity in early stages of age-related maculopathy. *Investigative Ophthalmology and Visual Science* **33**: 3136–3142.

Mayer M, Ward B, Klein R, Talcott J, Dougherty R et al (1994) Flicker sensitivity and fundus appearance in pre-exudative age-related maculopathy. *Investigative Ophthalmology and Visual Science* **35**: 1138–1149.

McBain VA, Kumari R, Townend J and Lois N (2011) Geographic atrophy in retinal angiomatous proliferation. *Retina* **31**: 1043–1052.

McFarland RA and Evans JN (1939) Alterations in dark adaptation under reduced ocygen tensions. *American Journal of Physiology* **127**: 37-50.

McKeague C, Margrain TH, Bailey C and Binns AM (2014) Low-level night-time light therapy for age-related macular degeneration (ALight): study protocol for a randomised controlled trial. *Trials* **15**: 246.

McLeod DS, Taomoto M, Otsuji T, Green WR, Sunness JS et al (2002) Quantifying changes in RPE and choroidal vasculature in eyes with age-related macular degeneration. *Investigative Ophthalmology and Visual Science* **43**: 1986–1993.

McLeod DS, Grebe R, Bhutto I, Merges C, Baba T et al (2009) Relationship between RPE and choriocapillaris in age-related macular degeneration. *Investigative Ophthalmology and Visual Science* **50**: 4982–4991.

Melrose MA, Magargal LE, Goldberg RE and Annesley W (1987) Subretinal neovascular membranes associated with choroidal nonperfusion and retinal ischaemia. *Annals of Ophthalmology* **19**: 396–399.

Mendrinos E and Pournaras CJ (2009) Topographic variation of the choroidal watershed zone and its relationship to neovascularization in patients with age-related macular degeneration. *Acta Ophthalmologica* **87**: 290–296.

Merry G, Munk M, Dotson R, Walker M and Devenyi R (2016) Photobiomodulation reduces drusen volume and improves visual acuity and contrast sensitivity in dry age-related macular degeneration. *Acta Ophthalmologica* **95**: e270-e277.

Metelitsina TI, Grunwald JE, DuPont JC, Ying GS, Brucker AJ et al (2008) Foveolar choroidal circulation and choroidal neovascularization in age-related macular degeneration. *Investigative Ophthalmology and Visual Science* **49**: 358–363.

Metha AB, Vingrys AJ and Badcock DR (1993) Calibration of a color monitor for visual psychophysics. *Behavior Research Methods, Instruments and Computers* **25**: 371–383.

Michaelson I (1948) The mode of development of the vascular system of the retina, with some observations on its significance for certain retinal diseases. *Transactions of the Ophthalmological Societies of the United Kingdom* **68**: 137–180.

Michelson G, Patzelt A and Harazny J (2002) Flickering light increases retinal blood flow. *Retina* **22**: 336–343.

Midena E, Degli Angeli C, Blarzino M, Valenti M and Segato T (1997) Macular function impairment in eyes with early age-related macular degeneration. *Investigative Ophthalmology and Visual Science* **38**: 469–477.

Miller WH (1985) Cyclic GMP controls rod phototransduction. *Neuroscience Research* **2**: 127–132.

Mimoun G, Soubrane G and Coscas G (1990) Les drusen maculaires. *French Journal of Ophthalmology* **13**: 511-530.

Minassian D, Reidy A, Lightstone A and Desai P (2011) Modelling the prevalence of age-related macular degeneration (2010-2020) in the UK: expected impact of anti-vascular endothelial growth factor (VEGF) therapy. *British Journal of Ophthalmology* **95**: 1433–1436.

Mitchell P, Smith W, Attebo K and Wang JJ (1995) Prevalence of age-related maculopathy in Australia: the Blue Mountains Eye Study. *Ophthalmology* **102**: 1450–1460.

Mitchell P, Smith W and Wang JJ (1998) Iris color, skin sun sensitivity, and age-related maculopathy. *Ophthalmology* **105**: 1359–1363.

Mitchell P, Wang JJ, Smith W and Leeder S (2002) Smoking and the 5-year incidence of age-related maculopathy. *Archives of Ophthalmology* **120**: 1357–1363.

Mitchell J and Bradley C (2006) Quality of life in age-related macular degeneration: a review of the literature. *Health and Quality of Life Outcomes* **4**: 97.

Mitchell P, Korobelnik J, Lanzetta P, Holz F, Prünte C et al (2010) Ranibizumab (Lucentis) in neovascular age-related macular degeneration: evidence from clinical trials. *The British Journal of Ophthalmology* **94**: 2–13.

Mitchell P, Macfadden W, Möckel V, Lacey S and Dunger-Baldauf C (2017) Ranibizumab efficacy in nAMD using a treat and extend regimen: a comparison between the interventional TREND and non-interventional LUMINOUS studies. *Investigative Ophthalmology and Visual Science* **58**: 891.

Moenter VM, Glen FC and Crabb DP (2014) Age-related eye disease and risk of falling: a review. *International Journal of Ophthalmic Practice* **5**: 79–83.

Moher D, Liberati A, Tetzlaff J and Altman DG (2009) Preferred reporting items for systematic reviews and meta-analyses: the PRISMA statement. PLOS Medicine 6: e1000097.

Mokwa NF, Ristau T, Keane PA, Kirchhof B, Sadda SR et al (2013) Grading of Age-Related Macular Degeneration: Comparison between Color Fundus Photography, Fluorescein Angiography, and Spectral Domain Optical Coherence Tomography. *Journal of Ophthalmology* **2013**: 385915.

Moore L, Niermeyer S and Zamudio S (1998) Human adaptation to high altitude: Regional and life-cycle perspectives. *Yearbook of Physical Anthropology* **41**: 25–64.

Moosmann B and Behl C (2008) Mitochondrially encoded cysteine predicts animal lifespan. *Aging Cell* **7**: 32–46.

Mori F, Konno S, Hikichi T, Yamaguchi Y, Ishiko S et al (2001) Pulsatile ocular blood flow study: decreases in exudative age related macular degeneration. *British Journal of Ophthalmology* **85**: 531–533.

Moseley M, Bayliss S and Fielder A (1988) Light transmission through the human eyelid: in vivo measurement. *Ophthalmic and Physiological Optics* **8**: 229–230.

Mousa SA, Lorelli W and Campochiaro PA (1999) Role of hypoxia and extracellular matrix-integrin binding in the modulation of angiogenic growth factors secretion by retinal pigmented epithelial cells. *Journal of Cellular Biochemistry* **74**: 135–143.

Moyer BR and Barrett JA (2009) Biomarkers and imaging: physics and chemistry for noninvasive analyses. *Bioanalysis* **1**: 321-356.

Mullins R, Russell S, Anderson D and Hageman G (2000) Drusen associated with aging and age-related macular degeneration contain proteins common to extracellular deposits associated with atherosclerosis, elastosis, amyloidosis, and dense deposit disease. *Federation of American Societies for Experimental Biology Journal* **14**: 835–846.

Mustafi D, Engel AH and Palczewski K (2009) Structure of cone photoreceptors. *Progress in Retinal and Eye Research* **28**: 289–302.

Nakajima T, Nakajima E, Shearer TR and Azuma M (2013) Concerted inhibition of HIF-1α and -2α expression markedly suppresses angiogenesis in cultured RPE cells. *Molecular and Cellular Biochemistry* **383**: 113–122.

Neale B, Fagerness J, Reynolds R, Sobrin L, Parker M et al (2010) Genome-wide association study of advanced age-related macular degeneration identifies a role of the hepatic lipase gene (LIPC). *Proceedings of the National Academy of Sciences* **107**: 7395–7400.

Neelam K, Nolan J, Chakravarthy U and Beatty S (2009) Psychophysical function in age-related maculopathy. *Survey of Ophthalmology* **54**: 167–210.

Ngai LY, Stocks N, Sparrow JM, Patel R, Rumley A et al (2011) The prevalence and analysis of risk factors for age-related macular degeneration: 18-year follow-up data from the Speedwell eye study, United Kingdom. *Eye* **25**: 784–793.

Nickla D and Wallman J (2010) The Multifunctional Choroid. *Progress in Retinal and Eye Research* **29**: 144-168.

Nikonov S, Lamb T and Pugh E (2000) The role of steady phosphodiesterase activity in the kinetics and sensitivity of the light-adapted salamander rod photoresponse. *Journal of General Physiology* **116**: 795–824.

Nishijima K, Ng YS, Zhong L, Bradley J, Schubert W et al (2007) Vascular endothelial growth factor-A is a survival factor for retinal neurons and a critical neuroprotectant during the adaptive response to ischemic injury. *American Journal of Pathology* **171**: 53–67.

Nivison-Smith L, Milston R, Madigan M and Kalloniatis M (2014) Age-related macular degeneration: linking clinical presentation to pathology. *Optometry and Vision Science* **91**: 832–848.

Nordgaard CL, Karunadharma PP, Feng X, Olsen TW and Ferrington DA (2008) Mitochondrial Proteomics of the Retinal Pigment Epithelium at Progressive Stages of Age-Related Macular Degeneration. *Investigative Opthalmology and Visual Science* **49**: 2848–2855.

Norman G (2010) Likert scales, levels of measurement and the 'laws' of statistics. *Advances in Health Sciences Education* **15**: 625–632.

Norton TT, Corliss DA and Bailey JE (2002) *The psychophysical measurement of visual function*. 1st edition. Woburn, MA. Butterworth-Heinemann.

O'Neill-Biba M, Sivaprasad S, Rodriguez-Carmona M, Wolf J and Barbur J (2010) Loss of chromatic sensitivity in AMD and diabetes: a comparative study. *Ophthalmic and Physiological Optics* **30**: 705–716.

Ohh M, Park CW, Ivan M, Hoffman MA, Kim TY et al (2000) Ubiquitination of HIF requires direct binding to the beta-domain of the vHL protein. *Nature Cell Biology* **2**: 423–427.

Ohnaka M, Nagai Y, Kimura M, Chihara T, Nakagawa K et al (2017) Two-year outcome of aflibercept for treatment-naïve patient with neovascular age-related macular degeneration using modified treat-and-extend regimen. *Investigative Ophthalmology and Visual Science* **58**: 890.

Oubraham H, Cohen SY, Samimi S, Marotte D, Bouzaher I et al (2011) Inject and extend dosing versus dosing as needed: a comparative retrospective study of ranibizumab in exudative age-related macular degeneration. *Retina* **31**: 26–30.

Owen CG, Jarrar Z, Wormald R, Cook DG, Fletcher AE et al (2012) The estimated prevalence and incidence of late stage age related macular degeneration in the UK. *British Journal of Ophthalmology* **96**: 752–756.

Owsley C, Jackson GR, White M, Feist R and Edwards D (2001) Delays in rod-mediated dark adaptation in early age-related maculopathy. *Ophthalmology* **108**: 1196–202.

Owsley C, McGwin G, Scilley K and Kallies K (2006) Development of a questionnaire to assess vision problems under low luminance in age-related maculopathy. *Investigative Ophthalmology and Visual Science*. **47**: 528-535.

Owsley C, McGwin G, Jackson GR, Kallies K.and Clark M (2007) Cone- and rod-mediated dark adaptation impairment in age-related maculopathy. *Ophthalmology* **114**: 1728–1735.

Owsley C, McGwin G, Clark ME, Jackson GR, Callahan MA et al (2016) Delayed Rod-Mediated Dark Adaptation Is a Functional Biomarker for Incident Early Age-Related Macular Degeneration. *Ophthalmology* **123**: 344–351.

Owsley C, Clark ME and McGwin G (2017) Natural History of Rod-Mediated Dark Adaptation over 2 Years in Intermediate Age-Related Macular Degeneration. *Translational Vision Science and Technology* **6**: 15.

Oyster C (2006) *The Human Eye: Structure and Function*. 1st edition. *Cary*, NC. Sinauer Associates Inc.

Padnick-Silver L, Weinberg AB, Lafranco FP and Macsai MS (2012) Pilot study for the detection of early exudative age-related macular degeneration with optical coherence tomography. *Retina* **32**: 1045–1056.

Pallikaris IG, Kymionis GD, Ginis HS, Kounis G, Christodoulakis E et al (2006) Ocular rigidity in patients with age-related macular degeneration. *American Journal of Ophthalmology* **141**: 611–615.

Panda-Jonas S, Jonas JB and Jokobczyk-Zmija M (1996) Retinal pigment epithelial cell count, distribution, and correlations in normal human eyes. *American Journal of Ophthalmology* **121**: 181–189.

Park YG, Rhu HW, Kang S and Roh YJ (2012) New Approach of Anti-VEGF Agents for Age-Related Macular Degeneration. *Journal of Ophthalmology* **2012**: 637316.

Pauleikhoff D, Barondes M, Minassian D, Chisholm I and Bird A (1990a) Drusen as risk factors in age-related macular disease. *American Journal of Ophthalmology* **109**: 38–43.

Pauleikhoff D, Chen JC, Chisholm I and Bird A (1990b) Choroidal perfusion abnormality with age-related Bruch's membrane change. *American Journal of Ophthalmology* **109**: 211–217.

Pauleikhoff D, Spital G, Radermacher M, Brumm G, Lommatzsch A et al (1999) A fluorescein and indocyanine green angiographic study of choriocapillaris in age-related macular disease. *Archives of Ophthalmology.* **117**: 1353–1358.

Pauleikhoff D, Löffert D, Spital G, Radermacher M, Dohrmann J et al (2002) Pigment epithelial detachment in the elderly. *Graefe's Archive for Clinical and Experimental Ophthalmology* **240**: 533–538.

Paun CC, Ersoy L, Schick T, Groenewoud J, Lechanteur YT et al (2015) Genetic Variants and Systemic Complement Activation Levels Are Associated With Serum

Lipoprotein Levels in Age-Related Macular Degeneration. *Investigative Opthalmology and Visual Science* **56**: 7766–7773.

Paupoo A, Mahroo O, Friedburg C and Lamb T (2000) Human cone photoreceptor responses measured by the electroretinogram a -wave during and after exposure to intense illumination. *Journal of Physiology* **529**: 469–482.

Pavlidis M, Stupp T, Georgalas I, Georgiadou E, Moschos M et al (2005) Multifocal electroretinography changes in the macula at high altitude: a report of three cases. *International Journal of Ophthalmology* **219:** 404–412.

Pelli DG (1997) The video toolbox software for visual psychophysics: transforming numbers into movies. *Spatial Vision* **10**: 437–442.

Pepperberg D, Birch D and Hood D (1997) Photoresponses of human rods in vivo derived from paired-flash electroretinograms. *Visual Neuroscience* **14**: 73–82.

Phipps J, Guymer R and Vingrys A (2003) Loss of cone function in age-related maculopathy. *Investigative Ophthalmology and Visual Science* **44**: 2277–2283.

Phipps J, Dang TM, Vingrys AJ and Guymer RH (2004) Flicker perimetry losses in age-related macular degeneration. *Investigative Ophthalmology and Visual Science* **45**: 3355–3360.

Piguet B, Palmvang IB, Chisholm IH, Minassian D and Bird A (1992) Evolution of age-related macular degeneration with choroidal perfusion abnormality. *American Journal of Ophthalmology* **113**: 657–663.

Polak K, Schmetterer L and Riva CE (2002) Influence of flicker frequency on flicker-induced changes of retinal vessel diameter. *Investigative Ophthalmology and Visual Science* **43**: 2721–2726.

Polyak S (1949) Retinal structure and colour vision. *Documenta Ophthalmogica* **3**: 24–56.

Pons M and Marin-Castaño ME (2011) Nicotine Increases the VEGF/PEDF Ratio in Retinal Pigment Epithelium: A Possible Mechanism for CNV in Passive Smokers with AMD. *Investigative Opthalmology and Visual Science* **52**: 3842–3853.

Pournaras CJ, Logean E, Riva CE, Petrig BL, Chamot SR et al (2006) Regulation of subfoveal choroidal blood flow in age-related macular degeneration. *Investigative Ophthalmology and Visual Science* **47**: 1581–1586.

Pow DV and Sullivan RP (2007) Nuclear kinesis, neurite sprouting and abnormal axonal projections of cone photoreceptors in the aged and AMD-afflicted human retina. *Experimental Eye Research* **84**: 850–857.

Priya RR, Chew EY and Swaroop A (2012) Genetic Studies of Age-related Macular Degeneration. *Ophthalmology* **119**: 2526–2536.

Prünte C and Niesel C (1988) Quantification of choroidal blood-flow parameters using indocyanine green video-fluorescence angiography and statistical picture analysis. *Graefes Archive for Clinical and Experimental Ophthalmology* **226**: 55–58.

Querques G, Georges A, Ben Moussa N, Sterkers M and Souied EH (2014) Appearance of regressing drusen on optical coherence tomography in age-related macular degeneration. *Ophthalmology* **121**: 173–179.

Rabin R and De Charro F (2001) EQ-SD: a measure of health status from the EuroQol Group. *Annals of Medicine* **33**: 337–343.

Ramakrishnan S, Anand V and Roy S (2014) Vascular endothelial growth factor signaling in hypoxia and inflammation. *Journal of Neuroimmune Pharmacology* **9**: 142-160.

Ramrattan RS, Van Der Schaft TL, Mooy CM, De Bruijn WC, Mulder PH et al (1994) Morphometric analysis of Bruch's membrane, the choriocapillaris, and the choroid in aging. *Investigative Ophthalmology and Visual Science* **35**: 2857–2864.

Redmond TM, Yu S, Lee E, Bok D, Hamasaki D et al (1998) Rpe65 is necessary for production of 11-cis-vitamin A in the retinal visual cycle. *Nature Genetics* **20**: 344–351.

Regillo CD, Brown DM, Abraham P, Yue H, Ianchulev T et al (2008) Randomized, Double-Masked, Sham-Controlled Trial of Ranibizumab for Neovascular Age-related Macular Degeneration: PIER Study Year 1. *American Journal of Ophthalmology* **145**: 239–248.

Rein D, Wittenborn J, Zhang X, Honeycutt A, Lesesne S et al (2009) Forecasting age-related macular degeneration through the year 2050: the potential impact of new treatments. *Archives of Ophthalmology* **127**: 533–540.

Remington L (2012) *Clinical Anatomy of the Visual System*. 3rd edition. St Louis, Elsevier Butterworth-Heinemann.

Remsch H, Spraul CW, Lang GK and Lang GE (2000) Changes of retinal capillary blood flow in age-related maculopathy. *Graefe's Archive for Clinical and Experimental Ophthalmology* **238**: 960–964.

Remulla JF, Gaudio R, Miller S and Sandberg M (1995) Foveal electroretinograms and choroidal perfusion characteristics in fellow eyes of patients with unilateral neovascular age-related macular degeneration. *British Journal of Ophthalmology* **79**: 558–561.

Roberts C and Torgerson D (1999) Baseline imbalance in randomised controlled trials. *British Medical Journal* **319**: 185.

Robinson J, Bayliss S and Fielder A (1991) Transmission of light across the adult and neonatal eyelid in vivo. *Vision Research* **31**: 1837–1840.

Rodriguez-Carmona M, O'Neill-Biba M and Barbur JL (2012) Assessing the Severity of Color Vision Loss with Implications for Aviation and Other Occupational Environments. *Aviation, Space, and Environmental Medicine* **83**: 19–29.

Rogala J, Zangerl B, Assaad N, Fletcher EL, Kalloniatis M et al (2015) In vivo quantification of retinal changes associated with drusen in age-related macular degeneration. *Investigative Ophthalmology and Visual Science* **56**: 1689-1700.

Rosenfeld PJ, Brown DM, Heier JS, Boyer DS, Kaiser PK et al (2006) Ranibizumab for Neovascular Age-Related Macular Degeneration. *New England Journal of Medicine* **355**: 1419–1431.

Rosenfeld PJ (2011) Bevacizumab versus Ranibizumab for AMD. New England Journal of Medicine 364: 1966–1967.

Ross RD, Barofsky JM, Cohen G, Baber WB, Palao SW et al (1998) Presumed macular choroidal watershed vascular filling, choroidal neovascularization, and systemic vascular disease in patients with age-related macular degeneration. *American Journal of Ophthalmology* **125**: 71–80.

Rosser DA, Cousens SN, Murdoch IE, Fitzke FW and Laidlaw DH (2003) How Sensitive to Clinical Change are ETDRS logMAR Visual Acuity Measurements? *Investigative Opthalmology and Visual Science* **44**: 3278-3281.

Roth F, Bindewald A and Holz FG (2004) Keypathophysiologic pathways in age-related macular disease. *Graefe's Archive for Clinical and Experimental Ophthalmology* **242**: 710–716.

Rushton W and Campbell F (1954) Measurement of rhodopsin in the living human eye. *Nature* **174**: 1096–1097.

Sahni JN, Czanner G, Gutu T, Taylor SA, Bennett KM et al (2017) Safety and acceptability of an organic light-emitting diode sleep mask as a potential therapy for retinal disease. *Eye* **31**: 97–106.

Sallo F, Peto T, Stanescu-Segall D, Vogt G, Bird A et al (2009) Functional aspects of drusen regression in age-related macular degeneration. *British Journal of Ophthalmology* **93**: 1345–1350.

San Giovanni JP, Chew EY, Clemons TE, Davis MD, Ferris FL et al (2007) The relationship of dietary lipid intake and age-related macular degeneration in a case-control study: AREDS Report number 20. *Archives of Ophthalmology* **125**: 671–679.

Sandberg MA, Weiner A, Miller S, Gaudio AR (1998) High-risk characteristics of fellow eyes of patients with unilateral neovascular age-related macular degeneration. *Ophthalmology* **105**: 441-447.

Sarks J, Sarks S and Killingsworth MC (1988) Evolution of geographic atrophy of the retinal pigment epithelium. *Eye* **2**: 552–577.

Sarks J, Sarks S and Killingsworth M (1994) Evolution of soft drusen in age-related macular degeneration. *Eye* **8**: 269–283.

Sarks J, Arnold J, Ho I, Sarks S and Killingsworth M (2011) Evolution of reticular pseudodrusen. *British Journal of Ophthalmology* **95**: 979–985.

Sato E, Feke GT, Menke MN and Wallace-McMeel J (2006) Retinal haemodynamics in patients with age-related macular degeneration. *Eye* **20**: 697–702.

Sawa M, Ueno C, Gomi F and Nishida K (2014) Incidence and characteristics of neovascularization in fellow eyes of Japanese patients with unilateral retinal angiomatous proliferation. *Retina* **34**: 761–767.

Schatz A, Breithaupt M, Hudemann J, Niess A, Messias A et al (2014) Electroretinographic assessment of retinal function during acute exposure to normobaric hypoxia. *Graefe's Archive for Clinical and Experimental Ophthalmology* **252**: 43–50.

Schick T, Ersoy L, Lechanteur YT, Saksens NT, Hoyng CB et al (2016) History of sunlight exposure as a risk factor for age-related macular degeneration. *Retina* **36**: 787–790.

Schlanitz F, Baumann B, Kundi M, Sacu S, Baratsits M et al (2017) Drusen volume development over time and its relevance to the course of age-related macular degeneration. *British Journal of Ophthalmology* **101**: 198–203.

Schlingemann RO (2004) Role of growth factors and the wound healing response in age-related macular degeneration. *Graefe's Archive for Clinical and Experimental Ophthalmology* **242**: 91–101.

Schmidt-Erfurth U, Eldem B, Guymer R, Korobelnik JF, Schlingemann RO et al (2011) Efficacy and Safety of Monthly versus Quarterly Ranibizumab Treatment in Neovascular Age-related Macular Degeneration: The EXCITE Study. *Ophthalmology* **118**: 831–839.

Schmidt-Erfurth U, Kaiser PK, Korobelnik JF, Brown DM, Chong V et al (2014) Intravitreal Aflibercept Injection for Neovascular Age-related Macular Degeneration: Ninety-Six–Week Results of the VIEW Studies. *Ophthalmology* **121**: 193–201.

Schultz DW, Klein ML, Humpert AJ, Luzier CW, Persun V et al (2003) Analysis of the ARMD1 locus: evidence that a mutation in HEMICENTIN-1 is associated with age-related macular degeneration in a large family. *Human Molecular Genetics* **12**: 3315–3323.

Schultz-Larsen K, Lomholt RK and Kreiner S (2007) Mini-Mental Status Examination: a short form of the MMSE was as accurate as the original MMSE in predicting dementia. *Journal of Clinical Epidemiology* **60**: 260-267.

Schuman SG, Koreishi AF, Farsiu S, Jung S, Izatt JA et al (2009) Photoreceptor Layer Thinning over Drusen in Eyes with Age-Related Macular Degeneration Imaged In Vivo with Spectral-Domain Optical Coherence Tomography. *Ophthalmology* **116**: 488–496.

Scilley K, Jackson GR, Cideciyan AV, Maguire MG, Jacobson SG (2002) Early age-related maculopathy and self-reported visual difficulty in daily life. *Ophthalmology* **109**: 1235–1242.

Seddon J, Willett W, Speizer F and Hankinson S (1996) A prospective study of cigarette smoking and age-related macular degeneration in women. *Journal of the American Medical Association* **276**: 1141–1146.

Seddon JM, Rosner B, Sperduto RD, Yannuzzi L, Haller JA et al (2001) Dietary fat and risk for advanced age-related macular degeneration. *Archives of Ophthalmology* **119**: 1191-1199.

Seddon JM, Cote J, Davis N and Rosner B (2003) Progression of Age-Related Macular Degeneration. *Archives of Ophthalmology* **121**: 785–792.

Seddon JM, Cote J, Page WF, Aggen SH and Neale MC (2005) The US twin study of age-related macular degeneration: relative roles of genetic and environmental influences. *Archives of Ophthalmology* **123**: 321–327.

Seddon JM, George S and Rosner B (2006) Cigarette smoking, fish consumption, Omega-3 Fatty Acid intake, and associations with age-related macular degeneration: the US Twin Study of age-related macular degeneration. *Archives of Ophthalmology* **124**: 995–1001.

Semenza GL (2012) Hypoxia-Inducible Factors in Physiology and Medicine. *Cell* **148**: 399–408.

Senra H, Ali Z, Balaskas K and Aslam T (2016) Psychological impact of anti-VEGF treatments for wet macular degeneration: a review. *Graefe's Archive for Clinical and Experimental Ophthalmology* **254**: 1873–1880.

Shahid H, Khan JC, Cipriani V, Sepp T, Matharu BK et al (2012) Age-related macular degeneration: the importance of family history as a risk factor. *British Journal of Ophthalmology* **96**: 427–431.

Shankar A, Mitchell P, Rochtchina E, Tan J and Wang JJ (2007) Association between circulating white blood cell count and long-term incidence of age-related macular degeneration: the Blue Mountains Eye Study. *American Journal of Epidemiology* **165**: 375–382.

Sharma RK and Ehinger BJ (2003) Adler's physiology of the eye. 10th edition. St Louis: Mosby.

Shelley EJ, Madigan MC, Natoli R, Penfold PL and Provis JM (2009) Cone degeneration in aging and age-related macular degeneration. *Archives of Ophthalmology* **127**: 483–492.

Shen L, Hoffmann TJ, Melles RB, Sakoda LC, Kvale MN et al (2015) Differences in the Genetic Susceptibility to Age-Related Macular Degeneration Clinical Subtypes. *Investigative Opthalmology and Visual Science* **56**: 4290–4299.

Sheridan CM, Pate S, Hiscott P, Wong D, Pattwell DM et al (2009) Expression of hypoxia-inducible factor-1alpha and -2alpha in human choroidal neovascular membranes. *Graefe's Archive for Clinical and Experimental Ophthalmology* **247**: 1361–1367.

Shi YH and Fang WG (2004) Hypoxia-inducible factor-1 in tumour angiogenesis. *World Journal of Gastroenterology* **10**: 1082-1087.

Shienbaum G, Gupta OP, Fecarotta C, Patel AH, Kaiser R et al (2012) Bevacizumab for neovascular age-related macular degeneration using a treat-and-extend regimen: clinical and economic impact. *American Journal of Ophthalmology* **153**: 468-473.

Silber MH, Ancoli-Israel S, Bonnet MH, Chokroverty S, Grigg-Damberger MM et al (2007) The visual scoring of sleep in adults. *Journal of Clinical Sleep Medicine* **3**: 121-131.

Sivapathasuntharam C, Sivaprasad S, Hogg C and Jeffery G (2017) Ageing retinal function is improved by near infrared light (670nm) that is associated with corrected mitochondrial decline. *Neurobiology of aging* **52**: 66-70.

Sivaprasad S, Arden G, Prevost AT, Crosby-Nwaobi R, Holmes H et al (2014) A multicentre phase III randomised controlled single-masked clinical trial evaluating the clinical efficacy and safety of light-masks at preventing dark-adaptation in the treatment of early diabetic macular oedema (CLEOPATRA): study protocol for a randomised controlled trial. *Trials* **15**: 458.

Sivaprasad S and Arden G (2016) Spare the rods and spoil the retina: revisited. *Eye* **30**: 189-192.

Sivaprasad S, Bird A, Nitiahpapand R, Nicholson L, Hykin P et al (2016) Perspectives on reticular pseudodrusen in age-related macular degeneration. *Survey of Ophthalmology* **61**: 521-537.

Smick K, Vilette T, Boulton M, Brainard G, Jones W et al (2013) Blue light hazard: New knowledge, new approaches to maintaining ocular health. *Report of a Roundtable Sponsored by Essilor of America*. New York City, New York.

Smith W and Mitchell P (1998) Family history and age-related maculopathy: The Blue Mountains Eye Study. *Australian and New Zealand Journal of Ophthalmology* **26**: 203–206.

Smith W, Mitchell P and Leeder SR (2000) Dietary fat and fish intake and age-related maculopathy. *Archives of Ophthalmology* **118**: 401-404.

Smith W, Assink J, Klein R, Mitchell P, Klaver CC et al (2001) Risk factors for age-related macular degeneration: Pooled findings from three continents. *Ophthalmology* **108**: 697–704.

Smith RT, Chan JK, Busuoic M, Sivagnanavel V, Bird AC et al (2006) Autofluorescence characteristics of early, atrophic, and high-risk fellow eyes in age-related macular degeneration. *Investigative Ophthalmology and Visual Science* **47**: 5495–5504.

Snodderly DM (1995) Evidence for protection against degeneration by carotenoids and antioxidant vitamins. *American Journal of Clinical Nutrition* **62**: 1448–1461.

Sodi A, Matteoli S, Giacomelli G, Finocchio L, Corvi A et al (2014) Ocular surface temperature in Age-related macular degeneration. *Journal of Ophthalmology* **2014**: e281010.

Solberg Y, Rosner M and Belkin M (1998) The Association Between Cigarette Smoking and Ocular Diseases. *Survey of Ophthalmology* **42**: 535–547.

Song WY, Lee SC, Lee ES, Kim CY and Kim SS (2010) Macular thickness variations with sex, age, and axial length in healthy subjects: a spectral domain-optical coherence tomography study. *Clinical and Epidemiological Research* **51**: 3913-3918.

Souied EH, Devin F, Mauget-Faysse M, Kolar P, Wolf-Schnurrbusch U et al (2014) Treatment of exudative age-related macular degeneration with a designed Ankyrin repeat protein that binds vascular endothelial growth factor: a phase I/II study. *American Journal of Ophthalmology* **158**: 724–732.

Spaide R (2007) Ranibizumab According to Need: A Treatment for Age-related Macular Degeneration. *American Journal of Ophthalmology* **143**: 679–680.

Sparrow J, Ueda K and Zhou J (2012) Complement dysregulation in AMD: RPE-Bruch's membrane- choroid. *Molecular Aspects of Medicine* **33**: 1–17.

SPECTRI (2014) A study investigating the efficacy and safety of lampalizumab intravitreal injections in participants with geographic atrophy secondary to age-related macular degeneration (SPECTRI). *https://clinicaltrials.gov/ct2/show/NCT02247531*. [Accessed 15th May 2017].

Spraul CW, Lang GE and Grossniklaus HE (1996) Morphometric Analysis of the Choroid, Bruch's Membrane, and Retinal Pigment Epithelium in Eyes With Age-Related Macular Degeneration. *Investigative Ophthalmology and Vision Science* **37**: 2724–2735.

Spraul CW, Lang GE, Grossniklaus HE and Lang GK (1999) Histologic and Morphometric Analysis of the Choroid, Bruch's Membrane, and Retinal Pigment Epithelium in Postmortem Eyes With Age-Related Macular Degeneration and Histologic Examination of Surgically Excised Choroidal Neovascular Membranes. *Survey of Ophthalmology* **44**: 10–32.

Srinivasan S, Swaminathan G, Kulothungan V, Raman R and Sharma T (2017) Prevalence and the risk factors for visual impairment in age-related macular degeneration. *Eye* **31**: 846–855.

Staurenghi G, Bottoni F, Lonati C, Autelitano A and Orzalesi N (1992) Drusen and "Choroidal filling defects": a cross-sectional survey. *Ophthalmologica* **205**: 179–186.

Stefánsson E, Geirsdóttir A and Sigurdsson H (2011) Metabolic physiology in age related macular degeneration. *Progress in Retinal and Eye Research* **30**: 72–80.

Stelmack J, Szlyk JP, Stelmack TR, Demers-Turco P, Williams RT et al (2004a) Psychometric properties of the Veterans Affairs Low-Vision Visual Functioning Questionnaire. *Investigative Ophthalmology and Visual Science* **45**: 3919–3928.

Stelmack J, Szlyk JP, Stelmack T, Babcock-Parziale J, Demers-Turco P et al (2004b) Use of Rasch person-item map in exploratory data analysis: a clinical perspective. *Journal of Rehabilitation Research and Development* **41**: 233–241.

Stelmack J and Massof RW (2007) Using the VA LV VFQ-48 and LV VFQ-20 in Low Vision Rehabilitation. *Optometry and Vision Science* **84**: 705–709.

Stelmack J, Tang XC, Reda DJ, Moran D, Rinne S et al (2007) The Veterans Affairs Low Vision Intervention Trial (LOVIT): design and methodology. *Clinical Trials* **4**: 650–660.

Strauss O (2005) The retinal pigment epithelium in visual function. *American Physiological Society* **85**: 845–881.

Strimbu K and Tavel J (2010) What are biomarkers? *Current Opinion in HIV and AIDS*. **5**: 463-466.

Sturr JF, Zhang L, Taub HA, Hannon DJ and Jackowski MM (1997) Psychophysical evidence for losses in rod sensitivity in the aging visual system. *Vision Research* **37**: 475–481.

Sullivan GM and Artino AR (2013) Analyzing and interpreting data from likert-type scales. *Journal of Graduate Medical Education* **5**: 541–542.

Sunness JS, Massof RW, Johnson MA, Bressler NM, Bressler SB et al (1989) Diminished foveal sensitivity may predict the development of advanced age-related macular degeneration. *Ophthalmology* **96**: 375–381.

Sunness JS, Rubin G, Applegate C, Bressler N, Marsh M et al (1997) Visual function abnormalities and prognosis in eyes with age-related geographic atrophy of the macula and good visual acuity. *Ophthalmology* **104**: 1677–1691.

Sunness JS, Gonzalez-Baron J, Applegate CA, Bressler NM, Tian Y et al (1999) Enlargement of atrophy and visual acuity loss in the geographic atrophy form of age-related macular degeneration. *Ophthalmology* **106**: 1768–1779.

Sunness JS, Margalit E, Srikumaran D, Applegate CA, Tian Y et al (2007) The long-term natural history of geographic atrophy from age-related macular degeneration: enlargement of atrophy and implications for interventional clinical trials. *Ophthalmology* **114**: 271–277.

Suter M, Remé C, Grimm C, Wenzel A, Jäättela M et al (2000) Age-related macular degeneration. The lipofusion component N-retinyl-N-retinylidene ethanolamine detaches proapoptotic proteins from mitochondria and induces apoptosis in mammalian retinal pigment epithelial cells. *Journal of Biological Chemistry* **275**: 39625–39630.

Szigeti A, Tatrai E, Varga B, Szamosi A, DeBuc D et al (2015) The effect of axial length on the thickness of intraretinal layers of the macula. *PLOS One* **10**: e0142383.

Tan J, Wang JJ, Liew G, Rochtchina E and Mitchell P (2008a) Age-related macular degeneration and mortality from cardiovascular disease or stroke. *British Journal of Ophthalmology* **92**: 509–512.

Tan J, Wang JJ, Flood V, Rochtchina E, Smith W et al (2008b) Dietary Antioxidants and the Long-term Incidence of Age-Related Macular Degeneration. *Ophthalmology* **115**: 334–341.

Tan J, Wang JJ, Flood V and Mitchell P (2009) Dietary fatty acids and the 10-year incidence of age-related macular degeneration. *Archives of Ophthalmology* **127**: 656–665.

Tano Y and Ohji M (2010) EXTEND-I: safety and efficacy of ranibizumab in Japanese patients with subfoveal choroidal neovascularization secondary to age-related macular degeneration. *Acta Ophthalmologica* **88**: 309–316.

Tao Y and Jonas J (2010) Refractive error and smoking habits in exudative age-related macular degeneration in a hospital-based setting. *Eye* **24**: 648–652.

Taylor HR, West S, Munoz B, Rosenthal F, Bressler S et al (1992) The long-term effects of visible light on the eye. *Archives of Ophthalmology* **110**: 99-104.

Taylor CT and Cummins E (2009) The role of NF-kappaB in hypoxia-induced gene expression. *Annals of the New York Academy of Sciences* **1177**: 178–184.

Terry L, Cassels N, Lu K, Acton J, Margrain T et al (2016) Automated Retinal Layer Segmentation Using Spectral Domain Optical Coherence Tomography: Evaluation of Inter-Session Repeatability and Agreement between Devices. *PLOS One* **11**: e0162001.

Thomas M and Lamb T (1999) Light adaptation and dark adaptation of human rod photoreceptors measured from the a-wave of the electroretinogram. *Journal of Physiology* **518**: 479–496.

Thornton J, Edwards R, Mitchell P, Harrison R, Buchan I et al (2005) Smoking and age-related macular degeneration: a review of association. *Eye* **19**: 935–944.

Tinjust D, Kergoat H and Lovasik JV (2002) Neuroretinal function during mild systemic hypoxia. *Aviation, Space and Environmental Medicine* **73:** 1189–1194.

Trichonas G and Kaiser PK (2013) Aflibercept for the treatment of age-related macular degeneration. *Ophthalmology and Therapy* **2**: 89–98.

Toth CA, Narayan SA, Hee MR, Fujimoto JG, Birngruber R et al (1997) A comparison of retinal morphology viewed by optical coherence tomography and by light microscopy. *Archives of Ophthalmology* **115**: 1425-1428.

Ueda-Arakawa N, Ooto S, Nakata I, Yamashiro K, Tsujikawa A, Oishi A et al (2013) Prevalence and Genomic Association of Reticular Pseudodrusen in Age-Related Macular Degeneration. *American Journal of Ophthalmology* **155**: 260–269.

Ugurlu S, Altundal A and Ekin M (2017) Comparison of vision-related quality of life in primary open-angle glaucoma and dry-type age-related macular degeneration. *Eye* **31**: 395–405.

Üretmen Ö, Akkinodot C, Erakgün T and Killi R (2003) Color Doppler Imaging of Choroidal Circulation in Patients with Asymmetric Age-Related Macular Degeneration. *Ophthalmologica* **217**: 137–142.

Vadlapatla R, Vadlapudi A and Mitra A (2013) Hypoxia-Inducible Factor-1 (HIF-1): A potential target for intervention in ocular neovascular diseases. *Current Drug Targets* **14**: 919-935.

Van Newkirk MR, Nanjan MB, Wang JJ, Mitchell P, Taylor HR et al (2000) The prevalence of age-related maculopathy: The visual impairment project. *Ophthalmology* **107**: 1593–1600.

Vanderbeek BL, Zacks DN, Talwar N, Nan B, Musch DC et al (2011) Racial differences in age-related macular degeneration rates in the United States: a longitudinal analysis of a managed care network. *American Journal of Ophthalmology* **152**: 273–282.

Varma R, Foong AW, Lai MY, Choudhury F, Klein R et al (2010) Four-year incidence and progression of age-related macular degeneration: the Los Angeles Latino Eye Study. *American Journal of Ophthalmology* **149**: 741–751.

Vingerling J, Dielemans I, Hofman A, Grobbee D, Hijmering M et al (1995) The prevalence of age-related maculopathy in the Rotterdam Study. *Ophthalmology* **102**: 205–210.

Vingrys AJ and Garner LF (1987) The effect of a moderate level of hypoxia on human color vision. *Documenta Ophthalmologica* **66:** 171–185.

Virgili G and Bini A (2007) Laser photocoagulation for neovascular age-related macular degeneration. *Cochrane Database of Systematic Reviews* **18**: CD004763.

Wald G and Brown PK (1958) Human rhodopsin. *Science* **127**: 222–226.

Wang JJ, Mitchell P and Smith W (1998) Refractive error and age-related maculopathy: The Blue Mountains Eye Study. *Investigative Ophthalmology and Visual Science* **39**: 2167–2171.

Wang JJ, Klein R, Smith W, Klein BE., Tomany S et al (2003a) Cataract surgery and the 5-year incidence of late-stage age-related maculopathy. *Ophthalmology* **110**: 1960–1967.

Wang JJ, Foran S, Smith W and Mitchell P (2003b) Risk of age-related macular degeneration in eyes with macular drusen or hyperpigmentation: the Blue Mountains Eye Study cohort. *Archives of Ophthalmology* **121**: 658–663.

Wang JJ, Rochtchina E, Lee AJ, Chia EM, Smith W et al (2007) Ten-year incidence and progression of age-related maculopathy: the Blue Mountains Eye Study. *Ophthalmology* **114**: 92–98.

Wang S and Linsenmeier RA (2007) Hyperoxia Improves Oxygen Consumption in the Detached Feline Retina. *Investigative Opthalmology and Visual Science* **48**: 1335–1341.

Wang JS and Kefalov VJ (2011) The cone-specific visual cycle. *Progress in Retinal and Eye Research* **30**: 115–128.

Wang Q, Kocaoglu OP, Cense B, Bruestle J, Jonnal RS et al (2011) Imaging retinal capillaries using ultrahigh-resolution optical coherence tomography and adaptive optics. *Investigative Ophthalmology and Visual Science* **52**: 6292-6299.

Wang Y, Han Y, Zhang R, Qin L, Wang M et al (2015) CETP/LPL/LIPC gene polymorphisms and susceptibility to age-related macular degeneration. *Scientific Reports* **5**: 15711.

Wangsa-Wirawan N and Linsenmeier R (2003) Retinal oxygen: fundamental and clinical aspects. *Archives of Ophthalmology* **121**: 547-557.

Watson A and Pelli D (1983) QUEST: a Bayesian adaptive psychometric method. *Perception and Psychophysics* **33**: 113–120.

Weikel KA, Chiu CJ and Taylor A (2012) Nutritional modulation of age-related macular degeneration. *Molecular Aspects of Medicine* **33**: 318–375.

Weissman L, De Souza-Pinto N, Stevnsner T and Bohr V (2007) DNA repair, mitochondria, and neurodegeneration. *Neuroscience* **145**: 1318–1329.

West J (2004) Human adaptation to extreme altitude. *Integrative and Comparative Biology* **44**: 663.

Williams PT (2009) Prospective Study of Incident Age-Related Macular Degeneration in Relation to Vigorous Physical Activity during a 7-Year Follow-up. *Investigative Opthalmology and Visual Science* **50**: 101–106.

Winn B, Whitaker D, Elliott D and Phillips N (1994) Factors affecting light-adapted pupil size in normal human subjects. *Investigative Ophthalmology and Visual Science* **35**: 1132–1137.

Wong T, Klein R, Klein BE and Tomany S (2002) Refractice errors and 10-year incidence of age-related maculopathy. *Investigative Ophthalmology and Visual Science* **43**: 2869–2873.

Wong TY, Chakravarthy U, Klein R, Mitchell P, Zlateva G et al (2008) The natural history and prognosis of neovascular age-related macular degeneration: a systematic review of the literature and meta-analysis. *Ophthalmology* **115**: 116-126.

Wong-Riley M (2010) Energy metabolism of the visual system. *Eye and Brain* **2**: 99-116.

Wong W, Su X, Li X, Cheung CG, Klein R et al (2014) Global prevalence of age-related macular degeneration and disease burden projection for 2020 and 2040 : a systematic review and meta-analysis. *The Lancet Global Health* **2**: 106–116.

Woo S, Ahn J, Morrison MA, Ahn SY, Lee J, Kim KW et al (2015) Analysis of Genetic and Environmental Risk Factors and Their Interactions in Korean Patients with Age-Related Macular Degeneration. *PLOS One* **10**: e0132771.

Wood A, Binns A, Margrain T, Drexler W, Považay B et al (2011) Retinal and Choroidal Thickness in Early Age-Related Macular Degeneration. *American Journal of Ophthalmology* **152**: 1030–1038

World Health Organisation (2009) Causes of blindness and visual impairment. *http://www.who.int/blindness/causes/en* [Accessed: 12th May 2017].

Wright AF, Chakarova CF, Abd El-Aziz MM and Bhattacharya SS (2010) Photoreceptor degeneration: genetic and mechanistic dissection of a complex trait. *Nature Reviews Genetics* **11**: 273–284.

Wu G, Weiter JJ and Santos S (1990) The macular photostress test in diabetic retinopathy and age-related macular degeneration. *Archives of Ophthalmology* **108**: 1556-1558.

Wu WC, Kao YH, Hu PS and Chen JH (2007) Geldanamycin, a HSP90 inhibitor, attenuates the hypoxia-induced vascular endothelial growth factor expression in retinal pigment epithelium cells in vitro. *Experimental Eye Research* **85**: 721–731.

Wu L, Tao Q, Chen W, Wang Z, Song Y et al (2013) Association between Polymorphisms of Complement Pathway Genes and Age-Related Macular Degeneration in a Chinese Population. *Investigative Opthalmology and Visual Science* **54**: 170–174.

Wu J, Uchino M, Sastry SM and Schaumberg DA (2014) Age-related macular degeneration and the incidence of cardiovascular disease: a systematic review and meta-analysis. *PLOS One* **9**: e89600.

Wykoff CC, Pugh CW, Harris AL, Maxwell PH and Ratcliffe PJ (2001) The HIF pathway: implications for patterns of gene expression in cancer. *Novartis Foundation Symposium* **240**: 212-225.

Wykoff CC, Ou WC, Brown DM, Croft DE, Wang R et al (2017) Randomized Trial of Treat-and-Extend versus Monthly Dosing for Neovascular Age-Related Macular Degeneration. *Ophthalmology Retina* **116**: 57–65.

Yang SS, Zuo CG, Xiao H, Mi L, Luo G et al (2016) Photoreceptor dysfunction in early and intermediate age-related macular degeneration assessed with mfERG and spectral domain OCT. *Documenta Ophthalmologica* **132**: 17-26.

Yang Z, Camp N, Sun H, Tong Z, Gibbs D et al (2006) A Variant of the HTRA1 Gene Increases Susceptibility to Age-Related Macular Degeneration. *Science* **314**: 992–993.

Yannuzzi L, Negrao S, Lida T, Carvalho C, Rodriguez-Coleman H et al (2001) Retinal angiomatous proliferation in age-related macular degeneration. *Retina* **21**: 416–434.

Yates JW, Sepp T, Matharu BK, Khan JC, Thurlby DA et al (2007) Complement C3 variant and the risk of age-related macular degeneration. *New England Journal of Medicine* **357**: 553–561.

Yau KW and Hardie RC (2009) Phototransduction motifs and variations. *Cell* **139**: 246–264.

Yehoshua Z, Wang F, Rosenfeld PJ, Penha FM, Feuer WJ et al (2011) Natural history of drusen morphology in age-related macular degeneration using spectral domain optical coherence tomography. *Ophthalmology* **118**: 2434–2441.

Yehoshua Z, Gregori G, Sadda SR, Penha FM, Goldhardt R et al (2013) Comparison of drusen area detected by spectral domain optical coherence tomography and color fundus imaging. *Investigative Ophthalmology and Visual Science* **54**: 2429–2434.

Yenice E, Sengun A, Soyugelen-Demirok G and Turacli E (2015) Ganglion cell complex thicknesses in nonexudative age-related macular degeneration. *Eye* **29**: 1076-1080.

Young R and Bok D (1969) Participation of the retinal pigment epithelium in the rod outer segment renewal process. *Journal of Cell Biology* **42**: 392–403.

Young R (1971) The renewal of rod and cone outer segments in the rhesus monkey. *Journal of Cell Biology* **49**: 303–318.

Young TA, Wang H, Munk S, Hammoudi DS, Young DS et al (2005) Vascular endothelial growth factor expression and secretion by retinal pigment epithelial cells in high glucose and hypoxia is protein kinase C-dependent. *Experimental Eye Research* **80**: 651–662.

Yu Y, Reynolds R, Fagerness J, Rosner B, Daly M et al (2011) Association of variants in the LIPC and ABCA1 genes with intermediate and large drusen and advanced age-related macular degeneration. *Investigative Ophthalmology and Visual Science* **52**: 4663–4670.

Yuda K, Inoue Y, Tomidokoro A, Tamaki Y and Yanagi Y (2010) Nerve fiber layer thickness in exudative age-related macular degeneration in Japanese patients. *Graefe's Archive for Clinical and Experimental Ophthalmology* **248**: 353–359.

Zawadzki RJ, Jones SM, Olivier SS, Zhao M, Bower BA et al (2005) Adaptive-optics optical coherence tomography for high-resolution and high-speed 3D retinal in vivo imaging. *Optics Express* **13**: 8532–8546.

Zayit-Soudry S, Moroz I and Loewenstein A (2007) Retinal pigment epithelial detachment. *Survey of Ophthalmology* **52**: 227–243.

Zhang L, Sonka M, Folk JC, Russell SR and Abramoff MD (2014) Quantifying disrupted outer retinal-subretinal layer in SD-OCT images in choroidal neovascularisation. *Investigative Ophthalmology and Visual Science* **55:** 2329-2335.

Zhang Y, Rha J, Jonnal R and Miller D (2005) Adaptive optics parallel spectral domain optical coherence tomography for imaging the living retina. *Optics Express* **13**: 4792–4811.

Zhao J, Frambach DA, Lee PP, Lee M and Lopez P (1995) Delayed macular chorio-capillary circulation in age-related macular degeneration. *International Ophthalmology* **19**: 1–12.

Zheng Y, Wu X, Lin X and Lin H (2017) The Prevalence of Depression and Depressive Symptoms among Eye Disease Patients: A Systematic Review and Meta-analysis. *Scientific Reports* **7**: 460453.

Zhou H, Zhao X, Johnson EJ, Lim A, Sun E et al (2011) Serum carotenoids and risk of age-related macular degeneration in a chinese population sample. *Investigative Ophthalmology and Visual Science* **52**: 4338–4344.

Zhu W, Wjeyakumar A, Syed AR, Joachim N, Hong T et al (2017) Vision-related quality of life: 12 month aflibercept treatment in patients with treatment-resistant neovascular age-related macular degeneration. *Graefe's Archive for Clinical and Experimental Ophthalmology*. **255**: 475-484.

Zweifel SA, Spaide RF, Curcio CA, Malek G and Imamura Y (2010) Reticular Pseudodrusen Are Subretinal Drusenoid Deposits. *Ophthalmology* **117**: 303–312.

Appendix I. Table of studies included in literature review

Title	Participants	Methods	Results	Conclusion	Notes
Reduced choroidal foveolar blood flow in eyes with increasing AMD severity (Grunwald et al., 2005).	189 in total 26 control eyes. 163 eyes with early AMD characteristics divided into 3 subgroups: (1) 56 eyes of drusen >63µm and no RPE changes. (2) 88 eyes of drusen >63µm and some RPE hyperpigmentary changes. (3) 19 eyes of drusen >63µm and CNV in non-study eye (13 of which had RPE hyperpigmentary changes in the study eye also).	Laser Doppler flowmetry (LDF) used to assess foveolar choroidal blood velocity, volume and flow. Laser diode beam 670nm, intensity 20mW, probing laser beam diameter 200µm 3 continuous 30s measurements of choroidal circulation taken per eye of which 12s of stable measurement was selected for analysis. Differences in mean circulatory parameters assessed by analysis of variance and test of linear trend.	Choroidal blood velocity (average): Controls (0.43). AMD 1 (0.38). AMD 2 (0.38). AMD 3 (0.37) arbitrary units. Increased risk of CNV was associated with decreased velocity (linear trend test). Choroidal blood volume (average): Controls (0.26). AMD 1 (0.25). AMD 2 (0.23). AMD 3 (0.20) arbitrary units. Choroidal blood flow (average): Controls (9.80). AMD 1 (7.78). AMD 2 (7.49). AMD 3 (6.54) arbitrary units. Increased risk of CNV was associated with decreased flow (linear trend test). Linear trend of velocity and flow remain statistically significant when adjusted for age and hypertension (important as increasing age causes decreased flow in controls).	Decreasing choroidal blood flow with increasing AMD features. Result suggests foveolar choroidal blood flow is lower than normal in eyes with AMD and correlates to the fundus features associated with risk of CNV development i.e. choroidal blood velocity, volume and flow all decrease progressively with an increase in severity of AMD features. Results are suggestive that disturbances in the choroidal circulation could hinder the normal diffusion of substances across the RPE-Bruch's membrane complex thus promoting an ischaemic environment. Author points out that loss of PRs during AMD may result in a reduced oxygen demand and decreased choroidal flow.	Also changes to the intensity and coherence of laser light produced by AMD can theoretically affect the hemodynamic measurements, the comparison of LDF relative blood flow measurements between normal and AMD eyes is open to question. Compares study to those measuring pulse amplitude however relationship between choroidal blood flow and pulse amplitude is not clearly established.
Regulation of sub-foveal choroidal blood flow in age-related macular degeneration (Pournaras et al., 2006).	56 eyes in total 1 eye of each participant used, split over 3 groups: (1) 19 'young' controls (age 24-44yrs) (2) 24 controls (age 50-84yrs) with mild	Laser Doppler flowmetry used to assess changes in foveolar choroidal blood velocity, volume and flow induced by increased perfusion pressure (achieved through isometric exercise). Measurements were taken at 3 points: rest, standing and squatting.	Squatting induced a significant increase in perfusion pressure (20-23%) that was similar in all groups. Measurements at the end of squatting as follows: Choroidal blood velocity (average): Young controls (3.0), elderly controls (5.7), AMD (7.3) arbitrary units.	New vessels lack ability to regulate increased blood flow in nAMD. An acute systemic increase in BP (perfusion pressure) does not induce a significant change in choroidal blood flow in young or elderly subjects with early AMD. However in the presence of nAMD blood flow increases significantly.	Highlights again that LDF data may be corrupted by changes in the laser light-scattering properties of sampled (AMD) tissue – hence physiological stimulus of exercise is used in this study. Exercise is used in order to eliminate tissue scatter as cause of error with LDF (LDF subfoveal

	macular pigmentary disturbances. (3) 23 subjects (age 45-86yrs) with subfoveal CNV caused by AMD.		Choroidal blood volume (average): Young controls (1.3), elderly controls (-2.9), AMD (0.5) arbitrary units. Choroidal blood flow (average): Young controls (7.3), elderly controls (6.7), AMD (12.4) arbitrary units. Measurements for group 1 and 2 were not significantly different from baseline (before squatting). In the AMD blood volume and (significantly) blood flow increased following the exercise when compared to group 2.	During exercise BP in the ophthalmic artery increases in parallel with that of the brachial artery. Therefore to find no increase in choroidal flow from before to after exercise (as with group 1 and 2) indicates a vascular resistance against the new perfusion pressure (brought about by either contraction of arteriole smooth muscle or contraction of pericytes surrounding the capillaries). The results suggest choroidal dysregulation of the AMD group which would allow over-perfusion in nAMD leading to increased exudation and bleeding.	choroidal flow is largely constant in healthy volunteers in spite of changes in perfusion pressure caused by exercise). Author states that: new vessels have immature fenestrated endothelial cells, inadequate numbers of pericytes and inadequate sites of contact between endothelial cells and pericytes hence control of vascular diameter is poor.
Delayed macular chorio-capillary circulation in age-related macular degeneration (Zhao et al., 1995).	42 eyes in total. 34 eyes with AMD (dry or nAMD, any stage of progression). 8 Age-matched controls.	Scanning laser ophthalmoscope (SLO) fluorescein video-angiography used. The retina was divided into 8 sections for analysis. Choriocapillary filling time was recorded in each sector (the time between the initial choroidal filling and the time at which choriocapillary filling was demonstrable in the entire sector). Filling time was correlated with the participant's drusen number, size, type, area and degree of confluence. Areas of slow filling by neo-vascularisation complexes were not considered when assessing the presence of delayed choriocapillary circulation.	Macular choriocapillary filling time was prolonged in AMD. Mean macular filling time for controls was 1.71s. Mean macular filling time for AMD participants was 3.29s. 5s was deemed as a delayed filling time (mean normal macular choriocapillary filling time plus 3 standard deviations), this was met by 26% of the AMD eyes tested. Delayed choroidal filling in AMD was widespread and not confined to the macular region. Filling was more delayed nasally to the fovea (as opposed to temporally), inferiorly to the fovea (as opposed to superiorly) and near the fovea (as opposed to in the periphery). A greater incidence of GA of the RPE was found in AMD eyes with delayed choroidal filling (statistically significant when age corrected). Also a trend towards a higher incidence of CNV in	AMD causes delayed choroidal filling which is proportional to drusen characteristics Results suggest clinically evident or hydrophobic drusen deposits impair bi-directional metabolic exchange across Bruch's membrane culminating in CC atrophy. The biochemical characteristics of the drusen may cause more impediment in one direction i.e. CCs decline but RPE preserved. In these eyes it is hypothesised the CC atrophy triggers a wound healing response to the ischaemia leading to CNV. Eyes with delayed choroidal filling had less, but more confluent drusen in the inner subfield. Therefore the composition of the confluent drusen could be used to identify those predisposed to delayed filling (this is opposite to Paulikoff et al. 1990, the author speculates due to study	Author comments on previous fluorescein angiographic analysis of choroidal filling times stating the short vascular filling time, fast outflow of fluorescein from the capillaries and frame speed of 1 photo per second limits precise analysis of filling times with this technique. A SLO gives 60 frames per second to improve this and provides better resolution of the short choriocapillary filling time. Areas of blocked choroidal fluorescence such as the xanthophyll containing foveal areas and RPE hyperpigmentation could not be analysed hence it is possible that the incidence

			AMD eyes with delayed choroidal filling was found (not statistically significant).	design, populations or disease severity). Less fluorescence of the inner subfield drusen in eyes with delayed filling suggests hydrophobic drusen (likely to impede the exchange of metabolites between the RPE and CCs).	of delayed filling has been under-estimated. Results similar to Pauleikoff et al. (1990).
Color Doppler imaging of choroidal circulation in patients with asymmetric age-related macular degeneration (Üretman et al., 2003).	52 eyes in total 26 participants who had dry AMD in one eye and nAMD in the fellow eye.	Laser Doppler flowmetry of the ophthalmic artery, nasal posterior ciliary artery and temporal posterior ciliary artery was performed in order to assess the blood flow velocity (peak systolic and end diastolic) alongside vessel pulsatilities and resistivity.	It must be remembered that these comparisons are between dry AMD and nAMD eyes (not controls). In eyes with CNV, systolic and diastolic velocities were lower for each vessel with the exception of systolic velocity of the nasal posterior ciliary artery. In eyes with CNV, the pulsativity and resistivity index was higher for each vessel to a statistically significant degree.	Decreased perfusion in nasal and temporal posterior ciliary arteries in nAMD more-so than dry AMD Results indicate that impaired choroidal blood flow could contribute to the pathophysiological process of CNV in eyes with AMD by predisposing the retina to ischaemia and hypoxia. It is still only speculated as to whether impaired blood flow plays a causative role in CNV development or whether it is secondary to CNV development.	Author states that all differences found in velocity were not statistically significant.
Retrobulbar circulation in patients with age-related maculopathy (Dimitrova et al., 2002).	22 eyes for study (1). 42 eyes for study (2). 44 participants with exudative AMD recruited over both trials alongside 32 age-matched controls. 11 with early AMD (drusen >63µm and/or atrophy of the RPE <175µm). 33 with late AMD (7 had PED, 18 had	2 separate trials: (1) Study of retrobulbar circulation in stages of AMD (2) Study of retrobulbar circulation in patients with unilateral exudative AMD Color doppler imaging used to measure peak systolic velocity, end diastolic velocity, pulsatility and resistivity in the central retinal, posterior ciliary and ophthalmic arteries.	In the posterior ciliary artery the pulsatility and resistivity (1.13 and 0.66) were significantly higher in the late AMD group than in the controls (0.97 and 0.61) this was statistically significant. No such difference was found within the other vessels analysed. No significant differences found between early AMD participants and controls. In unilateral exudative AMD participants the end diastolic velocity was lower in the posterior ciliary artery of the fellow eye (2.48) when compared to the exudative (2.64) and control group (3.11). The pulsatility and resistivity index of this	Circulatory dysfunction of the posterior ciliary artery was found (therefore the choroid) which may be related to AMD pathology. Irregularities in the retrobulbar circulation are not present in early AMD however manifest in later stages of the disease. Author speculates that increased scleral rigidity with AMD progression causes increased resistivity to choroidal blood flow and as a consequence a decrease in end diastolic velocity/increase in pulsatility and resistivity.	Author adds that results for central retinal artery circulation are reliant on blood pressure/ posture during measurement hence cannot be relied upon when comparing between trials. Results consistent with Mori et al., 2001. Choroidal circulation in fellow eyes of unilateral nAMD is also compromised hence studies should not use them as a

	CNV, 8 had disciform scarring).		vessel was also higher for the exudative eye (1.15 and 0.67) when compared to both the fellow eye (1.14 and 0.66) and controls (0.97 and 0.61) however this was found not to be statistically significant.	.	representative of true circulation in early AMD.
Ocular blood flow velocity in Age-related Macular Degeneration (Friedman et al., 1995).	50 eyes in total (age range 50-87, 75yrs median). 23 eyes with nAMD. 27 eyes with dry AMD (soft drusen without the presence of RPE detachment of CNV). 74 aged-matched controls.	Color Doppler imaging used to measure blood flow velocity (mean peak systolic and end-diastolic) and vessel pulsatility in the ophthalmic artery, central retinal artery and vein, temporal and nasal short posterior ciliary arteries and the four vortex veins.	Vessel pulsatility was found to be higher in participants with AMD (statistically significant for the nasal short posterior ciliary artery and central retinal artery). The pulsatility of the arteries that perfuse the eye is higher with the presence of AMD: Subjects whose pulsatility measures were in the upper tertile for the temporal short ciliary artery, central retinal artery and the nasal short posterior ciliary artery were 3, 3 and 11 times more likely to have AMD than those in the lower tertile. Systolic and diastolic velocities tended to be lower in patients with AMD across all age groups (statistically significant for the temporal short posterior ciliary artery and central retinal artery).	It is suggested that the higher pulsatility, combined with a lower end diastolic velocity, is evidence of an increase in the resistance of the short posterior ciliary arteries (indicating a decrease in the compliance of the choroidal vessels, combined with a decrease in their calibre in the presence of AMD). The author suggests that the decrease of compliance of the choroidal vessels is initiated by deposition of lipid in the sclera/Bruch's membrane resulting in decreased perfusion (ischaemia), higher intravascular pressure or both which leads to impaired RPE transport, then drusen accumulation etc. IOP, hypertension, pulse pressure and smoking variables were found not to be significantly associated with AMD status.	Author states that the pulsatility index is derived from the ratio of diastolic to systolic velocity and is less dependent on Doppler angle, machine settings, physiological conditions (hypertension) than measurements of absolute velocity. See Figure 4 for proposed sequence of AMD pathogenesis.
Drusen and 'Choroidal filling defects': a cross-sectional survey (Staurenghi et al., 1992).	126 eyes in total 68 eyes with hard drusen (<50µm, round lesions with sharply defined borders). Average age 65yrs. 58 eyes with soft drusen (>50µm, ill	Cross sectional study. Retrospective data taken from participants recruited to an ongoing case-control study. Fluorescein-angiography images analysed in order to categorise drusen and identify choroidal filling defect.	19.1% (13 of 68) Participants with hard drusen had a choroidal filling defect. 50% (29 of 58) participants with soft drusen had a choroidal filling defect. No delayed filling correlation was found associated with IOP, hypertension or diabetes. A significant difference between the mean ages of the 2 groups was found.	Results suggest an association between soft drusen and a choroidal filling defect. Eyes with abnormal choroidal filling tend to have fewer drusen that are less densely distributed in the central region (within 1600µm of the fovea).	A deficiency of blood flow in this area not related to AMD (a true choroidal filling defect). A decrease in the effusion (flow) of dye from the choroidal capillaries. Lower penetration of dye into Bruch's membrane due

	defined borders). Average age 72yrs. Also FFA characteristics used to diagnose. Those with both were designated into the group of their predominant drusen type.	Choroidal filling defect defined as adjacent areas, extending over at least 2 disk areas of choroidal hypofluorescence still evident at the end of the venous laminar phase.	This had no bearing on the mean age of participants with choroidal filling defects (69yrs hard drusen and 68yrs soft drusen).	The prolonged choroidal filling phase observed using FFA is likely to be associated with hydrophobic material in Bruch's membrane leading to an overall thickening of the layer. Evidence suggests this causes difficulty with metabolite transportation from the RPE to the choroid and results in choriocapillary irregularity. Author recognises that the criteria used (the appearance of a prolonged choroidal filling phase during FFA) cannot be used to diagnose a perfusion defect with 100% certainty as it could be caused by:	to altered composition (hydrophobic drusen altering the diffusion characteristics and binding properties of fluorescein).
Pulsatile ocular blood flow study: decreases in exudative age-related macular degeneration (Mori et al., 2001).	90 eyes in total. 10 participants with dry AMD, 11 participants with nAMD. 69 age-matched controls. Participants with hypertension were included in the study.	Pulsatile ocular blood flow (POBF) and pulse amplitude (PA) taken with participants in sitting position using a computerised tonometer (gives a measurement of total choroidal blood flow). The mean of 5 pulses was recorded. Also recorded was: systolic/diastolic blood pressure, IOP (Non-contact tonometer), refractive error (Autokeratorefractometer) and axial length (A-scan biometric ultrasound).	Participants with nAMD had a lower PA (median 1.2mmHg) than those with dry AMD (median 2.2mmHg) and controls (2.0mmHg). Participants with nAMD had a lower POBF (median 372.7µl/min) than those with dry AMD (607.0µl/min) and controls (547.4µl/min). 30% decrease in POBF for nAMD participants when compared to controls and those with dry AMD. No significant differences in PA or POBF were found between those with dry AMD and the controls. No significant differences were found in age, systolic and diastolic blood pressures, IOP, refractive error and axial length between AMD and control participants.	The total choroidal flow is lower in participants with nAMD, hence results correlate with those finding lower blood flow velocity in the short posterior ciliary arteries. Thickening of Bruch's membrane (associated with prolonged filling time observed in FFA) may induce increased vascular resistance of the choroid and decreased choroidal blood flow, leading to ischaemia. Choroidal blood flow was found to be lower in the centre of the fovea for participants with dry AMD (when compared to controls) by Grunwald et al., 1998. These results do not correlate and suggest that only local choroidal flow in the centre of the fovea may decrease however total choroidal flow does not.	Results do not correlate with Lang et al. 1994. The author suggests axial length was not accounted for by Lang et al., 1994. When a POBF decrease was reported for dry AMD participants. Decreased total choroidal flow may induce CNV via angiogenic factor induced by hypoxia. Stated by Chen et al. 2001. The disease activity of the nAMD is unknown: disciform scar or active CNV?

Presumed macular choroidal watershed vascular filling, choroidal neovascularisation and systemic vascular disease in patients with age-related macular degeneration (Ross et al., 1998).	94 eyes in total. 74 patients with age-related macular degeneration (mean age 75.1yrs) 20 age-matched controls (referred for a uniocular condition and underwent videoangiography on their 'healthy' fellow eye). Eyes with dry AMD were classified as having multiple drusen, GA or both (17.6% of AMD cohort). Eyes with nAMD were classified as having CNV, PED or both (82.4% of cohort).	Retrospective study of randomly selected indocyanine green videoangiograms (25mg dye in 1.25ml solvent followed by 5ml saline flush). Images taken every 2s for 30s and then intermittently for 30mins. The record of each participant was assessed, including results of a complete ocular examination, FFA, contact lens biomicroscopy and current systemic medication (used to derive info on hypertension, diabetes, coronary disease and vascular disorders).	41 of 74 AMD eyes (55.4%) exhibited presumed macular choroidal watershed vascular filling (PMWF) versus 3 of 20 (15%) control participants (none of which displayed PMWF near or adjacent to the fovea). Hypertension was noted in 24 of 41 (58.5%) participants with AMD and PMWF versus 9 of 33 (27.3%) participants with AMD and no PMWF. No significant difference was found when comparing the incidence of coronary heart disease, hypertension, vascular disease and diabetes in the AMD versus control groups. 5 of 13 (38.5%) eyes with dry AMD versus 36 of 61 (59.0%) eyes with nAMD exhibited PMWF of which 33 of 41 (80.5%) exhibited PMWF through or adjacent to the fovea. Of the 41 participants with AMD and PMWF 36 (87.8%) had CNV. In 33 (91.7%) the CNV arose from the watershed zone or its margin.	Results of previous angiographic studies indicate that the choriocapillaries consist of lobular beds, each acting as an independent unit with no functional adjoining connection of blood streams. Results documented here suggest watershed zones represent areas susceptible to ischaemia. Numerous watershed zones of the short posterior ciliary arteries and vortex veins meet at the highly metabolically active macular. Combined with a high pressure gradient and rapid blood flow this area is particular vulnerable to hypoxic assault. Participants with dry AMD and large PMWF zones may be at a higher risk of CNV development, destruction of these zones or improvements to their flow may aid in preventing AMD progression. Data supports theory that underlying systemic vascular disease such as hypertension further augments the tendency for PMWF in the presence of AMD.	Indocyanine green results of Hayashi and Laey. 1985. May be corrupted by poor eligibility criteria. Diabetes showed a negative correlation with PMWF. Possibly explained by diabetic systemic autonomic neuropathy, which can involve ocular uveal sympathetic pathways. (Choroidal sympathetic denervation could alter microvascular perfusion gradients or increase choroidal blood flow, thus minimising ischaemia and the tendency for PMWF). Study limited by low number of controls and participants with systemic complications of a vascular origin. Author suggests AMD pathogenesis theory (page 76).
Changes of retinal capillary blood flow in age-related maculopathy (Remsch et al., 2000).	47 eyes in total 10 eyes with early AMD (drusen >63µm and/or RPE atrophy <175µm) 13 with nAMD. 10 with end stage AMD (fibrotic scarring)	HRF two-dimensional confocal scanning laser Doppler flowmetry used to record retinal capillary blood volume, flow and velocity in 6 retinal sectors (I-IV over foveal region, V-VI outside vascular arcades) Classification based on ophthalmic examination, FFA. Systemic vascular disorder was excluded.	Participants with early AMD showed no significant change in choroidal volume, flow or velocity in any sector when compared to controls. Participants with nAMD showed significantly higher flow in areas I, II and IV and higher volume in areas III and IV when compared to controls. Participants with end-stage (fibrotic) AMD showed a reduction of velocity in	Results show a marked disturbance of retinal capillary blood flow in participants with nAMD (raised blood flow) and end-stage AMD (reduced perfusion). Early vascular abnormalities cannot be used as a risk factor for AMD development in children of those currently affected.	Author remarks that this technique cannot be compared directly to conventional laser Doppler flowmetry. Raised blood flow could be due to auto-regulative vascular response due to compromised metabolism, hence cannot be used as an

	14 normal eyes of children of participants with AMD (Mean age 46yrs, versus mean age of AMD participants of 72yrs)	Heart rate, blood pressure and IOPs monitored.	sectors II and IV and a reduction of volume and flow in sectors I-IV. In children of AMD participants in changes were found when compared to the control group.		AMD pathogenesis model with complete certainty.
Evolution of age-related macular degeneration with choroidal perfusion abnormality (Piguet et al., 1992)	96 eyes in total (all over 57yrs old). 46 had drusen in both eyes. 50 had drusen in one eye and dry or nAMD in the fellow eye. Participants recruited from an existing longitudinal study of AMD had visible drusen and underwent FFA. GA and PED were not included in this study.	Cross sectional study in which fluorescein angiography (FFA) was used. As opposed to normal rapid filling, abnormal choroidal perfusion was classified as a continuous area of prolonged, patchy choroidal fluorescence during the transit phase of the angiogram This pattern of choroidal filling is characteristically seen in participants with known choroidal hypoperfusion as part of a general vascular disorder.	A long choroidal filling phase was identified in 32 eyes (normal dye transit in 64 eyes). The number of new lesions associated with vision loss (a reduction of 2 Snellen lines or more) was significantly greater in eyes with prolonged choroidal filling (12 of 32 [37.5%], P<0.1) than in those with normal perfusion (9 of 64 [14%]). 17 of the 32 eyes (53.1%) with prolonged choroidal filling had GA whereas 9 of the 64 eyes (14%) with normal dye transit had GA (P<0.001). Newly developed GA caused vision loss in 7 of the 32 eyes (21.9%) with prolonged choroidal filling. CNV manifested in 4 eyes with prolonged choroidal filling (12.5%) and 7 eyes with normal dye transit (10.9%).	Evidence suggests that eyes with prolonged choroidal filling are more at risk of vision loss (through the development of GA) than those without the clinical sign. During early stages nAMD causes a greater degree of visual loss however it is expected that long term vision loss caused by progressive GA can be more detrimental. Failure of the RPE to deliver diffusible substances to the choroid may result in the choriocapillaries being unable to change from a sinusoidal system to a tubular arrangement (seen in most capillary beds).	The age, gender and period of review were not statistically significant. The degree of vision loss was on average 3 lines with newly developed GA and 5 lines with CNV. Potential pathway suggested: slow filling of the choriocapillaries indicates a change in blood flow likely to be brought about by the accumulation of deposits in Bruch's membrane which impair metabolic exchange.
Pulsatile ocular blood flow in asymmetric exudative age related macular degeneration (Chen et al., 2001).	74 eyes in total 37 participants categorised into 3 groups: (1) 21 with drusen in 1 eye and nAMD in the fellow eye, (2) 9 with a disciform scar in 1 eye and drusen in the fellow eye,	Pulsatile ocular blood flow (POBF) was performed using an OBF tonometer on a seated participant. 5 pressure pulses were also averaged in order to determine the pulse amplitude (PA). IOPs were also measured using contact tonometry. Blood pressure was taken and ocular perfusion pressure (OPP) was calculated.	Group 1 nAMD eyes had higher POBF than their fellow eyes with drusen only (when corrected for IOP and OPP). Eyes with disciform scarring in group 2 had lower POBF than their fellow eyes with drusen only. The IOP and OPP showed no significant difference between the fellow eyes of groups 2 and 3 but marginal significant difference between the eyes in group 1.	POBF was different between the fellow eyes of the individuals was asymmetric nAMD. Because the calculated OPP was not seen to be different between the 2 eyes in a single subject, it is speculated that the discrepancy in POBF may originate in a more distal vessel i.e. the retrobulbar vessels or the eye wall itself. The asymmetric pulsation found could have 2 causes: the pulsatile	Author states POBF measures choroidal circulation and contribution from retinal blood flow is negligible. However, there is still a contribution. Krakau. 1995. and Langham et al. 1989 give more detail on the floors of this technique. Author recognises POBF is not a flawless technique: the components of pulsatile blood flow to the total blood

	(3) 7 with a disciform scar in 1 eye and CNV in their fellow eye. Strict and numerous criteria stated for grading AMD and eligibility.		No statistically significant differences found between age, sex or blood pressure between the groups. The correlation of POBF to the CNV lesion size was insignificant.	components of the choroidal blood flow are dynamically influenced during the development of nAMD. A disciform scar may replace an active CNV, disorganise the choriocapillary-Bruch's membrane complex and damage the outer retina (thus decreasing the need and supply of the choroidal vessels in this eye). Reversely eyes with active CNV are likely to attract more blood flow to feed the new vessel growth. Alternatively increased asymmetrical scleral rigidity is more pronounced in the CNV eyes of group 1 and drusen eyes of group 2 (unlikely).	flow is unclear and ranges from 50-80%. There is high inter-individual variation and factors such as age, sex, hypertension, blood velocity, blood viscosity may affect readings. Results of group 3 possibly corrupted by 2 participants with leaking disciform scars and CNV in their fellow eye.
Topographic variation of the choroidal watershed zone and its relationship to neovascularisation in patients with age-related macular degeneration (Mendrinos and Pournaras, 2009).	50 eyes in total. ICG video-angiograms reviewed of 50 participants (20 male, 30 female). Mean age was 78.7yrs (range 55-94yrs). AMD was classified via reviewing the FFA of each participant. All forms and stages of nAMD were included. Cases of AMD with no clearly visible WZ were not used. CNV Graded using the Treatment of age-related macular degeneration with photo-dynamic therapy study group. 1999. Scale.	Cross sectional retrospective study using digital indocyanine green (ICG) video-angiography WZ zones were classified due to shape: Stellate pattern: consists of a vertical portion (corresponding to the WZs between the medial and lateral PCAs) associated with multiple, smaller, triangular zones (corresponding to the WZs between the branches of the lateral PCA). Vertical WZ only: running vertically through the ONH and fovea. Angle-shaped WZ: running at an angle through the ONH and fovea.	CNV occurred within the WZ in 88% of participants. In the remaining 12% CNV occurred at the WZ margin. Stellate pattern (60% participants): the triangular WZs are seen to meet in the centre of the macular. CNV occurred within the centre of these WZs in all cases. Vertical WZ only (36% participants): CNVs were located in the area at which the WZ passes through the fovea in 66.7% of cases. In the remaining cases the CNV was found at the temporal margin of the WZ and extended towards the fovea. An occult CNV was found in 13 of 50 participants (1 with an angle-shaped WZ, 5 with a vertical WZ and 7 with a stellate pattern). Predominantly classic CNV was found in 15 of 50 participants (5 with a vertical WZ and 10 with a stellate pattern).	A part of every watershed zone involved the macular region (even if it did not course through the fovea directly). The area at which WZs meet is an area of relatively poor blood flow supply and is consequently most vulnerable to ischaemic disorders. As in the majority of participants WZs met at the macular region it is this area that is anatomically predisposed to chronic ischaemia more than any other part of the posterior choroid. Combined with: Delayed filling and lowered perfusion pressure of the macular vasculature could predispose to AMD. Findings agree with Hayashi and De Laey (1985), Ross et al. (1998). and Giovanni et al. (1994) however this study only incorporated participants	Anatomically the choroidal blood supply comes from 2 posterior ciliary arteries (PCAs). In vivo studies on the choroidal vascular bed show that the PCAs and all their choriocapillary branch are segmentally structured and thus behave like end-arteries (individually supplying only one portion of tissue). Each choriocapillaris lobule functions as an independent unit with no anastomoses with adjacent lobules. The borderline area between territories of 2 end-arteries is defined as a watershed zone (WZ). Author states ICG is a highly protein-bound dye that provides enhanced imaging of the choroidal vessels in comparison to fluorescein

			Minimally classic CNV was found in 6 of 50 participants (1 with a vertical WZ and 5 with a stellate pattern).	with nAMD (hence higher percentages of CNV found in relation to WZs). Also no control group used and technique requires subjective interpretation of the angiogram to determine WZ boundaries.	which rapidly leaks out of the vasculature.
Quantification of choroidal blood-flow parameters using indocyanine green video-fluorescence angiography and statistical picture analysis (Prünte and Niesel, 1988).	10 eyes in total. 5 participants with dry AMD (determined by the presence of hard drusen, hyperpigmented RPE and RPE atrophy) 5 age-matched controls.	ICG Videoangiography. A solution of 0.3 mg/kg ICG was dissolved in 0.02 ml/kg of water and injected into the cubital vein. Picture processing analysis software was used in order to enhance the obtained images.	The arteriole filling time was delayed in those with AMD ($P<0.05$). The capillary peak filling time was delayed in those with AMD ($P<0.01$). Control participants displayed a lower coefficient of variance of grey values (CVG) indicating a higher perfusion rate.	The reduced perfusion found of AMD participants is likely to be due to morphological changes caused by the disease. More research is necessary to determine specifics of choroidal disruption.	
Localised reticular pseudodrusen and their topographic relation to choroidal watershed zones and changes in choroidal volumes (Alten et al., 2013).	60 eyes in total. 30 patients (22 females, 8 males) of mean age 76.7yrs. 30 age-matched controls. Participants were only eligible if they displayed reticular pseudodrusen (RPD) smaller than $10mm^2$ in the macular area. Signs of conventional soft or hard drusen, CNV, PED or GA were excluded.	Multiple techniques used. Fundoscopy, fundus auto fluorescence (FAF), infrared reflectance (IR) and fluorescein angiography (FFA) were used to determine eligibility. Indo-cyanine green angiography (ICG) used to classify shape of WZ. Confocal scanning laser ophthalmology (cSLO) was used to quantify the area affected by RPD. Spectral domain-optical coherence tomography (SD-OCT) was used to calculate choroidal volume and thickness.	WZs were detected in 83.3% of RPD eyes and 40% of controls. A stellate pattern was present in 40%, a vertical WZ was present in 44% and an angle-shaped WZ was present in 16.0% of RPD eyes studied. Correlation between the presence and localisation of RPD with the pattern of WZ was unable to be made due to lack of numbers. Mean retinal area affected by RPD was $7.45mm^2$. This area was localised fully or partially within the WZ of 22 out of 25 study eyes (88.0%). Mean choroidal volume was reduced significantly in the study group ($4.49mm^3$) versus the controls ($5.85mm^3$). $P<0.05$.	RPD development and progression may be driven by ischaemia starting with diffuse loss of small choroidal vessels and submacular choroidal thinning (confirmed by the presence of WZs combined with reduced choroidal volume and thickness). Areas of RPD were never situated nasally to the ONH and most frequently found superiorly to the fovea. The author speculates that RPD are likely to originate from rod rather than cone PR metabolism due to their position in the outer macular.	RPD are most frequently found between the superior fovea and superior temporal arcade (visible via cSLO, FAF, IR and SD-OCT). They have a punctate white/grey appearance close to the fovea (as opposed to yellow, ill-defined drusen). An average RPD diameter is between 50-400µm. Subjective interpretation of WZ via ICG is not ideal.

			Mean choroidal volume and choroidal thickness in the area most affected by RPD were both diminished to 0.85mm^3 and 171µm when compared to the same area within controls (1.11mm^3 and 225µm).		
The association between drusen extent and foveolar choroidal blood flow in age-related macular degeneration (Berenberg et al., 2012).	239 eyes in total. 157 participants with AMD (mean age 71yrs). Mean systolic blood pressure 137mmHg, mean diastolic blood pressure 75mmHg. CNV in the study eye (and any other ocular pathology) was excluded.	Foveolar blood flow velocity, volume and flow measured using laser Doppler flowmetry. 670nm diode laser beam with 20mW intensity (beam diameter 200µm). 3 continuous 30s measurements of the choroidal circulation were obtained of which a stable 12s section was used for analysis. Individual druse area, total drusen area and shortest distance between the druse edge and the fovea measurements were recorded by specially developed fundus camera software and assessed manually by a grader.	Total number of drusen within 3000µm of the foveola ranged from 1-846 (median 126). Total drusen area ranged from 0.001mm^2-9.62mm^2 (median 1.65mm^2). Average druse area ranged from 0.001mm^2-0.097mm^2 (median 0.01mm^2). For every 1- mm^2 increase in total drusen area, volume decreased by 0.0061 (P=0.03) and flow decreased by 0.23 (P=0.049). Association after age adjustment became less strong. For every 0.01- mm^2 increase in average druse area, the volume decreased by 0.0149 (P=0.001) and flow decreased by 0.495 (P=0.003). Remained statistically significant after adjustment for age (P=0.004) and (P=0.017). The number of drusen was not significantly associated with choroidal circulatory measurements.	Results suggest that in participants with dry AMD, eyes with a larger extent of drusen, as measured by total drusen area and average druse area, tend to have decreased choroidal blood volume and flow (which suggests that the area covered by drusen may be an important determinant of disease risk). Results indicate as drusen coalesce with advancing AMD there is a larger negative effect on choroidal blood volume and flow. A reduction of choroidal blood flow may also propagate drusen formation as it slows the removal of waste products from the RPE-Bruch's complex. Results indicate that total drusen area is more correlated with decreased flow than actual number of drusen.	Advantage of manual assessment of drusen: better discernment of drusen versus non-drusen, decreased false positives and false negatives. Advantage of computer assessment of drusen: reduced grading time, improved quantitative data, use of technical advances in digital image manipulation. There is a possibility that blood flow measurements are affected directly by the presence of drusen i.e. drusen interfere with laser Doppler blood flow measurement.
Association of risk factors for choroidal neovascularisation in age-related macular degeneration with decreased foveolar choroidal circulation (Xu et al., 2010).	298 eyes in total. 269 study eyes in total from 204 non-exudative participants recruited (mean age 71yrs) of which 55.9% were female. 6.4% were current smokers. 44.6% had a history of systemic hypertension. 61.8%	Laser Doppler flowmetry measurements from the centre of the foveola were performed to obtain data on blood velocity, volume and flow. Measurements were taken on a seated participant using a 670nm laser beam (20mW intensity). Blood pressure and IOP (Goldmann tonometry) data was also taken.	A significant inverse correlation was observed between age and choroidal blood flow and volume (P<0.0001 for both). Patients with increasing age tend to have lower choroidal blood flow and volume (maintained following adjustment for all other risk factors). A significant inverse correlation was observed between spherical correction and choroidal blood flow (P=0.006) and volume (P=0.04). Patients with more	The results of the study indicate flow and volume (but not velocity) decrease with age. This is likely due to age-related changes in capillary structure (decreases in lumen diameter and choriocapillary density). Systemic hypertension does appear to be related to irregularities in choroidal blood flow. It is speculated that hypertension may contribute to AMD pathogenesis through	No significant correlation between choroidal blood flow and actual blood pressure at the time of measurement was found. No correlation with race, eye colour or kidney disease was found however the author states this is not conclusive due to small numbers of participants

	had a history of cardiac disease. 8.8% had a history of kidney disease. 58.4% had RPE hypertrophy. 29 Controls used from previous study of which one eye used in each (Grunwald et al.1998).	Structured questionnaire used to obtain information on age, gender, race, smoking, medical history, eye colour and family history of AMD.	hyperopia tended to have lower choroidal blood flow and volume. Patients with a history of hypertension had choroidal blood volume (0.21 AU) and flow (6.94 AU) which were significantly lower than those observed in patients without hypertension (0.25 [P=0.007] and 7.97 [P=0.003] AU). Patients with RPE hypertrophy had average choroidal blood volume (0.22) and flow (6.94) which were significantly lower than those of eyes without hypertrophy (0.25 [P=0.01] and 7.78 [P=0.04] AU).	promoting an ischaemic environment (leading to WZ hypoxia and CNV). RPE hyperpigmentation was associated with decreased blood flow, it is suggested that hypoxia may play a role in the formation of RPE changes through moderating RPE proliferation and migration.	within the cohort of which these sub-categories apply. No association with smoking, cardiac disease or gender was found however the author states this is likely to be connected with the involvement of other pathogenic mechanisms that are not related to ischaemia or hypoxia i.e. oxidative damage and inflammatory pathways.
Age-related macular degeneration: choroidal ischaemia? (Coleman et al., 2013).	69 eyes in total. 52 patients recruited: 18 controls, 23 dry AMD, 28 nAMD.	High resolution ultrasound (20mHz ultrasound scans on each eye using a B-scan immersion technique). A prototype instrument of the authors design was used (based on a wavelet analysing technique and passing data through VDU based software for analysis). Fundus photography, OCT and ICG was measured in order to identify AMD type.	Technique able to separate visible areas of tissue from areas of fluid via their boundaries. In dry AMD, the wavelet descriptors showed a reduction in boundary contrast meaning decreased fluid to tissue ratio when compared to control eyes (indication of choroidal ischaemia in dry AMD). In nAMD there was an increased boundary enhancement which could be caused by an enhanced blood supply or other causes such as inflammation of microvascular anomalies.	Results confirm a principal correlation of dry AMD and choroidal dysfunction. It is hypothesised that ischaemia, primarily of Sattler's layer of the choroid, exists in nearly all cases of dry AMD. This smooth muscle endothelial dysfunction of the terminal arterioles would reduce the production of nitric oxide (a messenger molecule produced by the endothelium) leading to dysfunction. Alternatively the arteriolar damage may be caused by parasympathetic neuronal deterioration leading to reduced perfusion of the extracellular region surrounding the RPE.	Author speculates that pharmaceutical agents such as sildenafil, tadalafil and niacin could aid with increased choroidal perfusion and delay AMD pathogenesis.
Morphometric analysis of Bruch's membrane, the choriocapillaris, and the choroid	120 eye in total. 25 eyes with advanced AMD. 95 controls.	Histological analysis. After fixation in formaldehyde a horizontal tissue block of the ONH and macular was	The changes relating to normal ageing were recorded as: An increase in Bruch's membrane from 2.0µm to 4.7µm on average. A decrease of choriocapillaris from 0.75 (1st decade)	Results indicate that capillary density diminished in a linear fashion with increasing age. The reason for this is unknown. In eyes with AMD the decrease in capillary density and diameter was	

in aging (Ramrattan et al., 1994).		dehydrated and embedded in paraffin. 7µm thick sections were then stained for light microscopy analysis. Measurements included thickness of Bruch's membrane, lumen diameter and choroidal thickness at the fovea.	to 0.41 (10^{th} decade). A decrease in choriocapillaris diameter from 9.8µm (1^{st} decade) to 6.5µm (10^{th} decade). With regards to normal and pathological macular differences: The thickness of Bruch's membrane did not significantly differ from normal in areas of basal laminar deposit or GA. It was however thinner in areas of disciform scarring. Choriocapillaris diameter was significantly decreased in areas of GA and disciform scarring.	significantly larger than comparable normal counterparts. The presence of basal laminar deposits, GA or disciform scarring is associated with a reduction of choriocapillary density most likely by induced hypoxia derived from interference with diffusion across the RPE – PR complex. Results suggest that the choriocapillaris diameter is not related to the thickness of Bruch's membrane hence an alternate theory based on increased weight of Bruch's applying pressure onto the vasculature below can be dispelled.	
Histologic and morphometric analysis of the choroid, Bruch's membrane, and the retinal pigment epithelium in post-mortem eyes with age-related macular degeneration and histologic examination of surgically excised choroidal neovascular membranes (Spraul et al., 1999)	80 eyes in total. 19 eyes with dry AMD. 21 eyes with nAMD. 40 controls.	Histological analysis. Eyes were opened horizontally and examined via the use of a dissection microscope in order to diagnose as dry AMD, nAMD or control. The ONH and macular were removed, dehydrated in ethyl alcohol and 5µm thick sections were stained with acid-schiff before being slide mounted. The presence and severity of basal laminar deposit (BLD) was assessed alongside the number and type of drusen, thickness of the RPE, Bruch's membrane and the choroid. The density and diameter of capillaries and choroid vessels was also noted. As a secondary investigation the same procedure and	The density of large choroidal vessels was significantly reduced in both the nAMD (13.6 vessels mm^{-1}) and dry AMD (3.5 vessels mm^{-1}) when compared to controls (0.51 vessels mm^{-1}) however this was only significant for veins ($P<0.001$). Choriocapillary density was increased in the AMD groups: nAMD (0.61), dry AMD (0.63) in comparison to controls (0.51). A significant difference was found between the AMD and control group regarding the amount of BLD present. No such difference was found between AMD groups. The difference in drusen found (in terms of the percentage of eyes within each group was as follows: Hard drusen: nAMD (73%), dry AMD (77%), controls (57%).	The presence of AMD in any form results in increased BLD. Excess BLD is likely to disrupt the fragile balance of RPE derived factors required for healthy vasculature maintenance by hindering diffusion across Bruch's membrane. Results with regards to thickness correlate with Ramrattan et al. (1994). The result suggests that deposition of BLD within Bruch's membrane does not cause a significant change in its thickness. Choriocapillary findings differ to Ramrattan et al. (1994) however the choriocapillary characteristics measured in this study were in the majority from eyes at less advanced stages of AMD. As a result it has been determined that in early AMD the choriocapillaris appear to be relatively unchanged.	BLD is a material composed mostly of wide spaced collagen embedded in a granular matrix associated with membrane bound structures and fibronectin. It may be produced by damaged RPE cells. Read pg 529 for more information on pathogenesis theory.

		measurements were applied to surgically removed CNVM's.	Soft drusen: nAMD (64%), dryAMD (62%), controls (3%). More Bruch's membrane breakages were documented in nAMD than dry AMD or control groups. No difference in RPE thickness was found between the groups.	Soft, diffuse and large drusen alongside BLD are associated with development of AMD. Calcification and fragmentation of Bruch's membrane appears synonymous with nAMD development.	
Increased scleral rigidity and age-related macular degeneration (Friedman et al., 1989).	58 eyes in total. 29 patients with AMD most of which had either a disciform scar or drusen and pigmentary changes. 50 age-matched controls.	Contact Tonometry. Goldmann, Perkins (to verify Goldmann reading) and Schiotz tonometry performed on each participant. Initially an ultrasound A-scan was performed in order to determine axial length and fundus photos were taken to grade the AMD. Scleral rigidity was estimated using a Friedenwald nonogram[2] by graphically plotting the applanation IOP.	IOP in those with AMD was slightly lower on average than controls (not significant). Schiotz scale readings were lower in those with AMD when compared to controls and when paired with IOP readings the combination resulted in the difference of scleral rigidity (of both eyes) between the 2 groups being statistically significant (RE: P=0.0003, LE: P=0.009). Mean standard deviation of Perkins was: AMD (RE: 0.023, LE: 0.024). Mean standard deviation of Scleral rigidity was: AMD (RE: 0.018, LE: 0.020).	The author proposes that in AMD the blood flow within the intra-scleral portion of the vortex veins is compromised (Friedman et al., 1977) resulting in increased scleral rigidity.	Diagram available within the journal regarding proposed pathogenesis of AMD as speculated by Friedman et al. (1989).
Ocular rigidity in patients with age-related macular degeneration (Pallikaris et al., 2006).	76 eyes in total One eye of 32 participants with AMD (16 nAMD and 16 dry AMD). Mean age 69yrs. 44 age-matched control participants. Mean age 65yrs. Any pathology known to interfere with	Ocular rigidity measurement. An ocular rigidity measurement device was used to measure the pressure-volume relation and the ocular rigidity coefficient of each participant whilst undergoing cataract extraction. 200µl of salt solution was injected through the limbus into the anterior chamber in 4.5µl steps whilst the subsequent IOP rise was measured in intervals up to 30mmHg.	A rigidity coefficient was calculated as the slope of the pressure versus volume of salt solution curve (pressure range of 10-30mmHg). No statistically significant difference in ocular rigidity was found between those with and those without AMD (when both nAMD and dry AMD groups are merged). Rigidity coefficient: AMD: $0.0142\mu l^{-1}$. Control: $0.0125\mu l^{-1}$. P=0.255.	The findings indicate increased scleral rigidity in nAMD only. This has the potential to hamper vortex vein flow leading to increased choriocapillary resistance and induced hypoxia. Another possible cause of AMD development is speculated to initiate with RPE damage. The author states that the study is limited by the fact that participants had undergone photodynamic therapy prior to cataract extraction.	Results do not correlate with Friedman et al. (1989) as no sig difference was found between AMD and control participants. Difference likely due to study design i.e. Friedman et al. (1989) using a non-invasive method of scleral rigidity measurement. Also Friedman et al. (1989) used a cohort likely to be over-representing those with nAMD as opposed to dry AMD.

	aqueous drainage was ineligible.		The average ocular rigidity measurements were significantly higher in nAMD participants than controls (P=0.014) and in nAMD than those with dry AMD (P=0.004).	This has the potential to influence ocular rigidity measurements.	
Deep retinal vascular anomalous complexes in advanced age-related macular degeneration (Hartnett et al., 1996).	24 eyes in total. 14 with a retinal vascular anomalous complex (RVAC) : 11 participants were characterised as having a RVAC (mean age 79yrs). 3 additional patients developed a RVAC over the course of research and were subsequently included. Of the 14 with a RVAC, 13 also had a PED and 8 had an intra-retinal haemorrhage.. 10 age-matched participants with PED and CNV but no RVAC.	Cross sectional retrospective study using fluorescein angiography (FFA). Patients were selected from a computer search of records. Their FFAs were reviewed in order to determine the presence of a retinal vascular anomalous complex (RVAC) via secondary filling after the choroidal arterioles. RVACs were identified by the evidence of at least 1 dipping retinal arteriole into a deep vascular complex or at least 1 arteriole descending into a deep retinal space to a vascular communication.	PEDs that developed were similar in size and position to areas of drusen. ICG displayed a delay in choroidal filling adjacent to areas of drusen. Intraretinal haemorrhages, microaneurysms or telangiectatic vessels were found in 12 eyes, 11 of which had a RVAC. 3 of the 14 participants had either cardiovascular disease or hypertension and 2 had NIDDM (without signs of diabetic retinopathy).	Findings suggest evidence of disease at the RPE-Bruch's membrane level consistent with the emergence of a hypoxic environment via the accumulation of drusen. This is suggested as the precursor to RVAC development (and the following CNV as seen in nAMD). Results point towards an early alteration in the macular retinal vasculature in which the RVAC is likely to be a latter result. The presence of a PED may provide an additional hypoxic challenge by further removing the choroidal circulation from the outer retina.	An RVAC is an anomalous leaking vascular structure, found in the deeper retina (which is normally devoid of vessels). It is fed by 1 or more retinal arterioles. Media opacities, small pupils and IOLs in the elderly cohort made viewing of some RVACs difficult.
Refractive error and choroidal perfusion characteristics in patients with choroidal neovascularisation and age-related macular degeneration (Böker et al., 1993)	106 eyes in total. 186 study eyes who had CNV secondary to AMD (mean age 71yrs) were collected of which 80 were removed due to lack of (or poor quality) fluorescein angiograms.	Fluorescein angiography used to confirm presence of CNV membrane and reviewed for the determination of choroidal perfusion characteristics (classified as prolonged fluorescence during the transit phase). Refractive error was taken to be the spherical equivalent of the last refraction value that had been obtained prior to the	The risk for development of CNV increased with an increasing degree of hyperopia. Results show that an eye with a refractive error of +3.00-4.00D is 6.2 times more likely to develop nAMD than an emmetropic eye. Eyes within the +3.00D-+4.00D subgroup were found to be at most risk for nAMD development when compared to others (refraction range from +6.00 to -6.00D).	Results suggest that the hyperopic eye has a statistically significantly increased risk of developing AMD. As the sclera ages it becomes increasingly rigid, this has the potential to compromise the choroidal circulation by obstructing venous outflow. An obstruction of the choroidal veins will lead to an increase in choroidal vascular pressure which could ultimately contribute to CNV formation.	The finding is supported further by the fact that the prevalence of hyperopia recorded during the study was likely to have been a low estimate (due to nuclear cataract induced myopic shifting of the cohort). Those ineligible included: dry AMD, degenerative myopia, angioid streaks

	90 participants had unilateral CNV, the remaining had bilateral CNV. Healthy controls used (no number specified) from a general German population based study.	participants symptoms relating to AMD (as nAMD is likely to cause a hyperopic shift).	Myopic refractive error had little impact on the relative risk of developing CNV. Participants afflicted with bilateral nAMD tended to be older (mean age 73.1yrs) than those with unilateral CNV (mean age 70.9yrs. This was statistically significant, P=0.027). Abnormal choroidal perfusion was identified in 66.4% of angiograms reviewed.	This theory is supported by increased age in the bilateral nAMD participants. In hyperopic, shorter eyes the effects of scleral stiffening combined with a slightly thicker sclera lead to increased venous outflow obstruction when compared to myopic and emmetropic eyes. Delayed filling of choroidal vessels probably indicates a change in blood flow. This may manifest secondary to Bruch's membrane thickening and the appearance of drusen.	Uses good diagram of possible pathogenesis by Friedman et al., 1987.
Choroidal filling in age-related macular degeneration: indocyanine green angiographic findings (Giovannini et al., 1994).	177 eyes in total. 103 with nAMD. 42 with dry AMD (mean age >70yrs). 32 age-matched controls. 2 observers used for grading and analysis.	Indocyanine green videoangiography used (alongside FFA to aid diagnosis) VDU based software applied to analyse data and increase the definition of each image obtained. The earliest part of the angiography (the choroidal blush) was used to evaluate filling. A lack of a 'blush' at the centre of the macular during filling is indicative of poor perfusion within this area.	A statistically significant difference with regards to delayed choroidal filling was observed between those with and without AMD (P<0.005): In 59% of AMD participants delayed choroidal filling was observed. In 23% of control participants delayed choroidal filling was observed. 71% of CNVs seen were present at WZs. 52% of CNVs grew inside or at the margin of areas displaying delayed filling.	Results suggest a relationship between delayed choroidal filling and the presence of AMD. There was no significant difference between the filling pattern of those with classic and occult CNV hence a filling pattern alone cannot be used to determine the proposed AMD subtype that may develop. Results further underline correspondence between CNV development and WZs. This emphasised inadequate choroidal circulation in those with nAMD. Delayed filling sites are likely to represent areas of ischaemia and could be target by laser therapy to delay AMD progression.	Author states that ICG is a more accurate tool to assess choroidal filling that FFA. Using FFA it was difficult to differentiate between delayed filling due to blockage of fluorescence by deposits within Bruch's membrane. ICG uses infra-red investigation hence can better penetrate the barrier posed by Bruch's membrane.
Choroidal blood flow and progression of age-related macular degeneration in	82 eyes in total. 41 participants with unilateral nAMD were enrolled. Their fellow	Laser Doppler flowmetry (785nm beam) and laser interferometry used in this observational longitudinal study.	Of 37 participants 17 developed CNV over the course of the study and 20 did not. Lower choroidal blood flow (P=0.0071), higher AMD grade and lower PA	Analysis showed that blood flow and PA are risk factors for the development of CNV. This suggests that a lower choroidal perfusion is a risk factor for development of nAMD	This study used 2 independent methods of assessing blood flow. Metelitsina et al. (2008) only

the fellow eye in patients with unilateral choroidal neovascularisation (Boltz et al., 2010).	eyes (the study eye) were used as controls. 37 participants completed the study. 6 of which had systemic hypertension, 8 of which were current smokers and 9 of which were past smokers). Study eyes were graded according to the 'Age-related maculopathy staging system' based on fundus photos. Participants were excluded if they had diabetes, glaucoma or lens opacification of a degree that affected blood flow measurements.	FFA was used to confirm the absence of CNV in the non-exudative eye. Study ran over 3 years. Each participant underwent a screening visit (to check for eligibility) and a maximum of 7 study visits (where blood pressure, pulse rate, blood flow, blood volume, PA and contact IOP measurements were taken).	(P=0.0068) had statistically significant influences on the development of CNV. Also it was suggested that the more advanced the nAMD in the study eye was in direct relation to the risk of CNV development in the fellow eye. Systemic blood pressure and IOP showed no significant correlation with CNV development.	in the fellow eye of participants with unilateral CNV. A higher grading of CNV also correlates with a risk of development of CNV in the fellow eye. Author notes that a comparable study by Metelitsina et al. (2008) had a wide inclusion criteria (typically ophthalmic features of AMD and no signs of CNV) hence the proportion of eyes that developed AMD in their study was much smaller. Follow-up times were also more variable hence Metelitsina et al. (2008) observed a small increase in hemodynamic parameters over time in those eyes in which CNV did not develop (whereas a continuous decline has been suggested by this study, possibly due to the smaller number of participants who did not develop CNV).	used laser Doppler flowmetry which is susceptible to scattering properties of the tissue in question and also the media (laser interferometry can aid in overcoming this).
Retinal haemodynamics in patients with age-related macular degeneration (Sato et al., 2006).	33 eyes in total. 25 participants with AMD (all sub types graded via the AREDS scale). 9 age-matched controls. All participants underwent an ophthalmic examination (IOP, VA and a health-check) at screening.	Laser Doppler flowmetry used to measure vessel diameter, velocity and flow in the major temporal retinal arteries. A red 675nm beam was used to determine the velocity. 50 measurements were recorded per second for 2 seconds. The pulsatility ratio (PR), pulsatility index (PI) and resistivity index (RI) were calculated from velocity traces.	Values of PR (7.7), PI (1.8) and RI (0.84) were significantly higher in AMD participants than in controls (4.2, 1.4 and 0.75 respectively). There was no significant difference found in the mean velocity, diameter or flow between all levels of AMD and the controls. Mean velocity in mm/s was: 31.9 in controls, 34.5 in early, AMD and 29.5 in nAMD. Diameter in µm was: 106 in controls, 110 in early AMD and 120 in nAMD.	Typically an increased PR, PI and RI are an indication of increased vascular resistance to flow and/or decreased vascular compliance (in which case flow would also be reduced, which was not found in this study). These results point towards a more generalised circulatory abnormality proximal to the eye, specifically it is likely that participants with AMD have a stiffer, less compliant arterial vasculature leading to the eye (and that the loss of compliance of these larger blood vessels is due to age-	

	Those with additional ocular disease or a history of ocular operation were excluded.		Flow in µl/min was: 8.4 in controls, 10.7 in early AMD, and 10.2 in nAMD.	related degenerative changes in collagen and elastin). Results indicate that AMD and cardiovascular disease share the same modifiable risk factors. Treatments aimed at preventing systemic arterial rigidity may also slow or prevent the onset of AMD.	
Functional loss in age-related Bruch's membrane change with choroidal perfusion defect (Chen et al., 1992).	14 eyes in total. 8 eyes of 8 participants identified as having delayed choroidal filling from FFA. 6 controls with visible drusen but no vascular abnormality. The fundus appearance, visual acuity and age range (mean 63-64yrs) was similar in all participants.	Fluorescein angiography was used to identify the presence prolonged choroidal filling phase. Dark adapted static perimetry was performed on 8 eyes with prolonged choroidal filling and 6 eyes with a similar number of drusen but no manifest choroidal perfusion abnormality. Each participant was dark adapted for 45 minutes. Scotopic threshold was measured using a Humphrey automated perimeter (central 30-2 programme with background illumination off and a size V blue stimulus presented) and using fine matrix mapping (a VDU based threshold test).	In eyes without delayed perfusion no discrete areas of increased threshold were found. In contrast, 7 of the 8 eyes with delayed filling displayed discrete areas of scotopic threshold elevation (up to 3.4 log units). These areas corresponded to regions of perfusion abnormality. On fine matrix mapping, eyes with normal choroidal filling had a mean scotopic threshold above normal of 0.7 log units (7dB) beyond 5° from fixation. Eyes with choroidal perfusion abnormality showed a mean background threshold above normal of 1.0 log unit (10dB). 7 of these 8 eyes also had discrete areas of scotopic threshold elevation above normal of 1.8 (18dB) to 3.4 log units (34dB). The area of depressed sensitivity always corresponded with the area of slow choroidal filling when fine matrix mapping and FFA results were compared.	Eyes with the angiographic sign of slow choroidal filling have a higher threshold than eyes with normal choroidal filling. These participants had a similar fundus appearance and VA to the controls however reported more readily the need for increased light intensity for reading and slow recovery of vision after exposure to bright light. The results suggest that a more diffuse pigment epithelial or retinal dysfunction must be present either as a result of, or as a precursor to the accumulation of deposits within Bruch's membrane. It is suggested that the drusen might account for both the perfusion abnormality and functional loss by acting as a diffusion barrier between the RPE and choroid.	Small number of participants in this study.
Choroidal perfusion abnormality with age-related Bruch's membrane change	100 eyes in total. 115 participants (all >60yrs age) were recruited of which 100 met the eligibility criteria of drusen in both eyes or unilateral	Fluorescein angiography (FA) was used to analyse the presence of delayed choroidal filling. Filling was deemed abnormal if there was seen to be a continuous area of prolonged,	26 of the 100 eyes displayed a prolonged choroidal filling phase (PCFP), the other 74 were classified as having normal circulation characteristics. There was no statistically significant difference in age or sex of both groups.	Results suggest that angiographic appearance of the choroidal perfusion is modified in some AMD participants. The angiographic appearance cannot be assumed to imply a perfusion deficit alone as this may	Author explains FA dye can adhere to deposited molecules within Bruch's membrane which slows the speed of its diffusion and gives a false impression of delayed filling.

(Pauleikhoff et al., 1990).	nAMD/PED and drusen in the fellow eye.	patchy choroidal fluorescence in the transit phase of the FA extending over at least 5 disc diameters. Fundus photos were collected in order to analyse drusen characteristics (within 1600µm of the fovea, classified by number and density).	Eyes with a PCFP tended to have few drusen of less density in the macular area when compared to those without a choroidal defect (65.4% of eyes with a PCFP had >20 drusen centrally in comparison to 81.1% of eyes without a PCFP also 0% of eyes with a PCFP had confluent drusen in comparison to 31.1% of eyes without a PCFP). No significant difference was found in size/fluorescence or density/number of drusen in the peripheral retina.	be caused by accumulated deposits in Bruch's membrane. It can only be speculated as which clinical sign if causative of AMD pathogenesis (reduced perfusion or increased Bruch's thickness).	
Foveolar choroidal circulation and choroidal neovascularization in age-related macular degeneration (Metelitsina et al., 2008).	193 eyes in total. 135 participants with dry AMD of any grade (none of which displayed CNV at the time of enrolment) were recruited. Mean age was 70yrs. Longitudinal, prospective study in which participants were reviewed at various intervals: 101 were reviewed at 1yr, 89 at 2 years, 87 at 3 years, 59 at 4 years and 27 at 5 years. Participants were screened for other ocular diseases before being enrolled into the study.	Laser Doppler flowmetry was used to determine foveolar choroidal blood velocity, volume and flow. A 670nm diode laser beam of intensity 20mW was used to obtain blood flow readings. All measurements, including fundus photography, IOP and blood pressure were taken at baseline and follow-up visits.	CNV developed in 28 of 18 participants eyes during the course of the study. Baseline measurements of mean foveolar volume and flow in those who developed CNV were 24% (P<0.0001) and 20% (P=0.0007) lower than that observed in the 165 eyes in which CNV did not develop. There was no statistically significant difference in velocity of these groups. In the eyes that developed CNV foveolar volume and flow decreased annually on average by 9.6% and 11.5% before the formation of CNV, whereas in the eyes that did not, they increased by 6.7% (P=0.006) and 2.8% (P=0.004). In eyes in which CNV developed perfusion pressure (P=0.04) and drusen size (P=0.004) were increased when compared to those who did not develop CNV. Eyes with lower baseline flow were found to be more likely to show visual loss of 3 or more lines when compared to eyes with a higher baseline flow (P=0.005).	The results suggest that decreases in the choroidal circulation (particularly foveolar volume and flow) precede the development of CNV. The results strongly suggest that ischaemia has a role in the pathogenesis of AMD. The study suggests that a decrease in the delivery and diffusion of oxygen or metabolites may have a role (or be a causative factor) in the formation of CNV by triggering the formation of hypoxia-inducible genes i.e. VEGF.	Study results agree with those of: Mori et al., 2001; Chen et al., 2001 ; Üretmen et al., 2003 ; Rigas et al., 2004.

Color Doppler imaging discloses reduced ocular blood flow velocities in non-exudative age-related macular degeneration (Ciulla et al., 1999).	50 eyes in total. 25 participants with dry AMD (mean age 73yrs) were compared to 25 age-matched control subjects (Mean age 70.2yrs). Participants were eligible if they displayed: soft drusen >63µm, hyper/hypopigmentation of the RPE or GA. Anyone with signs of nAMD were excluded from this study. Participants were also excluded if they showed a history of diabetes, ophthalmic artery/venous occlusion, additional ocular disease or hypertensive retinopathy	Colour Doppler imaging was used to measure peak systolic and end-diastolic velocity in the ophthalmic, central retinal and nasal/temporal posterior ciliary arteries. A resistivity index (RI) was calculated from the peak systolic and end-diastolic velocity. Participants initially underwent tests to identify BCVA (logMAR), IOP (Goldmann) and FFA (in order to ensure no nAMD).	All velocities are recorded in cm/s. Cut-off for P was 0.0125. Nasal posterior ciliary artery results: mean end-diastolic velocity 1.45 with AMD and 1.95 in controls (25% decrease with AMD. P=0.0012, highly significant). Peak systolic velocity 6.02 with AMD and 7.34 in controls (18% decrease with AMD. P=0.00175 nearly significant). The resistivity index showed no significant difference. Temporal posterior ciliary artery results: mean end-diastolic velocity 1.54 with AMD and 1.88 in controls (18% decrease with AMD. P=0.0160 nearly significant). Peak systolic velocity 6.47 with AMD and 7.07 in controls (P=0.1733 not significant). The resistivity index showed no significant difference. Central retinal artery results: mean end-diastolic velocity 1.37 with AMD and 1.95 in controls. No significant difference in peak systolic velocity recorded. The resistivity index was 0.83 with AMD and 0.76 in controls (P=0.0007). No correlation was found between BCVA and velocity or area of RPE mottle/drusen and velocity however these measurements are of 'bulk' choroidal flow and not specifically the macular region. No differences were found between the groups for the ophthalmic artery. There was no statistically significant difference in age, BCVA or IOP of the subjects from both groups.	Results suggest that there are retrobulbar vascular changes (decreases in flow velocity), particularly in the nasal and temporal posterior ciliary arteries in the presence of AMD. In the posterior ciliary arteries (which supply the choroid) it was found that participants with AMD displayed a trend towards lower peak systolic and end-diastolic velocity. The findings of the central retinal artery may point to a secondary autoregulatory response in which retinal perfusion decreases in this vessel due to the decreased metabolic requirements (caused by RPE atrophy) during AMD. Classic pathogenesis theory quoted: Ageing of RPE causes accumulation of metabolic debris which leads to progressive engorgement of the RPE cells and to drusen formation. This in turn leads to dysfunction of the RPE which causes choroidal vasculature decline due to loss of angiographic factors.	Alternate theory proposed: Scleral thickening and stiffening via the deposition of lipid with age causes impaired choroidal perfusion which in turn adversely affects the metabolic transport function of the RPE. Finding with regards to RI do not correlate to Friedman et al., 1997. Differences may be due to the broader eligibility criteria used (both dry and nAMD).

Choroidal perfusion perturbations in non-neovascular age related macular degeneration (Ciulla et al., 2001).	21 AMD and 21 controls. AMD patients: Over 50yrs with soft drusen >63 microns, hyper/hypopigmentation or GA in fellow eye. nAMD in study eye. Controls: No AMD, diab ret, ocular pathology.	ICG angiography. Images processed in 6 locations including and around macular. Area dilution analysis: Speed of which ICG enters choroidal vasculature measured via plotting dilation curves.	No difference in perfusion characteristics in controls. Speed of 10% filling time was longer in AMD Px's than in normals for 4 perifoveal regions. Speed of 63% filling time was longer in AMD Px's than in normals for 4 perifoveal regions (this remained significant when other 2 peripapillary regions also included in analysis).	Subjects with AMD showed significant delays and heterogeneity of filling within perifoveal region when compared to age-matched controls. This indicates changed relating to vasculature in AMD show preferential involvement of perifoveal choroid.	
Subretinal neovascular membranes associated with choroidal non-perfusion and retinal ischemia (Melrose et al., 1987).	1 eye described in detail throughout the paper. Case document of a 75yr old woman suffering from systemic hypertension, arthritis and confluent drusen (without the appearance of subretinal haemorrhage) in her RE. Her left macular was scarred from previous nAMD.	Fluorescein angiography was used for assessment following hospital based diagnosis of the patient (based on symptoms of central vision loss and ophthalmologist evaluation).	Angiography displayed a normal choroidal and retinal filling pattern except for marked choroidal non-perfusion in the foveal region (which appeared early and persisted through all stages of the angiogram). The eye was treated with krypton-laser-photocoagulation in order to try and prevent disciform scarring.	Results indicate poor foveolar choroidal perfusion in association with nAMD. It is speculated that the cause may be linked to occlusion of the short posterior arteries secondary to spasm, oedema or direct injury. The case is consistent with studies showing a higher incidence of CNV in the fellow eye of patients with a history of nAMD. The author also speculates that the patient's light complexion and blue irides were also in agreement with studies suggesting caucasians are at a high risk of AMD development.	Documented in the style of a case-report hence minimal detail provided. First documented evidence of localised choroidal non-perfusion and associated CNV. In final paragraph the author indicates that 200 AMD cases have been reviewed. No numbers are provided with regards to results however.
A fluorescein and indocyanine green angiographic study of choriocapillaries in age-related macular disease (Pauleikhoff et al., 1999).	100 eyes in total. 12 Participants had early AMD only (classified by bilateral soft drusen). 88 participants had early AMD and nAMD in their fellow eye.	Fluorescein angiography was used to identify a distinct area of slow and patchy choroidal hypofluorescence during the early phase. Indocyanine green video-angiography (ICG) was used to identify a distinct area of reduced diffuse background	During early AMD a prolonged choroidal filling phase (PCFP) was observed in 26% of eyes using FFA and 32% of eyes using ICG. The predominant ocular characteristic associated with PCFP was the presence of localised areas of RPE atrophy. This was found in 28% of eyes with PCFP and only 6% without PCFP (P=0.005).	A PCFP can be interpreted as a sign of reduced choroidal perfusion in AMD. A change in the diffusional characteristics of Bruch's membrane is the speculated cause. Subsequently a PCFP can be used as a risk factor for GA development. To what extent PCFP contributes toward loss of VA due to AMD is unknown, but the sign could be	ICG confirmed as more accurate that FFA with regards to identifying PCFP.

	Mean age of participants was 72.6yrs.	fluorescence during the early phase. Drusen characteristics (number, size, density and fluorescence), BCVA and AMD status of the fellow eye was also documented.	A PCFP was associated with confluent drusen, of which 66% of eyes with PCFP displayed (P=0.01) and RPE atrophy patches (P=0.005) in the study eye. Eyes with PCFP tended to have a higher density of drusen inside 1600μm around the fovea. (P=0.01). There was also an association between PCFP and GA in the fellow eye (P=0.03).	used as a clinical indicator of visual prognosis.	
Foveal electroretinograms and choroidal perfusion characteristics in fellow eyes of patients with unilateral neovascular age-related macular disease (Remulla et al., 1995).	67 eyes in total. 67 patients with unilateral nAMD (age 61-89) recruited from a larger group study investigating prevalence of CNV and ERG implicit times. Exclusion criteria included media opacification significant enough to impact on fundus appearance.	Fluorescein angiogram used to identify delayed choroidal filling (characterised by a non-uniform fluorescence extending over at least 5 disc diameters of the posterior pole persisting through the onset of the venous phase). Foveal ERGs were elicited with a 4° white stimulus flickering at 42Hz presented by a hand held, dual beam stimulator ophthalmoscope. Responses were monitored with a CL electrode and quantified by Fourier analysis with regards to amplitude and implicit time	The mean for foveal cone ERG implicit time was 38.3ms for participants with delayed filling and 37.0ms for those without filling defects (This was statistically significantly. P=0.0167). ERG implicit times averaged 1ms slower (P=0.0167) and were more likely to be delayed (P=0.0078) in eyes with abnormal choroidal perfusion (retained when corrected for age, acuity and drusen extent). 42% of eyes studied displayed a choroidal perfusion defect. Participants with prolonged choroidal perfusion had a tendency to have more extensive macular drusen. ERG implicit time was positively correlated to the extent of macular drusen (which was also almost significantly associated with poor choroidal perfusion).	Prolonged choroidal perfusion was associated with a foveal cone ERG implicit time that was slower or more likely to be delayed. Results suggest the focal ERG can be added to impaired sensitivity in the dark and slowed dark adaptation as an objective measure of retinal malfunction related to AMD. It is hypothesised that the angiographic finding in participants with AMD is reflective of outer retinal ischaemia, resulting in foveal cone ERGs of normal amplitude but delayed implicit time.	
Occlusion of the posterior ciliary artery. I. Effects on choroidal circulation (Hayreh and Baines, 1972).	85 eyes in total. In-vivo 85 rhesus monkey eyes.	Fluorescein angiography (FA) was used in order to assess the macular choroidal circulation following induced arterial occlusion. Lateral orbitotomy was performed in order to gain	During lateral and medial PCA occlusions, the filling of the choroid supplied by the occluded artery was found to be delayed and incomplete. The delayed filling observed was specific to the occluded vessel i.e. neighbouring areas of choroidal vasculature supplied	The results indicate that a reduction in perfusion pressure in an end artery i.e. the PCAs has the potential to leave the macular in a hypoxic state. Any pathology that has the potential to interrupt choroidal blood flow (such as AION	In a corresponding review article (Hayreh. 1990) the author states from other studies that WZs between the choriocapillary lobules are arranged in a honeycomb formation and that WZs exist between

		access to the posterior ciliary arteries (PCAs) which were cauterised (occluded) near the site of entry into the eyeball. The lateral PCA was occluded in 31 eyes. The medial PCA was occluded in 17 eyes and all PCAs were occluded in 37 eyes.	by additional vessels were unaffected by the occlusion. Following PCA occlusion in all cases the retinal circulation remained unaffected No specific details provided or statistical analysis documented.	or senile degeneration) may have a pathogenesis involving ischaemia. Due to the nature of the filling the author speculates about watershed zones (WZs) between each segmental area of delay. The WZs location and number depend on the number of PCAs and short PCAs present and also their anatomical position. Watershed zone (WZ) definition: the border between the territories of distribution of any 2 end arteries (e.g. the nasal and posterior short ciliary arteries).	every aspect of the choroidal vasculature arrangement i.e. the PCAs and the short PCAs. The short PCAs and the choriocapillaries etc.
Changes in the choriocapillaris associated with senile macular degeneration (Kornzweig, 1977).	107 eyes in total. All eyes were attained post mortem. 26 eyes with established AMD, 5 with early AMD and 76 age-matched controls. All measurements were taken with a micrometer.	Histological Analysis. The retina and choroid were removed from the globe and placed in 7.5% buffered formalin solution for fixation. Then both were transferred into 3% trypsin solution and incubated at 38°C for 30mins (in order for the choroid to lose its pigment). The specimen was then placed into a petri dish and the larger choroidal vessels were removed. Bruch's membrane was dried onto a slide and stained with Schiffs (PAS) reagent and counterstained with hematoxylin in order to allow measurement of the finer choroidal vasculature.	Choriocapillary appearance in controls: A visible network of closely packed capillaries separated by inter-capillary septa (a dividing line of tissue). Lumen width ranged from 20-28 microns and septa width from 8-12 microns. Choriocapillary appearance in the presence of AMD: Thickening of the inter-capillary septa was noted (diameters between 20-24 microns were recorded). Narrowing of the lumen was also documented (12-20 microns). There appeared to be loss of cellular content of the capillaries with many lacking nuclei and only being sustained by the thickened septa. Distinct areas of capillary atrophy were observed in 59% of AMD eyes reviewed.	It is suspected that septa thickening and lumen narrowing is likely to have an impact on oxygen availability to the macular. In effect, a condition of hypoxia may develop which can lead to atrophy of the RPE via disrupting the photoreceptor cone cell function. Visible areas of atrophy may also contribute by causing focal hypoxia.	
Relationship between RPE and	11 in total.	Histological analysis	GA patient: Area outside atrophic zone: 92% RPE coverage, 72% vascular area, 13.9µm	Different pathogenesis for dry and nAMD.	Take into consideration the small sample size.

choriocapillaries in Age-related macular degeneration (McLeod et al., 2009).	3 age-matched controls, 5 subjects with GA, 3 subjects with nAMD.	Post-mortem analysis of the choroid. Globes opened at limbus and AC removed, then photographed with a digital microscope camera to assess pigmentary changes in retina (RPE atrophy) and CNV scarring. Choroids then dissected from sclera and assessed for alkaline phosphatase (APase) activity. Overlying pigment bleached with H_2O_2 and monitored daily until underlying CC visible. Photographs then taken and analysed with computer assisted morphometric technique.	capillary diameter (all comparable with controls). At border of atrophic zone: 38.1% RPE coverage, 52.3% vascular area, 10.3µm capillary diameter (all reduced). In atrophic zone: 1.8% RPE coverage, 38.0% vascular area, 7.9µm capillary diameter (all severely reduced). nAMD patient: 1mm peripherally from CNV: 95.9% RPE coverage, 39.6% vascular area, 13.9µm capillary diameter (RPE coverage and capillary diameter comparable with controls, vascular area severely reduced). Linear relationship between loss of RPE and CCs in GA. Linear relationship between loss of RPE and CC diameter in GA. Loss of fenestrations in endothelium of constricted CCs suggesting functional changes.	RPE removal causes CC atrophy likely as CCs require bFGF, VEGF, endothelin-1 and insoluble molecules to maintain endothelial integrity). For dry AMD this correlates with theory of RPE atrophy initiating secondary PR and CC loss (CC either constricts and loses fenestrations or degenerates to atrophy). For wet AMD results correlate with theory of choroidal vascular insufficiency preceding RPE dysfunction. Choroidal blood flow impairment leads to foveal ischaemia and then to neovascularisation in wet AMD.	
Quantifying changes in RPE and choroidal vasculature in eyes with age-related macular degeneration (McLeod et al., 2002).	6 eyes in total. Both eyes of 2 donors with AMD and 1 control donor (aged 70yrs). 1 donor (aged 84yrs) had systemic hypertension and a 10 year history of GA (RE) alongside a disciform scar (LE). Another donor (Age 95yrs) had cardiovascular disease and was registered sight	Histological Analysis. The retina and choroid was dissected from the sclera and incubated in alkaline phosphatase (APase). Pigment was then bleached with 30% H_2O_2 until the underlying vasculature was visible (at which point the tissue was slide-mounted). Computer assisted image and metamorphic analysis was then performed. A photomicroscope was used to take 1x1mm images which were enhanced for definition and clarity.	Regions of GA eyes with complete RPE atrophy demonstrated a substantial loss of choroidal blood vessels (only 42.7% vascular area found at the posterior pole). A 100% loss of RPE in eyes with GA was associated with a 51% mean decrease of vascular density in that area. Capillaries that remained within these regions were found to have constricted lumens (statistically significant $P<0.0001$, no figures provided). Analysis of the disciform scar revealed that underlying new vessels were highly constricted. Control subject results:	The normal ageing changes that occur within the choroid, Bruch's membrane, RPE and photoreceptors become pathologic as a result of AMD related histologic changes. The density of choroidal capillaries decreases considerably with age and substantially more in the presence of AMD. Results indicate that atrophy of RPE is more severe than loss of choriocapillaries. Loss of RPE does not result in complete underlying capillary loss (however surviving capillaries are less functional which	Removal of the retina and choroid from the eyecup may could mechanical loss of RPE. Similarly eyes with extended death-to-enucleation times (>20hrs) may have artificial RPE loss also. The percentage RPE area may be underestimated in the subjects with GA as unhealthy (but still functional RPE) may have no pigment and, therefore, would have been excluded from the analysis.

	impaired due to GA (RE) and advanced dry AMD (LE).		99-100% of RPE intact. 87.2% vascular area at the posterior pole which decreased to 78.9% at equator areas.	has the potential to result in ischaemia).	Results correlate well with Ramrattan et al. (1994).
Effects of hypoxia on retinal pigmented epithelium cells: protection by antioxidants (Castillo et al., 2002).	Cultured RPE cells of bovine origin. Bovine eyes obtained from a local abattoir, placed on ice and transferred to the laboratory for RPE culture within 2hrs. Undefined number of source eyes documented.	In Vitro RPE model. The RPE cells were accessed via resection of the retina. The tissue was then incubated for 45mins at 37°C with collagenase followed by further incubation with trypsin-EDTA. The remaining suspension was concentrated via centrifugation and cultivated for 7-10days before being plated out for analysis. A percentage of healthy RPE cells cultivated were then incubated for 72hrs at 3% O_2 in order to induce hypoxia. Before incubation some cells were introduced to 300µm of vitamin C (VC) or 10m*M* of N-acetylcysteine (NAC) antioxidant. RPE apoptosis was revealed via a Hoechst staining agent.	Hypoxic ATP and normoxic ATP were 1.5 and 2.5µM/25,000 cells respectively ($P<0.001$). Cells treated with antioxidant prior to hypoxia displayed increased ATP availability when compared to cells not treated with VC or NAC. As a result a significantly lower number of apoptotic cells were found when RPE cells were treated with VC or NAC. The induction of apoptosis (nuclear fragmentation) by hypoxia was confirmed by the typical DNA smear on agarose gel electrophoresis.	Incubation of RPE cells under hypoxia induced a reduction of intracellular ATP via the increase of lactate dehydrogenase (LDH). The results indicate that hypoxia can cause cell death of RPE through an oxidative stress-related mechanism. The data suggests that RPE cells suffer apoptosis when normal aging changes are accompanied by hypoxia. The effect of VC and NAC introduction appeared to have a protective function against free radical attack triggered via hypoxia. This is likely to be due to improved protection of mitochondrial membranes.	
Hypothermia reduces secretion of vascular endothelial growth factor by cultured retinal pigment epithelial cells (Coassin et al., 2010).	Cultured RPE cells (unspecified species of origin). The ARPE-19 strain was used.	In Vitro RPE model. RPE cells (ARPE-19 strain) were grown in culture for up to 5 days under normoxic (20% O_2) and hypoxic (1% O_2) conditions at temperatures ranging from 27°C to 40°C. Conditions were achieved using an incubating chamber via which gas could be introduced and temperature modified.	Hypothermia reduced RPE cell metabolism in a temperature dependant fashion. Metabolism was reduced by 31% and 17% at 27°C and 34°C when compared to cells grown at 37°C ($P<0.0001$). Hypothermia also reduced VEGF secretion which was reduced by 38% at 34°C when compared to cells cultured at 37°C ($P<0.0001$). Conversely VEGF secretion was significantly increased by	A hypoxic environment (such as that made possible by AMD pathogenesis) resulted in increased VEGF secretion. Hypothermia decreases both VEGF secretion and cellular metabolism of cultured RPE cells. Temperature manipulation is suggested as a possible treatment of AMD via reducing the energy consumption of the suffering	It is unknown as to whether hypothermia inhibits or promotes the secretory pathways of other growth factors which may influence RPE activity e.g. inflammatory factors (HIF-1). The safety of temperature manipulation has not been investigated long term and would be difficult to achieve in an ocular model. If

		VEGF levels were measured by the enzyme-linked immunosorbent assay (ELISA) and cell metabolic activity was measured by a fluorescent cell metabolic assay.	32% at 40°C when compared to those grown at 37°C (P<0.0001). Hypoxia increased VEGF secretion by 84% at 37°C when compared to cells cultivated under normoxic conditions (P<0.0001). Hypothermia decreased the hypoxia induced VEGF secretion by 30% at 34°C compared to cells grown under hypoxic conditions at 37°C (P<0.0001).	photoreceptors, reducing the metabolic activity of the RPE and as a result minimising VEGF secretion. This could be achieved by cooling the choroidal circulation.	successful chronic reduction of VEGF secretion could result in capillary atrophy.
Role of hypoxia and extracellular matrix-integrin binding in the modulation of angiogenic growth factors secretion by retinal pigmented epithelial cells (Moussa et al., 1999).	Cultured RPE cells of human origin. Undefined number of source eyes documented. 96 samples of RPE cells were cultured in Dulbecco's modified Eagle's medium and demonstrated to be a pure population before manipulation.	In Vitro RPE model. Refer to paper for specific detail on method. RPE cells were transferred into 96 well plates and incubated at room temperature for 60mins in order to set into position. Extra-cellular matrix (ECM) protein was added to all samples of which 48 were subjected to either normoxia (20% O_2) or hypoxia (1% 0_2) within a humidified incubator.	RPE cells maintained under hypoxic conditions showed a time-dependent linear increase in VEGF in their media. There was significantly more VEGF present (2 fold) under hypoxic conditions when compared to normoxic samples (P<0.01). A decrease of FGF2 was also recorded under hypoxic conditions. Under normoxic conditions there was an initial rise in VEGF in the sample which reached a plateau after 24hrs.	Exposing RPE cells to hypoxic conditions results in the up-regulation of VEGF. Thickening of Bruch's membrane is due in part to accumulation of type IV collagen. This could disrupt the adhesion of RPE cells to their basement membrane and contribute to their dysfunction.	Integrins are receptors that mediate the attachment between a cell and its surroundings. Hypoxia increases VEGF mRNA by a combination of upregulation of transcription and increased mRNA stabilization.
Effect of hypoxic stress in RPE cells: Influence of antioxidant treatments (Bellot et al., 2001).	Cultured RPE cells of rabbit origin. Donor eyes were immediately incubated in Dulbecco's modified Eagle's medium following enucleation. Sheets of RPE layer	In Vitro RPE model. The RPE cells were cultured in flasks (of which the purity of cell culture was verified via morphology testing). The cultures were separated and exposed to 1 of 2 oxygen	LDH activity in the culture medium significantly increased when RPE cells were incubated under hypoxic conditions (P<0.05). The intracellular content of ATP (recorded in mmol/25,000 cells) was reduced under hypoxic conditions (0.20) when compared to normoxia (1.30).	Most damage occurred when RPE cells were incubated within ischaemic conditions (hypoxia and glucose deprivation). Hypoxia induces LDH activity and ATP reduction which has the potential to cause apoptosis (as	LDH is an enzyme that aids in the production of energy. Its levels tend to rise in response to cellular damage. Experimentally induced ischaemia has the potential to create oxygen-free

	were removed from the eyecup and incubated in 0.1% trypsine and EDTA solution for 90mins.	levels (21% or 3% O_2). Half the cultures were treated with glucose and half were incubated without glucose (in order to simulate an ischaemic condition). Lactate dehydrogenase (LDH) activity and ATP cell content was used to determine the damage sustained by the RPE cells under each condition. 3 culture subgroups were treated with 1 of 3 antioxidants (thioproline, vitamin C or trolox) prior to hypoxic exposure.	DNA fragmentation of the hypoxic cells was demonstrated using an agarose gel electrophoresis test. Thioproline significantly prevented LDH activity (and ATP reduction) in hypoxic (1.25) and ischaemic cells (1.40) when compared to controls (0.30 and 1.1). Vitamin C did significantly prevented LDH activity and ATP reduction in ischaemic (hypoxia + glucose deprivation) but not purely hypoxic conditions. Trolox had no effect on LDH release or ATP levels under any condition.	demonstrated by the DNA fragmentation). Certain antioxidants appear to have a protective effect upon the RPE however more research is necessary to identify the optimum subtype.	radicals which in turn can induce apoptosis.
Vascular endothelial growth factor-A is a survival factor for retinal neurons and a critical neuroprotectant during the adaptive response to ischemic injury (Nishijima et al., 2007).	Rat animal model. Male pigmented Long-Evans rats used.	In-vivo animal model. Transient ischaemia was induced in the RE by surgical constriction of the optic sheath for 60minutes. VEGF-A isoforms (120 and 164), placental growth factor-1 (PIGF-1) and VEGF-E were administered intravitreally. FA was used to visualise vascular leakage. The eyes were then enucleated so that the VEGF levels could be determined by immunosorbent assay. 3µl of a VEGF neutralising antibody was also injected intravitreally into a sample of rats once per week over 6 weeks.	The number of apoptotic cells peaked at 12 and 24 hours after transient ischaemia (following the reperfusion of the ganglion cell and inner nuclear layer). Few apoptotic cells were found in the outer nuclear layer (due to its blood supply from the choroidal vasculature). Intraocular injection of VEGF-A just after reperfusion reduced apoptosis in the retina (in a dose-dependent manner). At 24 hours after reperfusion the number of apoptotic cells were reduced by 51.2% by the VEGF120 isoform (20pmol, $P<0.01$) when compared to the control group. A 20pmol dose of VEGF164 reduced the number of apoptotic cells by 46.7% ($P<0.01$) 12hrs after ischaemic assault.	VEGF-A has an initial anti-apoptotic effect on vascular endothelial cells under duress. Treatments aiming at reducing VEGF levels may cause secondary damage via eradicating its natural neuro-protective function. Exposure to the two most prevalent VEGF-A isoforms is effective in protecting neuronal cells in both the ganglion cell layer and inner nuclear layer after ischaemic assault. VEGF164 usage was seen to cause vascular leakage however hence the isoform is too potent for use as a neuro-protectant against AMD.	Documented details available on the retinal effect of ischaemia. See page 5 ‘Exogenous VEGF-A reduces long-term ischaemia-induced retinal damage’.

Hypoxic regulation of vascular endothelial growth factor in retinal cells (Aiello et al., 1995)	Cultured RPE cells of bovine origin. Some human donor cells also used.	In Vitro RPE model. All cells were cultured in Dulbecco's modified Eagles medium and exposed for various periods to 0% O_2. Hypoxia was achieved via a VDU controlled incubator RNA expression of VEGF was evaluated using northern blot analysis. Retinal endothelial growth assays (Hoechst-33258 dye) were used to assess the VEGF specific proliferative potential.	In a normoxic state the retinal pericytes, RPE cells and endothelial cells produced low levels of VEGF. Normoxic and hypoxic values were: Retinal pericytes: normoxic (0.1), hypoxic (0.9). RPE cells: normoxic (0.075), hypoxic (0.2). Endothelial cells: normoxic (0.05), hypoxic (0.4) (Units unknown). Retinal endothelial cells expressed less VEGF than RPE cells (P=0.1) and pericytes (P=0.1). VEGF expression was 6.1 and 2.5 fold greater in pericytes than RPE and endothelial cells respectively. VEGF expression was first noted at <10% O_2 and was maximum at <5% O_2 for exposures up to 24hrs. Increased VEGF expression was first recorded after 4hrs and reached a maximum value at 18hrs.	VEGF is a likely candidate for mediating retinal neovascularization (arising from ischaemic ocular disorders). VEGF mRNA expression is stimulated by hypoxia, likely to be pathologically induced by poor blood flow perfusion. Retinal pericytes, endothelial and RPE cells all have the potential to induce VEGF production. The author suggests laser photocoagulation of VEGF neutralising antibodies in order to prevent ocular neovascularization. VEGF levels were reversed in all cells by reinstitution of normoxia and reached a normative level within 24hrs.	
Sustained delivery of a HIF-1 antagonist for ocular neovascularisation (Iwase et al., 2013).	Mouse and rabbit animal model. The experiment used Doxorubicin (DXR) and Daunorubicin (DNR) which inhibit HIF-1 and perturb retinal function as demonstrated by ERG testing. Pathogen free C57BL/6 mice were used and Dutch belted rabbits.	In-vivo animal model. DXR was diluted into a nanoparticle polymer (synthesised by centrifugation). It was then delivered via intraocular injection in order to reduce HIF response and prevent CNV formation. Eyes were analysed at 1, 4, 7 and 14 days after injection. At 14 days the total area of CNV was measured following fluorescein perfusion.	VEGF levels were reduced significantly in those treated with DXR. 10µm DXR administered to mice was found to suppress VEGF formation for 35 days. The same amended dose in rabbits caused 105 days of VEGF suppression). The CNV and retinal NV area was significantly reduced in mice that were administered DXR after 14 days when compared to controls. Laser induced CNV results:	Anti-VEGF shows a benefit in preventing the progression of ocular neovascularization however it doesn't result in regression. Anti-VEGF combined with anti-platelet derived growth factor (PDGF-B) has resulted in regression suggesting that combination treatment shows promise. The author suggests that the suppression of HIF-1 is comparable to a combination therapy as HIF activity is not specific to the transcription of just one protein.	

		CNV was induced in a number of mice via laser-photocoagulation of Bruch's membrane. A number of mice were placed in 75% O_2 7 days after birth and returned to normoxia at day 12 in order to induce retinal neovascularization (NV).	Control area (0.02mm^2), 10mg DXR area (0.005 mm^2). P<0.001. Hypoxia induced retinal NV results: Control area (1.5 mm^2), 1mg DXR area (0.5 mm^2). P<0.001. See paper for full figures (substantial).	The results also confirm a strong role for HIF in AMD pathogenesis. DXR pending results of further testing on concentration may act as a promising treatment or alternative to ranibizumab.	
Geldanamycin, a HSP90 inhibitor, attenuates the hypoxia-induced vascular endothelial growth factor expression in retinal pigment epithelium cells in vitro (Wu et al., 2007).	Cultured RPE cells of human origin. RPE cell line (R-50) was cultivated overnight and distributed into 6 well plates.	In Vitro RPE model. After cultivation the RPE was moved into a hypoxic chamber where it was exposed to 1% O_2 conditions for 48hrs. A cell proliferation assay was used to identify the effect of hypoxia on cell growth. An immunosorbent (ELISA) assay was used to identify VEGF and bFGF release from the RPE. A selection of samples were pre-treated with geldanamycin (GA) 1hr prior to hypoxic exposure.	The cultured RPE cells under hypoxic conditions showed no obvious cell death as seen by morphological observation and cell proliferation assay. The hypoxic environment caused a 3.4 fold increase in the level of VEGF production when compared to original levels. VEGF concentration was documented as 500 and 900pg/ml in the control group in comparison to 900 and 1500pg/ml in the study group (after 24 and 48hrs hypoxic exposure). P<0.05. bFGF levels showed no significant change in levels under hypoxic conditions. Samples pre-treated with GA displayed reduced expression levels of VEGF.	The results indicate that VEGF expression is dependent on HSPs (particularly HSP90). Hypoxia was found to cause an increase in VEGF expression which under the artificial environment may have induced an anti-apoptotic effect. The author speculates that the HSP90 inhibitor (GA) induces reduction of HIF-1α levels and its downstream transcriptional activity (resulting in decreased VEGF expression). Using a HSP90 inhibitor as a clinically therapeutic agent for nAMD may be viable pending on further testing.	The study results conflict with that of Castillo et al. 2002 and Osborne et al. 1997 in which hypoxia induced apoptosis was seen in cultured RPE cells after 72hrs. A longer timescale may have given results that conform and the difference in RPE cell line used could have caused the conflicting results.
Hypoxia/ Reoxygenation induces CTGF and PAI-1 in cultured human retinal pigment epithelium cells (Fuchshofer et al., 2009).	Cultured RPE cells of human origin. The study aimed to investigate how hypoxia/re-oxygenation affects connective tissue growth factor (CTGF), plasminogen activator inhibitor-1 (PAI-1),	Lab based: immunoblot and immunoassay analysis used. Cultured RPE cells were kept in a hypoxic chamber and exposed to 1% O_2 for 12.36hrs before a 24hr reoxygenation period. The expression of various proteins was assessed by	No changes were notable at a microscopic level between the morphology of normoxic and hypoxic cells. Exposure to hypoxia caused a marked increase in the CTGF protein level (2.8 fold increase when compared to controls).	Hypoxia increases the expression of CTGF and PAI-1 at a transcriptional level. This can be prevented via the blockage of HIF-1 activity and reduced via antioxidant usage. The results indicates that the process of hypoxia/re-oxygenation increases pro-fibrinogenic factors and ECM components of RPE cells, leading to speculation that hypoxia	

	collagen type IV and fibronectin.	immunohistochemistry (Northern and Western blot analysis). Actinomycin D was added in order to examine whether hypoxia induced transcription of CTGF to PAI-1. Cells were prevented from HIF-1 activation by the addition of siRNA in a number of samples. Coenzyme Q10 and ascorbic acid (antioxidants) were introduced to a number of samples.	The PAI-1 protein level expression also increased following hypoxic exposure. A 1.7 and 2.5 fold increase was found after 12 and 24hrs. Following re-oxygenation levels of CTGF, PAI-1 and HIF-1 all showed a marked increase when compared to controls. Blocking HIF-1 expression prevented the increase in CTGF and PAI-1 previously observed under hypoxic conditions. The introduction of antioxidants caused a reduction of CTGF and PAI-1 mRNA expression by 2.2 and 1.8 fold in comparison to untreated samples.	may play a role in ECM deposit accumulation (drusen formation) seen during AMD. Increase CTGF expression found in CNV membranes is likely due to hypoxia mediated activation of VEGF and transforming growth factor.	
Concerted inhibition of HIF-1 alpha and-2 alpha expression markedly suppresses angiogenesis in cultured RPE cells (Nakajima et al., 2013)	Cultured RPE cells of human origin.	Lab based: immunoblot and immunoassay analysis used. Human ARPE-19 cells were cultured and introduced to hypoxia via the usage of an AnaeroPack chemical (0.1% O_2). Cell damage was quantified by measuring levels of LDH (an indicator of cell death and membrane breakage). A LDH cytotoxicity detection kit was utilised. VEGF activity was also detected using an immunoassay. HIF protein was identified using immunoblotting.	Hypoxia caused HIF-1α increase until the 24hr stage and HIF-2α increase until the 36hr stage. In correlation with HIF stabilization VEGF levels were also raised (After 24hrs hypoxic exposure levels were significantly raised when compared to controls). VEGF mRNA was inhibited by nearly 50% when HIF-1α activity was blocked using si-RNA. VEGF levels were not affected by the blocking of HIF-2α. However a combination block of both HIF-1α and HIF-2α gave the largest reduction in VEGF levels. VEGF release levels (in pg/VEGF/ml.medium): after 24hrs normoxia (250), hypoxia (500) and after 48hrs normoxia (600), hypoxia (1900).	The increased level of HIF isoforms during hypoxia is likely to be due to inhibition of O_2 dependent proteasomal degradation. Increased HIF-1α stabilisation induces increased VEGF transcription. Both HIF isoforms seem to be important in the upregulation of angiogenic factors during hypoxia. Inhibition of HIF-1α alone or a combination HIF inhibition may have the potential to be useful in targeted therapy however HIF is an important inducer of protein autophagy and RPE clearance hence this method would have to be approached with caution.	The author states that HIF-1 is the 'master switch' for control of cellular responses in hypoxia. HIF-1 isoforms are short lived under physiological conditions due to their hydroxylation by HIF prolylase. In hypoxia HIF isoforms stabilise and mediate angiogenesis or cell proliferation/survival processes.
Expression of hypoxia-inducible factor -1 alpha and -2 alpha in human	6 eyes in total. 6 eyes of 6 nAMD participants (aged 65-86yrs) were assessed	Lab based: immunoassay analysis used. This was not a post-mortem study. Each participant	HIF-1α and/or HIF-2α were detected in 5 of 6 CNVM's analysed. Half of the total endothelial cells and all macrophages (located in the stroma) were found to have both HIF isoforms.	The results suggest that HIF-1α and/or HIF-2α play a role in VEGF up-regulation and CNVM formation under hypoxic conditions.	HIF is a transcription factor that activates the expression of pro-angiogenic gene VEGF in response to hypoxia.

choroidal neovascular membranes (Inoue et al., 2007).	for the expression of HIF isoforms within their CNVM's.	underwent ocular surgery (submacular) in order to allow the CNVM to be obtained following its classification using FA. Once obtained the CNVM was tested for HIF presence (unspecified specifics of assay).		HIF was not detected within RPE cells raising the suspicion that another mechanism causes VEGF up-regulation at this location.	
Expression of hypoxia-inducible factor -1 alpha and -2 alpha in human choroidal neovascular membranes associated with age-related macular degeneration (Sheridan et al., 2009).	12 surgically excised subfoveal CNVM's used. The CNVM's were obtained from 9 participants with AMD and 3 with punctate inner choroidopathy (PIC). 26 control participants were also recruited.	Lab based: histological and immunoassay analysis used. . Specimens were fixed with formalin and embedded in wax. 5mm sections were then cut, mounted on slides, de-waxed and stained for histological (with haematoxylin and eosin) or immunohistochemical analysis.	HIF-1α was detected in 7 of 12 specimens (5 AMD and 2 PIC). HIF-2α was detected in 8 of 12 specimens (8 AMD). Within the outer retina of CNVM (containing capillaries and endothelial cells) both isoforms of HIF were found in 10 of 12 specimens. Within the inner retina (containing RPE and macrophages) both isoforms of HIF were found in 5 of 10 specimens. HIF-1α was less than HIF-2α expression. The presence of at least one HIF isoform was found in 10 of 12 CNVM's caused by AMD. HIF-1α was found in the RPE of 55% of samples. The presence of VEGF was found in all 12 samples and tended to be co-localised with HIF.	The results suggest that the central RPE cells are exposed to hypoxic insult during AMD pathogenesis. Blocking HIF activity has a potential therapeutic use however may lead to impaired wound healing. Also this action does not impact on the underlying disease pathway and hence will not resolve the disease activity (and promote a sustained hypoxic environment via preventing new vessel growth). The results confirm that hypoxia induces the expression of pro-angiogenic factors through the HIF transcriptional complex and that both HIF isoforms appear to have the ability to transcribe VEGF. Expression of HIF in RPE cells suggests that at some stage during AMD pathogenesis the RPE is hypoxic. Less long term hypoxia (due to the acute nature) of PIC onset may result in reduced HIF-2α. AMD pathogenesis seems more chronic in progression when compared hence HIF levels differ. Also fewer PIC samples were collected hence the results are less reliable.	Morphological analysis displayed that study and control eyes had a similar and distinctive cellular distribution consisting of a relatively avascular, fibrous stromal core to the CNVM and a peripheral zone rich in cells. Outside of this RPE degenerates and macrophages were found scattered throughout the tissue neighboured by capillaries and endothelial cells. This result differs from others as both HIF isoforms were found in-situ, not just HIF-1α only which has been documented in cultured RPE cells. The author states that the fact that anti VEGF injections are required to be repeated may indicate that the underlying hypoxic signal behind AMD pathogenesis remains present.

Retinal oxygen metabolism in exudative age-related macular degeneration (Geirsdottir et al., 2014).	166 eyes in total. 46 eyes of 46 nAMD participants and 120 eyes of 120 healthy controls were used. All participants were Caucasian. nAMD participants had not undergone any treatment prior to clinical testing. Those with longstanding AMD (disciform scarring) or additional ocular/systemic pathology were not eligible.	Microperimetry and OCT used. Oximeter used to provide oxygen saturation readings of the retinal circulation (not the choroid). Pre-trial measurements of blood pressure, finger pulse oximetry, IOP and heart rate were taken alongside a questionnaire regarding medical history and smoking status. A dual-wavelength non-invasive retinal oximeter (Oxymap T1) was used to record measurements of oxygen saturation via a light wavelength and absorption methodology. Images provided were analysed by Oxymap Analyzer software.	No difference was found between the arteriolar oxygen saturation between the AMD participants and the healthy controls (P=0.16). There was a statistically significant oxygen saturation difference found within the venuoles of the AMD and control groups, with the saturation being higher in the presence of AMD. In healthy individuals, venous oxygen saturation decreases by 0.16 percentage points for each year of age, while in AMD, the oxygen saturation increases by 0.40 percentage points per year. The arteriovenous difference decreases with age in AMD, while it increases in healthy individuals. Alternatively similar results may be as a consequence of less O_2 demand by the damaged retinal tissue.	The results suggest that retinal oxygen metabolism may be abnormal in patients with nAMD. Venous oxygen saturation appeared to be higher in the presence of AMD and continued to increase with age. Arteriovenous difference in oxygen saturation was less in AMD participants indicating that less oxygen is being extracted from the retinal vessels in the presence of AMD. This reduced oxygen saturation (assuming blood flow is not increased) results in less oxygen reaching the macular tissues. The data indicates that the retinal circulation is contributing less oxygen to the retina in AMD when compared to normal eyes. The oxygen consumption of the retina is likely to be abnormally low with nAMD. High oxygen saturation in vessels may reflect reduced oxygen delivery from vasculature to tissue as with results found in the presence of diabetic retinopathy (Hardarson and Stefánsson, 2012).	The author provides a good breakdown of studies performed: (Grunwald et al., 1998; Metelitsina et al., 2008; Boltz et al., 2010; Sato et al., 2006; and Remsch et al., 2000). The control group in this study was not age-matched to the study group and only vessels equal to or larger than 8 pixels could be measured due to the reliability of the oximeter (small vessels would've provided more accurate results). The author also suggests that another explanation for reduced oxygen delivery to tissue may be related to capillary non-perfusion and vessel wall thickening.
Hypoxia-induced metabolic stress in retinal pigment epithelial cells is sufficient to induce photoreceptor degeneration (Kurihara et al., 2016)	In vivo analysis using mouse and human cultivated RPE cells and functional analysis (ERG) using mouse models to demonstrate effect of induced hypoxia on photoreceptors	Electroretinography was performed on dark adapted, anaesthetised mice engineered to have choriocapillary defect. The defects exhibited were then compared to the retinal damage as induced by hypoxia (immunochemical analysis). Human RPE cells with induced hypoxia (3% oxygen chamber)	Mouse model: 1st signs of hypoxia (HIF reactivity) was noticed 6/12 post induction. Hypoxia in RPE induced severely distended basal infoldings, accumulation of lipid droplets within RPE cells, RPE cell hypertrophy and progressive thickening of Bruch's membrane (9/12 post induction) Human RPE:	Chronic HIF-2alpha mediated metabolic stress in RPE cells is enough to induce PR dysfunction and/or degradation. How this occurs: Hypoxia alters the RPE secretome (secretions). Hypoxic RPE shut down glucose and lipid oxidation (restoration) and commit to glycolysis (breaking down glucose	

		were also assessed for retinal damage. RPE cells were also modified to induce HIF stabilization and assessed for retinal damage.	HIF target gene VEGF-A was upregulated after exposure to low oxygen. Hypoxia triggered CC vasodilation. Removing VHL Causes RPE lipid droplet accumulation within 3/7. Severely distended basal infolding and increased thickness of BM occurred after 14/7. The effect of RPE hypoxia caused sensory defects. PR degeneration was observed along with significant functional impairments of both rod and cone driven-pathways	for energy). This allows RPE to gain energy more quickly however doubles their glucose intake. Since RPE is main supplier of glucose to neurosensory retina this impacts photoreceptor function and survival.	

Appendix II. ALight trial published protocol

McKeague et al. Trials 2014, 15:246
http://www.trialsjournal.com/content/15/1/246

TRIALS

STUDY PROTOCOL Open Access

Low-level night-time light therapy for age-related macular degeneration (ALight): study protocol for a randomized controlled trial

Claire McKeague[1], Tom H Margrain[1], Clare Bailey[2] and Alison M Binns[1,3*]

Abstract

Background: Age-related macular degeneration (AMD) is the leading cause of blindness among older adults in the developed world. The only treatments currently available, such as ranibizumab injections, are for neovascular AMD, which accounts for only 10 to 15% of people with the condition. Hypoxia has been implicated as one of the primary causes of AMD, and is most acute at night when the retina is most metabolically active. By increasing light levels at night, the metabolic requirements of the retina and hence the hypoxia will be considerably reduced. This trial seeks to determine whether wearing a light mask that emits a dim, green light during the night can prevent the progression of early AMD.

Methods/design: ALight is a Phase I/IIa, multicentre, randomized controlled trial. Sixty participants (55 to 88 years old) with early AMD in one eye and neovascular AMD (nAMD) in the fellow eye will be recruited from nAMD clinics. They will be randomized (in the ratio 1:1), either to receive the intervention or to be in the untreated control group, stratified according to risk of disease progression. An additional 40 participants with healthy retinal appearance, or early AMD only, will be recruited for a baseline cross-sectional analysis. The intervention is an eye mask that emits a dim green light to illuminate the retina through closed eyelids at night. This is designed to reduce the metabolic activity of the retina, thereby reducing the potential risk of hypoxia. Participants will wear the mask every night for 12 months. Ophthalmologists carrying out monthly assessments will be masked to the treatment group, but participants will be aware of their treatment group. The primary outcome measure is the proportion of people who show disease progression during the trial period in the eye with early AMD. A co-primary outcome measure is the rate of retinal adaptation. As this is a trial of a CE-marked device for an off-label indication, a further main aim of this trial is to assess safety of the mask in the cohort of participants with AMD.

Trial registration: International Standard Randomised Controlled Trials Register: ISRCTN82148651

Keywords: Age-related macular degeneration, Biomarker, Hypoxia, Light mask, Randomized controlled trial

Background

Age-related macular degeneration (AMD) is the leading cause of blindness in the developed world [1] and is responsible for more than 50% of visual impairment registrations in the UK [2]. For the majority of people with AMD, there is no treatment. The remaining 10 to 15% of people with the advanced, neovascular, form of the disease (nAMD) are mainly treated with intra-ocular injections of ranibizumab, an anti-vascular endothelial growth factor agent [3]. Follow-up treatment for these patients is long-term and places a significant burden on the UK National Health Service. Indeed, advanced AMD currently costs the British economy £1.2 billion to £3.7 billion per annum [2,4,5]. Furthermore, the disease is associated with depression, falls and social isolation [6,7]. Given this significant socioeconomic problem, there is a great need to evaluate potential therapeutic interventions that attempt to treat the disease at an early stage, to prevent vision loss from occurring.

* Correspondence: alison.binns.1@city.ac.uk
[1]School of Optometry and Vision Sciences, Cardiff University, Cardiff CF24 4 LU, UK
[3]Division of Optometry and Visual Science, School of Health Sciences, City University, London EC1V 0HB, UK
Full list of author information is available at the end of the article

Age-related macular degeneration is characterized by the dysfunction and death of photoreceptors in the central retina. There is an increasing amount of evidence to suggest that hypoxia plays a major role in its pathogenesis [8,9]. This has been attributed to various factors, including a disruption of choroidal circulation [10-13], and thickening and deposition of drusen at Bruch's membrane [9,14]. The latter increases the distance over which oxygen must travel to reach the retinal pigment epithelium from the choroidal circulation. Disease-related changes to Bruch's membrane also impair the diffusion of nutrients and growth factors, which consequently exacerbates choroidal perfusion abnormalities, promoting further hypoxia [8,15].

Even in the healthy retina, intraretinal oxygen profiles obtained from animals show that the oxygen tension at the proximal side of the photoreceptor inner segments is close to zero in darkness [16,17]. This is attributable to the metabolic demand of the 'dark current' in the retina's approximately 120 million rods [18]. When this limited supply of oxygen to the outer retina is further compromised by the changes to the choroidal circulation and Bruch's membrane that occur in AMD, hypoxia may result. This hypoxia could be the precursor for increased vascular endothelial growth factor production and apoptosis [19,20].

The fragile balance between metabolic demand and oxygenation is exemplified functionally by the adverse effects of hypoxia on colour vision [21-23], dark adaptation [24,25], mesopic sensitivity [26] and the electroretinogram [12,27-29]. To date, there is no direct evidence of the effect of hypoxia on visual function in AMD. However, there is evidence that scotopic threshold elevation and prolonged electroretinogram implicit times are associated with areas of reduced choroidal blood flow in AMD [30,31] and pilot data from our laboratory show a transient reduction in scotopic thresholds in an individual with early AMD whilst inhaling oxygen.

Environmental manipulation of light levels can substantially reduce the metabolic demands on the outer retina, thereby reducing the need for oxygen, and potentially providing an intervention that would delay the progression of conditions with a hypoxic aetiology [32]. A pilot study by Arden et al. [33] found no adverse effects from the provision of low-level night lighting over the course of 12 months in individuals with diabetic retinopathy [33]. Furthermore, a recent clinical trial in patients with diabetic macular oedema who wore a low-level light mask during the night for 6 months reported a reduction in oedema and an improvement in functional measures, which was attributed to the obviation of night-time hypoxia [34]. In this trial, we will be using the same intervention (low-level light therapy) to determine its ability to prevent the development of AMD.

Methods/design

Trial objectives

The primary aim of this study is to collect preliminary Phase I/IIa proof-of-concept trial data from people with early AMD in one eye and advanced nAMD in the fellow eye, recruited from a hospital nAMD clinic, in order to assess the impact of low-level night-time light therapy, compared with no intervention, on disease progression in the eye with early AMD. A further main aim of this trial is to assess safety of the mask in the cohort of participants with AMD.

The secondary aims of the study are to:

1. Establish the effect of low-level night-time light therapy, compared with no-treatment control, on secondary outcome measures, including: change in drusen volume from baseline in the eye with early AMD; ranibizumab retreatment rates in the fellow eye with nAMD; progression of early AMD on the basis of change in functional outcome measures; change in health-related quality of life (assessed using the EuroQol EQ-5D instrument); change in self-reported visual function assessed using the 48-item Veterans Affairs Low-Vision Visual Functioning Questionnaire (VA LV VFQ-48).
2. Establish the acceptability of low-level night-time light therapy in people with AMD by monthly qualitative interviews.
3. Determine the effect of low-level night-time light therapy on sleep patterns by conducting the Pittsburgh Sleep Quality Index (PSQI) questionnaire every month with both intervention arms by interview with the study investigator.
4. Establish the relationship between baseline functional biomarker outcomes and the severity of AMD (assessed using the simplified Age-Related Eye Disease Scale (AREDS) and initial drusen volume).
5. Evaluate the ability of all clinical tests to act as prognostic biomarkers for AMD progression.
6. Evaluate the ability of all clinical tests to act as predictive biomarkers for low-level night-time light therapy in people with AMD.
7. Compare the sensitivity of all clinical tests to disease progression over 12 months.

Study design and setting

ALight is a Phase I/IIa prospective proof-of-concept randomized controlled trial, consisting of two parallel groups. Trial recruitment and data collection will take place at the Medical Retina Clinic, Bristol Eye Hospital. Additional cross-sectional data will be collected from people with healthy eyes, or only early signs of AMD, at the Cardiff University School of Optometry and Vision Sciences.

Eligibility criteria

Inclusion criteria

- Between the ages of 55 and 88 years.
- Early Treatment of Diabetic Retinopathy Study (ETDRS) visual acuity of 0.3 logMAR (Snellen 20/40 or 6/12) or better in the test eye.
- Early AMD in the study eye.
- nAMD in the fellow eye, within a month of the third Ranibizumab injection (trial only).
- Willing to adhere to allocated treatment for duration of trial.

Exclusion criteria

- Ocular pathology other than macular disease.
- Significant systemic disease or medication known to affect visual function.
- Systemic disease that would compromise participation in a 1-year study (trial only).
- Insufficient English language comprehension.
- Cognitive impairment as determined using an abridged Mini Mental State Examination [7].
- Oxygen mask worn at night.

Suspension criteria for the trial

- Participant wishes to discontinue the study.
- Serious adverse events (for example, conversion to nAMD in the test eye) or unexpected changes in clinical status.

Interventions

Participants allocated to the treatment group will be given a 12-weekly disposable light mask (Polyphotonix Medical, UK) that presents organic light-emitting diode illumination (peak output 502 nm) to both eyes, to be used overnight for 12 weeks. Light masks will be replaced every 12 weeks at the participant's routine appointment at the nAMD clinic so that the total duration of mask usage is 12 months.

The mask provides a luminance of 75 photopic cd/m^2. When adjusted for the spectral sensitivity of rod photoreceptors, this equates to 186 scotopic cd/m^2 [35]. Light transmission by the human eyelid has been found to range between 0.3% and 2% for light in the region of 500 to 505 nm [36-38]. Under these conditions, the pupil diameter in people in the age group 60 to 85 years is approximately 4 mm [39]. This will result in a retinal illuminance in the order of 23 scotopic Td (assuming an eyelid transmission of 1%).

The masks will be pre-programmed to function only between specific hours, that is, 8 pm to 8 am, to prevent misuse. Outside of these hours, they will not illuminate if worn. The mask is activated when a touch sensor on the device is gently covered with a finger for 3 seconds. It will deactivate if not worn continuously for the first 15 minutes, and after that, the light will remain on for the remainder of the 8-hour period.

Treatment acceptability will be evaluated during a monthly interview with the study investigator. Compliance data will be obtained at the monthly visit from the treatment group both (i) through evaluation of a diary of mask usage, and (ii) objectively through data collected on a chip in the mask itself (based on a sensor which logs when the mask is in contact with the face). This provides precise data on the hours the mask is worn each night by each participant. As each mask is programmed with the unique participant identification code, compliance data stored on-chip will be non-identifiable except via the password-protected electronic database.

The current management of patients with early AMD involves advising on lifestyle factors, such as stopping smoking and improving diet. The only other intervention that is based on evidence from a robust randomized controlled trial is the provision of a nutritional supplement consisting of high-dose antioxidants plus zinc. This AREDS group formula (vitamin C, 500 mg; vitamin E, 400 IU; beta carotene, 15 mg and zinc, 80 mg) has been shown to reduce risk of progression from early to advanced AMD by around 20% over 5 years in people with specific features of AMD [40]. However, a recent systematic review by the Cochrane Collaboration indicated that there may be an increased risk of mortality in individuals taking vitamin E and beta carotene supplementation [41]. As this is a recently published document, its advice is not reflected in the current guidelines for the management of AMD. For this reason, the low-level light therapy will be compared with a no-treatment control, rather than with the AREDS group formula as the best current intervention.

Participants in both groups will receive routine ophthalmological care for the eye with nAMD (that is, ranibizumab injections). If the eye with early AMD converts to nAMD, the participant will proceed to ranibizumab treatment for this eye also, and will be withdrawn from the study.

Outcome measures

This study includes two co-primary outcome measures, reflecting structural status and functional status.

1. The proportion of people who show 'disease progression' in the eye with early AMD during the 12 months of the study based on an increase in drusen volume beyond test-retest repeatability limits or a progression to advanced AMD. Software available for the Cirrus optical coherence tomography (OCT) system allows automated assessment of drusen volume. Irrespective of initial drusen

volume, approximately 50% of people with AMD show a significant increase in drusen volume over the 12-month study period, that is, beyond test-retest 95% confidence intervals [42]. Conversion to advanced disease will also be considered to be an indicator of disease progression in this analysis. Data from a trial on a similar group indicates that about 10% of people meeting our inclusion criteria will develop advanced AMD within 12 months [43]. Hence, 60% of participants might be expected to show progression based on increased drusen volume or progression to late AMD. The development of advanced AMD will be determined on the basis of ophthalmologist diagnosis at the monthly follow-up appointments at the nAMD clinic.

2. The rate of retinal adaptation (time taken for photoreceptors to recover their sensitivity after being exposed to a bright adapting light).

Secondary outcome measures include: the change in drusen volume over the 12 month follow-up period; the number of ranibizumab retreatments required during the year in the fellow eye with nAMD (assessed through review of medical records at the end of 12 months); changes in visual function including chromatic thresholds, visual acuity and psychophysical 14 Hz flicker thresholds; self-report outcome measures, including health-related quality of life (EQ-5D) and visual function (VFQ-48) [44]; a sleep quality questionnaire (PSQI) and a semistructured interview (conducted monthly by interview) to determine intervention acceptability.

To obtain detailed information about the time course of any therapeutic action, the primary and the first of the secondary outcome measures (based on drusen volume) will be assessed at baseline and then at monthly intervals (using OCT images obtained at the regular nAMD clinic follow-up appointments).

Participant timeline

The study flow diagram (Figure 1) outlines the appointment schedule. In brief, potential participants are identified at their first visit to the nAMD clinic. At the second visit (1 month later), informed consent will be obtained, and screening tests and baseline questionnaires will be carried out. At the third monthly visit, baseline functional tests will be carried out, and participants will be randomly assigned to either the treatment or intervention group. Participants in both intervention groups will attend a short, monthly follow-up appointment following their routine appointment at the nAMD clinic throughout the year. Final outcome data will be collected from control and intervention groups at a 12-month follow-up appointment, scheduled to follow a regular visit to the nAMD clinic.

Participants in the cross-sectional baseline study will attend Cardiff University or the Bristol Eye Hospital for one visit only.

Recruitment

Sixty participants will be recruited to the trial. Ophthalmologists will identify potential trial participants who are attending for their first appointment at the nAMD clinic at Bristol Eye Hospital, and will provide them with an information sheet and ask for their permission to be contacted by the study investigators. The potential participants will be contacted at least 2 days after their receipt of the information sheet, and invited to meet the study investigator at their next visit to the nAMD clinic (approximately 1 month later) to discuss the trial, provide consent if they choose to participate, and carry out some basic screening tests. Participants will be informed after this screening visit whether they are eligible to take part in the study. Owing to the low number of patients required to participate in the study it is planned for the trial and data collection to take place principally at a single NHS centre, that is, the Bristol Eye Hospital. If needed, additional participants will be recruited from supplementary recruitment centres to ensure that targets are met.

Forty control participants and participants with grade 1 AMD (AREDS simplified scale [45]) for the baseline cross-sectional analysis will be recruited by local optometrists in Bristol and Cardiff, from a database of elderly volunteers, from the Bristol Eye Hospital, from the list of research volunteers at the Cardiff University Eye Clinic and from staff and students of Cardiff University.

Randomization

Participants will be stratified according to risk of AMD progression (using the AREDS simplified scale [45]), and randomly allocated to receive either the light mask or no intervention in a 1:1 ratio using computer-generated random permuted blocks (both groups will continue to receive ranibizumab injections as required for the fellow eye). The study investigator will be provided with three piles of envelopes by the chief investigator, in order to randomize the participant to either the intervention or control arm of the study. Each pile relates to a different stratum of randomization, that is, grade 2, 3 or 4 of AMD, according to the AREDS simplified scale. The envelopes in each pile will be numbered, and will contain the randomization allocation for each participant.

Masking

It is not appropriate in this study to use a sham treatment, since a non-illuminated mask may have a physiological effect on the retina and patients would be aware that they weren't perceiving light and so would be unmasked to their intervention group. The study investigator who

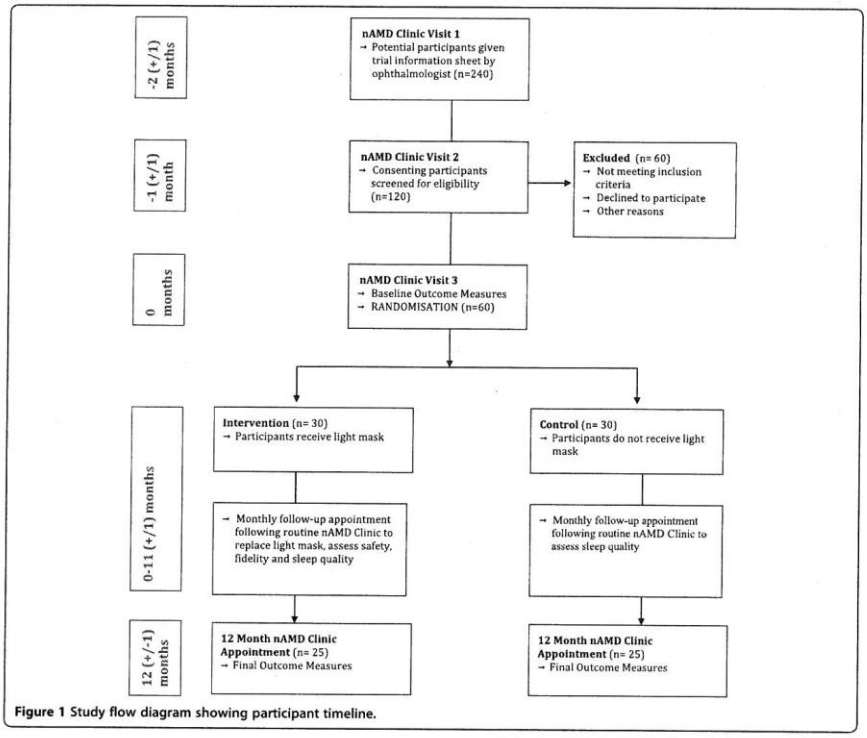

Figure 1 Study flow diagram showing participant timeline.

collects the outcome data will also be providing the masks and instructions on its usage and, hence, will not be masked to the intervention group. However, the potential for experimenter bias is limited, as the primary outcome measure, disease progression, is an objective measurement carried out by automated computer software. The ophthalmologists who are seeing the participants for their regular ranibizumab injections will be masked, which will prevent any bias in their retreatment decisions for the fellow eye.

Data collection methods

Screening visit

Following a discussion of the study, and the obtaining of informed consent, the study investigator will question the participant regarding ocular and medical history. Retinal photographs will be taken if they have not already been acquired, and repeated if image quality is insufficient to allow evaluation. The OCT and fundus photographs will be assessed to check for eligibility. The Van Herick angle of drainage will be measured, media clarity will be assessed for each eye and the lens graded according to the Lens Opacities Classification System III grading scale [46]. Visual acuity will be assessed in each eye using the ETDRS chart, following a brief refraction, if necessary. An abridged version of the Mini Mental State Examination will be used to assess for cognitive impairment (5 min; [7]).

Those still deemed eligible for inclusion in the study will also complete several questionnaires, through verbal interview with the investigator: visual function (VA LV VFQ-48) [44]; health-related quality of life (EQ-5D); sleep quality (PSQI) [47]; smoking history (pack years); vitamin supplementation; ethnic origin.

Baseline assessment

Optical coherence tomography images and fundus photographs obtained during the participant's routine visit

to the ranibizumab clinic will be obtained and analyzed to assess drusen volume and AMD grade, according to the AREDS simplified scale [45]. If the images are of insufficient quality, additional images will be captured.

The ETDRS visual acuity will be assessed in each eye. Chromatic thresholds will be measured for the eye with early AMD using the Colour Assessment and Diagnosis test [48] (City Occupational Ltd). Contrast thresholds to a 14 Hz flickering stimulus will be measured for the eye with early AMD using the procedure outlined by Dimitrov et al. [49]. The rate of parafoveal cone dark adaptation will be determined for the eye with early AMD using a psychophysical procedure described previously [50]. Thresholds will be determined using a psychophysical method, based on a '3 down, 1 up' staircase paradigm [50]. An array of white light-emitting diodes behind a diffusing filter will be used to light-adapt photoreceptors in the central 43.6° of the test eye (the output of the white light-emitting diodes will be modified by a Lee filter, HT015, to provide a retinal illuminance of 5.20 log phot Td.s^{-1}, providing a bleach of 85% cone photopigment and 74% rhodopsin). All light levels fall within the safety guidelines set out in British Standard BS EN 15004-2 (2007) [51]. There will be an initial training phase, of around 5 minutes, then the adapting light will be presented, and finally recovery of visual thresholds will be monitored for 25 minutes after exposure to the adapting light.

Those individuals who are assigned to the treatment group will then be given a light mask, and provided with written and oral instructions on its use. There will also be a reprise of the key information provided in the participant information letter about follow-up appointments. Participants will be given written copies to take home of the PSQI questionnaire that will be used in the monthly interview.

Monthly assessment

The investigator will access the OCT images and medical records of all participants after they have attended the ranibizumab clinic for each monthly follow-up appointment. This will allow measurement of drusen volume on a monthly basis, which will allow the final analysis to include an assessment of the time course of any therapeutic action. Additionally, reviewing medical records will facilitate monitoring of the conversion rate to advanced AMD in the control and intervention groups in the eye with early AMD at baseline, and of ranibizumab retreatment rates in the eye with nAMD, for adverse event reporting purposes.

Participants in both intervention groups will attend a short, monthly follow-up appointment following their routine ranibizumab clinic appointment, during which both groups will complete the PSQI sleep quality questionnaire. In addition, the treatment group will bring their mask along to each monthly visit to allow objective compliance data (nightly hours of use) to be exported from the device, retraining in mask use if required, functionality of the mask to be checked, masks to be replaced every 12 weeks, and a semistructured interview to be carried out to determine the acceptability of the intervention. These data will be used to address secondary objectives 2 and 3.

Final (12-month) visit

This visit will be the same as the baseline visit with the addition of a final semistructured interview assessing the acceptability of the intervention, and the questionnaires (PSQI, VA LV VFQ-48, Euroqol).

Baseline cross-sectional study

The 40 participants recruited only to the cross-sectional part of the study will undergo the tests outlined in the baseline assessment visit of the trial.

Statistical methods

It should be noted that, as a Phase I/IIa proof-of-concept study, this research is designed to assess the acceptability of this therapy for the participants, and to provide preliminary data to support a larger Phase III randomized controlled trial in the future, and so is not powered to detect small effect sizes. To maximize retention, all follow-up visits will be timed to coincide with scheduled appointments at the nAMD clinic. We will aim to recruit 60 people, which, allowing for 15% dropout through the year, should leave a final cohort of 51. This will be sufficient to detect a 50% reduction in people showing progression at a probability level of 0.2, with a power of 80%, and a change in the time constant of cone adaptation of 1 minute to be detected at a probability level of 0.05, with a power of 80%. The additional 40 participants enrolled into the cross-sectional part of the study will allow a total cohort of $n = 100$ to address secondary aim 4.

Analysis will be carried out on an intention-to-treat basis. There will be no interim analysis, but conversions to nAMD in the eye with early AMD at baseline, and ranibizumab retreatments for the fellow eye, will be recorded at each participant visit to the nAMD clinic for safety monitoring purposes.

This trial will primarily be concerned with providing information about the safety of the device in the treatment of AMD, and the magnitude of any treatment effect. On this basis, descriptive statistics will be carried out to summarize the demographic characteristics of the two groups, as well as the proportion of individuals showing disease progression in each group, the magnitude of changes in secondary outcome measures, including drusen volume, measures of visual function, and the self-report tests, and the fellow eye retreatment rates.

The primary outcome measure will be the proportion of patients demonstrating disease progression at 12 months.

Comparisons will be performed using stratified Mantel-Haenszel tests and presented as forest plots.

Formal statistical analysis will also include linear regression analysis to investigate changes in drusen volume controlling for intervention arm, baseline drusen volume and patient characteristics (such as age, vitamin supplement intake and history of smoking). Analysis of covariance (ANCOVA) will be carried out to compare the change in secondary outcome measures (for example, drusen volume, functional tests, self-report measures) and the ranibizumab retreatment rates over 12 months between the two intervention arms, controlling for the characteristics listed previously. Note that all analysis except for the ranibizumab retreatment rate pertains to the eye with early AMD. This will address secondary aim 1. To meet our fourth secondary aim, which is to establish the relationship between baseline functional biomarker outcomes and the severity of AMD, we will carry out a one-way analysis of variance (ANOVA) to compare the mean results at baseline between participants with grades of AMD in each group on the AREDS simplified scale. This analysis will take place when the baseline data collection is complete. To assess the ability of the clinical tests to act as prognostic and predictive biomarkers, receiver operating characteristics curves will be constructed to plot the sensitivity and specificity of the baseline measures in predicting outcomes within the control and intervention arms, respectively. This will address secondary aims 5 and 6. When the trial is completed, linear regression analysis will be used to determine how well the change in the functional measures relate to the change in our primary outcome measure (drusen volume), which is a validated biomarker for disease progression. This will address the seventh secondary aim.

Trial management

The chief investigator has ultimate responsibility for the trial management, assisted by the trial management group. Any important protocol modifications will be communicated to all relevant parties (investigators, research ethics committee, NIHR CRN Portfolio, trial registry, journals, NHS Research and Development, device manufacturer, funding body) by the chief investigator.

A trial steering committee has been established, which will also act as a data monitoring committee. In addition to annual meetings, the committee will be issued with information about any adverse events throughout the course of the study, so that they can decide whether it is appropriate for the study to be terminated. A 3-monthly newsletter will be issued to all investigators and the steering committee, updating on recruitment and other issues, throughout the trial.

Safety monitoring

All adverse events (AEs) and serious adverse events (SAEs) will be recorded. The chief investigator (AB) will be provided with an update of AEs every month and all SAEs within two working days. This trial does not involve a medicinal product or life-threatening procedure. Hence, the risk of a SAE is low. However, one potential SAE is an increased rate of progression to nAMD in the eye with early AMD at baseline. Although this is at odds with the literature, it is not an impossible outcome. Another potential SAE would be an increased rate of recurrence of nAMD in the fellow eye (resulting in increased ranibizumab retreatment rates). Conversion to nAMD and Ranibizumab retreatment requirement in the fellow eye will be determined by ophthalmologists at the monthly ranibizumab clinic, and recorded by the study investigator through assessment of medical records after each monthly ranibizumab appointment.

Wong et al. [52] carried out a meta-analysis of studies, which had looked at the progression to choroidal neovascularization in the fellow eye when free of advanced disease at study inception. They reported that the cumulative 1-year incidence of nAMD in the 426 patients enrolled in the five studies that evaluated this outcome was 12.2% (confidence interval, 1.7% to 30.6%). Therefore, we have placed an upper limit on the number of people expected to convert to nAMD per month of $n \times (30.6\% / 12 \text{ months})$, where n is the number of people in the trial who are using the light therapy light mask.

The chief investigator will assess the nature of the AEs and SAEs for seriousness, causality and expectedness. Following the initial report, follow-up data may be requested by the chief investigator. Where the SAE is both related and unexpected, the chief investigator will notify the Trial Steering Committee, the trial sponsor, the National Research Ethics Service North West, and the device manufacturer, who will notify the Medicines and Healthcare Regulatory Agency within 15 days of receiving notification of the SAE.

Data management

Any trial data will be recorded on spreadsheets using the numerical identifier for each patient. These data will be non-identifiable. All paper records will also use the unique numerical identifier, which will be non-identifiable. The only identifiable personal data will be the paper and electronic copies of the patient database. The paper copy will not be transferred between Cardiff University and the Bristol Eye Hospital, and will be kept in a locked filing cabinet at all times. The electronic database will be stored on a secure Cardiff University computer drive, which is accessible from Bristol and Cardiff via a password-protected connection. The study database will be checked for integrity every month by

the chief investigator. At the end of the trial, the data will belong to Cardiff University. At this time, Polyphotonix Medical Ltd (the manufacturer) will have access to the results. Anonymized data will be available for verification at any time by the funding body, the College of Optometrists, on request. Neither the College of Optometrists, nor Polyphotonix Medical Ltd. will influence the data collection or analysis. All data will be kept for 15 years, in line with Cardiff University's Research Governance Framework Regulations for clinical research.

Dissemination

A summary of the trial protocol is available to the public through the International Standard Randomised Controlled Trials Register. Any interested individuals may contact the chief investigator for further information. Results will be published in peer-reviewed journals and at International Conferences. The chief investigator has ultimate responsibility for the scientific content of any publications. Dissemination of results to trial participants will take place through a summary-of-findings newsletter sent at the end of the trial to those individuals who indicate a desire to receive an update. Dissemination to the wider community of people with AMD will take place through publication in the Macular Society's members' magazine, *Digest*, and through presentations at such events as the Macular Society 'Top Doctors' conference. Neither the funding body (the College of Optometrists), the light mask manufacturer (Polyphotonix Medical Ltd), nor the sponsor (Cardiff University) will influence the presentation or the publication of the research.

Ethical considerations

The study has been approved by the National Research Ethics Service North West, and is registered with the International Standard Randomised Clinical Trials Register. A notice of no objection has been obtained from the Medicines and Healthcare Regulatory Agency. The trial will be conducted in adherence with the Declaration of Helsinki and the Good Clinical Practice guidelines. The chief investigator and the research team will preserve the confidentiality of participants in accordance with the Data Protection Act 1998.

Audits and inspections

The trial is liable to inspection by the College of Optometrists as the funding organization. The study may also be liable to inspection and audit by Cardiff University under their remit as sponsor.

Discussion

In this article, we present a clinical trial protocol to evaluate the effect of low-level night-time light therapy in patients with early AMD. To our knowledge, this is the first randomized controlled trial of its kind in AMD. This study will provide the foundation for future large-scale clinical trials. With the prediction of longer life expectancy in the future, the prevalence of AMD and its associated social and economic problems will continue to increase unless a treatment is developed that will stop its progression.

Trial status

This protocol aims to establish the therapeutic benefit of low-level light therapy on disease progression in AMD. Recruitment will begin in April 2014 and continue until February 2015. Data collection will take place from June 2014 to April 2016.

Abbreviations

AE: adverse event; AMD: age-related macular degeneration; ANCOVA: analysis of covariance; ANOVA: analysis of variance; AREDS: age-related eye disease scale; CE: Conformité Européenne; ETDRS: Early Treatment of Diabetic Retinopathy Study; nAMD: neovascular age-related macular degeneration; OCT: optical coherence tomography; PSQI: Pittsburgh Sleep Quality Index; SAE: serious adverse event; VALVVFQ-48: 48-item Veterans Affairs Low-Vision Visual Functioning Questionnaire.

Competing interests

None of the authors has any financial interest in the device, or any other aspect of this trial.

Authors' contributions

CM: design, manuscript writing, final approval of the manuscript. TM: conception and design, critical revision and final approval of manuscript. CB: design, critical revision and final approval of manuscript. AB: conception and design, manuscript writing and final approval of the manuscript. All authors read and approved the final manuscript.

Funding

This trial is funded by a research grant from the College of Optometrists, UK. The device manufacturer, Polyphotonix Medical Ltd, is providing the light masks and technical support for the trial free of charge. Both the College of Optometrists and Polyphotonix have the right to review manuscripts bearing their name before publication, but the chief investigator has ultimate authority over the protocol, trial conduct and content of any publications.

Sponsor contact details

Dr K Pittard Davies, Cardiff University Research, Innovation and Enterprise Services, Cardiff University, 7th Floor, 30-36 Newport Rd, Cardiff CF24 0DE.

Author details

[1]School of Optometry and Vision Sciences, Cardiff University, Cardiff CF24 4 LU, UK. [2]Bristol Eye Hospital, Lower Maudlin Street, Bristol BS1 2LX, UK. [3]Division of Optometry and Visual Science, School of Health Sciences, City University, London EC1V 0HB, UK.

Received: 13 December 2013 Accepted: 23 May 2014
Published: 24 June 2014

References

1. Resnikoff S, Pascolini D, Etya'ale D, Kocur I, Pararajasegaram R, Pokharel GP, Mariotti SP: **Global data on visual impairment in the year 2002.** *Bull World Health Organ* 2004, **82**:844–851.
2. Bunce C, Xing W, Wormald R: **Causes of blind and partial sight certifications in England and Wales: April 2007-March 2008.** *Eye (Lond)* 2010, **24**:1692–1699.
3. The CATT Research group: **Ranibizumab and Bevacizumab for Neovascular Age-Related Macular Degeneration.** *N Engl J Med* 2011, **364**:1897–1908.
4. Economics A: *Future Sight Loss UK (1): the Economic Impact of Partial Sight and Blindness in the UK Adult Population.* London: Royal National Institute of Blind People; 2009.

5. Cruess AF, Zlateva G, Xu X, Pauleikhoff D, Lotery A, Mones J, Buggage R, Schaefer C, Knight T, Goss TF: **Economic burden of bilateral macular degeneration multi-country observational study.** *Pharmacoeconomics* 2008, **26**:57–73.
6. Dargent-Molina P, Favier F, Grandjean H, Baudoin C, Schott AM, Hausherr E, Meunier PJ, Breart G: **Fall-related factors and risk of hip fracture: the EPIDOS prospective study.** *Lancet* 1996, **348**:145–149.
7. Margrain TH, Nollett C, Shearn J, Stanford M, Edwards RT, Ryan B, Bunce C, Casten R, Hegel MT, Smith DJ: **The Depression in Visual Impairment Trial (DEPVIT): trial design and protocol.** *BMC Psychiatry* 2012, **12**:57.
8. Feigl B: **Age-related maculopathy - linking aetiology and pathophysiological changes to the ischaemia hypothesis.** *Prog Retin Eye Res* 2009, **28**:63–86.
9. Stefánsson E, Geirsdóttir A, Sigurdsson H: **Metabolic physiology in age related macular degeneration.** *Prog Retin Eye Res* 2011, **30**:72–80.
10. Ciulla TA, Harris A, Martin BJ: **Ocular perfusion and age-related macular degeneration.** *Acta Ophthalmol Scand* 2001, **79**:108–115.
11. Ciulla TA, Harris A, Kagemann L, Danis RP, Pratt LM, Chung HS, Weinberger D, Garzozi HJ: **Choroidal perfusion perturbations in non-neovascular age related macular degeneration.** *Br J Ophthalmol* 2002, **86**:209–213.
12. Feigl B: **Age-related maculopathy in the light of ischaemia.** *Clin Exp Optom* 2007, **90**:263–271.
13. Metelitsina TI, Grunwald JE, DuPont JC, Ying G-S, Brucker AJ, Dunaief JL: **Foveolar choroidal circulation and choroidal neovascularization in age-related macular degeneration.** *Invest Ophthalmol Vis Sci* 2008, **49**:358–363.
14. Sarks S, Cherepanoff S, Killingsworth M, Sarks J: **Relationship of basal laminar deposit and membranous debris to the clinical presentation of early age-related macular degeneration.** *Invest Ophthalmol Vis Sci* 2007, **48**:968–977.
15. Ciulla TA, Harris A, Chung HS, Danis RP, Kagemann L, McNulty L, Pratt LM, Martin BJ: **Color Doppler imaging discloses reduced ocular blood flow velocities in nonexudative age-related macular degeneration.** *Am J Ophthalmol* 1999, **128**:75–80.
16. Ahmed J, Braun RD, Dunn R, Linsenmeier RA: **Oxygen distribution in the macaque retina.** *Invest Ophthalmol Vis Sci* 1993, **34**:516–521.
17. Wangsa-Wirawan ND, Linsenmeier RA: **Retinal oxygen: fundamental and clinical aspects.** *Arch Ophthalmol* 2003, **121**:547–557.
18. Hagins WA, Ross PD, Tate RL, Yoshikami S: **Transduction heats in retinal rods: tests of the role of cGMP by pyroelectric calorimetry.** *Proc Natl Acad Sci USA* 1989, **86**:1224–1228.
19. Witmer AN, Vrensen GFJM, Van Noorden CJF, Schlingemann RO: **Vascular endothelial growth factors and angiogenesis in eye disease.** *Prog Retin Eye Res* 2003, **22**:1–29.
20. Dunaief JL, Dentchev T, Ying G-S, Milam AH: **The role of apoptosis in age-related macular degeneration.** *Arch Ophthalmol* 2002, **120**:1435–1442.
21. Karakucuk S, Oner AO, Goktas S, Siki E, Kose O: **Color vision changes in young subjects acutely exposed to 3,000 m altitude.** *Aviat Space Environ Med* 2004, **75**:364–366.
22. Connolly DM, Barbur JL, Hosking SL, Moorhead IR: **Mild hypoxia impairs chromatic sensitivity in the mesopic range.** *Invest Ophthalmol Vis Sci* 2008, **49**:820–827.
23. Vingrys AJ, Garner LF: **The effect of a moderate level of hypoxia on human color vision.** *Doc Ophthalmol* 1987, **66**:171–185.
24. Connolly DM, Hosking SL: **Aviation-related respiratory gas disturbances affect dark adaptation: a reappraisal.** *Vis Res* 2006, **46**:1784–1793.
25. Brinchmann-Hansen O, Myhre K: **The effect of hypoxia upon macular recovery time in normal humans.** *Aviat Space Environ Med* 1989, **60**:1183–1186.
26. Connolly DM, Hosking SL: **Oxygenation state and mesopic sensitivity to dynamic contrast stimuli.** *Optom Vis Sci* 2009, **86**:1368–1375.
27. Tinjust D, Kergoat S, Lovasik JV: **Neuroretinal function during mild systemic hypoxia.** *Aviat Space Environ Med* 2002, **73**:1189–1194.
28. Feigl B, Stewart IB, Brown B, Zele AJ: **Local neuroretinal function during acute hypoxia in healthy older people.** *Invest Ophthalmol Vis Sci* 2008, **49**:807–813.
29. Pavlidis M, Stupp T, Georgalas I, Georgiadou E, Moschos M, Thanos S: **Multifocal electroretinography changes in the macula at high altitude: a report of three cases.** *Ophthalmologica* 2005, **219**:404–412.
30. Chen JC, Firzke FW, Pauleikhoff D, Bird AC: **Functional loss in age-related Bruch's membrane change with choroidal perfusion defect.** *Invest Ophthalmol Vis Sci* 1992, **33**:334–340.
31. Remulla JF, Gaudio AR, Miller S, Sandberg MA: **Foveal electroretinograms and choroidal perfusion characteristics in fellow eyes of patients with unilateral neovascular age-related macular degeneration.** *Br J Ophthalmol* 1995, **79**:558–561.
32. Arden GB: **The absence of diabetic retinopathy in patients with retinitis pigmentosa: implications for pathophysiology and possible treatment.** *Br J Ophthalmol* 2001, **85**:366–370.
33. Arden GB, Gunduz MK, Kurtenbach A, Volker M, Zrenner E, Gunduz SB, Kamis U, Ozturk BT, Okudan S: **A preliminary trial to determine whether prevention of dark adaptation affects the course of early diabetic retinopathy.** *Eye (Lond)* 2010, **24**:1149–1155.
34. Arden GB, Jyothi S, Hogg CH, Lee YF, Sivaprasad S: **Regression of early diabetic macular oedema is associated with prevention of dark adaptation.** *Eye (Lond)* 2011, **25**:1546–1554.
35. Wyszechki G, Stiles WS: *Colour Science: Concepts and Methods, Quantitative Data and Formulae.* New York: John Wiley; 1982.
36. Moseley MJ, Bayliss SC, Fielder AR: **Light transmission through the human eyelid: *in vivo* measurement.** *Ophthalmic Physiol Opt* 1988, **8**:229–230.
37. Robinson J, Bayliss SC, Fielder AR: **Transmission of light across the adult and neonatal eyelid *in vivo*.** *Vis Res* 1991, **31**:1837–1840.
38. Ando K, Kripke DF: **Light attenuation by the human eyelid.** *Biol Psychiatry* 1996, **39**:22–25.
39. Winn B, Whitaker D, Elliott DB, Phillips NJ: **Factors affecting light-adapted pupil size in normal human subjects.** *Invest Ophthalmol Vis Sci* 1994, **35**:1132–1137.
40. Age-Related Eye Disease Study Research Group: **A randomized, placebo-controlled, clinical trial of high-dose supplementation with vitamins C and E, beta carotene, and zinc for age-related macular degeneration and vision loss: AREDS report no. 8.** *Arch Ophthalmol* 2001, **119**:1417–1436.
41. Bjelakovic G, Nikolova D, Gluud LL, Simonetti RG, Gluud C: **Antioxidant supplements for prevention of mortality in healthy participants and patients with various diseases.** *Cochrane Database Syst Rev* 2012, **3**:CD007176.
42. Yehoshua Z, Wang F, Rosenfeld PJ, Penha FM, Feuer WJ, Gregori G: **Natural history of drusen morphology in age-related macular degeneration using spectral domain optical coherence tomography.** *Ophthalmology* 2011, **118**(12):2434–2441.
43. Neelam K, Hogg RE, Stevenson MR, Johnston E, Anderson R, Beatty S, Chakravarthy U: **Carotenoids and co-antioxidants in age-related maculopathy: design and methods.** *Ophthalmic Epidemiol* 2008, **15**(6):389–401.
44. Stelmack JA, Szlyk JP, Stelmack TR, Demers-Turco P, Williams RT, Moran D, Massof RW: **Psychometric properties of the Veterans Affairs Low-Vision Visual Functioning Questionnaire.** *Invest Ophthalmol Vis Sci* 2004, **45**:3919–3928.
45. Ferris FL, Davis MD, Clemons TE: **A simplified severity scale for age-related macular degeneration: AREDS Report No. 18.** *Arch Ophthalmol* 2005, **123**:1570–1574.
46. Chylack LT Jr, Wolfe JK, Singer DM, Leske MC, Bullimore MA, Bailey IL, Friend J, McCarthy D, Wu SY: **The Lens Opacities Classification System III. The Longitudinal Study of Cataract Study Group.** *Arch Ophthalmol* 1993, **111**(6):831–836.
47. Buysse DJ, Reynolds CF, Monk TH, Berman SR, Kupfer DJ: **The Pittsburgh Sleep Quality Index: a new instrument for psychiatric practice and research.** *Psychiatry Res* 1989, **28**:193–213.
48. O'Neill-Biba M, Sivaprasad S, Rodriguez-Carmona M, Wolf JE, Barbur JL: **Loss of chromatic sensitivity in AMD and diabetes: a comparative study.** *Ophthalmic Physiol Opt* 2010, **30**:705–716.
49. Dimitrov PN, Robman LD, Varsamidis M, Aung K-Z, Makeyeva GA, Guymer RH, Vingrys AJ: **Visual function tests as potential biomarkers in age-related macular degeneration.** *Invest Ophthalmol Vis Sci* 2011, **52**:9457–9469.
50. Gaffney AJ, Binns AM, Margrain TH: **The topography of cone mediated dark adaptation in age-related maculopathy.** *Optom Vis Sci* 2011, **88**:1080–1087.
51. British Standards Institution: *BS EN ISO 15004-2:2007: Ophthalmic Instruments. Fundamental Requirements and Test Methods. Light Hazard Protection.* London: 2007.
52. Wong TY, Chakravarthy U, Klein R, Mitchell P, Zlateva G, Buggage R, Fahrbach K, Probst C, Sledge I: **The natural history and prognosis of neovascular age-related macular degeneration: a systematic review of the literature and meta-analysis.** *Ophthalmology* 2008, **115**(1):116–126.

doi:10.1186/1745-6215-15-246
Cite this article as: McKeague *et al.*: Low-level night-time light therapy for age-related macular degeneration (ALight): study protocol for a randomized controlled trial. *Trials* 2014 **15**:246.

Appendix III. Calibration of a LCD monitor

Prior to calibration the luminance output of the monitor was non-linear. Therefore the output was 'Gamma corrected' to ensure linear output in accordance with the methods described by Metha et al. (1993). In brief, a 'Gamma model' was fitted to the non-linear luminance output using the Excel Solver function (Figure App II.1). This allowed the derivation of output luminance as a function of grey scale monitor output. Direct measurement of the luminance output of the monitor at various grey scale values allowed the calculation of the grey scale value needed to give a desired luminance. This allowed the derivation of a 'Gamma function' (Table App II.1) which when applied to the LCD monitor resulted in a linear luminance output.

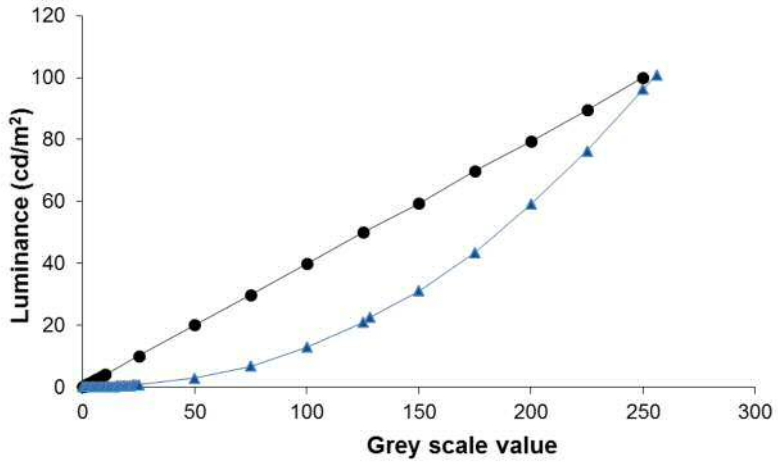

Figure App II.1. Pre- (triangle) and post- (circle) calibration luminance output of the LCD monitor.

Table App II.1. Gamma function values calculated throughout the duration of the ALight clinical trial.

Date	Gamma Function
08/07/14	2.230375
31/10/14	2.215787
12/12/14	2.223671
26/01/15	2.210972
25/02/15	2.221308
24/03/15	2.223629
21/04/15	2.218070
19/05/15	2.209280
30/06/15	2.221618
14/07/15	2.227637
02/09/15	2.221134
18/11/15	2.191009
27/01/16	2.175951
23/02/16	2.188395
04/04/16	2.215031
07/06/16	2.231966
08/08/16	2.209406
12/10/16	2.222900

Appendix IV. Dark adaptation MATLAB code

DARK ADAPTATION EXPERIMENT – Alight trial

```
%First written 3/3/90 by Tom Margrain.
%This version was modified on 13/5/14 by T.Margrain and G.Robinson.
%This version is specific to the 4 degree target used for the Alight
trial.
%The Programme is set up for dilated Px at 140cm. DA over 25mins
%Calibration is for the NEC MultiSync PA241w Monitor.

clear all
```

%1st step: input coordinates and sizes for fixation cross and spot stimulus:

```
%Stimulus specifics:
%How many pixels of the monitor equate to 1 retinal degree at 140cm?
%How large (in retinal degrees) will the stimulus be?
%Spot positioning (1st and 3rd numbers = horiz, 2nd and 4th = vert)
pixelsPerDegree=88.86;
SpotSize=4;
SpotSize=(SpotSize*pixelsPerDegree)/2;
offsetCenteredspotRect = [960-SpotSize, 600-SpotSize, 960+SpotSize,
600+SpotSize];
SurroundRectInner      =      [960-SpotSize-10,      600-SpotSize-10,
960+SpotSize+10, 600+SpotSize+10];

%Fixation cross specifics:
%What thickness/size/colour [R,G,B] will the fixation cross be?
LineThickness = 7;
LineLength=600;
LineSpectrum = [256 256 256];
```

%2nd step: input specifics of the test prior to bleach:

```
%How long will the test run?
durationInSeconds = 1500;
%How will the programme know when a button has been pressed (a response
given)?
KbName('UnifyKeyNames');
%Which VDU screen will be used? Which window will the test run in?
try
whichScreen = 0;
window = Screen(whichScreen, 'OpenWindow');
white = WhiteIndex(window); % pixel value for white colouring in this
window
black = BlackIndex(window); % pixel value for black colouring in this
window
%What sounds will be used throughout the test?
correctSound = sin(2*pi*100*[0:0.00125:2.0]);
incorrectSound = sin(2*pi*40*[0:0.00125:2.0]);
NewFilterSound = sin (2*pi*200*[0:0.00125:10.0]);
%Dark adaptation specifics:
%Step-size is based on 4-2 staircase method used by Dimitrov et al.
(2011).
incrementStep = 0.4;
SpotLuminance = 1.95;
%How can you escape the programme in event of an error?
escapeKey = KbName('ESCAPE');
```

```
%Set up a various counters to record data throughout the test:
response = 0;
responseCounter = 0; %Counts patients responses throughout test
reversalCounter = 1; %Counts number of reversals (reset after each
threshold)
DarkAdptCounter = 0; %Counts number of times a DA threshold is recorded
presentationCounter=1; %Counts total number of presentations shown
dataCounter=1; %Counts total number of reversals shown
thresholdCounter = 1;%Counts total number of threshold points

%Set up filter parameters:
%The 2nd and 3rd ND filters are set as 0 until put into place
AdjustmentFilter1 = 1.2; %This is the optical density of the first ND
filter.
AdjustmentFilter2 = 0; %This is the optical density of the second ND
filter
AdjustmentFilter3=0; %This is the optical density of the third ND
filter

%Create a line to flag when the stimulus is reaching its lowest
luminance for a 2nd time during threshold testing:
SecondNDFIlterFlag = 0;
resultTime = 1;
resultThreshold = 1;
BreakFlag=0;

%Create a window at the start of the experiment in which instructions
can be displayed:
Screen(window, 'FillRect', 0);
%Write experiment details and instructions into the created window
Screen('DrawText', window, 'DARK ADAPTATION VERSION 2 12-05-14', 700,
800, white);
Screen('DrawText', window, '10s to start bleach', 800, 400, white);
Screen(window, 'Flip');
%Inform the investigator when to apply the bleaching source
WaitSecs (10);
Screen ('DrawText', window, 'Start bleach now', 800, 400, white);
Screen(window, 'Flip');
WaitSecs (60);
%Inform the investigator when half the bleaching time has subsided
Screen('DrawText', window, '1 minute complete, the beep will sound
when 10s remain', 600, 400, white);
Screen(window, 'Flip');
WaitSecs (50);
%Inform the investigator (via a beep) when there is 10s of bleaching
time left
cf = 750;                    % This is the carrier frequency (Hz).
sf = 15050;                  % This is the sample frequency (Hz).
d = 1.0;                     % This is the duration (s).
n = sf * d;                  % This is the number of samples.
s = (1:n) / sf;              % This prepares the sound data from the
video card.
s = sin(2 * pi * cf * s);    % This is the sound modulation
sound(s, sf);                % This presents the sound from the sound
card.
pause(d + 0.5);              % This ends the sound.
WaitSecs (10);
%Inform the investigator when threshold testing is to begin
Screen ('DrawText', window, 'Press any key to begin', 750, 800,
white);
```

```
Screen('DrawText', window, 'Bleach finished', 800, 400, white);
Screen(window, 'Flip');
%Wait until a key is pressed before the testing begins and hide the
mouse cursor
KbWait;
Screen('HideCursorHelper', window);
```

%3rd step: set up procedures following bleach – before threshold testing begins

```
%Set up a timer to record duration of testing from when 1st key is
pressed
startTime = now;
durationEachThreshold = 1;
numberOfSecondsRemaining = durationInSeconds;
SecondsRemaining = durationEachThreshold;

%Calibrate the screen as soon as the 1st key is pressed
MinScreenLum = 0.12;
GammaFunc = 2.227637;
MaxScreenLum = 99.36;

%Now start the experiment loop (i.e. threshold testing via 4-2
staircase)
fprintf('Experiment started'),
%Record what time threshold testing began and for how long it proceeds
StartExptSecs = GetSecs;
while GetSecs - StartExptSecs < durationInSeconds
%Ensure that threshold testing re-enters the experiment loop and
doesn't stop until commanded
stopRule = 1;
while stopRule > 0

%Calculate the grey scale required for desired spot luminance
%To do this raise spot luminance by the power of 10 to 'un-log' it
GammaCorrectSpotLum = 255*(((10^SpotLuminance)-
MinScreenLum)/MaxScreenLum)^(1/GammaFunc);

%Make the fixation cross 3x brighter than the spot stimulus
LineSpectrum = [GammaCorrectSpotLum*3.0; GammaCorrectSpotLum*3.0;
GammaCorrectSpotLum*3.0];

%Write the spot luminance on the corner of the screen in blue text
Screen('DrawText', window, ['GammaCorr: ' num2str(SpotLuminance,4)],
1700, 1100, [0,0,240]);

%Ensure the fixation cross is visible before and after the stimulus
appears
Screen('DrawLine', window, [LineSpectrum], 960-LineLength, 600,
960+LineLength, 600 ,LineThickness);
Screen('DrawLine', window, [LineSpectrum], 965, 600-LineLength, 965,
600+LineLength ,LineThickness);
```

%4th step: begin stimulus presentation for threshold testing

```
%Create the spot stimulus – with fixation cross lines superimposed
Screen('FillOval', window, [GammaCorrectSpotLum GammaCorrectSpotLum
0], offsetCenteredspotRect);
Screen('DrawLine', window, [LineSpectrum], 960-LineLength, 600,
960+LineLength, 600 ,LineThickness);
```

```
Screen('DrawLine', window, [LineSpectrum], 965, 600-LineLength, 965,
600+LineLength ,LineThickness)
%Present the stimulus
Screen(window, 'Flip');
%After 200ms remove the stimulus but keep fixation cross lines.
WaitSecs (0.2);
%Write the spot luminance on the corner of the screen in blue text
again
Screen('DrawText', window, ['GammaCorr: ' num2str(SpotLuminance,4)],
1700, 1100, [0,0,240]);
%Ensure the fixation cross remains even after the stimulus has
disappeared
Screen('DrawLine', window, [LineSpectrum], 960-LineLength, 600,
960+LineLength, 600 ,LineThickness);
Screen('DrawLine', window, [LineSpectrum], 965, 600-LineLength, 965,
600+LineLength ,LineThickness);
Screen(window, 'Flip');
%Record the exact time at which the stimulus was taken off the screen.
ResponseSecs = GetSecs;
```

%5th step: record responses to stimulus presentation

```
%Record if any key has been pressed during stimulus presentation
while 1
[ keyIsDown, timeSecs, keyCode ] = KbCheck;
if keyIsDown

%If the ESC key is pressed then break the loop and end the programme
if keyCode(escapeKey)
BreakFlag=1;
break
end

%If the patient pressed a key within a given timescale then record a
'correct response'
if (timeSecs - ResponseSecs)<0.6;
response = 1;
sound(correctSound)

%If the patient pressed a key too late then record an 'incorrect
response'
else
response = -1;
sound (incorrectSound)
break
end

%Avoid kbcheck reporting multiple events as loop is repeated
while KbCheck;
end
break
end

%If no response is made by the patient to the stimulus...
%Record the time and how long it has been since a presentation
SecsNow = GetSecs;
timeSincePresentation = (SecsNow - ResponseSecs);
if timeSincePresentation > 1;
%This means that the patient did not identify the stimulus (response
incorrect)
response = -1;
break
```

```
end
end
%If the ESC key is pressed then break the loop and end the programme
if BreakFlag==1
break
end

%Record the time and brightness of each presentation made
presentationTime(presentationCounter)= (GetSecs - StartExptSecs);
presentationThreshold(presentationCounter)=           SpotLuminance-
AdjustmentFilter1-AdjustmentFilter2-AdjustmentFilter3;
presentationCounter = presentationCounter + 1;

%Adjust the next stimulus presented based on the response given
%If there is a correct response:
if response > 0;
if incrementStep > 0.0; %Indicates the threshold was raised on the
last presentation
%Record the time and brightness of the current threshold (to which a
correct response has been given)
resultTime (thresholdCounter) = (GetSecs - StartExptSecs);
resultThreshold (thresholdCounter) = SpotLuminance-AdjustmentFilter1-
AdjustmentFilter2-AdjustmentFilter3;
thresholdCounter = thresholdCounter + 1;
stopRule = -1; %Indicates to the programme that a correct answer has
been logged and a threshold has been recorded
end
%Ensure that the next presentation given is reduced in brightness by
0.3 log units
incrementStep = -0.3;
WaitSecs (0.5+(2*(rand(1.0))));
End

%If there is an incorrect response:
if response < 0;
incrementStep = 0.1;
WaitSecs (rand(1.0));
end
%Ensure that the next presentation is increased brightness of 0.1 log
units
SpotLuminance = SpotLuminance + incrementStep;
if SpotLuminance > 2
SpotLuminance = 2;
end

%6th step: Reset stimulus intensity when minimum luminance is reached
if SpotLuminance < -0.5;
SecondNDFIlterFlag = SecondNDFIlterFlag + 1;
%Make a sound to alert the investigator a new filter is required
sound (NewFilterSound)
% Ensure the programme knows if this is the 1st or 2nd filter being
brought down
if SecondNDFIlterFlag == 1
%By what value will the brightness be attenuated by the filter?
AdjustmentFilter2 = 2.1;
%How long does the investigator have to bring the filter down?
WaitSecs (10.0)
%Reset the stimulus intensity to maximum brightness with filter in
place
SpotLuminance = SpotLuminance + AdjustmentFilter2;
end
```

```
%Repeat process with a 1.8ND filter if patient reached minimum
brightness again
if SecondNDFIlterFlag == 2
AdjustmentFilter3 = 1.8;
WaitSecs (10.0)
SpotLuminance = SpotLuminance + AdjustmentFilter3;
end
end
end %This ends the search for a threshold

% What happens if the esc key is pushed during this?
if BreakFlag==1
break
end
end
```

%7th step: Generate results

```
%Bring the cursor back
Screen('ShowCursorHelper', window);

%Converts row of presentation times and threshold values into column
format
presentationTime = presentationTime (:);%
presentationThreshold = presentationThreshold (:);
%Plot every recorded presentation graphically
plot(presentationTime, presentationThreshold,'b*')
xlabel('Time(s)')
ylabel('Log Threshold')
axis ([0 1500 -5 1.5])
hold on
%Converts row of correct-response times and correct-response threshold
values into column format
resultTime = resultTime(:);
resultThreshold = resultThreshold(:);
%Plot every recorded correct-response graphically
plot(resultTime, resultThreshold,':ko')
%Fit the final exponential curve to the data
Starting = [1.2,5,40];
options=optimset('Display','off');
Estimates=fminsearch(@myfitExp,Starting,options,resultTime,resultThr
eshold);
fT = Estimates(1)
iT = Estimates(2)
Tau =Estimates(3)
ExpFitTime =0:2.0:300;
ExpFitThreshold   =   Estimates(1)+((Estimates(2)-Estimates(1))*exp(-
ExpFitTime./Estimates(3)));
plot(ExpFitTime, ExpFitThreshold,'r-','LineWidth',2)

%Close the window now that the data has been collected and graphically
plotted
Screen('CloseAll');

%Output all the data to Excel spreadsheet
presentationData = [presentationTime, presentationThreshold]
thresholdData = [resultTime, resultThreshold]
ExpFitTime=ExpFitTime(:);
ExpFitThreshold=ExpFitThreshold(:);
%What folder shall the results be sent to?
```

```
xlswrite('c:\Users\CAD     User\Desktop\Grant\Matlab     results\Dark
Adaptation Results.xls', presentationData,'Model','A14');
xlswrite('c:\Users\CAD     User\Desktop\Grant\Matlab     results\Dark
Adaptation Results.xls', thresholdData,'Model','D14');
xlswrite('c:\Users\CAD     User\Desktop\Grant\Matlab     results\Dark
Adaptation Results.xls', fT,'Model','H3');
xlswrite('c:\Users\CAD     User\Desktop\Grant\Matlab     results\Dark
Adaptation Results.xls', iT,'Model','H2');
xlswrite('c:\Users\CAD     User\Desktop\Grant\Matlab     results\Dark
Adaptation Results.xls', Tau,'Model','H4');
catch
Screen('CloseAll');
```

Appendix V. Flicker threshold MATLAB code

```
% 14 Hz FLICKER THRESHOLD: For Alight Trial use
%
% This programme uses a YES/NO, QUEST driven staircase to determine
contrast
% thresholds for a flickering gaussian blob.
% The code is adapted from Gaboiumdemo, kbDemo and QuestDemo.
% Ver. 1: T.Margrain (28-11-12).
% Modified for the Alight trial by T.Margrain and G Robinson (Mar
2014)
% This version uses a 14Hz Gaussian blob set for 2 degrees at 140cm
% viewing distance (Alight monitor: NEC Multisync PA241W)

% Modifications from V1 include:
% 'simple gamma correction' code obtained online from
% AdditiveBlendingForLinearSuperpositionTutorial.
% Lines of code that were not used before include:
% PsychImaging('AddTask', 'General', 'EnablePseudoGrayOutput') - this
line
% lets us call up all screen output in the range 0-1 (0-100%) rather
than
% grey scale.
%             PsychImaging('AddTask',             'FinalFormatting',
'DisplayColorCorrection',
% 'SimpleGamma');
% This line sets up simple gamma correction in the video output
'pipeline'
%  PsychColorCorrection('SetEncodingGamma', win, gamma); So, all
output is
% gamma corrected automatically.
% This version also allows the 'blob' to occupy a 0-1 range rather
than
% 0-0.5 (line 130). It also changes the slightly misleading variable
% "contrast" to the more accurate "luminance" i.e. the output is
threshold
% luminance (lines 167, 173). The final output (threshold) is log
luminance
% as a fraction of the max screen luminance in cd/m2.


% Step 1: Set up all the relevant parameters
% How many trials?
clear all
trialsDesired = 40;% How many trials?
wrongRight={'wrong','right'}; % What is correct response?
stimFreq = 14; % What is temporal frequency of flickering in Hz?
KbName('UnifyKeyNames'); % Allows keypad press to be recorded as a
response
escapeKey = KbName('ESCAPE'); % Ensures prog can be stopped if
necessary
format compact
avgfps = [];
contrastPresent = [];
falsePositive = 0; % Counts number of false positive responses
LineSpectrum = [256 256 256]; % Draw a line (colour [R,G,B]
LineLength =200;
LineThickness=5;
AssertOpenGL;
```

```
% This programme uses Psychophysics QUEST routines to determine
threshold
% to get these to work it is necessary to provide information about
the
% threshold we are looking for in particular an initial guess at the
% threshold and the standard deviation
% Provide our prior knowledge to QuestCreate, and receive the data
structure % "q".
participant=[];
while isempty(participant) % Display message to input subjects name
    participant=input('Subjects name please: ', 's');
end
tGuess=[];
while isempty(tGuess) % Display message to input an estimate of
threshold
    tGuess=input('Estimate threshold (e.g. -1): ');
end
tGuessSd=[];
while isempty(tGuessSd) % Display message to input an estimate of SD
    tGuessSd=input('Estimate the standard deviation of your guess,
above, (e.g. 2): ');
end
pThreshold=0.82;
beta=3.5;delta=0.01;gamma=0.5;
% beta controls the steepness of the psychometric function (Typically
3.5).
% delta is the fraction of trials on which the observer presses
blindly. %(Typically 0.01).
% gamma is the fraction of trials that will generate response 1 when
% intensity==-inf.
q=QuestCreate(tGuess,tGuessSd,pThreshold,beta,delta,gamma);
q.normalizePdf=1; % This adds a few ms per call to QuestUpdate, but
otherwise the pdf will underflow after about 1000 trials.

% Introduce try and catch failsafe to rescue code in event of prog
crash
try

% Select screen with maximum ID for output window:
screenid = max(Screen('Screens'));

% Open a fullscreen, onscreen window with gray background. Enable
32bpc
% floating point framebuffer via imaging pipeline on it, if this is
possible
% on your hardware while alpha-blending is enabled. We need alpha-
blending
% here to superimpose the gabor blob on the background. The programme
will
% abort if your graphics hardware is not capable of any of this.
PsychImaging('PrepareConfiguration');
PsychImaging('AddTask', 'General', 'FloatingPoint32BitIfPossible');

% Enable bitstealing aka PseudoGray shader: This line is needed so
that
% subsequent screen output is in the range 0-1 i.e. up to 100% of
screen % output. No need to call grey levels.
% It also increases the number of grey scales that can be generated
PsychImaging('AddTask', 'General', 'EnablePseudoGrayOutput');

% Set up the final video output pipeline to include gamma correction
```

```
PsychImaging('AddTask', 'FinalFormatting', 'DisplayColorCorrection',
'SimpleGamma');

% Finally open a window according to the specs given with above
% PsychImaging calls, clear it to a background color of 0.5 aka 50%
% luminance:
[win, winRect]=PsychImaging('OpenWindow',screenid, 0.5);
WaitSecs (0.5);

% Apply the gamma correction to all outputs to the screen. The default
value % here is gamma = 2 however Grant to update monthly throughout
Alight trial
gamma = 1 / 2.227637;
PsychColorCorrection('SetEncodingGamma', win, gamma);
WaitSecs (1);

% Enable alpha-blending, set it to a blend equation useable for linear
% superposition with alpha-weighted source. This allows to linearly
% superimpose gabor patches in the mathematically correct manner,
should
% they overlap. Alpha-weighted source means: The 'globalAlpha'
parameter in
% the 'DrawTextures' can be used to modulate the intensity of each
pixel of
% the drawn patch before it is superimposed to the framebuffer image,
i.e.
% it allows to specify a global per-patch contrast value:
Screen('BlendFunction', win, GL_SRC_ALPHA, GL_ONE);

% Query frame duration: We use it later on to time 'Flips' properly
for an
% animation with constant framerate:
ifi = Screen('GetFlipInterval', win);

% Create a gabor patch: This is 184x184 pixel matrix that has periperal
% values around zero and a central value of 1. The gray scale range
of the
% monitor is 1 at the centre of the gabor.
[x,y] = meshgrid(-100:100, -100:100);
whiteBlob = (exp(-((x/40).^2)-((y/40).^2)));

% Create blob movie, first determine frame rate
rate = 1/ifi;

% Determine number of frames avaliable for a given stimulus frequency
framesAvaliable = rate/stimFreq;

% Determine the step size to get through 360 degrees (1 cycle) in the
% number of frames avaliable
step = 360/framesAvaliable;

% Set up degrees, start a zero and increment in the loop according to
the
% step size
x=-180;

% Get the time at the very start to record the total experimental time
exptStart = Screen('Flip', win);

% Introduce experiment, wait for signal to start
```

```
%Screen('FrameRect', win ,[0,128,0], [540,300,740,500],1);
Priority(2);% Update the priority for Matlab i.e. Avoid interference
from OS

% Give instructions to the patient
Screen('DrawText', win, 'PUSH THE BUTTON WHEN YOU SEE THE CENTRE OF
THE CIRCLE FLICKER', 550, 283, [1,1,1]);

% Draw a white oval to use as a fixation target
Screen('FrameOval', win, [LineSpectrum], [760,400,1160,800]);
Screen ('Flip', win);
WaitSecs (4);
Screen('HideCursorHelper', win);
Screen ('Flip', win); % Flipping removes the text from the screen
```

```
% Step 2: Start main experiment loop (threshold testing begins)

for k=1:trialsDesired;
Screen('FrameOval', win, [LineSpectrum], [760,400,1160,800]);
Screen ('Flip', win);
% First pick up the threshold recommended by QUEST
tTest=QuestQuantile(q); % Recommended by Pelli (1987).

% Unlog tTest, this ensures that the luminance of the stimulus is
controlled
luminance = 10^tTest;

% Generate the textures to be displayed during each frame, assume 60Hz
so
% going from 1 to 120 will be a 2s presentation
for i=1:120;

%Need to change contrast to a fraction
Blob = whiteBlob * (luminance) * sind(x);
gabortex(i)=Screen('MakeTexture', win, Blob, [], [], 2);
x=x+step;
end;

% Wait a random period of time before giving the presentation
randomdelay = rand*6;
StartSecs = GetSecs;
timeNow=0;
while timeNow <randomdelay
SecsNow = GetSecs;
timeNow = (SecsNow - StartSecs);

% Command the keyboard to check for input
[ keyIsDown, timeSecs, keyCode ] = KbCheck;

% if a key is pushed:
if keyIsDown
falsePositive = falsePositive+1; % Count the incorrect responses
Beeper(400) % Sound to indicate response
while KbCheck; end % this avoids KbCheck reporting multiple events
end
end
```

```
% Was the stimulus seen or not seen?
response = 0;
count = 0; % This is needed to count the number of presentations
vbl = Screen('Flip', win);
tstart = vbl; % records the time the main presentation loop started
for i=1:120;
Screen('DrawTexture', win, gabortex(i),[],[],45);
Screen('FrameOval', win, [LineSpectrum], [760,400,1160,800]);

% Check the frame presentation time, does it always match the frame
refresh
% rate?
vbl = Screen('Flip', win, vbl + ifi/2);
lastTime = vbl;
count = count+1; % Will count up to 120

% check for keyboard for a correct response during presentation
[ keyIsDown, timeSecs, keyCode ] = KbCheck;
if keyIsDown % if a key is pushed this is what to do
response=1; % flags a correct response
break % breaks out of the presentation loop
end
end;

% Clear the screen of any residual gabor and get time stamp
tend = Screen ('Flip', win); % records the time the presentation
stopped
Screen('FrameOval', win, [LineSpectrum], [760,400,1160,800]);
Screen ('Flip', win);

% Check frames per second for this trial, store result in array avgfps
avgfps(k) = count / (tend - tstart);

% Now get the participants response
ResponseSecs = GetSecs;% gets the time the stimulus was flipped out

% Wait for a response for three seconds, if in the 1st second = correct
while 1
[ keyIsDown, timeSecs, keyCode ] = KbCheck; % Did they push a button?
if keyIsDown % This bit of code is only executed if a button is pushed
if (timeSecs - ResponseSecs)<1; % Was their response in time?
response = 1; %this 'flag' means the response was correct
Beeper (1000) % make a 'beep' sound to indicate correct response
recognised

else
response = 0; %this means the response was incorrect (in this case
too slow)
Beeper (600) % make a different sound to indicate response too slow
falsePositive = falsePositive+1;% counts the incorrect responses
break
end

while KbCheck; end % this avoids KbCheck reporting multiple events
break
end

% Now, if no button was pressed
SecsNow = GetSecs;
timeSincePresentation = (SecsNow - ResponseSecs);
```

```
% If no response within 1s of stimulus, its missed, get out of loop
if timeSincePresentation > 4;
break
end % waiting for response or time up
end

% Print the results for this particular trial
fprintf('Trial          %3d          at          %5.2f          is
%s\n',k,tTest,char(wrongRight(response+1)));
LuminancePresent(k)=tTest;

% Now update the QUEST routines with the last threshold value (this
is all in % logs) and let it know if the participant responded
correctly (1) or
% incorrectly (0)

% Add the new datum (actual test intensity and observer response) to
the
% database
q=QuestUpdate(q,tTest,response);
end

% Step 3: Obtain and export results

% Display cursor again now threshold testing has finished
Priority(0);% Resest normal priority
Screen('ShowCursorHelper', win);

% Ask Quest for the final estimate of threshold.
t=QuestMean(q); % Recommended by Pelli (1989) and King-Smith et al.
(1994).
sd=QuestSd(q);
fprintf('Final threshold estimate (mean±sd) is %.2f ± %.2f\n',t,sd);

% Determine total experimental time
exptEnd = Screen('Flip', win);
exptTotal = exptEnd - exptStart

% Print out the number of false positives
falsePositive

% Close onscreen window, release all resources:
Screen('CloseAll');

% Plot results onto graph for quick viewing
figure(1)
k=1:trialsDesired;
plot (k,avgfps)
xlabel ('Trial')
ylabel ('Frames / sec')

% Plot the stimuli presented
figure(2)
k=1:trialsDesired;
plot (k,LuminancePresent, 'ob')
xlabel ('Trial')
ylabel ('Log luminance')
```

```
% Transfer all the key data to Excel
LuminancePresent = LuminancePresent(:); % This changes the vector from
a row to a column
trialNumber = k(:);
today = now; % this represents the current date and time in Excel
name ={participant};
% Where to transfer the data to?
xlswrite('c:\Users\CAD User\Desktop\Grant\Matlab results\14Hz Flicker
Results.xls', today,'Sheet1','B3');
xlswrite('c:\Users\CAD User\Desktop\Grant\Matlab results\14Hz Flicker
Results.xls', today,'Sheet1','B4');
xlswrite('c:\Users\CAD User\Desktop\Grant\Matlab results\14Hz Flicker
Results.xls', name,'Sheet1','B5');
xlswrite('c:\Users\CAD User\Desktop\Grant\Matlab results\14Hz Flicker
Results.xls', exptTotal,'Sheet1','E3');
xlswrite('c:\Users\CAD User\Desktop\Grant\Matlab results\14Hz Flicker
Results.xls', trialNumber,'Sheet1','A8');
xlswrite('c:\Users\CAD User\Desktop\Grant\Matlab results\14Hz Flicker
Results.xls', LuminancePresent,'Sheet1','B8');
xlswrite('c:\Users\CAD User\Desktop\Grant\Matlab results\14Hz Flicker
Results.xls', t,'Sheet1','E4');
xlswrite('c:\Users\CAD User\Desktop\Grant\Matlab results\14Hz Flicker
Results.xls', sd,'Sheet1','E5');
xlswrite('c:\Users\CAD User\Desktop\Grant\Matlab results\14Hz Flicker
Results.xls', falsePositive,'Sheet1','E6');

% The following code allows the source error to be identified if the
programme does not run

catch
Screen('CloseAll');
rethrow(lasterror);
psychrethrow(psychlasterror);
end
```

Appendix VI. Cross sectional study consent form and CRFs

School of Optometry
Cardiff University
Maindy Road
Cardiff
CF24 4LU

Study Title: Low-Level Night-Time Light Therapy for Age-Related Macular Degeneration

Protocol: 11/01/15; Version: 16

Names of Researchers: Dr Alison Binns
Dr Tom Margrain
Mr David Grant Robinson

	Please initial
1. I confirm that I have read and understand the Alight participant information sheet dated 04/03/15. I have had the opportunity to consider the information, ask questions and have had these answered satisfactorily.	☐
2. I understand that my participation is voluntary and I am free to withdraw at any time without giving reason, without my medical care or legal rights being affected.	☐
3. I agree that my details can be used by the research team and understand that my personal details will be treated as **STRICTLY CONFIDENTIAL.**	☐
4. I agree to take part in the study in accordance with the terms set out in the consent form and ALight information sheet.	☐
5. I would like to receive a summary of the research findings at the end of the study.	☐

Name of Patient	Date	Signature
Name of person taking consent	**Date**	**Signature**

PART A: Patient Details

Today's date ☐☐ / ☐☐ / ☐☐☐☐ (d d / m m / y y y y)

Patient's **surname**

Patient's **first name**

Patient's date of birth ☐☐ / ☐☐ / ☐☐☐☐ (d d / m m / y y y y)

Patient's address _____

_____

_____

Patient's telephone number _____

PART B: Explain study; ask if patient wants to take part

	Yes	No
Has the patient read the study information sheet?	☐	☐
Has a full explanation of the study been provided?	☐	☐

Does the patient want to take part? ☐ Yes, consent ☐ Need more time, *review at next clinic* ☐ No

PART C: Audit Information

Gender ☐ Male ☐ Female

Ethnicity ☐ White ☐ Black / Black British ☐ Asian / Asian British ☐ Other Ethnic Group (please specify) _____

Patient ID ☐☐☐☐☐☐☐☐

THE COLLEGE OF OPTOMETRISTS

ALIGHT AMD LIGHT TRIAL

NHS University Hospitals Bristol NHS Foundation Trust

PART A: Patient ID

Study Eye (please tick appropriate box) Right ☐ Left ☐

Part B: Screening evaluation

	Right Eye				Left Eye			
LOCS III Grade	**NC**				**NC**			
	NO				**NO**			
	C				**C**			
	P				**P**			
Fundus Appearance								
AMD Status (early, nAMD, GA)								
Drusen volume								
Van Herick Grade *(Please tick appropriate box)*	G1	G2	G3	G4	G1	G2	G3	G4
AREDS Simplified Grade *(Please tick appropriate box)*	G0	G1	G2	G3	G4			

Visual Acuity	Right Eye	Left Eye
BCVA *(ETDRS number of letters)*		

PART C:

a) Check inclusion criteria	Yes	No
The patient is between 55-88 years old	☐	☐
The patient has visual acuity better than 40 letters in study eye	☐	☐
The patient has grade 0 or grade 1 AMD (AREDS simplified scale)	☐	☐
The patient can speak and understand English	☐	☐

If NO for any box above, the patient needs to be excluded: Skip to Part E

b) Check exclusion criteria	Yes	No
The patient has ocular pathology other than macular disease	☐	☐
The patient has a Van Herrick angle of 1 or 0	☐	☐
The patient has significant systemic disease known to affect visual function (e.g. diabetes, Parkinson's disease, Alzheimer's disease).	☐	☐
The patient has cognitive impairment (MMSE)	☐	☐
The patient is taking medication known to affect visual function	☐	☐

If YES for any box above, the patient needs to be excluded

PART D: Eligibility *Please tick the appropriate box*

Patient is eligible and wants to take part ☐ Patient is ineligible/does not want to take part ☐

PART E: Patient's name and investigator's signature

1) Re-state **patient's** name:_____ Date:_____

2) **Investigator's** signature:_____

Part F: Data Collection

Autorefractor Rx	RE	
	LE	

Quality of Fundus Photograph *(Tick appropriate box)*	RE	Acceptable		Unacceptable *(Repeat)*	
	LE	Acceptable		Unacceptable *(Repeat)*	
Quality of OCT Image *(Tick appropriate box)*	RE	Acceptable		Unacceptable *(Repeat)*	
	LE	Acceptable		Unacceptable *(Repeat)*	

Colour Vision

Diagnosis	
Certification	
r-g threshold	
y-b threshold	

14Hz Flicker Thresholds

Contrast Threshold	
Standard deviation	

Dark Adaptometry

Pupil Size *(mm)*

Cone Tau	
Time to RCB	

Appendix VII. Patient information sheet

Information Booklet for participants

Retinal Treatment and Research Unit
Clinical Research Unit
Bristol Eye Hospital
Lower Maudlin Street
Bristol
BS1 2LX

Tel: 0117 342 4770
Fax: 0117 342 4891

Dear Sir/Madam,

Cardiff University in collaboration with Bristol Eye Hospital would like to invite you to take part in our study investigating the effect of low-level night-time light therapy on age-related macular degeneration.

Before you decide, we would like you to understand why the research is being done and what it would involve for you. Please take the time to read this information sheet, feel free to talk to family and friends about the study if you wish. Before commencing the study we will go through the information sheet with you and answer any questions you may have. Please ask us if there is anything that is not clear.

What is this study about?

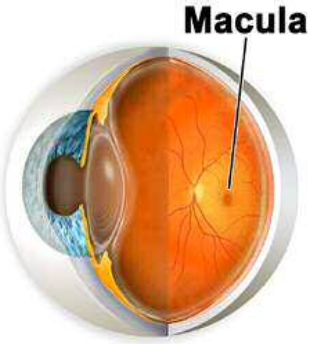

Age-related macular degeneration (AMD) is a common eye condition among people aged 50 or older. It damages the macula, the part of the retina that gives us clear, central vision. This makes activities such as reading, driving and recognising familiar faces more difficult. New evidence suggests that a lack of oxygen in the retina may be involved in the development of AMD, especially at night-time. By exposing the eye to very dim light during the night, more oxygen is available for the eye to function better. Practically, this would involve wearing a comfortable sleep mask at night that emits a very dim green light. The sleep mask is currently being evaluated in a similar study as a treatment for another eye condition, diabetic retinopathy.

The main aim of this study is to determine if wearing this sleep mask can stop the progression of early AMD.

This trial forms part of a postgraduate doctoral research project.
You have been asked to take part in this research because we are looking for 60 volunteers with early AMD in one eye and wet AMD in the other eye to help us find out how effective the sleep mask is at reducing the progression of both wet and early AMD. You would be randomly allocated either to receive a sleep mask to wear overnight for 12 months or to receive your usual hospital care only (your regular Lucentis ® clinic appointments).

What will happen to me if I take part?

1. Those who wish to take part in the study will have an **initial appointment** of up to 60 minutes with one of our team for you to ask any questions you may have and provide your consent to participating in the study. We will ask you some questions regarding your general health, vision, sleeping habits, vitamin supplementation, smoking history and memory, and let you know if you are eligible to take part in

the study. If you are eligible and wish to take part, we will ask for your GP details so that we can inform them that you are taking part in the study. If you are eligible to take part, we will also take several measurements at this point to measure the sensitivity of the eyes after a period of time in the dark. This appointment will take place just before your Lucentis ® clinic, so that no extra visits to the hospital are needed.

2. If you are eligible and willing to take part, a **second appointment** will take place just before your third Lucentis ® clinic. This will take around 75 minutes. We will put a drop in each eye to make your pupils larger, if not already inserted by the staff in the Lucentis ® clinic. We will then **take several measurements** to monitor the sensitivity of the eyes after a period of time in the dark and in response to a flickering target, and we will assess your colour vision. This will involve looking at a computer screen and reporting the presence of different targets by pressing a button. A computer will then decide if you are in **the treatment group** (given a light mask) or **the control group** (not given a light mask) on the basis of chance. If assigned to the treatment group, you will be shown how to use and fit the mask and you will receive written instructions to take home with you.

3. Each month, when you attend for your regular Lucentis ® clinic appointment, we will meet up with you at the clinic to see how you are getting on. We will also ask some questions about your sleep quality. This will take about 10 minutes. The light mask needs to be replaced every 12 weeks. At your monthly Lucentis® Clinic visits, if you are in the treatment group, we will ask you to bring along your used mask, so that we can check that it is working properly, provide you with a new fabric cover to the mask, and give you a new one to take home every 3 months. We will also access some electronic data on the mask, which tells us how many hours it has been worn each night for the past month. In addition, with your permission, the study investigators will access your medical records each month as you attend your regular clinic

appointments. This will allow us to monitor your vision, and the health of your eyes throughout the year.

4. At the end of the 12 month period, there will be a **final appointment** before your Lucentis ® clinic. This will take about 75 minutes and include the same tests as the second appointment, with the addition of some questions about how you found the treatment and a questionnaire about your sleeping habits. The sleep masks will then be returned to the study investigator.

What are the possible benefits of taking part?

If it is found to be effective, this therapy could slow or stop the progression of AMD. As this is the first trial of its kind, a larger study with more participants would then be carried out to confirm the results. All people who are found to be suitable and are enrolled in the trial will receive a complimentary £10 gift voucher.

What does the treatment involve?

1. If you are in the **control group**, you will receive treatment as usual for your eye with wet AMD, but will receive no additional treatment.

2. If you are in the **treatment group**, you will receive treatment as usual for your eye with wet AMD, and will be given a light mask to wear each night for a year.

3. The light mask consists of a fabric eye mask, containing a small plastic pod which houses light emitting diodes (LEDs). It is held in place by an adjustable fabric strap, which passes around the back of the head. The light mask provides a low level of illumination to the eyes at night, which shines through the eyelids to illuminate the back of the eyes when you are asleep. The light provided is approximately half as bright as the average brightness of a television set.

4. It is designed to be worn when you are in bed at night. The mask should be removed if you need to get up at any time during the night, for example to go to the bathroom.

Are there any risks involved?

1. Low-level night-time light therapy has been **shown to be safe**. However, because this is the first study in people with AMD, safety will be a priority in this study. We will be checking that sleep quality is not affected by a monthly check-up and checking the health of your eyes by looking at the photographs taken at your regular Lucentis® clinic.

2. It is not anticipated that you will experience any discomfort associated with the mask, however should you feel at all uncomfortable wearing the mask after your Lucentis injection, we advise you to discontinue wear for a few nights, until your eye feels less tender. We will ask you to report any such problems when we see you each month at the clinic.

3. The drops used to enlarge your pupil are the same as those used at every Lucentis ® clinic you attend. They may make your vision temporarily a little blurred and make you sensitive to bright lights for about 6 hours. During this time we advise you not to drive or to operate any dangerous machinery. Very rarely some people can develop an adverse reaction to these drops. In **less than 1 in 20,000 people** they may cause a rise in eye pressure, known as closed angle glaucoma. The symptoms of this can include, pain, a red eye and halos around lights. In the extremely unlikely event that this should occur, you should contact us urgently on the numbers shown below. If we are unavailable then you should go straight to eye casualty for assessment and treatment with other eye drops to bring the pressure back down.

Do I have to take part?

No – it is up to you whether you decide to take part or not. Participation in this study is purely voluntary. If you do decide to take part, you will be given this information sheet to keep and will be asked to sign a consent form. You can withdraw at any time without giving a reason. Please note that if you do not wish to take part in the study it will not affect your current or future care.

What if there is a problem?

If you do have a concern about any aspect of this study, you should ask to speak to the researchers (contact details below) who will do their best to answer your questions. If you remain unhappy and wish to complain formally, you can do this through the NHS Complaints Procedure – details can be obtained from the researchers.

What if I have any questions?

Please ask. We are very happy to discuss any aspect of the study. *Please do not send personal information regarding your medical status by e-mail, as this is not a secure means of communication.*

- **Grant Robinson (Robinsondg2@cf.ac.uk)**
- **Dr Alison Binns (BinnsAM@cf.ac.uk)**
- **Dr Tom Margrain (MargrainTH@cf.ac.uk)**
- **Tel: 02070408495**
- **School of Optometry and Vision Sciences, Cardiff University.**

Where can I seek independent advice?

For any concerns about your rights as a participant or any complaints, please contact the Patient Advice and Liaison Service (PALS), or call into our drop in service, located on Level 2, Queens Building, Bristol Royal Infirmary.

Contact the 'Patient Support and Complaints Team, Trust Headquarters, University Hospitals Bristol, Malborough Street, Bristol. BS1 3NU. (tel: 01173423604 or e-Mail pals@uhbristol.nhs.uk).

What will happen if I don't want to carry on with the study?

You are free to withdraw at any time without giving a reason; however we will retain non identifiable data collected up to your withdrawal. Please note that if you do not wish to take part in the study it will not affect your current or future care.

What if there is a problem?

In the unlikely event that harm should occur as a result of negligence associated with this study, cover is provided by the Cardiff University insurance policy.

Will my taking part in this study be kept confidential?

All information collected during the study will be processed and stored securely by the researchers using password-protected systems. Your personal information will be coded and only the researchers will be able to identify you during the study. All procedures are compliant with the Data Protection Act 1998. With your permission, if you decide to take part, we will inform your GP of your participation in the study.

What will happen to the results of the research study?

The study results will be analysed and presented at national and international meetings and in scientific journals. Identities of participating volunteers will not be revealed in any resulting published material. If you wish to be provided with a summary of the research findings at the end of the study please tick the appropriate box on the consent form.

Who is funding and reviewing the research?

This study is being organised by Cardiff University in collaboration with Bristol Eye Hospital, and funded by the College of Optometrists. The light mask manufacturer, Polyphotonix Medical Ltd, is providing the light masks free of charge. This study was reviewed and approved by the College of Optometrists, the Greater Manchester South Research Ethics Committee and UH Bristol NHS Foundation Trust.

Appendix VIII. ALight trial consent form and CRFs

Study Title: Low-Level Night-Time Light Therapy for Age-Related Macular Degeneration

Protocol: 22/09/14; Version: 15

Names of Researchers: Dr Alison Binns
Dr Tom Margrain
Mr Grant Robinson

	Please initial
6. I confirm that I have read and understand the ALight participant information sheet dated 22/09/2014. I have had the opportunity to consider the information, ask questions and have had these answered satisfactorily.	☐
7. I understand that my participation is voluntary and I am free to withdraw at any time without giving reason, without my medical care or legal rights being affected.	☐
8. I agree that my details can be used by the research team and understand that my personal details will be treated as STRICTLY CONFIDENTIAL.	☐
9. I understand that I will be selected for either the treatment or control group on the basis of chance and agree to comply with that treatment for the 12 month duration of the study.	☐
10. I agree to take part in the study in accordance with the terms set out in the consent form and ALight information sheet.	☐
11. I agree that the investigators may inform my GP that I am participating in this trial	☐
12. I agree that the investigators may access my medical records on a monthly basis.	☐
13. I would like to receive a summary of the research findings at the end of the study.	☐

Name of Patient	**Date**	**Signature**
Name of person taking consent	**Date**	**Signature**

SCREENING VISIT
PART A: Patient Details

Today's date ☐☐ / ☐☐ / ☐☐☐☐ (d d / m m / y y y y)

Patient's **surname** ☐☐☐☐☐☐☐☐☐☐☐☐☐☐☐☐☐☐☐☐

Patient's **first name** ☐☐☐☐☐☐☐☐☐☐☐☐☐☐☐☐☐☐☐☐

Patient's date of birth ☐☐ / ☐☐ / ☐☐☐☐ (d d / m m / y y y y)

Patient's Address _____

_____

_____

_____

Patient's Telephone number Daytime : _____

Mobile/other : _____

PART B: Explain study; ask if patient wants to take part

	Yes	No
Has the patient read the study information sheet?	☐	☐
Has a full explanation of the study been provided?	☐	☐

Does the patient want to take part?

☐ Yes, *sign consent form*

☐ Need more time, *review at next Lucentis clinic*

☐ No, *skip to part F*

PART C: Audit Information

Gender ☐ Male ☐ Female

Ethnicity

☐ White ☐ Black / Black British

☐ Asian / Asian British ☐ Other Ethnic Group (please specify) _____

Patient ID (initials + 4 digit code) ☐☐0 1☐☐☐☐

PART A: General Health

Medical Illnesses (*tick all that apply*)

☐ Diabetes ☐ Alzheimer's ☐ None

☐ Parkinson's ☐ Motor neurone disease

☐ Other: specify _____

Current medication

PART B: Ocular Status

	Right Eye				**Left Eye**			
BCVA *(ETDRS number of letters)*								
Ocular Diagnosis *(Tick all that apply)*	Early AMD		nAMD		Early AMD		nAMD	
	Normal		Geographic Atrophy		Normal		Geographic Atrophy	
	Other		*Please Specify…*		Other		*Please Specify…*	

PART C: Assessment of the Ocular Media and Fundus

	Right Eye				**Left Eye**			
LOCS III Grade	**NC**				**NC**			
	NO				**NO**			
	C				**C**			
	P				**P**			
Fundus Appearance								
AMD Status (early, nAMD, GA)								
Van Herick Grade ***Exclude if Grade ≤1***	G1	G2	G3	G4	G1	G2	G3	G4
AREDS Simplified Grade *(Please tick appropriate box)*	G0	G1	G2	G3	G4			

PART D: Cognitive Screening and Visual Function Questionnaire

Cognitive Screening Test

I would like you to repeat the following three words: APPLE, PENNY, TABLE

(Repeat until the patient registers all three words)

A1	What is the day?		Correct	Yes ☐	No ☐	
A2	What is the month?		Correct	Yes ☐	No ☐	
A3	What is the year?		Correct	Yes ☐	No ☐	
A4	Spell WORLD backwards	DLROW	Number correct	☐		

(Final cognitive screening question A5 follows the questions on visual function)

Cognitive Screening Test

What were the 3 words that I asked you at the beginning?

1) _____
2) _____
3) _____

(apple, penny, table)

Number correct _____

Did the patient pass the cognitive screen?

Yes (1) (day, year, month correct; 3/5 WORLD; remember at least 2 words)
No (0) **Patient is ineligible** *(Skip to Part E)*

PART E: a) Check inclusion criteria

	Yes	No
The patient is between 55-88 years old	☐	☐
The patient has visual acuity better than 40 letters in study eye	☐	☐
The patient is receiving treatment for neovascular AMD in one eye only	☐	☐
The patient has early AMD in the study eye	☐	☐
It is within 1 month of 3rd anti-VEGF injection	☐	☐
The patient is willing to adhere to treatment for the duration of the trial	☐	☐
The patient has sufficient hearing to permit use of the telephone	☐	☐
The patient can speak and understand English	☐	☐

If NO for any box above, the patient needs to be excluded: Skip to Part F

b) Check exclusion criteria	Yes	No
The patient has advanced AMD in both eyes	☐	☐
The patient has ocular pathology other than macular disease	☐	☐
The patient has systemic disease that would affect visual function or compromise participation in a one year study	☐	☐
The patient has cognitive impairment (MMSE)	☐	☐
The patient is taking medication known to affect visual function	☐	☐
The patient wears an oxygen mask at night	☐	☐
The patient has a history of falls or high risk of falling	☐	☐

If YES for any box above, the patient needs to be excluded: Skip to Part F

PART F: Eligibility *Please tick the appropriate box*

Patient is eligible and wants to take part (*go to Part F*) ☐

Patient is *ineligible/ does not want to take part (skip to part G*) ☐

PART G: Patient is eligible and wants to take part, record patient and GP contact details

Patient's telephone number	☐☐☐☐☐☐☐☐☐☐☐
Best days / times to contact patient?	
GP name	
GP address	
GP telephone number	☐☐☐☐☐☐☐☐☐☐☐

PART H: Patient's name and investigator's signature

1) Re-state **<u>patient's</u>** name:

_____

2) **<u>Investigator's</u>** signature:

_____

Date

PART I: Health Questionnaires *(Eligible participants only)*

Vitamin Supplementation

Are you currently taking vitamin supplements regularly? ☐ yes ☐ no

If so, for how many years have you been taking them? ☐ years

If known, what is the name of the vitamins you are taking?

Smoking History

1) Are you currently a smoker? ☐ yes ☐ no *(skip to Q4)*
2) How many cigarettes do you smoke per day? ☐ per day
3) For how many years have you been smoking? ☐ years
4) Have you ever smoked in the past? ☐ yes ☐ no (*skip Q5-7*)
5) How long ago did you give up? ☐ months ☐ years
6) On average how many cigarettes did you smoke each day? ☐ per day
7) For how many years did you smoke ☐ years

Part J: Dark Adaptometry

Study Eye (please tick appropriate box) Right ☐ Left ☐

Time of dilation **Drop used**

Full Dilation? **Time additional drop instilled?**

Yes		No	

Time bleach started **Pupil size (mm)**

Cone tau	
RCB	

Quality of data

Acceptable		Unacceptable *(repeat at baseline)*	

BASELINE VISIT

PART A: Patient ID

		0	1				

Study Eye (please tick appropriate box) Right ☐ Left ☐

PART B: Assessment of the Ocular Media and Fundus

Quality of Fundus Photograph *(Tick appropriate box)*	RE	Acceptable		Unacceptable *(Repeat)*	
	LE	Acceptable		Unacceptable *(Repeat)*	
Quality of OCT Image *(Tick appropriate box)*	RE	Acceptable		Unacceptable *(Repeat)*	
	LE	Acceptable		Unacceptable *(Repeat)*	

	Right Eye		**Left Eye**		
Fundus appearance					
Drusen Volume (study eye) 3mm^2					
Drusen Volume (study eye) 5mm^2					
AMD Status (early, nAMD, dry AMD)					
AREDS Simplified Grade *(Please tick appropriate box)*	G0	G1	G2	G3	G4

PART C: Reassessment of Participants Eligibility (Part 1)

Participant still meets eligibility criteria	Yes		No					
Participant still willing to participate in the study			Yes		No		Initial	

PART D: Tests of Visual Function

Study Eye (please tick appropriate box)	Right		Left	

	Right Eye	Left Eye
Auto-refraction		
Spectacle Prescription		

Visual Acuity	Right Eye	Left Eye
BCVA *(ETDRS number of letters)*		

Colour Vision

Diagnosis	
Certification	
r-g threshold	
y-b threshold	

14Hz Flicker Thresholds

Contrast Threshold	
Standard deviation	

Dark Adaptometry

Quality of data obtained at screening visit	Acceptable		Unacceptable	

If 'Unacceptable' then perform dark adaptometry and document results below.

				Time of dilation

	Drop used

Yes		No		**Full Dilation?**

Time of drop instillation				

Time bleach started				

Pupil Size *(mm)*	

Cone tau	
RCB	

PART E: Reassessment of Participants Eligibility (Part 2)

Participant still meets eligibility criteria	Yes		No	

Participant still willing to participate in the study	Yes		No		Initial	

PART F: Randomisation Record

Envelope Number													
Group Allocation	Intervention		Control										
Sleep masks provided	Date							Time					
		d	*d*	*m*	*m*	*y*	*y*		*24 hour clock*				

Sleep mask hours programmed for use (8 hour window)	Start Time					
	End Time					
		24 hour clock				

Sleep mask dates for use	Start Date						
		d	*d*	*m*	*m*	*y*	*y*
	End Date						
		d	*d*	*m*	*m*	*y*	*y*

Training provided	Date							Time					
		d	*d*	*m*	*m*	*y*	*y*		*24 hour clock*				

Reprise follow-up appointments information	Yes		No			
Copy of PSQI given	Yes		No			
£10 gift voucher given?	Yes		No		Declined	
GP information letter sent?	Yes		No			

MONTHLY VISIT

PART A: Patient ID

		0	1				

Study Eye (please tick appropriate box) Right ☐ Left ☐

Month of Study (1-11) ☐

PART B: Questionnaires

Semi-Structured Questionnaire

Have you experienced any new medical problems over the past month? If yes, please describe.	
How have you been getting on with your light mask?	
Have you been wearing the light mask every night?	
For approximately how many hours do you wear the mask at night?	
Has the light mask been comfortable to wear? Could you grade this on a scale of 1-10, where 1 is so comfortable that you aren't aware that the mask is there, and 10 is so uncomfortable that you can't bear to wear it.	
If the mask is not completely comfortable, please could you describe the sources of discomfort e.g. the strap, the pressure of the mask on the face,	
Have you experienced any problems with sleeping when using the light mask? If yes, do you feel that this due to the brightness of the light, or to the physical sensation of wearing the mask?	
Have you had any problems in operating the mask? If so, please describe.	
Do you have any concerns or questions about the mask and its use?	

Is there anything else you would like us to know about your experience of wearing the light mask?	

PART C: Current Mask Information

Current light mask start date						
	D	D	M	M	Y	Y
Current light mask end date						
	D	D	M	M	Y	Y
1) Compliance data exported? (Please tick appropriate box)		Yes		No		
2) Retraining provided? (Please tick appropriate box)		Yes		No		
3) New mask issued? (Please tick appropriate box)		Yes (go to part D)		No (go to part E)		

Part D: New Mask Information

4) New light mask start date						
	D	D	M	M	Y	Y
5) New light mask end date						
	D	D	M	M	Y	Y

Part E: Mask maintenance

1) New fabric strap fitted? (Please tick appropriate box)	**Yes**		**No**	

Part F: Monthly Medical Record Assessment

Quality of Fundus Photograph *(Tick appropriate box)*	RE	Acceptable		Unacceptable	
	LE				
Quality of OCT Image *(Tick appropriate box)*	RE	Acceptable		Unacceptable	
	LE				

	Right Eye				**Left Eye**
Fundus appearance					
Drusen Volume (study eye) 3mm²					
Drusen Volume (study eye) 5mm²					
AMD Status (early, nAMD, dry AMD)					
AREDS Simplified Grade *(Please tick appropriate box)*	G0	G1	G2	G3	G4

Conversion to wet AMD in study eye? (Please tick appropriate box)	**Yes – Withdraw from study and inform CI**		**No**	

Any other change in medical status (systemic / ocular)?	**Yes**		**No**	

FINAL VISIT

PART A: Patient ID			0	1				

Study Eye (please tick appropriate box) Right ☐ Left ☐

PART B: Assessment of the Ocular Media and Fundus

Quality of Fundus Photograph *(Tick appropriate box)*	RE	Acceptable		Unacceptable *(Repeat)*	
	LE	Acceptable		Unacceptable *(Repeat)*	
Quality of OCT Image *(Tick appropriate box)*	RE	Acceptable		Unacceptable *(Repeat)*	
	LE	Acceptable		Unacceptable *(Repeat)*	

	Right Eye		**Left Eye**	
LOCS III Grade	**NC**		**NC**	
	NO		**NO**	
	C		**C**	
	P		**P**	
Fundus Appearance				
AMD Status (early, nAMD, GA)				
Drusen Volume (study eye) 3mm²				
Drusen volume (study eye) 5mm²				

AREDS Simplified Grade *(Please tick appropriate box)*	G0	G1	G2	G3	G4

PART C: Tests of Visual Function

Study Eye (please tick appropriate box)	Right		Left	

Visual Acuity	Right Eye	Left Eye
BCVA *(ETDRS number of letters)*		

Colour Vision

Diagnosis	
Certification	
r-g threshold	
y-b threshold	

14Hz Flicker Thresholds

Contrast Threshold	
Standard deviation	

Dark Adaptometry

Pupil Size *(mm)*		Cone Tau	
		Time to RCB	

Appendix IX. Table of ALight trial baseline characteristics

				LOCS III grade				Smoking history	Supplement history
Study ID	Study group	AREDS grade	BCVA (ETDRS score)	NC	NO	C	P	Pack years	Years taken
MJ010001	Intervention	2	-0.04	2	2	1	1	15.00	0.0
MA010002	Intervention	4	0.22	2	2	1	1	0.00	3.0
MN010003	Intervention	2	-0.10	2	2	1	1	40.00	0.0
JC010004	Control	3	-0.12	0	0	0	0	50.00	0.0
JN010005	Control	4	-0.04	0	0	0	0	0.00	2.0
AS010006	Control	4	-0.06	1	1	1	1	5.60	0.5
EA010007	Control	4	0.30	2	2	2	1	20.00	0.0
JW010008	Control	3	0.16	2	2	2	1	0.00	0.0
FC010009	Intervention	3	0.24	0	0	0	0	5.75	0.0
JE010010	Intervention	3	0.08	0	0	0	0	19.60	0.0
JC010011	Control	3	0.22	2	2	2	0	5.25	2.0
CS010012	Intervention	4	0.24	2	2	0	0	5.25	2.0
LA010013	Control	3	0.26	2	2	2	0	0.00	0.0
JG010014	Intervention	3	0.18	2	2	1	1	0.00	0.0
GP010015	Control	4	0.10	2	2	1	0	0.00	0.0
CA010016	Intervention	4	0.02	0	0	0	0	3.00	2.0
JW010017	Control	2	0.28	0	0	0	0	0.00	0.0
GW010018	Intervention	3	-0.10	0	0	0	0	21.00	4.0
JB010019	Intervention	3	0.02	0	0	0	0	15.00	0.0
AN010020	Control	2	0.16	2	1	2	1	0.00	0.0
RJ010021	Intervention	3	-0.12	1	0	0	0	7.50	1.0
AB010022	Control	4	0.06	2	2	0	0	0.00	0.0
MB010023	Control	4	-0.04	2	2	0	0	5.00	2.0
RH010024	Intervention	2	0.28	2	2	2	1	30.00	0.0
CG010025	Control	2	0.00	2	2	1	1	42.00	0.0
MA010026	Control	4	0.20	2	1	1	1	0.00	1.0
DJ010027	Control	2	-0.16	2	1	1	0	15.00	0.0
KW010028	Intervention	2	0.20	2	2	0	0	0.00	0.0
MH010029	Control	3	0.10	0	0	0	0	45.00	1.0
JF010030	Control	4	-0.04	2	2	0	0	0.00	1.0
DB010031	Intervention	2	-0.16	2	2	1	1	52.50	0.0
AB010032	Intervention	3	0.08	2	2	2	1	0.00	5.0
SG010033	Intervention	3	0.02	0	0	0	0	0.00	2.0
GF010034	Intervention	3	0.30	2	2	1	0	0.00	0.0
RG010035	Intervention	2	0.02	0	0	1	0	70.00	0.0
ML010036	Control	3	0.20	2	2	2	1	0.00	0.0
WB010037	Intervention	4	0.20	2	2	2	0	0.00	0.0
HB010038	Control	4	0.18	1	1	0	0	2.25	0.0
JH010039	Control	4	0.08	2	2	1	1	0.00	0.0
BP010040	Intervention	4	0.26	0	0	0	0	30.00	0.0
BJ010041	Intervention	3	0.00	0	0	0	0	50.00	0.0
VB010042	Intervention	3	-0.04	0	0	0	0	0.00	1.0
JW010043	Control	3	0.06	2	2	2	0	5.00	0.0
NE010044	Control	2	-0.04	1	1	0	0	0.00	0.0
RH010045	Intervention	4	0.00	2	2	0	0	2.00	0.0
GL010046	Intervention	3	0.04	0	0	1	0	0.00	0.0
PS010047	Intervention	2	0.08	1	1	1	0	0.00	0.0

AW010048	Control	4	0.02	1	1	2	0	0.00	0.0
MM010049	Control	2	0.04	2	2	1	1	18.75	0.0
PC010050	Intervention	2	0.02	1	1	2	0	0.00	0.0
PR010051	Control	2	-0.04	2	2	2	1	62.50	0.0
DR010052	Control	3	0.00	2	2	2	2	0.00	0.0
IJ010053	Control	2	0.30	2	2	0	0	16.00	0.0
AH010054	Control	3	0.08	1	2	2	0	24.00	0.0
GC010055	Intervention	4	0.14	0	0	0	2	0.00	4.0
JL010056	Intervention	3	0.14	2	2	1	1	0.00	0.0
MP010057	Intervention	2	0.22	2	2	1	1	50.00	2.0
PB010058	Control	4	0.04	2	2	1	1	0.00	0.0
CE010059	Control	2	0.04	1	1	0	0	0.00	0.0
AW010060	Intervention	4	0.18	0	0	0	0	0.00	2.0

Study ID = study identification; AREDS Grade = Age Related Eye Disease Study Simplified Severity Grade (Ferris et al., 2005); BCVA = Best corrected visual acuity; ETDRS = Early Treatment Diabetic Retinopathy Study; LOCS III = Lens Opacities Classification System III (Chylack et al., 1993); NC = nuclear colour; NO = nuclear opalescence; C = cortical cataract; P = posterior subcapsular cataract

Appendix X. ALight trial 18-month post-hoc analysis

When the AMD status of participants who showed no disease progression during the trial was reviewed 6 months following their end-of-study visit, hospital records reported that following final data collection 3 control participants and no intervention participants had developed nAMD in the study eye. This equated to 5% (n=1) of the intervention group and 17% (n=5) of the control group converting to nAMD over 18 months. The mask wearer who converted to nAMD wore the mask for 70 nights prior to nAMD onset. When combined with 12-month disease progression data (n=8 intervention and n=14 controls) 38% (n=8) of the intervention group and 59% (n=17) of the control group showed disease progression over 18 months. This difference between study groups failed to reach statistical significance (Mantel-Haenszel test, Common Odds Ratio = 0.794, P=0.559).

For the purposes of this trial, drusen shrinkage was not included as an outcome measure as it was not possible to distinguish between regression preceding late stage AMD and regression which may indicate a reduction in disease severity. Post-hoc review of change in drusen volume for those who developed nAMD after their final study visit showed that 50% had shown significant drusen shrinkage throughout the trial. However, there was no significant difference (chi-squared test, P=0.57) in the proportion of those (intervention, 24%; control, 17%) showing drusen shrinkage between groups. The post-hoc review of AMD status 6 months after the final visit also showed that none of the intervention participants who displayed significant drusen shrinkage throughout the trial progressed to nAMD up to 18-months post randomisation.

Post-hoc sample size calculations suggest that a sample size of 381 per group would be required to detect an effect of the magnitude seen in the ALight trial (80% power, P=0.05) at 12 months. It was interesting to note that a greater number of participants

progressed to nAMD in the control group (n=3, 10%) in the 6 months following the trial than in the treatment group (where no further participants converted). In other words, by the time 18 months had elapsed since mask wear commenced, 38% of mask wearers and 59% of the control group had exhibited signs of disease progression in the eye with early AMD (with 5% of the intervention group and 17% of the control group converting to nAMD in this timeframe). Based on post hoc analysis of these data, if conversion to nAMD only was specified as a measure of disease progression and change in drusen volume was not considered, an approximate sample size of 103 per group would be required to detect an effect of the magnitude seen in the present study (80% power, P=0.05) if the follow-up was extended to 18 months. This suggests that further study of the longer term effectiveness of the intervention is of value; the 12 month follow up time may not have been long enough.